IMPACT OF HYDROPHILIC EMULSIFIER AND EMULSION MICROSTRUCTURE ON AROMA RELEASE OVER W/O/W EMULSIONS

By

Xiaolu Pu, MSc.

Thesis submitted to the University of Nottingham

for the degree of Doctor of Philosophy

Division of Food Sciences

School of Biosciences

University of Nottingham

Loughborough

LE12 5RD

May 2018

ABSTRACT

In this thesis, the impact of the interactions between the hydrophilic emulsifiers and aroma compounds as well as emulsion microstructure including droplet size, droplet size distribution, emulsion stability and creaming on aroma release over water-in-oil-in-water (w/o/w) emulsions was investigated.

Polyglycerol polyricinoleate (PGPR) was used as the only hydrophobic emulsifier to stabilise the internal water droplets in the primary water-in-oil (w/o) emulsion of the w/o/w emulsions throughout this research. Three hydrophilic emulsifiers investigated to stabilise the w/o droplets in w/o/w emulsions included a low molecular weight non-ionic surfactant, polyoxyethylene 20 sorbitan monolaurate (Tween 20), a chemically modified starch, octenyl succinic anhydride (OSA) starch and a protein, pea protein isolate (PPI), as the large molecular weight emulsifiers. The two emulsification methods of high shear mixing and stirred cell membrane emulsification were used. Controls of water and oil-in-water (o/w) emulsions were prepared with the formulation and process conditions as for the w/o/w emulsions. Emulsion microstructure was characterised in terms of droplet appearance, droplet size, droplet size distribution as well as emulsion stability over time. Both static and dynamic headspace analyses were carried out to investigate the aroma release behaviour over w/o/w emulsions.

The results showed that w/o/w emulsions were a suitable vehicle for short time aroma entrapment, which was most successful for the hydrophilic aroma

acetoin compared to the hydrophobic aromas acetyl pyridine and hexanal. This entrapment of the hydrophilic aroma resulted from the barrier of the oil phase in the w/o droplets to delay its diffusion or the PGPR micelles in the oil phase to entrap it in the polar inner core. The complex food emulsifiers OSA starch and PPI were for the first time successfully used in stirred cell membrane emulsification to produce similarly sized o/w and w/o/w emulsions. These were produced to eliminate the effect of droplet size in the study of aroma release. The release of aromas (i.e. diacetyl and 3-pentanone) was affected by the combination of the type of the hydrophilic emulsifier (Tween 20, OSA starch and PPI) and the type of the emulsion system (i.e. o/w and w/o/w emulsions) as well as the emulsion microstructure including droplet size, emulsion stability, interface thickness, creaming and diffusion of the internal water phase into the external water phase of w/o/w emulsions. The thinner interface laden by Tween 20 might lead to a quicker diffusion of the hydrophobic aroma 3-pentanone from the w/o droplets into w_2. OSA starch interacted with the hydrophilic aroma diacetyl and 3-pentanone, and PPI interacted with 3-pentanone. These findings help to better understand the effect of the hydrophilic emulsifier and emulsion microstructure on aroma release and present a novel study to produce similarly sized emulsion droplets with complex food emulsifiers.

ACKNOWLEDGEMENTS

I would like to express my first and deepest appreciation to my main supervisor, Dr Bettina Wolf, whose considerable contribution in help, support, guidance, patience, suggestion and encouragement throughout these years as well as her scientific contribution towards this thesis and for correcting my endless drafts.

Furthermore, I would also like to acknowledge to my additional supervisor, Dr Ian Fisk, who gave me much useful comments and advices for my study. I would also like to thank Dr Robert Linforth, who kindly provides a lot of useful discussions and suggestions in terms of using the equipment in laboratory, experiment design, statistical analysis and advices for the thesis.

I sincerely express my gratitude to Dr Marijana Dragosavac, who gave me so much help, support, guidance, suggestion and discussion over one year when I was working at Loughborough University. Also many thanks to Prof. Richard Holdich, Monika Pietrzak and Dr Morelli Serena for their help and support.

I must thank to China Scholarship Council for the scholarship covering the tuition fee and living fee for three years in my PhD study.

A special thanks to Alexandra Katharine McEntee, whose work stimulated the design of this PhD research.

I also must thank to the colleagues and staff who are now or were in the department of Food Sciences: Amelia, Clive, Deepa, Emily, Henghui, Hui, Joanne, Juyang, Natalie, Nicole, Qi, Ruben, Sasika, Steve, Xiaqiu, Xu and Zarani for their help, support and encouragement in the lab and office.

Finally, I would like to acknowledge my parents for their love and support. I would also like to give my honest thanks to my husband Yidong Liu for his love, support, encouragement and always standing by me since we were together. A special thanks to our little daughter Nuoxi for her kicking my stomach when I was writing up in pregnancy and her loveliness and happiness bringing to me when I was revising the thesis.

ABSTRACT ..... **I**

ACKNOWLEDGEMENTS ..... **III**

LIST OF ABBREVIATIONS AND SYMBOLS **1**

1 INTRODUCTION **7**

1.1 Overall aim and specific objectives 8

1.2 Structure of the thesis 9

1.3 Research dissemination 12

2 BACKGROUND TO THIS THESIS **13**

2.1 Emulsions 13

2.1.1 Single emulsions 13

2.1.2 Double emulsions 14

2.1.3 Emulsion instability 17

2.1.3.1 Gravitational separation 17

2.1.3.2 Flocculation 18

2.1.3.3 Phase inversion 19

2.1.3.4 Coalescence 19

2.1.3.5 Ostwald ripening 20

2.1.3.6 Double emulsion instability 20

2.2 Emulsifiers 23

2.2.1 Stabilisation mechanisms 25

2.2.1.1 Steric stabilisation 25

2.2.1.2 Electrostatic stabilisation 26
2.2.2 Emulsifier type 27
2.2.2.1 Low molecular weight surfactants 28
2.2.2.1.1 Classification by chemical structure 28
2.2.2.1.2 Hydrophilic lipophilic balance 29
2.2.2.1.3 Critical micelle concentration 31
2.2.2.1.4 Polyglycerol polyricinoleate 33
2.2.2.1.5 Polyoxyethylene 20 sorbitan monolaurate 35
2.2.2.2 Starch 36
2.2.2.2.1 Octenyl succinic anhydride starch 38
2.2.2.3 Protein 39
2.2.2.3.1 Pea protein isolate 41
2.3 Food flavours 43
2.4 Flavour release mechanisms 44
2.4.1 Partition coefficient and diffusion coefficient 46
2.4.1.1 Henry's law 46
2.4.1.2 Octanol-water partition coefficient 48
2.4.1.3 Fick's Law 49
2.4.2 Interactions between aroma compounds and food ingredients 49
2.4.2.1 Aroma-lipid interactions 50
2.4.2.2 Aroma-surfactant interactions 51
2.4.2.3 Aroma-starch interactions 52
2.4.2.3.1 Hydrophobic interaction 53

2.4.2.3.2 Hydrogen binding 53

2.4.2.4 Aroma-protein interactions 54

2.4.2.4.1 Hydrophobic and hydrogen binding 54

2.4.2.4.2 Covalent binding 57

2.5 Conclusions 59

3 MATERIALS AND METHODS 60

3.1 Materials 63

3.2 Methods 63

3.2.1 Preparation of w/o/w emulsions through high-shear mixing 63

3.2.2 Preparation of control o/w emulsions through high-shear mixing

.....65

3.2.3 Aroma addition 65

3.2.4 Analysis of emulsions 66

3.2.4.1 Microscopy 66

3.2.4.2 Droplet size measurement 67

3.2.5 Aroma release measurement 67

3.2.5.1 Static headspace analysis 69

3.2.5.2 Dynamic headspace analysis 72

3.2.6 Statistics 75

4 IMPACT OF AROMA HYDROPHOBICITY ON AROMA ENTRAPMENT IN A W/O/W EMULSION 76

4.1 Introduction 77

4.2 Methods specific to the results reported in this chapter 80

4.2.1 Sample preparation 80

4.2.2 Quantification of aroma entrapment 81

4.3 Emulsion microstructure..... 82

4.4 Aroma partitioning and entrapment 85

4.4.1 Hydrophilic aroma compound 85

4.4.2 Hydrophobic aroma compounds 87

4.5 Entrapment ratio..... 88

4.6 Conclusions 89

5 IMPACT OF HYDROPHILIC EMULSIFIER ON AROMA RELEASE FROM W/O/W EMULSIONS.....90

5.1 Introduction 91

5.2 Methods specific to the results reported in this chapter 92

5.2.1 Emulsion composition and aroma inclusion..... 92

5.2.2 Static headspace analysis..... 94

5.2.3 Dynamic headspace analysis..... 99

5.3 Emulsion microstructure during storage 100

5.4 Aroma release under static condition 110

5.4.1 Hydrophilic aroma..... 111

5.4.2 Hydrophobic aroma 115

5.5 Aroma release under dynamic condition 119

5.5.1 Hydrophilic aroma 120

5.5.2 Hydrophobic aroma 125

5.6 Conclusions 127

6 DROPLET SIZE CONTROL OF W/O/W EMULSIONS THROUGH STIRRED CELL MEMBRANE EMULSIFICATION 129

6.1 Introduction 129

6.2 Methods specific to the results reported in this chapter 136

6.2.1 Interfacial tension measurement 136

6.2.2 Viscosity measurement 137

6.2.3 Density measurement 137

6.2.4 Preparation of w/o/w emulsions through stirred cell membrane emulsification 138

6.2.4.1 Stirred cell membrane emulsification 138

6.2.4.2 Emulsion phases 140

6.2.4.3 Process parameters 141

6.2.5 Microscopy and image analysis 142

6.2.6 Droplet size measurement 143

6.3 Prediction of droplet diameter 144

6.3.1 Surface/ interfacial tension of all liquid phases 144

6.3.2 Viscosity 148

6.3.3 Density 149

6.3.4 Predicted droplet diameters 149

6.4 Effect of process parameters on droplet size 151

6.5 Effect of emulsifier concentration and rotational speed on emulsion microstructure 158

6.6 Emulsion stability 162

6.7 Conclusions 166

7 IMPACT OF HYDROPHILIC EMULSIFIER ON AROMA RELEASE OVER EMULSIONS GENERATED VIA STIRRED CELL MEMBRANE EMULSIFICATION AND THICKENED WITH XANTHAN GUM 167

7.1 Introduction 168

7.2 Methods specific to the results reported in this chapter 170

7.2.1 Sample formulations and process parameters 170

7.2.2 Xanthan gum addition and aroma inclusion 172

7.2.3 Emulsion characteristics 174

7.2.4 Assessing encapsulation efficiency 175

7.2.5 Aroma release measurement 178

7.3 Properties of emulsions prepared through stirrced cell membrane emulsification 180

7.3.1 Emulsion microstructure during storage 180

7.3.2 Creaming velocity 187

7.3.3 Emulsion viscosity with xanthan gum 189

7.3.4 Encapsulation efficiency 191

7.4 Aroma release under static condition 196

7.4.1 Hydrophilic aroma 196

7.4.2 Hydrophobic aroma 198

7.5 Aroma release under dynamic condition 200

7.5.1 Hydrophilic aroma 200

7.5.2 Hydrophobic aroma 203

7.6 Conclusions 206

8 OVERALL CONCLUSIONS AND FUTURE WORK..... 208

8.1 Conclusions 210

8.2 Future work 212

REFERENCES..... 215

LIST OF ABBREVIATIONS AND SYMBOLS

ABBREVIATIONS:

A	Total interfacial area of the dispersed phase
A'	Cross-sectional area
APCI-MS	Atmospheric pressure chemical ionisation - mass spectrometry
b	Blade height
C	Aroma concentration
C_a/ C_g	Aroma concentration in air or the gas phase at equilibrium
C_i	Total magnesium concentration initially added in the internal water phase of water-in-oil-in-water emulsions
CMC	Critical micelle concentration
C_{Mg}	Magnesium concentration in the external water phase of water-in-oil-in-water emulsions measured by the flame atomic absorption spectroscope over time
C_o	Aroma concentration in the oil phase
C_{oct}	Aroma concentration in octanol at equilibrium
C_t	Total aroma concentration prepared in a liquid sample
C_{water}	Aroma concentration in water at equilibrium
C_{w_1}	Aroma concentration in the internal water phase of water-in-oil-in-water emulsions
C_{w_2}	Aroma concentration in the external water phase of water-in-oil-in-water emulsions
$C_{(w_1+w_2)}$	Aroma concentration in the total water phase of water-in-oil-in-water emulsions
CTAB	Cetyltrimethylammonium bromide
CV	Coefficient of variation
C_w	Aroma concentration in water at equilibrium
C'_{w_1}	Aroma concentration initially added in the internal water phase of water-in-oil-in-water emulsions
C'_{w_2}	Aroma concentration initially added in the external water phase of water-in-oil-in-water emulsions

D	Stirrer diameter
d_{av}	Average droplet size
DS	Degree of substitution
$d_{3,2}$	Mean droplet size on surface area basis, also known as Sauter diameter
$d_{4,3}$	Mean droplet size on volume basis
EMG	Ethoxylated monoglyceride
EPI	Estimation program interface
g	Local acceleration due to gravity
G	Interfacial energy
GMS	Glycerol 1-monostearate
H	Henry's law constant at equilibrium
h	Heated
HLB	Hydrophilic-lipophilic balance
K	Association constant
K_{ae}	Air-emulsion partition coefficient
K_{ao}	Air-oil partition coefficient
K_{aw}	Air-water partition coefficient
K_{gc}	Gas-continuous phase partition coefficient of the aroma compound
K_{gl}	Gas-liquid partition coefficient
K_{mc}	Micelle-continuous phase partition coefficient
LMW	Low molecular weight
Log P	Octanol-water partition coefficient
m	Mass
ME	Membrane emulsification
Mg	Magnesium
$MgCl_2$	Magnesium chloride
M_L	Molecular weight of the hydrophilic region
M_T	Total molecular weight
Mwt	Molecular weight

NaCl	Sodium chloride
n_b	Number of impeller blades
NC46	N-creamer 46
N_g	Number of moles of the aroma in the gas phase
N_o	Number of moles of the aroma in the oil phase of oil-in-water emulsion
$N_{o'}$	Number of moles of the aroma in the oil phase of water-in-oil-in-water emulsions
n_p	Total number of binding sites per mole of protein
N_t	Total number of moles of the aroma added in a liquid sample
N_w	Number of moles of the aroma in the water phase of oil-in-water emulsions
n_{w_1}	Number of moles of the aroma initially added to the internal water phase
N_{w_1}	Number of moles of the aroma in the internal water phase of water-in-oil-in-water emulsions
n_{w_2}	Number of moles of the aroma initially added to the external water phase
N_{w_2}	Number of moles of the aroma in the external water phase of water-in-oil-in-water emulsions
N_{water}	Number of moles of the aroma in water
N_2	Nitrogen
o/w or ow	Oil-in-water
o/w/o	Oil-in-water-in-oil
OSA	Octenyl succinic anhydride
owP	Oil-in-water emulsions stabilised with pea protein isolate
owS	Oil-in-water emulsions stabilised with octenyl succinic anhydride starch
owT	Oil-in-water emulsions stabilised with Tween 20
p	Aroma partial pressure in air at equilibrium
PGPR	Polyglycerol polyricinoleate
PI	Isoelectric point

PPI	Pea protein isolate
PVA	Poly-vinyl alcohol
r	Droplet radius
Re	Reynolds number
r_p	Pore radius
r_{trans}	Transitional radius
SD	Standard deviation
SMILES	Simplified molecular input line entry specification
SSA	Specific surface area
SSL	Sodium stearol lactylate
t	Time
T'	Tank diameter
v	Creaming velocity
V_{bound}	Number of moles of the aroma compound bound per mole of protein
V_f	Molar concentration of the free volatile compound
V_g	Volume of the gas phase
V_l	Total volume of a liquid sample
V_{w1}	Volume of the internal water phase of water-in-oil-in-water emulsions
V_{w2}	Volume of the external water phase of water-in-oil-in-water emulsions
w	Water
w/o or w_1/o	Water-in-oil
w/o/w or w_1/o/w_2 or wow	Water-in-oil-in-water
w_1	Internal water phase of water-in-oil-in-water emulsions
w_2	External water phase of water-in-oil-in-water emulsions
wowP	Water-in-oil-in-water emulsions stabilised with pea protein isolate

wowS	Water-in-oil-in-water emulsions stabilised with octenyl succinic anhydride starch
wowT	Water-in-oil-in-water emulsions stabilised with Tween 20
wP	Water with pea protein isolate
WPI	Whey protein isolate
wS	Water with octenyl succinic anhydride starch
wT	Water with Tween 20
x	Predicted droplet diameter formed at a single membrane pore
x’	Distance of an aroma molecule transport
XG	Xanthan gum

SYMBOLS

γ	Oil-water interfacial tension (N/m)
δ	Boundary layer thickness (m)
η	Viscosity of the continuous phase (Pa·s)
π	Ratio of a circle's circumference to its diameter
ρ	Density of the continuous phase (kg/m^3)
ρ_d	Density of the dispersed phase (kg/m^3)
τ_{max}	Maximum shear stress at the membrane surface (Pa)
ϕ_m	Volume fraction of the micelles in the continuous phase
ϕ_o	Volume fraction of the oil phase in the oil-in-water emulsions
ϕ_w	Volume fraction of the water phase in the oil-in-water emulsions
$\phi_{w/o}$	Volume fraction of the water-in-oil emulsion in the water-in-oil-in-water emulsions
ϕ_{w_1}	Volume fraction of the water phase in the water-in-oil emulsions
ω	Angular velocity of the paddle stirrer (ras/s)

1 INTRODUCTION

A considerable number of natural and processed foods are partly or wholly based on emulsions, such as milk, cream, beverages, mayonnaise, sauces, butter, margarine and so on. Two phase liquid emulsions formulated with food oil and a food-grade aqueous phase either or both of which with added emulsifiers and/or stabilisers are a suitable delivery vehicle of aroma compounds. Whilst simple emulsions are well known as delivery vehicles for aromas soluble in the dispersed phase (Miettinen et al. 2002, van Ruth et al. 2002a, Malone et al. 2003, Paraskevopoulou et al. 2009, Arancibia et al. 2011), the potential of double emulsions, such as water-in-oil-in-water (w/o/w) emulsions to deliver aromas that diffuse into each phase is less well known (Dickinson et al. 1994, Brückner et al. 2007). It is necessary to formulate the w/o/w emulsion system with food grade emulsifiers such that their microstructure is stable as required (Garti 1997a, Frasch-Melnik et al. 2010, Pawlik et al. 2010, Sapei et al. 2012, Souilem et al. 2014). Hydrophobic emulsifiers are needed to induce into the oil phase to stabilise the internal water droplets of the primary w/o emulsion. It has been widely reported that polyglycerol polyricinoleate (PGPR) is a powerful emulsifier for this purpose (Bonnet et al. 2009, Márquez et al. 2010, Leal-Calderon et al. 2012). Hydrophilic emulsifiers are then required to stabilise the w/o droplets to form the w/o/w emulsion. There are a range of hydrophilic emulsifiers commonly used for w/o/w emulsions including low molecular weight surfactants, hydrophobically modified starches and proteins (Kawakatsu et al. 2001, Chiu et al. 2015).

Polyoxyethylene 20 sorbitan monolaurate (Tween 20), octenyl succinic anhydride (OSA) starch and pea protein isolate (PPI) are representatives of these three classes of emulsifiers. It is likely that the hydrophobic and the hydrophilic emulsifiers required to stabilise w/o/w emulsions interact with added aroma compounds through binding to aromas or solubilising aromas (Landy et al. 1996, Guichard 2002, Miettinen et al. 2002). This would lead to a reduction in the headspace intensity of aroma compounds or a decreased release rate over the emulsions. Droplet size, droplet size distribution and emulsion stability of w/o/w emulsions formulated by different hydrophilic emulsifiers may also have an influence on aroma release (Charles et al. 2000, van Ruth et al. 2002a, Mirhosseini et al. 2008).

1.1 OVERALL AIM AND SPECIFIC OBJECTIVES

The overall aim of this PhD research was to explore the impact of interaction between aroma compounds and hydrophilic emulsifiers and the impact of emulsion microstructure including droplet size, droplet size distribution and emulsion stability on aroma release behaviour over w/o/w emulsions using *in vitro* methods. To achieve this research aim, specific objectives were undertaken and these include:

I. Validation of preliminary data obtained via *in vitro* methods to investigate the impact of aroma hydrophobicity on aroma entrapment in a w/o/w emulsion processed via high shear mixing.

II. Manipulation of the interfacial design of w/o droplets in the w/o/w emulsions through varying type of emulsifier, i.e., a low molecular weight surfactant, a hydrophobically modified starch and a protein, prepared via high shear mixing to explore the impact of emulsifier type on aroma release using *in vitro* methods.

III. Manufacture of w/o/w emulsions stabilised with these three emulsifiers with narrow/controlled droplet size distribution through stirred cell membrane emulsification to better control emulsion microstructure.

IV. Exploring the aroma release mechanisms over these well-defined w/o/w emulsions using *in vitro* methods to investigate the aroma-emulsifier interaction.

1.2 STRUCTURE OF THE THESIS

The next thesis chapter, Chapter 2, introduces the background and fundamentals of two science areas related to this PhD research; emulsion science and flavour science. This emulsion science part covers emulsion types, emulsion instability, emulsifier function and the specific emulsifiers used in this research. With regard to flavour science, flavour definition and the mechanisms of flavour release including partition coefficients, laws of aroma compounds and aroma-ingredient interactions are reviewed.

In Chapter 3, the materials and methods are reported. All materials used in this PhD research are presented. For the methods, the preparation of w/o/w

emulsions and control o/w emulsions through high shear mixing is described. The aroma addition method is briefly reported. In the subchapter of emulsion characterisation methods, the evaluation of emulsion microstructure using microscopy and the measurement of droplet size distributions are provided. In the subchapter of aroma release measurement using *in vitro* methods, static headspace analysis and dynamic headspace analysis are generally introduced. Lastly, the statistical method applied for data analysis is described.

Chapters 4-7 constitute the main thesis chapters presenting all experimental results and their discussion. Each chapter also contains the methods specific to the results reported in this chapter. Chapter 4 reports the aroma entrapment in the internal aqueous phase of a w/o/w emulsion stabilised with pea protein isolate as affected by the aroma hydrophobicity. The methods including formulating the w/o/w emulsion, the addition of aromas and the aroma entrapment using *in vitro* methods specific to this chapter are shown. Chapter 5 reports the impact of the three for this PhD research selected hydrophilic emulsifiers Tween 20, octenyl succinic anhydride starch and pea protein isolate on aroma release over w/o/w and control o/w emulsions, in terms of emulsion microstructure and aroma-emulsifier interaction. The methods including emulsion formulation, aroma addition, headspace analysis parameters under static and dynamic conditions specific to this chapter are described. Chapter 6 presents the results and discussion of droplet size control of w/o/w emulsions stabilised with the aforementioned three hydrophilic emulsifiers through stirred cell membrane emulsification. The method including the measurement of interfacial tension, viscosity and density as material parameters required to

predict mean droplet size for the specific membrane emulsification process is described. Then the method of preparing w/o/w emulsions through stirred cell membrane emulsification, including the setup of membrane emulsification, emulsion phase formulation and process parameters of membrane emulsification, is reported. The methods of microscopy, image analysis and droplet size measurement used in this chapter are described. Chapter 7 reports and discusses the aroma release behaviour over these w/o/w and o/w control emulsions with similar droplet size also prepared via stirred cell membrane emulsification, and water as the simplest control, in order to investigate the interaction between the hydrophilic emulsifiers and the aromas. The methods including sample formulations, process parameters of membrane emulsification, xanthan gum addition to prevent droplet creaming, aroma addition, emulsion characteristics, magnesium encapsulation to measure the loss of the internal water phase in w/o/w emulsions and aroma release measurement parameters used in this chapter are described.

Finally, the overall conclusions of this research and suggestions for future work are presented in Chapter 8.

1.3 RESEARCH DISSEMINATION

The results obtained during this research are in preparation for publishing as follows:

Pu, X., Wolf, B., Dragosavac, M. M.. Droplet size control of water-in-oil-in-water emulsions stabilised with complex food emulsifiers generated via stirred cell membrane emulsification.

Pu, X., Wolf, B., Fisk, I.. Impact of hydrophilic emulsifier and emulsion microstructure on aroma release above water-in-oil-in-water emulsions.

The results obtained during this research have been presented as follows:

Pu, X., McEntee, A., Neille, M., Wolf, B., Fisk, I. (March 2014). Release behaviour of duplex emulsions. Poster presentation. 1st Food Structure and Functionality Forum, Amsterdam, The Netherlands.

Pu, X., McEntee, A., Neille, M., Wolf, B., Fisk, I. (April 2015). Aroma entrapment of duplex emulsions. Poster presentation. Trends in Flavour, Nottingham, UK.

Pu, X., Fisk, I., Wolf, B. (July 2015). Flavour release from duplex emulsions. Oral presentation. 3rd Nursten Postgraduate Flavour Symposium, Newcastle, UK.

2 BACKGROUND TO THIS THESIS

In this Chapter, the background related to this PhD research is introduced. Two aspects of the background are presented as follows: one is the emulsion aspect, including the emulsion type, the emulsion instability and the emulsifiers specific to this thesis; the other is the flavour aspect, including the definition of flavour and the principles of flavour release. The specific emulsifiers mentioned in Chapter 1 are reviewed because they were used in this research.

2.1 EMULSIONS

A food emulsion is a mixture of two or more immiscible liquid phases, one being present in the other in the form of droplets, with appropriate emulsifiers adsorbed at the interface (Madene et al. 2006). The suspended droplets are referred to as the dispersed phase, while the medium in which they are suspended is the continuous phase. The emulsion types are presented as follows.

2.1.1 Single emulsions

There are mainly two types of single emulsions as shown in Figure 2.1: oil-in-water (o/w) emulsion and water-in-oil (w/o) emulsion. They are the ones this research mainly has been focusing on.

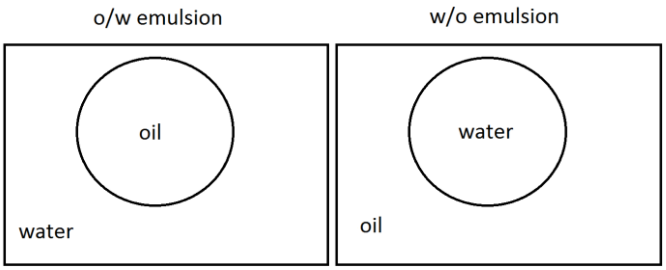


Figure 2.1 Schematic structure of an o/w emulsion and a w/o emulsion

An o/w emulsion consists of oil droplets dispersed in an aqueous phase. Examples include milk, cream, mayonnaises, salad dressing, beverages and soups in the food industry (McClements 2005). This type of emulsion is generally a conductor of electricity and can be diluted with water. A w/o emulsion is comprised of water droplets dispersed in an oil phase. Food examples are margarine and butter. It poorly conducts electricity and can be diluted with solvents or oil. The formation of o/w emulsions or w/o emulsions not only depends on the volume ratio of water to oil but also the type of emulsifier and the emulsification means. The choice of emulsifiers is discussed in section 2.2.

2.1.2 Double emulsions

Double emulsions, or duplex emulsions, are emulsions where the droplets of the dispersed phase contain even smaller dispersed droplets (Azhar et al. 2006). They are complex systems where o/w and w/o emulsion types exist simultaneously. Double emulsions were first explicitly described as “where one

emulsion is within the other" (Seifriz 1925), but it is only in the past 50 years that they have been widely studied (Garti 1997a). Most researches on double emulsions have been focused on the pharmaceutical field, but double emulsions have been gained interests in food area (Gerald et al. 2017).

Double emulsions are the simplest form of complex emulsions including water-in-oil-in-water (w/o/w) and oil-in-water-in-oil (o/w/o) emulsions. $w_1/o/w_2$ emulsions are the mostly investigated double emulsions in food, pharmaceutics and cosmetics industries (Leal-Calderon et al. 2007), and these are studied throughout this thesis. Figure 2.2 shows the structure of a $w_1/o/w_2$ emulsion, where larger oil droplets containing small inner water droplets are dispersed in the external aqueous phase.

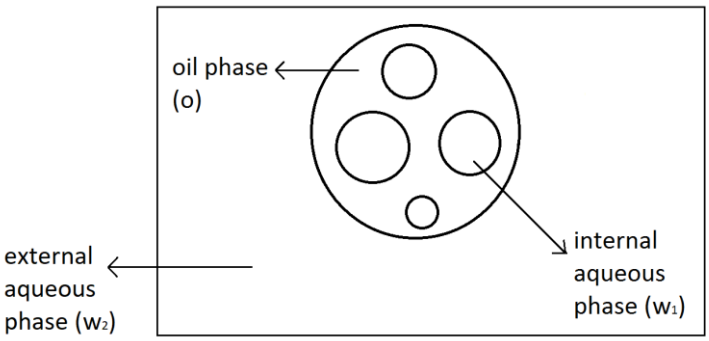


Figure 2.2 Schematic structure of a water-in-oil-in-water ($w_1/o/w_2$) emulsion

Due to the complex structure, $w_1/o/w_2$ emulsions have the advantage of potentially encapsulating or entrapping bioactive compounds including micronutrients and flavours in the internal droplets and/ or the oil phase to

slow or control their release and delivery as desired (Augustin et al. 2008, Lesmes et al. 2009, Giroux et al. 2013, Jiménez-Colmenero 2013). Based on this advantage, several new food products have been reported in the form of $w_1/o/w_2$ emulsions, such as salted cream (encapsulation of salt) and aromatic mayonnaises (Garti 1997b). Moreover, $w_1/o/w_2$ emulsions can be applied to reduce fat since some of the oil in the droplets is replaced by water. It has been reported that $w_1/o/w_2$ emulsions were used to replace the milk fat in cheese-like products to improve the nutritional quality by reducing fat level and saturated fatty acids contents, but also allowed consumers to still perceive a creamy and full-fat mouthfeel without full-fat content (Lobato-Calleros et al. 2006, Lobato-Calleros et al. 2009). A food application of low-calorie mayonnaise was reported, where a $w_1/o/w_2$ system with the same volume fraction of the dispersed phase and the same texture as a simple emulsion but with a lower oil content (due to the existence of the inter aqueous phase) was applied (Matsumoto et al. 1979). $w_1/o/w_2$ emulsions have also been shown to allow salt reduction, which enabled decreasing sodium amount without affecting consumer satisfaction with regard to saltiness (Malone et al. 2003, Lad et al. 2012, Chiu et al. 2015). They also can be taste masking and protect certain ingredients such as bitter peptides (Azhar et al. 2006) or sensitive probiotics such as lactobacillus acidophilus (Shima et al. 2006).

2.1.3 Emulsion instability

Unstable emulsions change properties over time, which is usually undesirable in the food industry. There are a range of basic instability processes encountered in simple emulsions, such as gravitational separation including creaming and sedimentation, flocculation, phase inversion, coalescence and Ostwald ripening shown in Figure 2.3 (Tadros 2013).

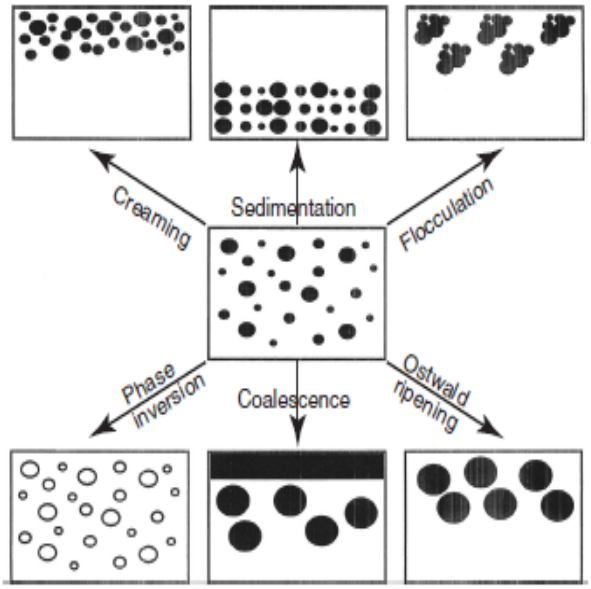


Figure 2.3 Schematic representation of emulsion instability processes (Tadros 2013)

2.1.3.1 Gravitational separation

Gravitational separation results from the density difference between the dispersed droplets and the continuous phase. If the emulsion droplets have a lower density than the surrounding liquid, they will tend to move upward,

which is referred to as creaming. The creaming velocity of an isolated spherical particle in a liquid can be determined by the Stokes' law in Equation 2.1 (McClements 2005):

$$v = -\frac{2gr^2(\rho_d - \rho)}{9\eta} \qquad \text{Equation 2.1}$$

where v is the creaming velocity, g is the local acceleration due to gravity, r is the radius of the droplet, ρ_d is the density of the dispersed phase, ρ is the density of the continuous phase and η is the viscosity of the continuous phase. Thus, the creaming velocity can be decreased mainly by producing smaller droplets and increasing the continuous phase viscosity. Creaming is more common in o/w food emulsions than sedimentation. The droplets reach the top of the emulsion and form a cream layer. The final thickness of the cream layer depends on the initial droplet volume fraction and the effectiveness of the droplet packing. The droplets in a creamed emulsion can be re-dispersed by mild agitation if they are not too strongly attracted to each other or there is no coalescence occurring. In contrast to creaming, sedimentation occurs if the emulsion droplets have a higher density than the surrounding liquid.

2.1.3.2 Flocculation

Flocculation is the process where two or more droplets collide to form aggregates without merging. The strength of droplet aggregation depends on the relative magnitude of the attractive and repulsive forces between droplets (Dickinson 1992). Flocculation causes the acceleration of the creaming rate and

coalescence (Borwankar et al. 1992). Flocculation can be either reversible (weak flocculation) or irreversible (strong flocculation termed coagulation). There are a variety of methods to control flocculation, such as applying mechanical agitation (e.g. stirring) and altering solvent conditions (e.g. pH, ionic strength, polarity or temperature).

2.1.3.3 Phase inversion

Phase inversion is the process where an emulsion system changes from an o/w type to a w/o type or vice versa, triggered by composition or environment changes such as temperature, volume fraction of the dispersed phase, additives, emulsifier type, emulsifier concentration and mechanical agitation (Brooks et al. 1998). It is an essential step in the manufacture of a number of food products including butter and margarine.

2.1.3.4 Coalescence

Coalescence occurs when the thin film separating the droplets is ruptured and two or more droplets merge together to form a larger droplet. In o/w emulsions, coalescence eventually leads to the formation of an oil layer on the top, which is referred to as oiling off (McClements 2005). In w/o emulsions, it leads to the accumulation of water at the bottom. Coalescence causes emulsion droplets to cream or sediment at a faster rate due to the increase in

their size. The occurrence of coalescence can be delayed by preventing droplet contact and interfacial film rupture.

2.1.3.5 Ostwald ripening

Ostwald ripening is a phenomenon where large droplets gradually grow by consuming smaller ones, due to mass transfer of the dispersed phase from one droplet to another through the continuous phase. In consequence, smaller droplets disappear and the droplet size distribution shifts to larger peak values with time. This phenomenon is driven by the interfacial free energy, where larger droplets have a lower interface energy due to their lower interfacial area to volume ratio. Ostwald ripening can be controlled by methods such as producing relatively large droplets, narrowing the droplet size distribution, decreasing the solubility of the dispersed phase in the continuous phase, decreasing the interfacial tension and so on.

2.1.3.6 Double emulsion instability

Double emulsions are less stable than single emulsions because they usually contain relatively larger droplets and have a greater tendency to coalescence than single emulsions (Dickinson et al. 1991). This is because of a larger interfacial area contained in double emulsions. The instability of double emulsions can be mainly seen at three levels: (1) between small internal water

droplets, (2) between large w/o droplets, (3) between the w/o droplets and the small droplets dispersed within it.

The mostly investigated instability phenomena in double emulsions is the swelling or shrinkage of the double emulsion in the presence of water migration in or out of the droplets (Garti 1997a). Water and water soluble materials transport in w/o/w emulsions are dominated by two pathways: swelling-breakdown mechanism and diffusion and/ or permeation through the oil film (Cheng et al. 2007). Coalescence of the small inner droplets with the oil droplet interface in w/o/w emulsions was reported, which was due to the rupture of the thin oil phase film that forms between the external water phase and the internal water phase (Ficheux et al. 1998). This lead to complete delivery of the small internal water droplets to the external water phase. In a w/o/w emulsion without osmotic pressure, the Laplace pressure associated with the small inner droplets lead to the water diffusion from the internal aqueous phase to the external aqueous phase (Mezzenga 2007). This effect can be reduced by dissolving a low molecular weight compound such as a salt or sugar into the internal aqueous phase to efficiently decrease the chemical potential of water and thus, to induce an osmotic pressure gradient opposing the Laplace pressure (Koroleva et al. 2003, Mezzenga et al. 2004). However, a concentration gradient or an osmotic pressure gradient between two aqueous phases exerted by the whole set of various molecules (surfactant, electrolytes, actives) has been widely reported as one of the mechanisms behind the diffusion process (Matsumoto et al. 1980, Pawlik et al. 2010, Zhu et al. 2018).

It is also found that even if the osmotic pressure was balanced, there was still salt diffusion from the internal phase to the external phase (Pawlik et al. 2010). Another route of water transport is through the thin lamellae of surfactant, which partially form in the oil layer due to fluctuations in its thickness (Jager-Lezer et al. 1997, Garti 1997b). Reverse micelles in the oil phase has previously been reported to transport water by entrapping water molecules inside and diffuse across the oil phase to the other aqueous phase (Sela et al. 1995).

It has been suggested that the diffusion of water and water soluble materials is a rate-determining step. Several methods have been presented to improve the stability of w/o/w emulsions and slow the diffusion rate (Garti 1997b). The methods consist of three categories: (1) stabilisation of the internal water droplets, (2) modification of oil phase, (3) stabilisation of the w/o droplets. The internal water phase is claimed to be best stabilised by reducing the size of the water droplets by mechanically or using more surface active emulsifiers, or increasing the viscosity of the internal water phase or forming microspheres. The approaches to modify oil contains the selection of proper oil phase and use of possible carriers, complexing agents and increase its viscosity. The stabilisation of the w/o droplets can be improved by using polymeric emulsifiers, macromolecular ampliphilies (polysaccharides and proteins) or colloidal solid particles to form strong and more rigid droplet film, which lead to a slow release of water soluble materials (Sela et al. 1995, Garti et al. 1996, Benichou et al. 2004). The molecular complexation of polymers and surfactants added to the external aqueous phase has also been reported to enhance the

stability of w/o/w emulsions and control of diffusion of encapsulant (Gerald et al. 2017).

2.2 EMULSIFIERS

The thermodynamic instability phenomenon of emulsions is due to the excess free energy associated with the surface of emulsion droplets (Jiao et al. 2008). The interfacial free energy is defined in Equation 2.2:

$$\Delta G = \gamma \Delta A \qquad \text{Equation 2.2}$$

where G is the interfacial energy, γ is the interfacial tension and A is the total interfacial area of the dispersed phase. The interfacial area of an emulsion increases after emulsification, which results in that dispersed droplets tend to come together to reduce the surface area and eventually revert back to the original two-phase system. In order to minimise this emulsion destruction effect, emulsifiers are added in emulsion systems to aid their formation and kinetic stability.

Emulsifiers, also known as surface-active agents, are defined as amphiphilic molecules. This is due to the coexistence of hydrophilic head groups that tend to attach to polar solvents (e.g. water) and hydrophobic tail groups that associate with non-polar solvents (e.g. oil). Figure 2.4 illustrates an example of the droplet surface adsorbed by low-molecular-weight surfactants in an o/w emulsion and a w/o emulsion.

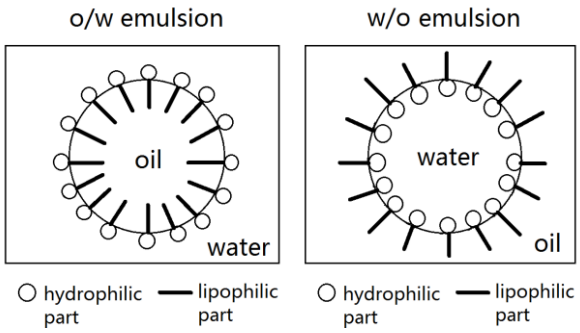


Figure 2.4 Schematic surface adsorbed by emulsifier molecules in an o/w emulsion and a w/o emulsion

An effective emulsifier used in an emulsion has three functions: binding strongly to the interface once adsorbed; rapidly lowering the interfacial tension at the newly formed oil-water interface; protecting the freshly produced droplets against flocculation or coalescence (Dickinson 2009).

Bancroft's rule (Davis 1996) is applied to aid the selection of an emulsifier and is indicative of which type of emulsion would be stabilised. It states that the phase in which a given emulsifier is most soluble will form the continuous phase of an emulsion. Thus, an oil-soluble emulsifier should stabilise w/o emulsions, while a water-soluble emulsifier should stabilise o/w emulsions. Whether an emulsifier is hydrophilic or lipophilic can be decided by the hydrophilic-lipophilic balance (HLB) as described in section 2.2.1.2. In a w/o/w emulsion system, two or more emulsifiers are typically required, one that is predominately hydrophobic stabilising the primary w/o emulsion and one that is predominately hydrophilic stabilising the secondary o/w emulsion. The

hydrophobic and hydrophilic emulsifiers are added to the oil and the external aqueous phase respectively.

2.2.1 Stabilisation mechanisms

Emulsifiers can stabilise the emulsion droplets through different stabilisation mechanisms. The two main mechanisms are steric and electrostatic stabilisations and they are present as follow.

2.2.1.1 Steric stabilisation

Steric stabilisation is a generic term that encompasses all aspects of the stabilisation of emulsion droplets adsorbed by emulsifiers such as surfactants, phospholipids, polysaccharides or proteins (Napper 1977). When two droplets get sufficiently close, their interfacial layers overlap and interact with each other. Steric stabilisations are a result of the intermingling and/ or compression of the interfacial layers (Tadros 2015). At close droplet separations, steric stabilisation can be strongly repulsive and prevent emulsion droplets from aggregating (Tadros 1991, Tadros 2015). Nonetheless, the overall magnitude, sign and range of steric stabilisation is dependent on the properties of the interfacial layers such as thickness, packing, flexibility, rheology and molecular interactions, and therefore is determined by the emulsifier type (McClements 2005, Tadros 2015). The strength of steric stabilisations increases with the thickness of the emulsifier adsorbed interface and the droplet size.

Steric stabilisation has the advantages of insensitive to pH and ionic strength, which are the main difference with electrostatic stabilisation. For example, it was reported that emulsion stabilised by modified starch through steric stabilisation were stable against changes in pH (3-9), ionic strength (0-25 mM $CaCl_2$) and temperature (30-90 °C) (Chanamai et al. 2002). However, a large amounts of emulsifier are usually required to cover the droplet surface and stabilise the droplets through steric stabilisation. Since steric stabilisation is strongly repulsive when droplets approach at short distance, sterically stabilised emulsion may weakly flocculate but they are unlikely to coalesce.

2.2.1.2 Electrostatic stabilisation

Electrostatic stabilisation usually occurs when the emulsion droplets have an appreciable electrical charge. Since all the droplets in an emulsion are generally stabilised by the same emulsifier type, emulsion droplets usually have similar charges. An isolated charged droplet is surrounded by a cloud of counterions. When two similarly charged droplets approach each other, their counterion clouds overlap and the repulsive interaction arises to prevent the droplets from aggregation (Cosgrove 2010). The magnitude and sign of the repulsion is dependent on the type and concentration of the emulsifier present at the droplet surface and the prevailing environmental conditions such as pH, temperature and ionic strength (McClements 2005).

When the electrical charge on the droplet surface is reduced (e.g., by changing the pH) or screened (e.g. by increasing the electrolyte concentration), the

electrostatic repulsion between droplets can be remarkably reduced. For example, β-lactoglobulin stabilised emulsions were found stable against flocculation at room temperature at pH 7 without salt addition due to the strongly electrostatic repulsion between droplets (Kim et al. 2002a, Kim et al. 2002b). However, these emulsions became unstable at a sufficiently high concentration of salt (150 mM) because this screened the electrostatic repulsion.

2.2.2 Emulsifier type

Low-molecular-weight (LMW) surfactants, hydrophobically modified starches and proteins are the emulsifier types used in this PhD research. They are the main types of emulsifiers applied in food emulsions. LMW surfactants are more surface-active or more efficient in stabilising emulsion droplets than macromolecules such as proteins and starches. The former forms a compact adsorbed layer at the oil-water interface and the latter two form a viscoelastic interface, which strongly influences the emulsion kinetic and thermodynamic stability (Capek 2004). Nonetheless, emulsions stabilised with proteins or starches are usually more stable against coalescence and Ostwald ripening than LMW surfactant stabilised emulsions (Aveyard et al. 2003, Yusoff et al. 2011). The stability of the emulsions stabilised with proteins or starches is attributed to their large molecular size and the fact that proteins or starches tend to adsorb strongly or irreversibly at the oil-water interface.

2.2.2.1 Low molecular weight surfactants

Low molecular weight surfactants, hereinafter referred to as surfactants, are small molecules and very mobile. They are particularly efficient at reducing the interfacial tension by rapidly adsorbing at the created oil-water interface during emulsification. The surfactant classification by chemical structure and HLB as well as two surfactants specific to this thesis are introduced below.

2.2.2.1.1 Classification by chemical structure

Surfactants can be grouped according to chemical structure. Table 2.1 (Griffin 1949, Stauffer 1999, Ushikubo et al. 2014) lists some examples of different surfactant types.

The hydrophobic region of a surfactant molecule is usually a long chain of fatty acids containing 10-20 carbon atoms (St Angelo 1989). The hydrophilic region of a surfactant may have a variety of functional groups. The hydroxyl groups and ethylene oxide chains comprise the hydrophilic solubilising groups for non-ionic surfactants. Carboxylates, sulfonates, sulphates and phosphates generally provide the solubilising properties of anionic surfactants. Amines and ammonium groups provide the solubilising groups in cationic surfactants. If both an anionic and a cationic group are present on the same molecule, the surfactant is zwitterionic.

Table 2.1 Examples of surfactant type (Griffin 1949, Stauffer 1999, Ushikubo et al. 2014)

Surfactant type	Representative	Example	Hydrophilic lipophilic balance (HLB)
Non-ionic	Monoglycerides	Glycerol 1-monostearate (GMS)	3.8
	Monoglycride derivatives	Ethoxylated monoglyceride (EMG)	13
	Sorbitan derivatives	polyoxyethylene 20 sorbitan monolaurate (Tween 20)	16.7
	Polyglycerol esters	Polyglycerol polyricinoleate (PGPR)	1.5
Anionic	Lactylates	Sodium stearol lactylate (SSL)	8.3
Cationic	Quaternary ammonium salts	Cetyltrimethylammonium bromide (CTAB)	15.8
Zwitterionic	Certain ingredients	Lecithin	9.7

2.2.2.1.2 Hydrophilic lipophilic balance

An alternative way of classifying surfactants is to use the hydrophilic-lipophilic balance (HLB). HLB is the balance between the hydrophilic region of a surfactant and its hydrophobic region, which governs the surfactant functionality at the interface and hence the surfactant utility in emulsions. It assigns a numerical value to surfactants, which provides a simple guide of surfactant selection. HLB can be calculated by Equation 2.3 (Stauffer 1999):

$$HLB = 20M_L / M_T \qquad \text{Equation 2.3}$$

Where M_L is the molecular weight of the hydrophilic region and M_T is the total molecular weight. Hence, the number scale varies from 0 for a pure hydrophobe up to 20 for a pure hydrophile.

Another method of calculating HLB is to sum the functional group values for the hydrophilic and hydrophobic regions in the surfactant, expressed in Equation 2.4 (Davis 1994):

$$HLB = \Sigma \text{ (hydrophilic group values)} - \Sigma \text{ (lipophilic group values)} + 7$$

Equation 2.4

Table 2.2 (Davis 1994) presents some examples of functional group numbers. As a result of HLB calculation by Equation 2.4, a low HLB value indicates a surfactant molecule with a predominantly hydrophobic character, while a high HLB number indicates a predominantly hydrophilic character (Norn 2015). In general, surfactants with a HLB in the range of 3-6 are good to use in w/o emulsions, while those with a HLB range varying in 7-9 are good wetting agents, and those with a HLB of 10-18 are good to use in o/w emulsions (Griffin 1949). Table 2.1 reports some HLB values of food surfactants (Griffin 1949, Stauffer 1999, Ushikubo et al. 2014).

Table 2.2 Examples of functional group numbers (Davis 1994)

	Functional group	Group number
Hydrophilic	$-SO_4Na$	38.7
	-COOH	2.1
Lipophilic	$-CH_2-$	0.475
	-CH-	

In practice, the average HLB of a blend of surfactants can be calculated according to the theoretical HLB values of the individual surfactants and the composition of the surfactant blend, which is used to determine the optimum HLB for a particular system. However, HLB only provides a one-dimensional description of the surfactant properties. It does not consider that the functional properties of some emulsifiers such as proteins are significantly influenced by temperature and solution conditions (Hasenhuettl et al. 2008).

2.2.2.1.3 Critical micelle concentration

When the surfactant concentration exceeds a critical value known as the critical micelle concentration (CMC), the molecules added in a liquid can form micelles (Rosen et al. 2012). When below the CMC, the addition of a small amount of surfactant results in a dramatic reduction of the equilibrium surface tension in the solution. Monomers of surfactant molecules are dominant, which are amphiphilic and have a high surface activity. But once above CMC when the solution is saturated with surfactants, any additional added molecules will form micelles, while the monomers remain at a constant concentration. There is very little influence on further reducing the equilibrium interfacial tension due to the little surface activity of micelles. CMC can indicate the minimum concentration of an emulsifier to sufficiently reduce the interfacial tension at which the maximum extent reduction in the interfacial tension at equilibrium was achieved. Nonetheless, the size of emulsion droplets produced during emulsification is more related to the dynamic interfacial

tension. Because it takes time for macromolecular emulsifiers to reach the equilibrium interfacial tension, which is usually much longer for the emulsification time scale. For example, the time required for the emulsifier to reach the equilibrium of the interfacial tension is approximately 1000 s for octenyl succinic anhydride (OSA) starch at 1 (% w/w) at 25 °C (Tesch et al. 2002), while that for Tween 20 at 0.1 (% w/w) is around 10 s at 20 °C (Schröder et al. 1998). Hence, a much higher emulsifier concentration above CMC is usually required to sufficiently reduce the interfacial tension.

Micelles have highly dynamic structures because they are only held together by relatively weak physical interactions compared to the thermal energy of the system (Israelachvili 2011). Figure 2.5 gives an example of the structure of a micelle of a hydrophilic emulsifier in water and a micelle of a hydrophobic emulsifier in oil.

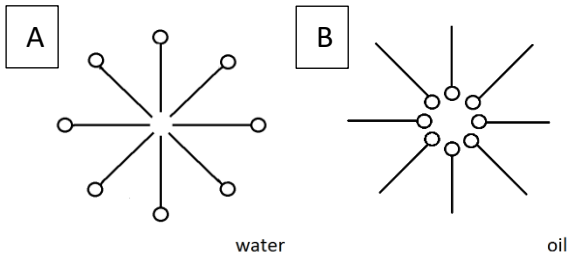
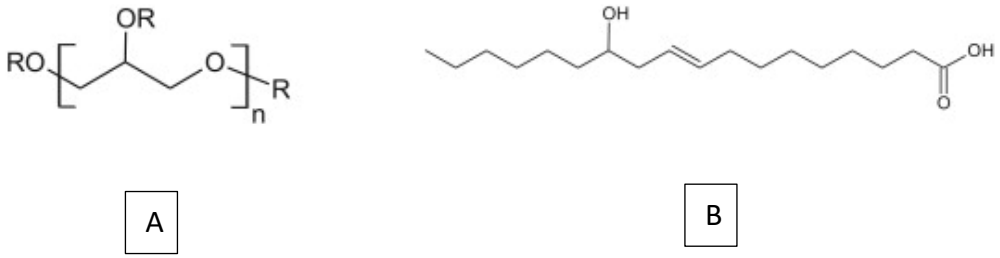


Figure 2.5 Schematic structure of A) a micelle of a hydrophilic emulsifier in water and B) a micelle of a hydrophobic emulsifier in oil

The inner core of the hydrophilic emulsifier micelle is non-polar due to the orientation of the individual surfactant molecules. The inner core can entrap oil-soluble ingredients in the carbon chains or between the oxyethylene chains. However, the inner core of the hydrophobic emulsifier micelle is polar thus can entrap water-soluble ingredients.

2.2.2.1.4 Polyglycerol polyricinoleate

Polyglycerol polyricinoleate (PGPR) is a commonly used hydrophobic surfactant. It is prepared by the esterification of condensed castor oil fatty acids with polyglycerol, where the condensed fatty acids were prepared by heating castor oil fatty acids in the absence of oxygen and have an average of around five fatty acid residues per molecule of the condensed product (Wilson et al. 1998). Figure 2.6 (Ushikubo et al. 2014) shows the structure of PGPR and ricinoleic acid.



A B

Figure 2.6 A) chemical structure of PGPR. R is a hydrogen, ricinoleic acid or polyricinoleic acid. The average value of n is about 3. B) chemical structure of ricinoleic acid. (Ushikubo et al. 2014)

The polyglycerol head region of PGPR has a high affinity for water and the polyricinoleate tail regions have a high affinity for oil (Bastida-Rodriguez 2013). The molecular weight of PGPR is around 3000 g/mol (Ushikubo et al. 2014). PGPR has a CMC value around 1.8 (% w/w) at 20 °C (Bahtz et al. 2016).

As a non-ionic surfactant, PGPR has been reported to be effective in the stabilisation of both single w/o emulsions and the internal water-oil interface of w/o/w emulsions (Fechner et al. 2007, Surh et al. 2007, Mun et al. 2010, Pawlik et al. 2012, Wolf et al. 2013). However, it is more widely used to modify the flow properties of chocolate and to modify fat-crystal properties (Garti et al. 1999, Hasenhuettl et al. 2008). Utilising PGPR, stable w/o emulsions can be formed at high water volume fractions such as 80%, due to the powerful water-binding capacity of the hydrophilic polyglycerol chain (Wilson et al. 1998). It has been reported that the entrapment yield of a polymeric dye mainly depended on the stability of the inner water droplets in a w/o/w emulsion, which was controlled by the PGPR concentration (Azhar et al. 2006). A yield of more than 90% was achieved with 4% PGPR in the oil phase and 0.5% sodium caseinate in the external water phase. The yield almost reached 100% when the PGPR concentration was increased to 8% at the same sodium caseinate concentration in the external water phase. The PGPR concentration could be reduced to 2% by adding 0.5% sodium caseinate in the internal water phase to obtain high yield and stable w/o/w emulsions, which indicated a possible synergistic effect between PGPR and sodium caseinate. Furthermore, it has been widely suggested that the availability of salt at the interface strengthens

the adsorption of PGPR molecules at the oil-water interfaces and improves the emulsion stability (Hino et al. 2000, Fechner et al. 2007, Pawlik et al. 2010, Wolf et al. 2013) through a range of polar head group-ion, polar head group-solvent and ion-solvent interactions (Chattopadhyay et al. 1992, Chattopadhyay et al. 1993). PGPR stabilised w/o emulsions were more stable with smaller droplet diameters and narrower size distribution, compared to those using Span 80, or using the combination of Span 80 and Tween 80, which was proposed to be due to the stable elastic interfaces formed by PGPR which hinder coalescence (Taylor 2011, Matos et al. 2014, Aditya et al. 2015).

2.2.2.1.5 Polyoxyethylene 20 sorbitan monolaurate

With regard to hydrophilic surfactants, the polysorbate family is one of the most hydrophilic or water soluble surfactants due to the polyoxyethylene chain. Among the non-ionic polysorbate group, polyoxyethylene 20 sorbitan monolaurate (Tween 20) with a short chain length of fatty acids has the highest HLB at 16.7. The chemical strcuture of Tween 20 is presented in Figure 2.7 {Obradović, 2017 #564}. The Tween 20 molecule consists of the polyoxyethylene chains linked with a sorbitan ring, which comprises the hydrophilic reigon of the surfactant, and an alkyl side chain that comprises the hydrophobic region (Cottrell et al. 2015). The molecular weight of Tween 20 is about 1228 g/mol and it has a CMC value of around 0.07 (% w/w) at 25 °C (Cottrell et al. 2015). Tween 20 is effective in stabilising o/w emulsions or w/o/w emulsions (Kawashima et al. 1992, Pawlik et al. 2010).

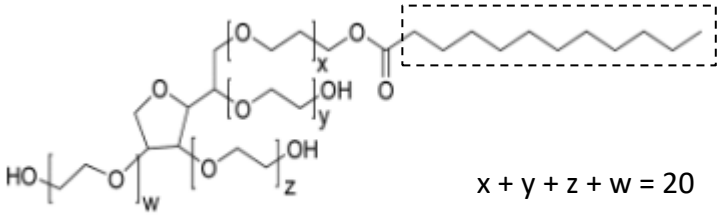


Figure 2.7 Schematic strcuture of Tween 20 {Obradović, 2017 #564}. Dotted box notes the alkyl chain.

2.2.2.2 Starch

Starch is a macromolecule consisting of a large amount of glucose units with α-(1→4) linear links and α-(1→6) branched links. It comprises two types of polymers amylose and amylopectin, shown in Figure 2.8 (Sweedman et al. 2013).

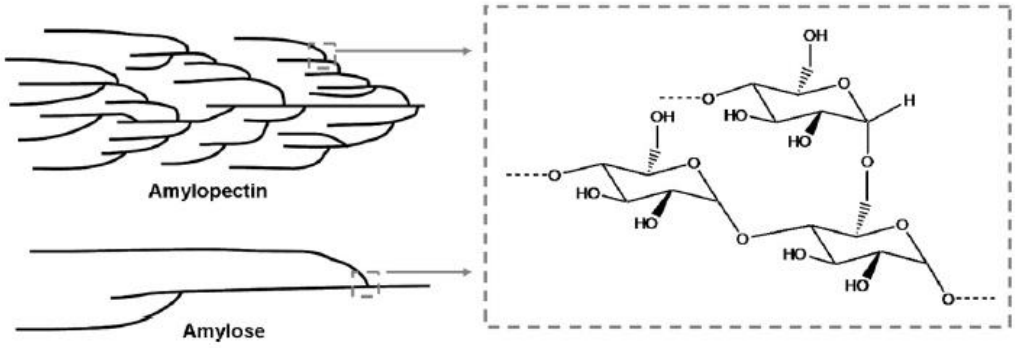


Figure 2.8 Schematic structures of amylose and amylopectin (Sweedman et al. 2013)

Amylose is of a molecular weight in the magnitude of 10^6 g/mol and with a few long-chain branches. Amylopectin is of a molecular weight in the magnitude of 10^8 g/mol and shorter branches (Taggart et al. 2009). Depending on botanical origin an average amylose makes up approximately 20-25% of a starch, whereas amylopectin makes up nearly 75-80%. Starch is contained in large amounts in staple food such as potato, wheat, maize and rice.

Native starch is a hydrophilic molecule that can be used as a texture stabiliser, but it generally has limited solubility in water. Native starch can be modified which involves the alteration of physical characteristics under heat or moisture conditions or the alteration of chemical characteristics by etherification, esterification, cross-linking and grafting (Hermansson et al. 1996). Starch that is used as an emulsifier should have the functionality of substantial surface activity at the oil-water interface for the formation and stabilisation of emulsion droplets (Dickinson 2003). Thus, native starches are chemically modified to be surface active with an amphiphilic character, usually by incorporating chemical groups with hydrophobic character into the hydrophilic polysaccharide backbone (Bhosale et al. 2006). Among all chemical modification, starch modified with octenyl succinic anhydride is permitted in food applications. It was reported that chemically modified starches were more surface active at air-water and toluene-water interfaces than native starch, and ocetnyl succinic anhydride starch lowered surface and interfacial tension at a large extent (Prochaska et al. 2007).

2.2.2.2.1 Octenyl succinic anhydride starch

Octenyl succinic anhydride (OSA) starch has been commonly used to stabilise o/w emulsions or w/o/w emulsions due to its strong surface activity and emulsifying and emulsion stabilising properties (Tesch et al. 2002, Nilsson et al. 2007, Yusoff et al. 2011, Dokić et al. 2012, Hadnađev et al. 2015, Krstonošić et al. 2015, Marefati et al. 2015). OSA starch is hydrophobically modified by the esterification reaction of short octenyl succinic anhydride chains with starch hydroxyl groups, whose structure is shown in Figure 2.9 (Shogren et al. 2000).

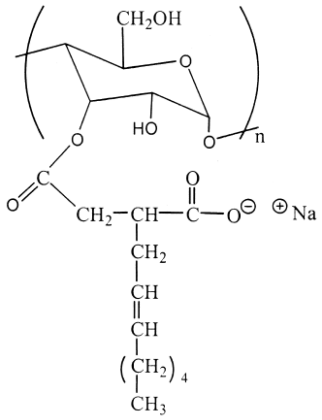


Figure 2.9 Schematic structure of OSA starch (Shogren et al. 2000)

The degree of substitution (DS) is expressed as the average number of moles of substituent groups per anhydroglucose unit (Singh et al. 2007). Each anhydroglucose unit has three hydroxyl groups at C2, C3 and C6 available for OSA substitution, so the maximum DS is 3 (Nilsson et al. 2007). The substitution preferentially occurs on C2 and C3 hydroxyl groups of anhydroglucose units

(Choi et al. 2002, Bai et al. 2011). In OSA starch, the typical DS is in the range of 0.01-0.2, while the range of 0.01-0.03 is allowed for food applications (Nilsson et al. 2007, Singh et al. 2007).

OSA starch can adsorb at the oil-water interface to form a viscous boundary layer where the hydrophobic OSA chains attach to the oil and the hydrophilic starch chains extend into the water, stabilising emulsion droplets through steric stabilisation (Bhosale et al. 2006). OSA starch is soluble in cold water and of low viscosity at high concentrations (Heinze 2000).

2.2.2.3 Protein

Proteins are macromolecules of amino acid chains joined by amide linkages. Some of the amino acid side chains are hydrophilic and some are hydrophobic. When a protein dissolves in water in a native folded configuration, most of the hydrophobic side chains are in the interior of the protein where they are not in contact with water, while the hydrophilic chains are on the exterior surface that are in contact with water as shown in Figure 2.10A (Stauffer 1999). If an oil phase is present, proteins unfold and adsorb at the oil-water interface: the hydrophobic chains originally located in the interior of the protein are exposed to oil, whereas the hydrophilic chains remain in water (Figure 2.10B). For globular proteins, they can adsorb at the interface with some hydrophobic regions facing the oil and the hydrophilic chains facing the water (Figure 2.10C). But once they adsorb at the interface, a globular protein often undergoes

structural rearrangements to maximise the number of contacts between hydrophobic regions and oil (Figure 2.10B).

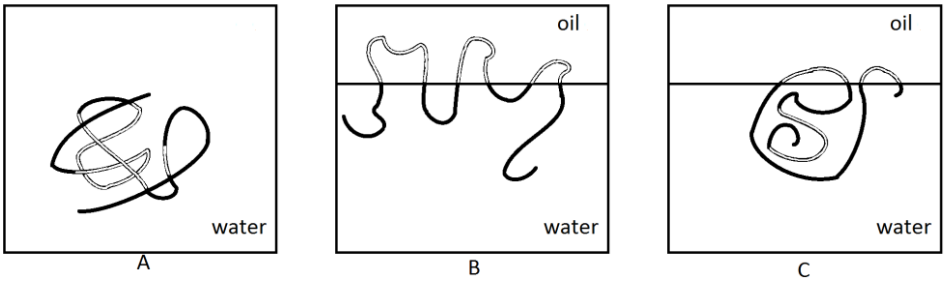


Figure 2.10 Schematic conformation of a protein (Stauffer 1999). A. protein dissolves in water in folded configuration. B. Protein unfolds at the interface. C. Globular protein adsorbs at the oil-water interface before rearrangement. Light section is the hydrophobic part of the chain and black section is the hydrophilic part.

Non-globular proteins are more flexible molecules and therefore rearrange more rapidly, while globular proteins are more rigid molecules and therefore rearrange their structure more slowly. Proteins can locate their loops and tails at the interface to form a thick viscoelastic layer to stabilise emulsions through the steric and electrostatic stabilisation (Garti 1997b, Dickinson 2010).

Proteins have a large molecular size. For example, β-casein has an approximate molecular weight of 24000 g/mol and α_{s1}-casein has a slightly smaller molecular weight (Hasenhuettl et al. 2008). β-casein and α_{s1}-casein are the two major components in casein. Casein is one of the most investigated milk proteins due

to its high surface activity (Dickinson 1997, Hemar et al. 1998). β-lactoglobulin as a milk protein formed in whey on cheese making has a molecular weight around 18400 g/mol (Hamada et al. 1995).

Since the interfacial layers adsorbed by proteins are usually electrically charged, protein-stabilised emulsions are particularly sensitive to environment changes such as temperature, pH, ionic strength and type of ion (McClements 2005). At pH values near the isoelectric point (PI) of the protein or at high ionic strength, the electrostatic repulsion between emulsion droplets may not be sufficiently large to prevent the droplets from aggregation. Globular proteins are sensitive to thermal treatment. They unfold and expose reactive nonpolar and sulfhydryl groups at a high enough temperature (McClements 2005). This increases the attractive interactions between droplets and hence leads to flocculation.

2.2.2.3.1 Pea protein isolate

Plant proteins are alternatives to replace animal proteins because they are cholesterol-free and low-fat food ingredients (Abd El-Hady et al. 2003). Although soybean proteins remain the primary source of plant-derived food proteins, pea protein has also drawn interests as it can be a substitute of soy protein due to its high nutritive value, similar functional properties and non-allergenic characteristic (Kaur et al. 2007, Barac et al. 2010, Adebiyi et al. 2011). Pea protein consists of legumin, vicilin and albumins, where legumin and vicilin are most abundant (O'Kane et al. 2005). Legumin is a very compact globular protein having a total molecular weight around 380000 g/mol. It consists of

acidic polypeptides located outside and basic polypeptides being the hydrophobic core of the protein (Gueguen et al. 1988). Vicilin is a globulin with a molecular weight of approximately 150000 g/mol. Vicilin is more surface-active at air-water and dodecane-water interfaces than legumin in their native forms (Dagorn-Scaviner et al. 1987). Pea proteins were reported to be more surface active at the oil-water interface than soy proteins (Ducel et al. 2004).

Pea proteins are used in the form of protein isolates and concentrates. Pea protein isolate (PPI) is made from pea flour by aqueous extraction and isoelectric precipitation of the protein (Owusu-Ansah et al. 1991). The protein content in pea isolate is more than 80%. PPI had an isoelectric point of around 4.3 at 20 °C, and it had been related to reduce the oil-water interfacial tension faster at pH 7 than at pH 2.4 (Gharsallaoui et al. 2009). At pH 7, PPI lead to a rapid decrease in the oil-water interfacial tension, followed by a slower decrease over time. The rapid decrease was attributed to the surface activity of pea globulins, while the slower decrease corresponded to a slow unfolding and molecular rearrangement such as intermolecular association or aggregation of the individual unfolded protein molecules at the interface. Accordingly, the emulsifying capacity of PPI in o/w emulsions is pH dependent. The highest emulsifying capacity of 70.8% was found at pH 7 and the lowest emulsifying capacity was at pH 4 (Gharsallaoui et al. 2012). High emulsifying capacity of PPI at pH values below 4 and above 5 is a result of the enhancement of intermolecular repulsions of charged amino and carboxyl groups between protein-stabilised oil droplets. At pH 4-5, the lack of electrostatic repulsions among emulsion droplets induces rapid coalescence.

2.3 FOOD FLAVOURS

Food flavour plays an essential role in the quality and acceptability of foods. It refers to aroma and taste. Aromas are volatile compounds and sensed by receptors in the nose. Tastes are non-volatile compounds and sensed by receptors in the tongue and the inside of the mouth (Thomson 1986). The flavour perception of a food constitutes a combination of aroma and taste (Taylor et al. 1996a, Taylor et al. 1996b).

Aroma is a broad sensation including 10000 or more different odours. Aroma compounds usually have a low molecular weight and their volatility depends on the chemical structure. They are present in food at extremely low level, 10-15 mg/kg or µl/l (Almonds et al. 2009). A great variety of aromas exist in foods such as fruits, vegetables and beverages. The complexity of food aromas can vary from as few as 15 compounds in a simple fruit to up to 100 compounds in complex cooked foods (Taylor et al. 2010). Examples of aroma compounds are given in Table 2.3. Taste is a sensation related to sweet, sour, salty, bitter and umami.

Table 2.3 Examples of aroma compounds

Aroma compounds	Odour	Occurrence
Benzaldehyde	Bitter, almond-like	Almonds, cherries, plums
(E, Z)-2, 6-nonadienal	Cucumber-like	Cucumbers
2-furfurylthiol	Roasted	Coffee
(R)-Limonene	Citrus-like	Orange juice

When food is consumed, flavour compounds are released from the food into the mouth. Volatile compounds reach the receptors, the olfactory tissue of the nasal cavity, when they pass back up through the nasopharynx into the nose and via the throat after being released by chewing (Almonds et al. 2009). Non-volatile compounds are perceived by receptor cells located in taste buds in the oral cavity.

2.4 FLAVOUR RELEASE MECHANISMS

Flavour release is the process of flavour compounds moving in the headspace from a food and afterwards to the receptors in the nose and mouth (Harrison 2000).

In this research the *in vitro* release of aroma compounds from w/o/w emulsions has been studied. When a w/o/w emulsion is in a closed environment, the aroma compounds are initially distributed among the oil, water, interfacial and headspace regions. Aroma distribution in each phase of a w/o/w emulsion and release into the gas phase (g) above the emulsion is a complex process with the following six steps: (1) diffusion of aroma molecules inside the internal water phase (w_1); (2) diffusion across the inner water-oil interface; (3) diffusion within the oil phase (o); (4) diffusion across the outer oil-water interface; (5) diffusion inside the external water phase (w_2); (6) diffusion across the air-emulsion interface. The diffusion of aroma molecules into each phase is very rapid,

generally in seconds. Aroma release over a w/o/w emulsion can therefore be perceived prior to placing it in one's mouth by sniffing the headspace.

Aroma release above a multiphase system is not only dependent on the availability of an aroma compound in the gas phase, but also is dependent on the affinity of the food ingredients for the aroma (Taylor et al. 2010). The availability of an aroma in the gas phase are determined by various physicochemical properties of an aroma compound, such as the molecular weight, vapour pressure, boiling point and partition coefficients. For example, the diffusion of an aroma compound in a food system and consequently its release in the gas phase is accelerated with decreasing chain length and decreasing molecular weight of the aroma (Voilley et al. 1996). The affinity of food ingredients for an aroma is caused by aroma-ingredient interactions, which often modify the overall aroma perception by reducing the aroma intensity in the gas phase. The interactions between an aroma compound and food ingredients are determined by both the nature of the aroma and the physicochemical properties of the food ingredients, such as molecular size, functional groups, shape and polarity (Landy et al. 1996, Druaux et al. 1997, van Ruth et al. 2000, Guichard 2002, Pays et al. 2002, McClements 2005). The factors that influence the release behaviour of an aroma compound are introduced in the following.

2.4.1 Partition coefficient and diffusion coefficient

This section introduces the basic physical processes that drive aroma release, including the partitioning as explained by Henry's law, the hydrophobicity as explained by the octanol-water partition coefficient (log P) and the mass transfer through diffusion as explained by Fick's law. The partition coefficients can be used to estimate the partitioning within a multiphase system and to understand loss rates during evaporative processes when these partition coefficients are applicable.

2.4.1.1 Henry's law

Aroma release only takes place when the equilibrium between the gas phase and the food system is disturbed. In other words, non-equilibrium is the driving force for the diffusion of flavour compounds. The static partition of flavour molecules between air and water, or the food product, at the thermodynamic equilibrium or the volatility of an aroma compound can be determined by the air-water or air-liquid partition coefficient (K_{aw}) in Henry's law (Nawar 1971):

$$K_{aw} = \frac{C_a}{C_w} \qquad \text{Equation 2.5}$$

and

$$H = \frac{p}{C_w} \qquad \text{Equation 2.6}$$

where C_a is the aroma concentration in air (molar fraction), C_w is the aroma concentration in water (molar fraction), H is the Henry's law constant and p is

the aroma partial pressure in air, all at equilibrium. The air-water partition coefficient is temperature affected as the log-transformed air-water partition coefficient is linearly related to the temperature (Kolb et al. 1992).

Henry's law is limited to a range of conditions (Taylor 1998, Fisk 2014). It is ideally considered that the aroma concentration is infinitely diluted. Many aroma compounds are non-ideal and do not follow Henry's law. Examples include compounds that dissociate such as organic acids, that associate such as in the formation of micelles, that chemically interact with a solvent such as vanillin in propylene glycol, or that are inherently chemically unstable over time such as intermediary by-products of lipid oxidation. Table 2.4 lists some examples of K_{aw} values at 20 °C. Estimation of K_{aw} can be derived from fundamental values such as the vapour pressure of an aroma compound, the molar volumes of the gas and liquid phases and the activity coefficient of the compound (Voilley et al. 1977).

Table 2.4 Examples of K_{aw} values of aroma compounds estimated from EPI SUITE (EPA's and Syracuse Research Corp., USA) at 20 °C

Aroma compounds	K_{aw}
Propan-2-ol	3.31×10^{-4}
Vanillin	8.79×10^{-8}
benzaldehyde	1.09×10^{-3}
Nonanone	1.5×10^{-2}
Limonene	1.3

2.4.1.2 Octanol-water partition coefficient

The octanol-water partition coefficient, or log P value, describes the hydrophobicity of an aroma compound (Poole et al. 2003). Log P is defined in Equation 2.7. It is proportional to the aroma concentration in octanol C_{oct} and its concentration in water C_w at equilibrium:

$$\text{Log P} = \log\left(\frac{C_{oct}}{C_w}\right) \qquad \text{Equation 2.7}$$

It should be noted that as the scale is logarithmic, small changes in log P lead to major differences in availability in the water phase. Aroma compounds vary in their log P values, which is typically positive for hydrophobic aromas and negative for hydrophilic ones. Table 2.5 lists some examples. Natural organic acids such as citric acid generally have low log P values (< -1) due to their low solubility in lipid, while much more lipid soluble compounds such as limonene and farnesol have large log P values (> 3).

Table 2.5 Examples of log P values of aroma compounds estimated from EPI SUITE (EPA's and Syracuse Research Corp., USA)

Aroma compounds	Log P
Ascorbic acid	-1.88
Citric acid	-1.67
Propan-2-ol	0.28
Vanillin	1.05
benzaldehyde	1.71
Nonanone	2.71
Limonene	4.83
Farnesol	5.77

2.4.1.3 Fick's Law

Under non-equilibrium conditions, the difference in aroma concentration between the liquid phase and the vapour phase is the driving force leading to the diffusion of the aroma compounds, with a flow of material from regions of high concentration to regions of low concentration. According to Fick's first law of diffusion, mass transfer through diffusion is explained in Equation 2.8 (Atkins et al. 2014):

$$\frac{d_m}{d_t} = -A'D\frac{d_C}{d_{x'}} \qquad \text{Equation 2.8}$$

where the mass transfer rate, mass (m) per unit time (t), is proportional to the concentration (C) gradient over a set distance (x') per unit cross-sectional area (A') and the diffusion coefficient (D). Diffusivity ranges, as described by the diffusion coefficient, depend on the food system, with rubbery systems having diffusion coefficients in the order of 10^{-14} to 10^{-13} m^2/s, oils of 10^{-11} m^2/s, water of 10^{-9} m^2/s and gases of 10^{-5} m^2/s (Fisk 2014).

2.4.2 Interactions between aroma compounds and food ingredients

Aroma availability in the gas phase over liquid systems can also be related to the interactions between the aroma compounds and the ingredients in a food system (Versic 1988). Thus, the formulation of a food system influences the extent and type of aroma interactions. Major food ingredients with respect to interactions are lipids, surfactants, carbohydrates and proteins.

2.4.2.1 Aroma-lipid interactions

As most aroma compounds are hydrophobic, oils and fats probably have the strongest impact on aroma release among all food ingredients (Doyen et al. 2001). The affinity of aromas for oils can be affected by the oil properties such as the oil polarity determined by the chain length. Hydrophobic aromas have higher affinity for oils with longer chain fatty acids (Harvey et al. 1995). Hydrophobic aromas can bind to lipids by weak and reversible van der Waals forces and unspecific hydrophobic interactions (Plug et al. 1993). Lipids act as solvents for hydrophobic aroma compounds. The distribution of aroma molecules in water and in oil can be determined by the octanol-water partition coefficient (section 2.4.1.2).

Given the only effect on the aroma release over an emulsion system is the interaction with the lipid phase, Equation 2.9 can be used to describe the air-emulsion partition coefficient (K_{ae}) (Buttery et al. 1973):

$$K_{ae} = 1 / (\phi_o / K_{ao} + \phi_w / K_{aw}) \qquad \text{Equation 2.9}$$

ϕ_o, K_{ao}, ϕ_w and K_{aw} are the oil volume fraction, the air-oil partition coefficient, the water volume fraction and the air-water partition coefficient, respectively. The equation originates from oil and water layers without any added emulsifiers. Thus, this equation does not take account of any potential interactions with emulsifiers, or their presence as a bulk ingredient in the food system. The equation has been used to predict the aroma distribution in o/w emulsions with the knowledge of K_{ao} and K_{aw} (Guyot et al. 1996). The difference in the K_{ae} between the theoretical value and the experimental value can be

used as the evidence of interactions between the aromas and food ingredients except for lipids (Meynier et al. 2005, Karaiskou et al. 2008).

2.4.2.2 Aroma-surfactant interactions

Some small low molecular weight surfactants such as Tweens may associate with the aroma compounds. The diffusion of water or water-soluble molecules through the oil-water interface of w/o/w emulsions may be either through thin lamellae of surfactants partially formed in the oil layer due to fluctuation of its thickness, or through the incorporation in micelles or reverse micelles (Cheng et al. 2007). Those micelles formed by hydrophilic surfactants such as Tween 20 in the aqueous phase have the capability of solubilizing hydrophobic aromas inside their oil-soluble interior. This increases the retention of hydrophobic compounds in the aqueous phase so that decreases the gas-liquid partition coefficient (K_{gl}). By using dynamic headspace analysis, it was found that the reduction in release of hydrophobic aroma compounds from o/w emulsions was due to the presence of Tween20 micelles with hydrophobic structures inside (Benjamin et al. 2014). A reduction in the gas-liquid partition coefficient under static headspace analysis was resulted from the Tween 20 micelles entrapping the hydrophobic aromas inside (van Ruth et al. 2002b). This study also reported that when Tween 20 was added to oil, Tween 20 formed reverse micelles in oil, which entrapped the hydrophilic aromas leading to a reduction in the gas-liquid partition coefficient. In a similar way, hydrophilic aromas can

solubilise inside micelles formed from hydrophobic surfactants such as PGPR in the lipid phase.

The partition coefficient of an aroma compound between the gas phase and a liquid with the addition of surfactant (K_{gl}) is described by Equation 2.10 (McClements 2005):

$$K_{gl} = \frac{K_{gc}}{[1 + \phi_m(K_{mc}-1)]} \qquad \text{Equation 2.10}$$

where K_{gc} is the gas-continuous phase partition coefficient of the aroma compound, ϕ_m is the volume fraction of the micelles in the continuous phase and K_{mc} is the micelle-continuous phase partition coefficient. It indicates that the higher the affinity of the aroma compound for the surfactant micelles ($K_{mc} >> 1$), the smaller the gas-liquid partition coefficient and the less aroma molecules release into the gas phase from the liquid.

2.4.2.3 Aroma-starch interactions

The interactions between starch and aroma compounds have been widely studied as starch is one of the most widely used food ingredients. Aroma-starch interactions can be divided into two types, hydrophobic interaction and hydrogen binding (Madene et al. 2006). Native starch, physically modified starch and chemically modified starch have been reported to have the same two types of interactions with aromas (Light 1990).

2.4.2.3.1 Hydrophobic interaction

The hydrophobic interaction is related to an inclusion complex with amylose forming a helix around the hydrophobic chain of aroma molecules, while amylopectin binds with water (Naknean et al. 2010). It is a non-covalent reversible binding and a starch with a high amylose content leads to greater binding of aroma compounds. The helical conformation of the complexes depends on the ligand type of the aroma molecules (Escher et al. 2000). The binding affinity of an aroma ligand for the linear starch fraction has been reported to increase with increasing chain length of amylose (Wulff et al. 2005). For chemically modified starch, the inclusion complexation ability decreases with increasing degree of substitution (Wulff et al. 1998).

2.4.2.3.2 Hydrogen binding

The hydrogen binding is formed between the hydrophilic part of the aroma compounds and hydroxyl groups of starch (Arvisenet et al. 2002). By using inverse gas chromatography to measure the retention of aroma compounds in a matrix, interactions between starches, including high amylose corn starch, wheat starch and β-cyclodextrin matrixes, and aroma compounds were reported to result from hydrogen binding (Delarue et al. 2000). Using the same method, aroma retention due to interactions with native starches, predominately through hydrogen bonding, was reported to increase in the following sequence: ester < ketone < aldehyde < alcohol (Boutboul et al. 2002b). A higher retention of 3, 7-dimethyl-2, 6-octadien-1-al was found after the

starch was physically modified under a specific thermal treatment compared to that with native starch. Another study about the impact of the nature and the treatment of starch on aroma retention using the same technology was also reported (Boutboul et al. 2002a). It was found that maltodextrin obtained from a physical and enzymatic treatment had the highest aroma retention, followed by pregelatinised starches produced by a physical treatment and an extruded high-amylose starch. Granular starches including native starches and acetylated starches obtained from a mild chemical treatment had the lowest aroma retention, which may be due to hydrogen bonding with aroma compounds. Aroma retention increased with the aroma polarity in the sequence: d-limonene < ethyl hexanoate < octanal < 1-hexanol.

2.4.2.4 Aroma-protein interactions

Aroma compounds can interact with proteins in two ways, reversible physical binding including hydrogen bonds, hydrophobic interactions and ionic bonds, and irreversible chemical binding via covalent linkages.

2.4.2.4.1 Hydrophobic and hydrogen binding

In most cases, aroma-protein interactions are reversible, usually hydrophobic interaction and hydrogen binding (Damodaran et al. 1980a). The reversible binding of an aroma compound obeys the Scatchard equation below:

$$V_{bound} / V_f = K (n_p - V_{bound}) \text{ at equilibrium} \qquad \text{Equation 2.11}$$

where V_{bound} is number of moles of the aroma compound bound per mole of protein, V_f is the molar concentration of the free volatile compound, K is the association constant and n is the total number of binding sites per mole of protein (Taylor et al. 2010). As binding proceeds, the protein can undergo conformational changes and more binding sites can become available. The binding affinity for aroma compounds is influenced by the chain length, the functional group and the structural state of the protein (Damodaran et al. 1981). Aromas only bind to proteins when the binding sites are not engaged in protein-protein or other interactions. Most of the proteins in various applications including gelation, thickening, emulsification and foaming adopt a globular structure that results from equilibrium between the physiochemical factors such as hydrophobic interactions, electrostatic interactions, hydrogen bonding, van der Waals forces and configurational entropy (McClements 2002). The functional properties of globular proteins are determined by the molecular structure and dynamics of the proteins under the environmental conditions. Factors such as pH, salts, temperature and high pressure, that influence protein conformation, can significantly change the aroma binding characteristics of proteins. The unfolding of proteins can increase the aroma binding by increasing the number of hydrophobic binding sites (O'Neill et al. 1988, Jouenne et al. 2000), or it can decrease the binding by modifying specific binding sites for aroma compounds (Suppavorasatit et al. 2012). Protein loops in water especially prefer interacting with aroma compounds (Figure 2.10A). Nonpolar aroma molecules can diffuse into the hydrophobic core of the protein and replace the intra- or intermolecular protein-protein hydrophobic

interactions. The amount of aroma adsorbed to proteins increases with the hydrophobicity of the proteins.

Most studies have been reported for the reversible binding of flavour molecules to β-lactoglobulin, casein, bovine serum albumin and soy proteins (O'Neill et al. 1987, Sostmann et al. 1998, Suryaprakash et al. 2000, Tavel et al. 2010, Bandyopadhyay et al. 2012). It has been reported that tested by headspace analysis, β-lactoglobulin at the oil-water interface in o/w emulsions limits release of hydrophobic aroma compounds from oil to water through hydrophobic interactions and thus induces a lower aroma perception, even if the addition of fat induced a greater change in aroma release than the addition of protein in water solution (Guichard et al. 2000). Using high performance liquid chromatography (HPLC), it was found that vanillin bound to bovine serum albumin mainly through hydrophobic interactions and bound to sodium caseinate mainly via hydrogen bonding (Chobpattana et al. 2002). Tested by an equilibrium dialysis method, vanillin was found to not bind to the denatured form of bovine serum albumin, while 2-octanone was bound both by the native form and the denatured form of bovine serum albumin (Burova et al. 2003). Soy glycinin and β-conglysinin have large similarities in primary structure to pea legumin and vicilin. Therefore, information on soy protein-aroma binding can be relevant for the consideration of pea protein-aroma interaction. Also using equilibrium dialysis, it has been reported that soy β-conglysinin binds to 2-nonanone through the hydrophobic interaction, while soy glycinin has no affinity for 2-nonanone (Damodaran et al. 1981). Measured by the combination of ultrafiltration and gas-liquid chromatography (GC), hexyl acetate was found

to have a binding affinity with native soy protein through hydrophobic interactions and the denaturation of the native protein by heat or acid leads to a loss for hexyl acetate bound to the protein (Semenova et al. 2002c). A few studies have been undertaken on the pea protein-flavour interaction, which also used the GC approach (Wang et al. 2014, Wang et al. 2015). Arginyl residues of pea protein was found to bind to diacetyl through weak and reversible interaction under GC analysis (Dumont et al. 1986). Vicilin, one of the major proteins in pea protein, was found to bind both aldehydes and ketones at pH 7.6 and pH 3.8 determined by GC (Heng et al. 2004). The other major protein in pea protein, legumin, only showed binding to aldehydes at pH 7.6.

2.4.2.4.2 Covalent binding

Certain aroma compounds, such as aldehydes, can form irreversible and covalent bonds with proteins (Meynier et al. 2003, Meynier et al. 2004). These include the formation of salts, amides and esters, the condensation of aldehydes with amino groups (NH_2) and sulfhydryl groups (SH). The condensation reaction is named as the Schiff base reaction, where a C=N bond in the free amino acids or the free amino groups of proteins, known as a Schiff base, is replaced by a C=O bond in the carbonyl groups of aroma compounds (Voilley et al. 1996). In the case of formaldehyde-protein interaction, formaldehyde reacts not only with the amino groups in proteins but also with the sulfhydryl groups. It has been reported that disulfides including diethyl,

dipropyl, dibutyl, diallyl and 2-furfuryl methyl bind irreversibly and covalently to ovalbumin when the pH of the aqueous solution increases to 8.0 or when the protein is denatured by heating, due to more free sulfhydryl groups available in the denatured protein (Adams et al. 2001). More disulfides were lost when the aroma compounds were added in the solution before heating than when the aromas were added after heating, which could result from greater reaction rate at the higher temperature and also the maximised availability of the sulfhydryl groups as the protein unfolded during the denaturation. The bound amount of 2-nonanone with bovine serum albumin increased with the concentration of sodium sulphate, sodium chloride, sodium bromide and sodium perchlorate (Damodaran et al. 1980a, Damodaran et al. 1980b). The anions modified the conformation of the protein and this modification was attributed to the ability of anions to bind the dipolar groups of the macromolecules. Using headspace solid-phase microextraction (SPME) and GC, it was found that upon heat or high pressure denaturation, the covalent interactions between trans-2-nonenal and whey protein isolate (WPI) were enhanced, while the hydrophobic interactions between 2-nonanone and WPI were weakened (Kuhn et al. 2008). The irreversibly bound amount of acetone and ethanol increased with the polarity of the proteins (Kim et al. 1988).

2.5 CONCLUSIONS

The literature review demonstrates the background of w/o/w emulsions including the emulsifiers used in this PhD research to stabilise w/o/w emulsions, and the factors that affect aroma release over w/o/w emulsions in relation to this research. Apart from the nature of aroma compounds, the ingredients in w/o/w emulsions, particularly the hydrophilic emulsifiers, can also have an influence on aroma release behaviour. Nonetheless, there are few studies reporting on the effect of the hydrophilic emulsifier type on aroma release behaviour over w/o/w emulsions. Thus, this research investigates the possible interaction between aroma compounds and different hydrophilic emulsifiers, and the impact of the emulsion microstructure formed with these emulsifiers on aroma release.

3 MATERIALS AND METHODS

In the present Chapter 3 the materials and methods used throughout this PhD research are introduced. Explicitly, this includes materials used to formulate water-in-oil-in-water (w/o/w) or oil-in-water (o/w) emulsions and their preparation based on the conventional method of high-shear mixing. Emulsions were formulated with the hydrophobic emulsifier polyglycerol polyricinoleate (PGPR) and a range of hydrophilic emulsifiers. Emulsions contained salt, which refers to sodium chloride unless other salt is mentioned. Salt was added to the internal water phase of the w/o/w emulsions to enhance the adsorption of PGPR at the oil-water interface (Hino et al. 2000, Pawlik et al. 2010, Wolf et al. 2013). The same molar concentration of salt was used in the external water phase of the w/o/w emulsions studied in Chapters 5-7 to induce osmotic pressure balance between two aqueous phases (Pawlik et al. 2010). Pea protein isolate (PPI) was chosen as the hydrophilic emulsifier to stabilise the w/o droplets in the w/o/w emulsions in the separate Chapter 4. Then three different hydrophilic emulsifiers were studied in Chapters 5-7, polyoxyethylene 20 sorbitan monolaurate (Tween 20), octenyl succinic anhydride (OSA) starch and PPI, representing a non-ionic low-molecular-weight surfactant, a modified starch and a protein respectively. Further detailed information on emulsion composition such as concentration of emulsifier, added salt and oil/water phase volume is provided in all of the main thesis Chapters (Chapter 4-7) reporting on the specific formulated emulsions. Further, Chapter 6 is dedicated to the preparation and characterisation of w/o/w emulsions with well defined

mean droplet size and droplet size spectrum through stirred cell membrane emulsification. Chapter 7 demonstrates applying these emulsions to aroma release analysis. Magnesium chloride hexahydrate ($MgCl_2 \cdot 6H_2O$) was chosen as a marker to be encapsulated in the internal water phase of the w/o/w emulsions manufactured by membrane emulsification for the measurement of water movement from the internal water phase to the external water phase, and magnesium is also one of the essential food micronutrients. As a thickening agent in the external water phase of w/o/w emulsions or the water phase of o/w emulsions produced by membrane emulsification, xanthan gum was used in order to prevent emulsion creaming otherwise affecting aroma release analysis. As controls, o/w emulsions with similarly sized mean droplet size and droplet size spectrum compared to w/o/w emulsions were also prepared by membrane emulsification. These corresponding methods are included in Chapter 7 together with the aroma release results. In terms of aroma release analysis, the description of the experimental set-up and protocol is part of this Chapter 3. The method of aroma addition to the different emulsions studied in this PhD research is explained in the relevant main Chapters. Initially three aroma compounds, acetoin, acetyl pyridine and hexanal, were studied in Chapter 4 as they cover a range of hydrophobicity with logP at -0.36, 0.49 and 1.97 respectively. Then two aroma compounds, diacetyl and 3-pentanone, were mainly investigated in Chapter 5 and 7, since they have different hydrophobicity, hydrophilic (diacetyl) and hydrophobic (3-pentanone), but the same molecular weight to eliminate the impact of molecular mass on aroma release behaviour. The physicochemical properties of the aroma compounds

including the logP, molecular weight (Mwt) and the air-water partition coefficient (K_{aw}) used for the aroma concentration calibration in Chapter 4, 5 and 7 were calculated at the temperature of 20 °C by Estimation Program Interface (EPI) Suite software (EPA's and Syracuse Research Corp., USA). They are reported in Table 3.1. 0.02% sodium azide was added to the water phase of emulsions in Chapter 4-7 to suppress microbial spoilage.

Table 3.1 Physicochemical properties of aroma compounds from EPI Suite at 20 °C

Aroma compound	CAS number	LogP	Mwt (g/mol)	K_{aw}	Density (g/cm^3)	Solubility (µg/l)
Diacetyl	431-03-08	-1.34	86.09	$5.44x10^{-4}$	0.990	10^9
Acetoin	513-86-0	-0.36	88.11	$4.21x10^{-4}$	1.012	$8.33x10^8$
Acetyl pyridine	1122-62-9	0.49	121.14	$5.23x10^{-7}$	1.08	$1.87x10^7$
3-pentanone	96-22-0	0.75	86.13	$3.63x10^{-3}$	0.815	$1.81x10^7$
Hexanal	66-25-1	1.97	100.16	$8.71x10^{-3}$	0.815	$3.53x10^6$

3.1 MATERIALS

Sodium chloride (NaCI) was purchased from Fisher Scientific (Loughborough, UK). Polyglycerol polyricinoleate (GRINDSTED PGPR 90) was kindly provided by DuPont Danisco (Kettering, UK). Polyethylene 20 sorbitan monolaurate (Tween 20), magnesium chloride hexahydrate ($MgCl_2 \cdot 6H_2O$) and sodium azide (NaN_3) were bought from Sigma Aldrich (Dorset, UK). Octenyl succinic anhydride (OSA) – waxy maize starch, N-creamer 46 (NC46), was supplied by Univar (Widnes, UK). Powdered pea protein isolate (PPI) was obtained from MyProtein (Northwich, UK). Xanthan gum (Keltro RD) was provided by CP KELCO (San Diago, USA). The aroma compounds, acetoin, acetyl pyridine, hexanal, diacetyl and 3-pentanone, were purchased from Sigma Aldrich (Dorset, UK). Sunflower oil was purchased from a local supermarket. Water used in all experiments was deionized water, produced on site. All materials were used as received from the supplier. All concentrations are provided on a weight by weight basis, unless stated otherwise.

3.2 METHODS

3.2.1 Preparation of w/o/w emulsions through high-shear mixing

A two-step emulsification method was used to produce the w/o/w emulsions. This type of preparing a w/o/w emulsion involves initially the processing of the internal w/o emulsion, which is then processed into the external water phase. To distinguish the two water phases, they were indexed with w_1 and w_2

referring to the internal water and external water phase respectively. Thus, in the following the complex emulsions are referred to as $w_1/o/w_2$ emulsions. Both processing steps were accomplished with a batch high-shear overhead mixer (Silverson L5M, Chesham, UK) fitted with an emulsor screen (Silverson, Chesham, UK) as described in the following. As mentioned in the preamble of this chapter, the exact composition of each emulsion analysed for aroma release is provided in the respective main thesis Chapter.

Initially the internal w_1/o emulsion was prepared. The oil phase (o) of this emulsion contained PGPR and was prepared by adding PGPR to the oil at the desired concentration followed by mixing on a magnetic stirrer at room temperature for at least 30 min. The internal water phase (w_1) contained NaCl and was prepared by mixing on a magnetic stirrer at room temperature for 5 min. w_1 was then slowly added into o under high-shear mixing at 7000 rpm for 4 min with the processing beaker immersed in an iced water bath (4-6 °C) to avoid overheating. This emulsion was prepared in 100 g batches at a ratio of w_1:o of 2:3 (w/w).

Then the w/o/w emulsion was prepared. The external water phase w_2 contained either Tween 20, OSA starch or PPI as the hydrophilic emulsifier at the desired concentration as specified in sections 4.2.1, 5.2.1, 6.2.4.2 and 7.2.1. The primary w_1/o emulsion was added to the previously prepared w_2 during high-shear mixing at 6700 rpm for 4 min with the processing beaker immersed in an iced water bath (4-6 °C). The mixing ratio of $(w_1/o):w_2$ was 3:7 (w/w) and batches of 100 g were processed. Aroma addition was shown in section 3.2.3.

3.2.2 Preparation of control o/w emulsions through high-shear mixing

In Chapter 5, o/w emulsions manufactured by high-shear mixing were prepared as the controls for w/o/w emulsions. The water phase contained Tween 20, OSA starch or PPI as the hydrophilic emulsifier at the same concentration as the w/o/w emulsions. The dispersed oil phase was added on the top of the continuous water phase and mixed using the same high-shear overhead mixer at 6700 rpm for 4 min with the processing beaker immersed in an iced water bath (4-6 °C). The mixing ratio of oil to water was 3:7 (w/w) and batches of 100 g were processed. Further details are reported in section 5.2.1.

3.2.3 Aroma addition

This PhD research was concerned with the aroma release above complex emulsions. The aroma compounds were added to the emulsions prior to or post processing at selected concentration and utilising methods outlined in the relevant main thesis Chapters. Here the stock solutions with varying aroma concentrations were prepared by dissolving varying amounts of aroma compounds in water. The stock solutions were either added to the internal water phase w_1 of the w/o/w emulsions before processing, or added to the external water w_2 phase of w/o/w emulsions before or after processing. The specific compositions and addition methods are described in detail in sections 4.2.1, 5.2.1 and 7.2.2.

3.2.4 Analysis of emulsions

Emulsions produced in this PhD research were generally analysed for droplet size. However, any w/o/w emulsion was first inspected on a microscope to confirm that their microstructure was that of a w/o/w emulsion. This method and the methods of image analysis and laser diffraction applied for droplet size analysis are described in the following. Also included in this chapter is the description of the quantification of aroma release above the emulsions. The design of the membrane emulsification protocol as outlined in Chapter 6 as well as the accomplishment of the aroma release studies in Chapter 7 required the quantification of a broader set of emulsion properties. These additional methods are introduced in Chapters 6 and 7.

Generally, emulsions were analysed immediately after manufacturing and then in regular intervals during storage at room temperature (21 ± 5 °C).

3.2.4.1 Microscopy

The microstructure of the w/o/w emulsions was visualised using an epifluorescence and transmitted light microscope (EVOS FL, Life Technologies, USA). Slides were prepared by placing a small drop of emulsion after dilution with water onto the slide and carefully sliding a cover slip over the sample. A bright field objective was selected using a magnification range of between x20 and x80. At least three randomly selected areas of each slide were imaged at each magnification and three slides were prepared for each emulsion.

3.2.4.2 Droplet size measurement

The droplet size distribution of the secondary emulsion droplets (the emulsified w_1/o emulsion) of the $w_1/o/w_2$ emulsions was analysed immediately after preparation and during storage using a laser diffraction particle size analyser (Beckman-Coulter LS 13 320, Meritics Ltd, Dunstable, UK) fitted with a universal liquid module using water as the dispersing medium. Measurement set up and analysis was controlled by the instrument's software package. Once the emulsion was dispersed in the water, three measurements were taken and the raw data averaged before analysis based on the input of the refractive indices of the dispersion medium (water) and the dispersed phase (oil). The values were 1.33 and 1.47 respectively. The imaginary part of the dispersed phase refractive index was set to 0. Each emulsion was analysed in triplicate. The results are reported as the mean droplet size on volume basis ($d_{4,3}$), the mean droplet size on surface area basis ($d_{3,2}$) also known as Sauter diameter, span and the specific surface area (SSA), averaged over the three replicate sample data and including their standard deviation. Droplet size distributions are presented as a percentage based volume density distribution.

3.2.5 Aroma release measurement

In this PhD research static and dynamic aroma release over the w/o/w emulsions was analysed through sampling the headspace intensity from an

emulsion sample directly into atmospheric pressure chemical ionisation - mass spectrometry (APCI-MS) equipment.

In static headspace analysis, aroma release measurement was carried out at different time slots once after the aroma compounds were added to the emulsions. The time when the aroma headspace intensity remained consistent between two continuous time slots was recorded as the equilibrium time. It provides information about how long it takes for aroma to reach equilibrium in the headspace in a sealed environment and also indicates the equilibrium in each phase of the w/o/w emulsion. Static headspace analysis is mainly determined by air-emulsion partitioning.

In dynamic headspace analysis, aroma compounds were allowed a certain time, which was the equilibrium time suggested by the former static headspace analysis, to equilibrate in emulsions in a sealed glass vial before analysis. Then the headspace atmosphere was constantly purged out of the vial containing the emulsion and trapped for sampling to the APCI-MS. This dynamic condition with headspace dilution and re-equilibration is an indication of the experience when consuming food and beverages. The dynamic headspace analysis is mainly determined by the interface between air and the emulsion. The idea was applied to gain insights into the factors that affect the dynamics of aroma release from the internal emulsion phases of oil and w_1 over time. The methods are described in detail in the following.

3.2.5.1 Static headspace analysis

As aforementioned, atmospheric pressure chemical ionisation - mass spectrometer (APCI-MS) (Ultima Micromass, Manchester, UK) was used to measure the aroma release into the static headspace above emulsions and control samples. The control samples were water and single o/w emulsions spiked with the same aroma as the w/o/w emulsion to be analysed. Their preparation is described in detail in sections 3.2.2, 4.2.1, 5.2.1 and 7.2.1. In either case, 50 ml of liquid sample were measured into a suitably sized glass bottle with a plastic lid containing a hole (approx. 3 mm diameter), which allowed for the fibre connected to the APCI-MS to pass through (Figure 3.1). This allowed obtaining a headspace volume of 84 ml for enough aroma amount in the headspace available for APCI-MS measurement. The headspace sampling rate into the APCI-MS was set at 5 ml/min and measured using an electronic flow meter (very-flow 500, Agilent Technologies, Berkshire, UK). The transfer line to the mass spectrometer was heated (140 °C) and the source was operated in positive ionisation mode (4Kv corona discharge). The compounds were maintained in selected ion mode (Table 3.2) with a dwell time of 0.1 s. The duration of analysis for each sample was seconds. The signal intensity was measured as relative peak height using the MassLynx 4.1 operation software (Micromass, Manchester, UK). The average headspace intensity including the standard deviation is reported over three replicate sample peak heights.

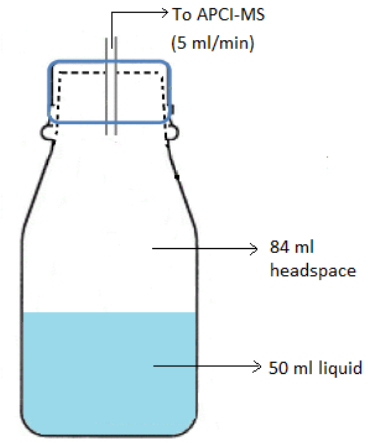


Figure 3.1 Schematic of set-up for the static headspace analysis using the APCI-MS

Table 3.2 List of ion mode of different aroma compounds used for the APCI-MS setting

Aroma compounds	Ion mode (= molecular weight + 1) (m/z)
Acetoin	89
Acetyl pyridine	122
Hexanal	101
Diacetyl	87
3-pentanone	87

Standard solutions of acetoin, acetyl pyridine and hexanal dissolved in water were prepared ranging in concentration from 3 mg/l to 935 mg/l in order to check the APCI-MS sensitivity and reproducibility by plotting standard curves calibrated with headspace intensity. The aroma standard solutions were freshly prepared in triplicate and allowed to equilibrate (20 min) before the static

headspace analysis through the APCI-MS. Aqueous calibration curves were generated, see Figure 3.2, where aroma headspace intensity is proportional to aroma concentration in liquid. The APCI-MS response was repeatable.

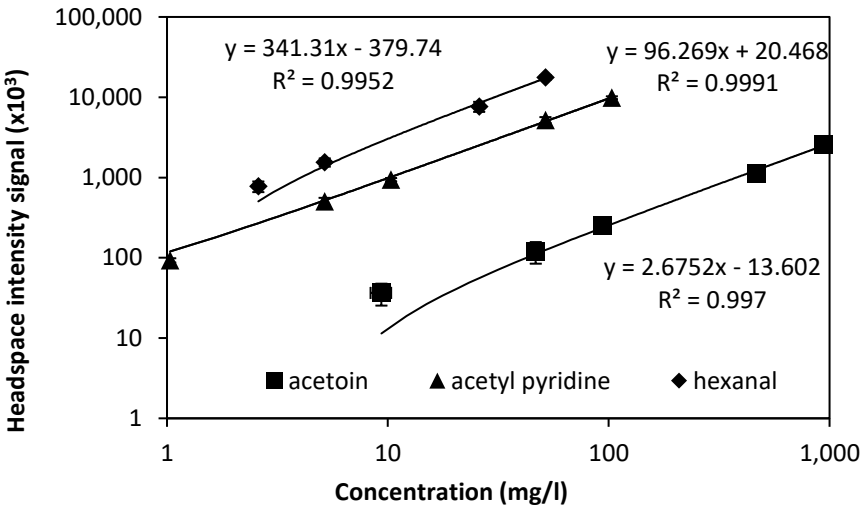


Figure 3.2 Calibration curves of acetoin, acetyl pyridine and hexanal

Diacetyl or 3-pentanone in water at 20 µl/l was freshly prepared and static headspace intensity was measured continuously to test the consistency of APCI-MS perception. Figure 3.3 shows diacetyl and 3-pentanone release maintained consistent in the static headspace above water over time.

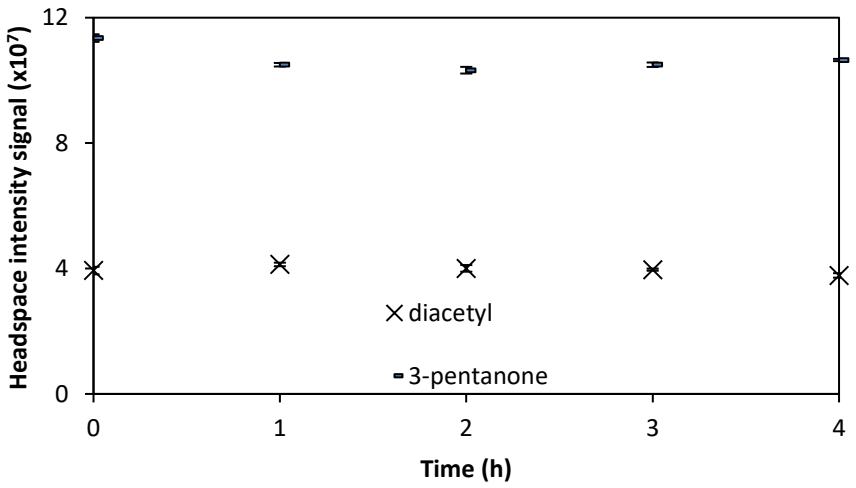


Figure 3.3 Static headspace intensity of diacetyl and 3-pentanone above water over time

3.2.5.2 Dynamic headspace analysis

The dynamic headspace of the samples was analysed using the same atmospheric pressure chemical ionisation - mass spectrometer (APCI-MS) and sampling rate was measured with the same gas flow meter as for the static headspace analysis (see section 3.2.5.1). A larger sample volume of 100 ml was measured into a glass bottle of the same size as used for static headspace analysis and a headspace volume of 34 ml was obtained (Figure 3.4), because a strong and persistent headspace signal should be observed during headspace dilution.

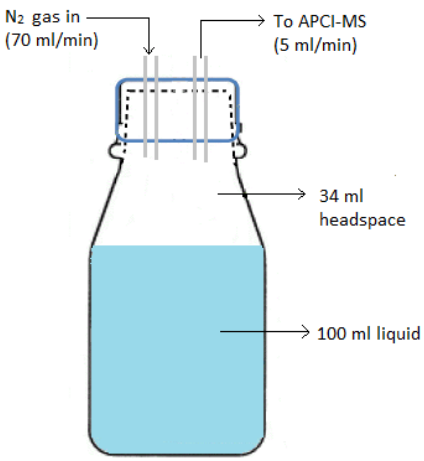


Figure 3.4 Schematic set-up for the dynamic headspace analysis using the APCI-MS

To purge the headspace, nitrogen gas (N_2) was introduced into the bottle at a flow rate of 70 ml/min, retracted from the bottle and passed into the APCI-MS at the lower flow rate of 5 ml/min, so there was a quick dilution of the headspace above the emulsions and a slow flow into the APCI-MS for continuous measurement. As in the case of the static headspace analysis, the transfer line of the mass spectrometer was heated (140 °C) and the source was operated in positive ionisation mode (4Kv corona discharge). The aroma compounds were measured in selected ion mode (Table 3.2) with a dwell time of 0.1 s over a 10 min period starting from the time when a peak signal intensity appeared. The signal intensities on the mass spectrums were recorded using the MassLynx 4.1 operation software (Micromass, Manchester, UK). Raw data was exported to Microsoft Excel and graphs were plotted as the average headspace intensity (%) including the standard deviation against time (min).

The first point of average headspace intensity was set to 100%. The points measured after the first point were divided by the first point of average headspace intensity.

20 µl/l diacetyl or 3-pentanone in pure water was freshly prepared and Figure 3.5 depicts an example of how the dynamic headspace intensity of diacetyl and 3-pentanone over pure water changed over time. Dynamic release behaviour was found to vary in the rate at which their intensity in the headspace decreased with time. At the end, the aroma amount remaining in the headspace also varied for the different systems.

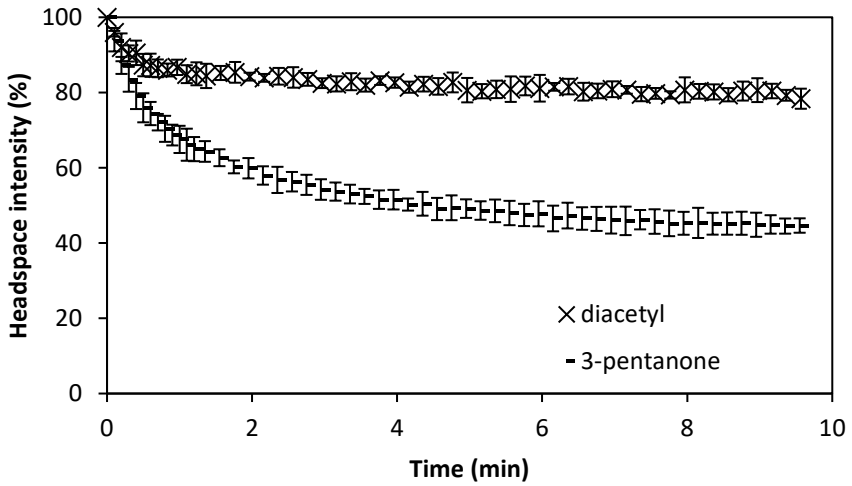


Figure 3.5 Dynamic headspace release of diacetyl and 3-pentanone above water

3.2.6 Statistics

The mean values and their standard deviations were calculated using the spreadsheet software Microsoft Excel. The two-factor ANOVA statistical analysis with Tukey post hoc test ($P < 0.05$) using the Expert Design software (Stat-Ease Inc., USA) was used to investigate if there was any interaction between those two factors (i.e. system type and emulsifier type). The one-way ANOVA and two-factor ANOVA statistical analyses with Tukey post hoc test ($P < 0.05$) using the SPSS software (IBM Statistics 21, USA) were carried out to explore how the data was significantly different from each other in statistics.

4 IMPACT OF AROMA HYDROPHOBICITY ON AROMA ENTRAPMENT IN A W/O/W EMULSION

In this Chapter, the results of the research on how aroma hydrophobicity affects aroma entrapment in w/o/w emulsions are presented. The method of how the aroma entrapment was quantified is described in this chapter considering both methods of aroma addition to the w/o/w emulsions applied in this PhD research: addition to the internal water phase (w_1) prior to the processing of the w_1/o emulsions into the external water phase w_2 and addition to the external water phase w_2 following processing of the w_1/o/w_2 emulsions. Static headspace intensity was measured and it was assumed that aroma entrapment in w_1 had occurred when the headspace intensity for the w/o/w emulsions for aroma addition to w_1 was lower than that for the w/o/w emulsions with aroma addition to w_2. Occurrence of aroma entrapment revealed that the headspace intensity of aroma compounds did not reach the equilibrium above the w/o/w emulsions or there was interaction between the aroma compounds and the ingredients in w/o/w emulsions that affected aroma release. Aroma entrapment was quantified over a relatively short time (20 min) after the emulsions were placed into sealed containers as the aroma concentration in w_1 would be identical to that in w_2 at equilibrium for a long enough time without other circumstances changing, e.g. heating and stirring, or without aroma-ingredient interactions.

4.1 INTRODUCTION

Aroma entrapment is a technology by which one or a mixture of aroma compounds is coated with or entrapped in another material or system (Madene et al. 2006). Entrapment can be used to maintain aroma compounds in a food product during storage, protecting aromas from undesirable interactions with other components of the food formulation, reduce aroma-aroma interactions, enhance aroma shelf-life and/or control aroma release (Reineccius 1991, Tari et al. 2002, Taylor et al. 2010). Nowadays, research on aroma entrapment tends to focus on slowing down aroma release and on triggering release systems activated typically by heat and mechanical stress (Taylor et al. 2010).

w/o/w emulsions can be used as entrapment vehicles of bioactive ingredients, such as aromas, salts and sugars, since their multiple compartment structures offer the possibility of entrapping substances within the primary or secondary internal droplet phase (Versic 1988, Raynal et al. 1993, Dickinson et al. 1994, Malone et al. 2003, Leal-Calderon et al. 2007, Frasch-Melnik et al. 2010, Souilem et al. 2014, Chiu et al. 2015). Besides a lower fat level in w/o/w emulsions compared to single o/w emulsions (the dispersed oil phase containing the internal water phase) can also reduce the interaction between the hydrophobic aromas and the fat-associated ingredients (Shamil et al. 1991, Malone et al. 2000, Doyen et al. 2001). Other entrapment systems include molecular entrapment such as cyclodextrin, physical entrapment in extruded carbohydrates such as maltodextrin (Chang et al. 2010), or through more

complex structures such as dried yeast cells for the entrapment of hydrophobic aroma compounds (Normand et al. 2005).

There are some publications reporting on aroma release over w/o/w emulsions. It has been reported that incorporating butanol (log P 0.84) into a sodium caseinate-stabilised w/o/w emulsion, the reduced release rate was due to the oil phase acting as a diffusional barrier, compared with a single o/w emulsion stabilised with the same protein (Dickinson et al. 1994). An increase in the fraction of the internal water phase of w/o/w emulsions lead to a decrease in perceived acidity of citric acid during consuming (Malone et al. 2003). Recent research has shown that changes in emulsifier concentration, oil type including soybean oil or a medium-chain triglyceride and oil content could significantly affect air-emulsion partition coefficients (Mao et al. 2014). This finding originated from a flavour-emulsifier binding effect, the hydrophobicity of flavour compounds and the polarity of oil. The aroma compounds reported in above literatures were initially added into the oil phase of o/w emulsions or into the internal aqueous phase of w/o/w emulsions before emulsion manufacturing. None of the cited literature reported whether the release of aroma compounds with different hydrophobicity was influenced by the location of initial aroma addition. It can be hypothesised that differences in aroma headspace intensity above w/o/w emulsions due to different location of aroma addition could affect the aroma release from a w/o/w emulsion based food product by consumers.

The purpose of this chapter was to investigate the entrapment of different aroma compounds in w/o/w emulsions stabilised with polyglycerol polyricinoleate (PGPR) and pea protein isolate (PPI). Three aromas, acetoin, acetyl pyridine and hexanal, were chosen to cover a range of hydrophobicity. PGPR was used as the hydrophobic emulsifier to produce the primary w/o emulsion and PPI was chosen as the hydrophilic emulsifier to further produce the w/o/w emulsion. For the static headspace analysis, 20 min was chosen for aroma equilibrium distribution in w/o/w emulsions based on literature suggesting that aroma release from o/w emulsions could reach equilibrium within 10 min (Mao et al. 2014).

It is assumed that at equilibrium and without any interaction between the aroma compounds and the ingredients in w/o/w emulsions, the initial addition way would not affect the aroma release in the headspace. Thus, when considering aroma concentration initially added to w_1, the number of moles of the aroma initially added to w_1 (n_{w_1}) should be identical to that initially added to w_2 (n_{w_2}). The number of moles of the aroma and the volume of w_2 are given by Equation 4.1 and 4.2 respectively. So the aroma concentration that should be initially added into w_1 (C'_{w_1}) was calculated by Equation 4.3 with the knowledge of fixed aroma concentrations initially added to w_2 (C'_{w_2}).

$$N = C * V \qquad \text{Equation 4.1}$$

$$V_{w_2} = V_{w_1} * (1 - \phi_{w/o}) / (\phi_{w/o} * \phi_{w_1}) \qquad \text{Equation 4.2}$$

$$C'_{w_1} = C'_{w_2} * (1 - \phi_{w/o}) / (\phi_{w/o} * \phi_{w_1}) \quad \text{Equation 4.3}$$

where N is the number of moles of the aroma in a phase, C is the aroma concentration in a phase, V is volume of a phase, V_{w_1} is the volume of w_1, V_{w_2} is the volume of w_2, $\phi_{w/o}$ is the volume fraction of the w/o emulsion in the w/o/w emulsion and ϕ_{w_1} is the volume fraction of the water phase in the w/o emulsion.

4.2 METHODS SPECIFIC TO THE RESULTS REPORTED IN THIS CHAPTER

4.2.1 Sample preparation

The internal water phase of the w/o/w emulsions, w_1, was a 1% NaCl solution. The oil phase, o, contained 6% of PGPR. The external water phase, w_2, contained 1.5% of pea protein isolate (PPI).

Three aroma compounds acetoin, acetyl pyridine and hexanal with the log P values from -0.36 to 1.97 were investigated. Acetoin was chosen as a representative of hydrophilic compounds, while acetyl pyridine and hexanal were chosen as representatives of hydrophobic compounds. They were added either to w_1 or w_2 prior to emulsification (utilising the process outlined in section 3.2.1) to prepare emulsions which are subsequently referred to as 'internal' or 'external' samples respectively. The aroma compounds were added at a concentration of either 10, 15 or 20 µl/l (low, mid, high) to w_2. This range of aroma concentration was chosen as it is the range of aroma amount

generally presented in food (Almonds et al. 2009). The solubility of the aromas (see Table 3.1) was also considered so that the three aroma concentrations are compatible for them to be solubilised in w_1.

According to Equations 4.1-3, a concentration for aroma addition to w_1 of 58, 87 and 116 µl/l at low, mid and high level, respectively, was obtained. Thus, if 20 min is sufficient for aroma compounds to reach equilibrium over w/o/w emulsions and there is no ingredient-aroma interaction, the headspace intensity of aroma addition to w_1 at equilibrium should be equivalent to that when aroma was initially added to w_2. Published values of the physicochemical properties including logP values, molecular weight, air-water partition coefficient and density considered for this prediction were introduced in Table 3.1.

Emulsions were prepared in triplicate and after a 20 min period submitted to headspace analysis.

4.2.2 Quantification of aroma entrapment

Aroma entrapment was assumed to have taken place when the headspace intensity above 'external' samples was higher than above 'internal' samples, illustrated in Figure 4.1.

The entrapment ratio was calculated to see the impact of log P on aroma release. For each aroma, this ratio was calculated with the headspace intensity

above ‘external’ samples divided by the headspace intensity above ‘internal’ samples determined 20 min after emulsion preparation. If the ratio is 1, it would mean ‘internal’ sample and ‘external’ sample would have the same headspace intensity, which suggests that there was no aroma entrapment and aroma distribution had reached equilibrium over the w/o/w emulsions.

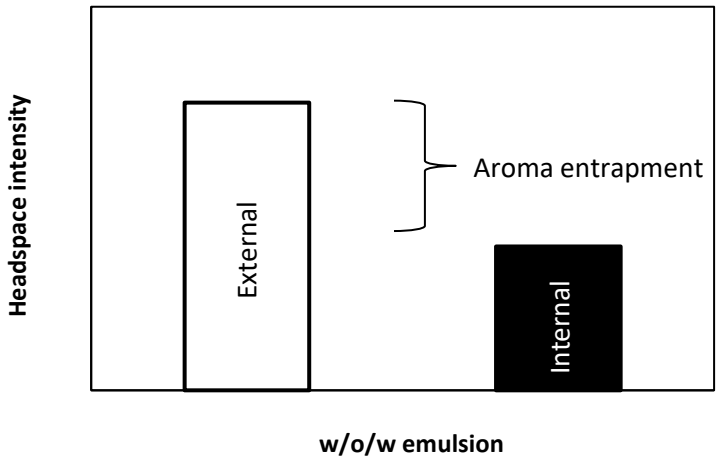


Figure 4.1 Schematic representation of aroma entrapment as indicated by the difference in mean headspace intensity between ‘external’ sample and ‘internal’ sample

4.3 EMULSION MICROSTRUCTURE

Figure 4.2A and B shows two micrographs of the same w/o/w emulsion taken at different magnification. The microstructure of w/o/w emulsions prepared with aroma addition had the same microstructure, so only micrographs of the

w/o/w emulsion in absence of aroma are shown. Oil droplets are clearly discernible. The dark appearance of the droplets is characteristic for emulsion droplets which themselves are emulsions (w/o in this case). Images taken at the lower magnification show evidence of the undissolved protein present in the emulsion as highlighted in Figure 4.2A.

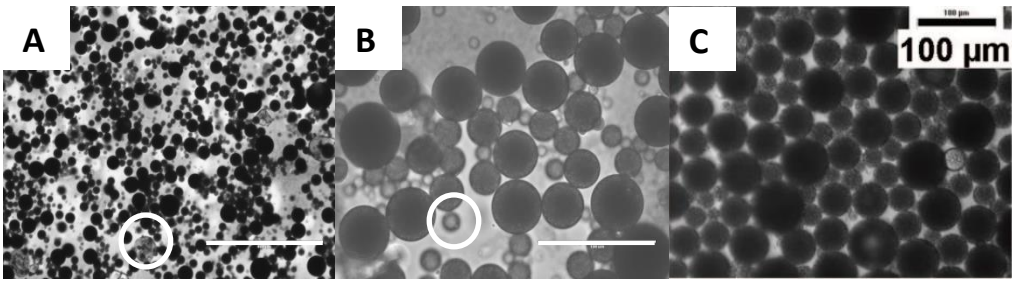


Figure 4.2 Micrographs of w/o/w emulsions stabilised with pea protein isolate as the hydrophilic emulsifier. The circles in image A indicate the protein (PPI). The circles in image B indicate small oil droplets containing few w_1 droplets with light appearance. Image C is a micrograph from the literature (Rojas et al. 2008). The scale bar in A represents 400 µm. The scale bar in B and C represents 100 µm.

A micrograph of a w/o/w emulsion from a publication (Rojas et al. 2008) is presented in Fig. 4.2C in order to proof that the microstructure shown under microscopy was w/o/w emulsions. This publication reported that the microscopy image confirmed the double-emulsion globules were completely

filled with many tiny w_1 droplets. Similar microscopic observation was also found in the previous literature (Lad et al. 2012).

Figure 4.3 shows the droplet size distribution of the w/o/w emulsion prepared without aroma, which is representative of the w/o/w emulsion droplet profile studied in this chapter. The droplet size spectrum is broad and the extended tail at small diameters is likely in part due to multiple scattering from the w_1 droplets internalised in the (larger) oil droplets (Kaimainen et al. 2015) or/and a certain fraction of small oil droplets containing few w_1 droplets with light appearance (Thompson et al. 2015), which are highlighted in Figure 4.2B. The mean Sauter diameter ($d_{3,2}$) of the w/o/w emulsions was 5.20±0.58 μm.

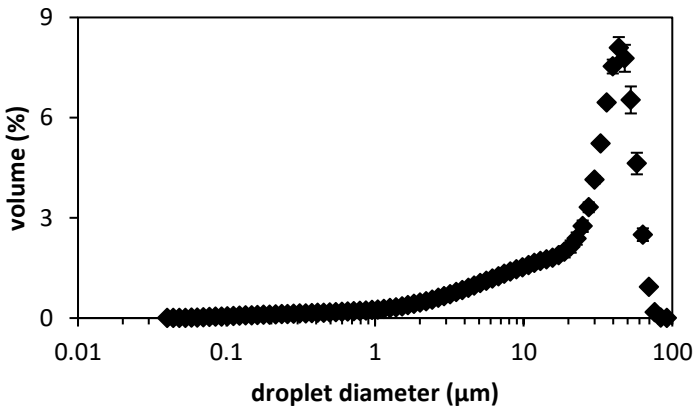


Figure 4.3 Averaged droplet size distribution of w/o/w emulsion

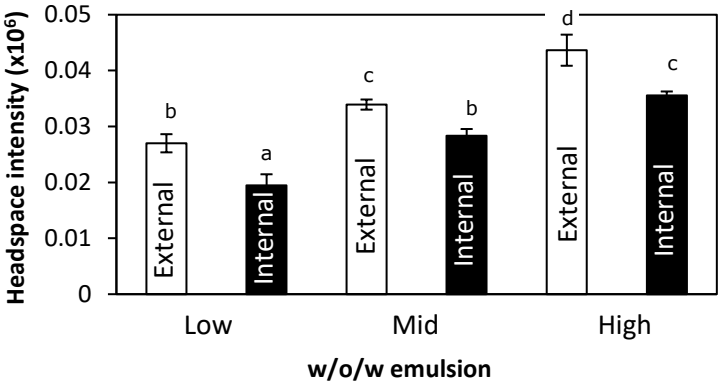
4.4 AROMA PARTITIONING AND ENTRAPMENT

The headspace intensity over the w/o/w emulsions was evaluated by APCI-MS through static headspace analysis. As outlined in the method section 4.2.1, one hydrophilic aroma compound acetoin (logP < 0) and two hydrophobic aromas acetyl pyridine and hexanal (logP > 0) were considered in this chapter. These aroma compounds were individually added to either w_1 or w_2 prior to emulsion preparation at low, mid or high concentration. Figure 4.4 shows the headspace intensity of the three aroma compounds above the w/o/w emulsion, both when the aroma compound was introduced to the internal or the external aqueous phase. Results graphs are presented in order of increasing logP value, that is increasing hydrophobicity, and results are shown for the three levels of addition investigated.

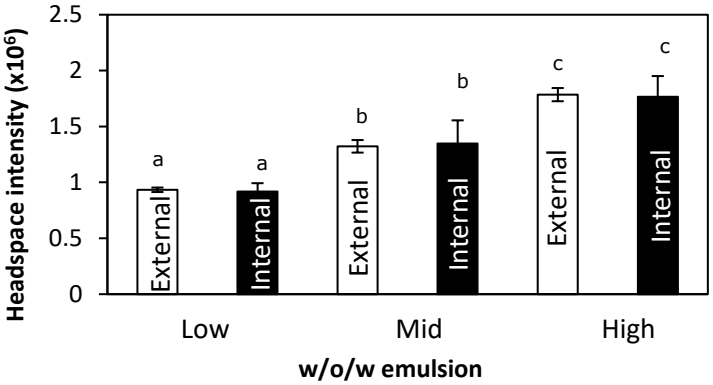
4.4.1 Hydrophilic aroma compound

When considering acetoin, the hydrophilic aroma compound included in this study, the headspace intensity of the 'internal' emulsion (aroma initially added to the internal aqueous phase) was significantly lower ($P < 0.05$) than that of the 'external' emulsion (aroma initially added to the external aqueous phase) (Figure 4.4A). The static headspace data were acquired 20 min after emulsion preparation. The fact that there was a difference between 'internal' and 'external' samples indicates that over this time scale there was a resistance to mass transfer/diffusion within the system and acetoin was being entrapped in the internal water phase of the w/o/w emulsion.

A



B



C

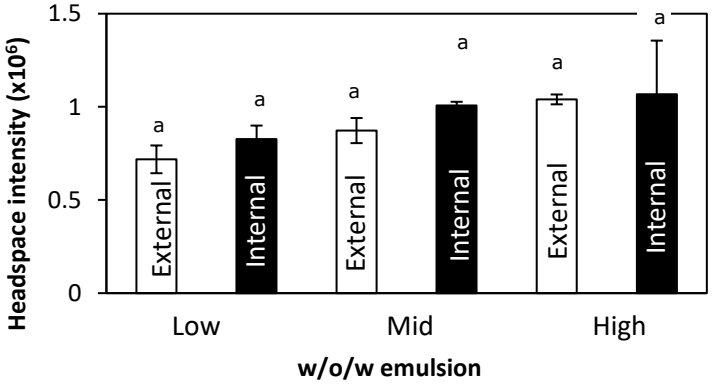


Figure 4.4 Static headspace intensity of A) acetoin B) acetyl pyridine C) hexanal above the w/o/w emulsion with concentration from low to high. Scales of the y-axis vary by target analyte. Different letters indicate statistically significant values ($P < 0.05$).

The results suggest that the headspace intensity of acetoin did not reach equilibrium. Since acetoin is hydrophilic, diffusion of acetoin from the internal aqueous phase to the external aqueous phase is presumed to be slowed by the hydrophobic barrier, the oil layer of the oil droplets. It also might be due to the PGPR micelles in the oil phase that are capable of entrapping hydrophilic aromas in the polar inner core as explained in section 2.2.2.1.3.

Not surprisingly, it also can be seen that increasing concentration of aroma compound inclusion resulted in a steady increase in the headspace response for both the 'external' emulsions and the 'internal' emulsions. It indicates the headspace intensity of acetoin was concentration dependent.

4.4.2 Hydrophobic aroma compounds

The headspace intensity of the more hydrophobic acetyl pyridine did not vary when comparing the phase to which it was added (Figure 4.4B), although there was a clear enhancement in headspace intensity within each aroma addition type with increasing concentration. It appears that in direct contrast to acetoin, the more hydrophobic compound acetyl pyridine was not entrapped in w_1 of the w/o/w emulsion. This is possibly due to its increased solubility in the hydrophobic phase.

There was a similar response for the hydrophobic aroma compound hexanal (Figure 4.4C), which has a higher logP than the other two aroma compounds.

There was no significant difference in the headspace intensity between the 'external' and the 'internal' emulsions ($P > 0.05$).

4.5 ENTRAPMENT RATIO

In order to better investigate the impact of log P on aroma release, the entrapment ratio of each aroma compound at each concentration is shown in Figure 4.5. It represents the entrapment behaviour of the duplex $w_1/o/w_2$ emulsion and a value above 1 indicates that the aroma is more efficiently entrapped within the inner aqueous phase of the w/o/w emulsion compared to addition of the aroma compound to the external water phase.

A decrease in entrapment ratio could be seen with an increase in logP across all samples. However, this is independent of concentration. Specifically, the entrapment ratio of acetoin was around 1.3, while that of acetyl pyridine and hexanal was around 1.0 and 0.9 respectively. As discussed previously, the resistance of the oil layer to the diffusion of the hydrophilic compounds acted to entrap the hydrophilic compounds within the inner phase. This highlights the importance of the basic physical properties of aroma compounds when considering their entrapment in w/o/w emulsions both for long term stabilisation of bioactives and the prediction of partitioning and release during food processing and oral processing.

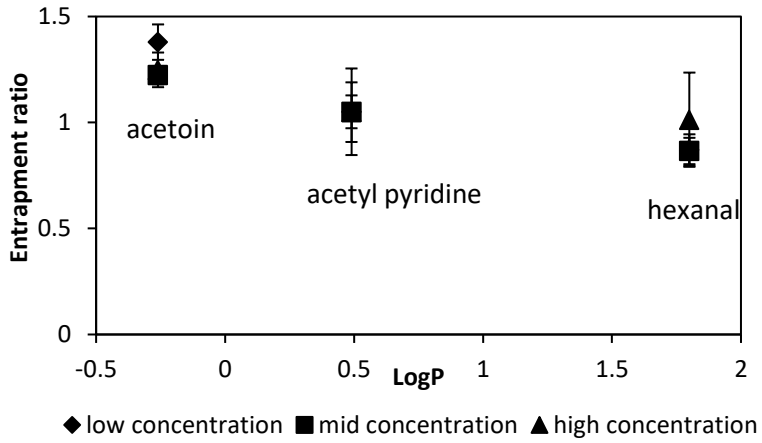


Figure 4.5 Entrapment ratio, as measured by differences in headspace of acetoin, acetyl pyridine and hexanal added into the internal or external water phases of w/o/w emulsions

4.6 CONCLUSIONS

The results shown in this chapter demonstrate that w/o/w emulsions are effective vehicles for the short-time aroma entrapment and probable delay release of hydrophilic aroma compounds. To further understand the aroma release behaviour over w/o/w emulsions, static headspace analysis for a longer term to reach equilibrium in the headspace intensity as well as dynamic headspace analysis after equilibrium should be explored. The impact of the interfacial design in terms of emulsifier type and emulsion microstructure (droplet size, droplet size distribution and emulsion stability) as well as the interactions between the aroma compounds and the emulsifiers in the system on aroma release also merits further investigation.

5 IMPACT OF HYDROPHILIC EMULSIFIER ON AROMA RELEASE FROM W/O/W EMULSIONS

In this chapter the research on the impact of the type of the hydrophilic emulsifier for the stabilisation of w/o/w emulsions on aroma release is reported. Types investigated included a low molecular weight non-ionic surfactant, polyethylene 20 sorbitan monolaurate (Tween 20), a chemically modified starch, octenyl succinic anhydride (OSA) starch, and a protein, pea protein isolate (PPI), as a large molecular weight emulsifier. Diacetyl and 3-pentanone were used as representative hydrophilic and hydrophobic aroma compound respectively. They were added into the emulsions after emulsion manufacture. The advantage of adding aroma compounds after emulsion preparation was to reduce aroma loss during processing, which could not be avoided due to exposure to open air during processing addition but was measurable. To isolate the impact of the oil phase (o) and the external aqueous phase (w_2) on aroma release, release behaviour over w_2 and single o/w emulsion was quantified in the same way as over the w/o/w emulsions. Emulsion microstructure characteristics are also presented to help understand the impact of droplet size and droplet size distribution of emulsions stabilised with these three different hydrophilic emulsifiers on aroma release. Both static headspace analysis and dynamic headspace analysis was carried out to characterise the aroma release behaviour. Static headspace analysis was used to investigate the equilibrium time an aroma reach in the headspace above w/o/w emulsions. After

equilibrium, dynamic headspace analysis was carried out to investigate whether the aroma was entrapped in the w/o/w emulsion microstructure leading to a slow release into the headspace.

5.1 INTRODUCTION

It is important to understand the interaction behaviour of aroma compounds with major ingredients in w/o/w emulsion microstructures. The ingredient-aroma interactions affect the release of selective aroma compounds in the headspace over the food during process, storage and human perception (Kinsella 1988, Bakker 1995).

The major ingredients in w/o/w emulsions include oil, water, hydrophobic emulsifier and hydrophilic emulsifier. Hydrophilic emulsifiers are used to stabilise the oil droplets with their internal water droplets. Low molecular weight surfactants, starches and proteins are the commonly used hydrophilic emulsifiers in food emulsions (section 2.2.2). Their interactions with aroma compounds have been discussed in sections 2.4.2.2-4. However, there are few studies reporting the comparison of the interactions between aromas and different emulsifiers in emulsions. A previous study showed that the headspace intensity of an aroma compound (3-methylbutyraldehyde) over w/o/w emulsions stabilised with Span 80 and OSA starch was higher than that over w/o/w emulsions stabilised with Span 80 and whey protein isolate (Brückner et al. 2007). The differences in release behaviour can result from the differences in the binding of aromas to different hydrophilic emulsifiers, which

implicates selecting appropriate hydrophilic emulsifiers for aroma release over w/o/w emulsions.

In the previous Chapter 4, it has been demonstrated that w/o/w emulsions stabilised with PPI could entrap hydrophilic aroma compounds in the internal water phase (w_1) for a short time. But the impact of emulsion microstructure and the aroma-emulsifier interactions on aroma release was not explored. It is hypothesised that aroma release above w/o/w emulsions depends on the nature of the aroma compounds, emulsion microstructure including the droplet size and emulsion stability, and the hydrophilic emulsifiers that possibly interact with aromas. Thus, the aim related to this chapter was to investigate the influence of hydrophilic emulsifiers and the emulsion microstructure on aroma release behaviour over w/o/w emulsions. Different from the aroma compounds used in Chapter 4, two new aromas were selected in this chapter considering that they represent the opposite hydrophobicity class and have the same molecular weight to eliminate the molecule size on release behaviour.

5.2 METHODS SPECIFIC TO THE RESULTS REPORTED IN THIS CHAPTER

5.2.1 Emulsion composition and aroma inclusion

Three emulsifiers, Tween 20, OSA starch and PPI (section 3.1), were chosen as a representative of low-molecular-weight surfactant, chemically modified starch and protein respectively. These three hydrophilic emulsifiers were used

in w_2 to investigate the effect of emulsifier type on aroma release over w/o/w emulsions.

w_1 contained 0.1 M NaCl. The salt concentration was chosen considering it should be not too high to have the impact on destabilising the w/o and w/o/w emulsions and also be sufficient to enhance the adsorption of PGPR molecules at the interface to produce stable w_1 droplets. This concentration was suggested from previous literature (Matos et al. 2013, Matos et al. 2014). o contained 4% PGPR and this concentration was advised by the literature (Pawlik et al. 2010). w_2 contained 2% Tween 20, 4% OSA starch or 1.5% PPI. These emulsifier concentrations were chosen considering they were sufficient to stabilise emulsion droplets, which was tested in the preliminary experiments and was also suggested from the literature (Pawlik et al. 2010, Chiu et al. 2017). w_2 also contained 0.1 M NaCl to balance the osmotic pressure between the two aqueous phases in the w/o/w emulsions. w/o/w emulsions were prepared using the method described in section 3.2.1. They were labelled 'wowT', 'wowS' and 'wowP' respectively. Controls of o/w emulsions consisting of 2% Tween 20, 4% OSA starch or 1.5% PPI in were prepared as described in section 3.2.2. These were named 'owT', 'owS' and 'owP' respectively. Five different water controls were also prepared: water; 0.1 M NaCl; 2% Tween 20 in 0.1 M NaCl; 4% OSA starch in 0.1 M NaCl; 1.5% PPI in 0.1 M NaCl. They were named 'w', 'NaCl', 'wT', 'wS' and 'wP' respectively. The controls of emulsifier solutions with salt addition were prepared to explore the impact of w_2 on aroma release. Samples were prepared in batches. All emulsions creamed due to the density difference between oil and water.

The two aroma compounds chosen were diacetyl and 3-pentanone. They have different hydrophobicity (see Table 3.1), hydrophilic for diacetyl and hydrophobic for 3-pentanone. These compounds have the same molecular weight (Mwt) to eliminate the effect of molecular mass on aroma release. The aroma was added to the emulsion after emulsion manufacture.

w/o/w emulsion microstructure and droplet size were observed utilising the methods described in section 3.2.4. This was to investigate the emulsion stability up to 7 days of storage, as 7 days is generally a minimum storage period for dairy products (Bishop et al. 1986). Microscopy observation and droplet size measurement were taken immediately after w/o/w emulsion manufacture in the absence or in the presence of aroma compounds. The corresponding results were named 'day of making'. Further measurements were undertaken 2 and 6 days after emulsion manufacture. These results were labelled 'day 2' and 'day 6' respectively.

5.2.2 Static headspace analysis

For the static headspace analysis, 45 ml of w/o/w emulsion or o/w emulsion was transferred to a glass bottle (a total volume of 134 ml) with a 25x6 mm magnetic stirrer bar at the bottom. 200 µl/l aroma standard solution in 0.1 M NaCl was prepared in a 100 ml volumetric flask. 5 ml of this aroma standard solution was added to each bottle to make a final aroma concentration of 20 µl/l. The resulting gas headspace volume was 84 ml. Once the aroma standard solution was added to a bottle, the bottle was immediately sealed followed by

stirring at 500 rpm for 1 min to ensure equal distribution of the aroma compound. All samples were analysed at room temperature (utilising the method described in section 3.2.5.1) with the first analysis taking place immediately after the mixing step was finished. The corresponding results were labelled '0 h'. Further measurements were undertaken 1 h, 2 h, 3 h and 4h after aroma addition and results were labelled '1 h', '2 h', '3 h', '4 h' respectively. A water standard with the same amount of aroma added was always measured at the same time. All samples were prepared in triplicate to test for reliability and repeatability of the procedure. The relative headspace intensity was calculated as the headspace intensity over the emulsion divided by that over aroma added to water measured at the same time (see Figure 3.3). This was due to the inconsistent equipment (APCI-MS) performance over the control of the experiment period. An equilibrium was considered to be reached when the relative headspace intensity was not different from the one measured at last time slot.

Theoretical aroma distributions at equilibrium for different systems including water, o/w emulsions and w/o/w emulsions were calculated by Equations 5.1-9, with the knowledge of the total number of moles of an aroma added to a liquid sample (N_t), the mass fraction of each phase, the volumes of the liquid sample and the gas phase above the liquid, the air-water partition coefficient (K_{aw}) (Table 3.1) and the octanol-water partition coefficient (log P). These equations only take account of the lipid-effect on aroma partitioning to reach equilibrium without the consideration of any impact of aroma-ingredient interactions. N_t equals to the initial aroma concentration added in a liquid (C_t =

20 µl/l) multiplying by the total liquid volume (V_l = 50 ml), which is 1 µl. For water system, K_{aw} is used, which is proportional to the aroma concentration in the gas phase (C_g) and the aroma concentration in water (C_{water}). Hence, the number of moles of the aroma in water (N_{water}) and the number of moles of the aroma in the gas phase (N_g) can be calculated according to K_{aw} and the volumes of the gas phase (V_g = 84 ml) and V_l in Equation 5.1 and 5.2 respectively.

$$N_{water} = N_t / (1 + V_g K_{aw} / V_l) \qquad \text{Equation 5.1}$$

$$N_g = N_{water} V_g K_{aw} / V_l \qquad \text{Equation 5.2}$$

For o/w emulsions, log P is also used, which is the ratio of the aroma concentration in the oil phase (C_o) and the aroma concentration in water phase (C_w). Thus, the number of moles of the aroma in the water phase (N_w), in the oil phase (N_o) and in the gas phase (N_g) can be calculated according to the volume fraction of the oil phase (ϕ_o = 0.3), log P, K_{aw}, V_g and V_l in Equation 5.3, 5.4 and 5.5 respectively.

$$N_w = N_t / (1 + \phi_o 10^{\log P} / (\phi_o - 1) + V_g K_{aw} / (V_l(1 - \phi_o))) \qquad \text{Equation 5.3}$$

$$N_o = N_w \phi_o 10^{\log P} / (\phi_o - 1) \qquad \text{Equation 5.4}$$

$$N_g = N_w V_g K_{aw} / (V_l(1 - \phi_o)) \qquad \text{Equation 5.5}$$

For w/o/w emulsions, it is considered that the aroma concentration in w_1 (C_{w_1}) should be equivalent to that in w_2 (C_{w_2}) at equilibrium. Here, log P is proportional to the aroma concentration in total water phase ($C_{(w_1 + w_2)}$) and C_o, while K_{aw} is proportional to C_g and $C_{(w_1 + w_2)}$. After manipulating equations, the

number of moles of the aroma in w_2 (N_{w_2}), in w_1 (N_{w_1}), in oil ($N_{o'}$) and in the gas phase (N_g) is given in Equation 5.6, 5.7, 5.8 and 5.9 respectively. $\phi_{w_1/o}$ is the volume fraction of the primary w/o emulsion in the w/o/w emulsion (i.e. 30%) and ϕ_{w_1} is the volume fraction of the water phase in the primary w/o emulsion (i.e. 40%).

$$N_{w_2} = N_t(1 - \phi_{w_1/o}) / ((1 + (\phi_{w_1} - 1)10^{\log P}\phi_{w_1/o} / (\phi_{w_1/o} + \phi_{w_1} - \phi_{w_1/o}\phi_{w_1}) + V_gK_{aw} / (V_l\phi_{w_1/o}\phi_{w_1} + V_l - V_l\phi_{w_1/o}))(\phi_{w_1/o}\phi_{w_1} + 1 - \phi_{w_1/o})) \quad \text{Equation 5.6}$$

$$N_{w_1} = N_{w_2}\phi_{w_1/o}\phi_{w_1} / (1 - \phi_{w_1/o}) \quad \text{Equation 5.7}$$

$$N_{o'} = N_{w_2}(1 + N_{w_2}\phi_{w_1/o}\phi_{w_1} / (1 - \phi_{w_1/o}))(\phi_{w_1} - 1)10^{\log P}\phi_{w_1/o} / (\phi_{w_1/o} + \phi_{w_1} - \phi_{w_1/o}\phi_{w_1}) \quad \text{Equation 5.8}$$

$$N_g = N_{w_2}(1 + N_{w_2}\phi_{w_1/o}\phi_{w_1} / (1 - \phi_{w_1/o}))\, V_gK_{aw} / (V_l\phi_{w_1/o}\phi_{w_1} + V_l - V_l\phi_{w_1/o}) \quad \text{Equation 5.9}$$

Therefore, theoretical aroma concentrations can be calculated with the number of moles of the aroma in a phase divided by the volume of the phase. Theoretical aroma concentrations at equilibrium in the gas phase and water are shown in Table 5.1A. Theoretical aroma concentrations at equilibrium in the gas phase, the water phase and the oil phase of o/w emulsions is presented in Table 5.1B. Theoretical aroma concentrations at equilibrium in the gas phase, w_1, o and w_2 of w/o/w emulsions are reported in Table 5.1C.

Table 5.1 Theoretical aroma distribution in each phase after equilibrium under static headspace analysis: A) water B); o/w emulsions; C) w/o/w emulsions. The unit for the aroma concentration in the water phase (C_w), in the oil phase (C_o), in the internal water phase (C_{w_1}) and in the external water phase (C_{w_2}) is µl/l. The unit for the aroma concentration in the gas phase (C_g) is $x10^{-2}$ µl/l.

A

	C_w	C_g
Diacetyl	19.98	1.09
3-pentanone	19.88	7.22

B

	C_o	C_w	C_g
Diacetyl	1.28	27.99	1.52
3-pentanone	47.00	8.36	3.03

C

	C_{w_1}	C_o	C_{w_2}	C_g
Diacetyl	24.12	1.10	24.12	1.31
3-pentanone	10.88	61.18	10.88	3.95

With these values in Table 5.1, the theoretical relative headspace intensity at equilibrium were calculated by the theoretical headspace concentration over w/o/w emulsions or o/w emulsions at equilibrium divided by that over water at equilibrium. As a result, the theoretical relative headspace intensity over w/o/w emulsions was 1.21 for the hydrophilic aroma diacetyl and 0.55 for the hydrophobic aroma 3-pentanone. The theoretical relative headspace intensity over o/w emulsions was 1.4 for diacetyl and 0.42 for 3-pentanone. For diacetyl, the relative headspace intensity over w/o/w emulsions at equilibrium is

theoretically less than that over o/w emulsions. It indicates that the hydrophilic aroma remains to a larger extent in w/o/w emulsions compared to o/w emulsions. This can be explained by the fact that the w/o/w emulsions contain more water due to additional presence of w_1. For 3-pentanone, the relative headspace intensity at equilibrium over w/o/w emulsions is theoretically more than that over o/w emulsions. It shows that the hydrophobic aroma remains to a lesser extend in w/o/w emulsions compared to o/w emulsions, which is because the w/o/w emulsions contain less oil due to w_1 inside the oil phase.

5.2.3 Dynamic headspace analysis

For the dynamic headspace analysis, 95ml of w/o/w emulsion or o/w emulsion or water control was placed into a glass bottle with a 25x6 mm stirrer bar at the bottom and stored at room temperature. 400 µl/l aroma standard solution containing 0.1 M NaCl was prepared in a 100 ml volumetric flask. 5 ml of the aroma standard solution was added into each bottle to obtain a final aroma concentration of 20 µl/l and a 34 ml headspace volume. The bottles were immediately sealed and stirred at 500 rpm for 1 min to ensure rapid distribution of the aroma compounds. The w/o/w emulsions were then stored without further mixing at room temperature and 24 h were allowed for the aroma equilibrium in the bottles before the dynamic headspace analysis. The o/w emulsions were kept for 4 h for aroma equilibration before dynamic headspace analysis. The periods were chosen to allow the system to reach equilibrium based on the results of the static headspace analysis (discussed in

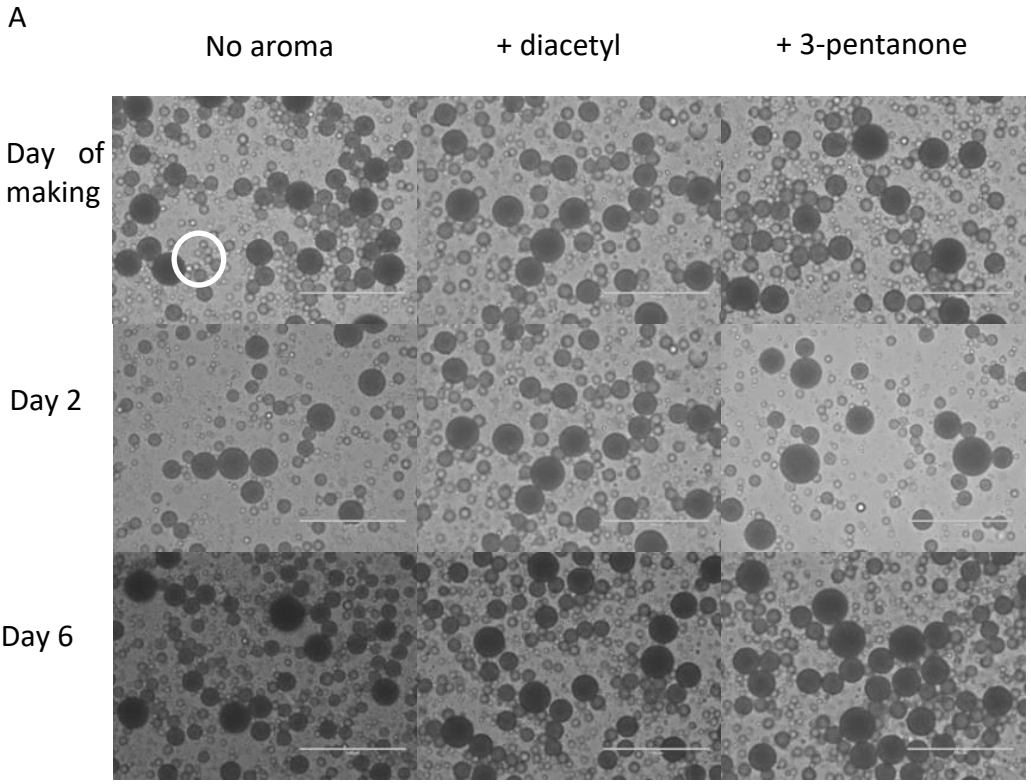
section 5.4). Dynamic headspace analysis was then carried out utilising the method in section 3.2.5.2.

5.3 EMULSION MICROSTRUCTURE DURING STORAGE

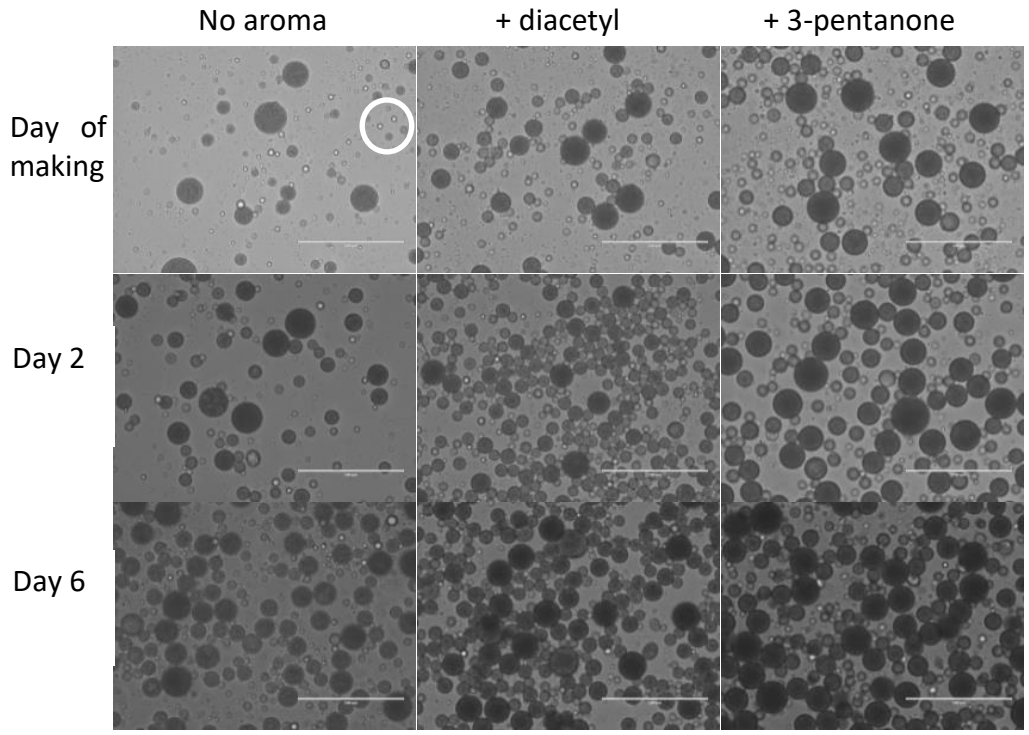
Emulsion microstructure observed by microscopy and droplet size distribution during storage was investigated to check the formation of w/o/w emulsions and emulsion stability. The results are shown in Figures 5.1-2 and Table 5.2.

Figure 5.1 illustrates the microstructure of Tween 20 (Figure 5.1A), OSA starch (Figure 5.1B) and PPI stabilised (Figure 5.1C) w/o/w emulsions in the absence or in the presence of the hydrophilic aroma (diacetyl) or the hydrophobic aroma (3-pentanone). All of the micrographs show the characteristics of a w/o/w emulsion as already described in section 4.3 confirming the successful preparation of the w/o/w emulsion samples. Some small dispersed droplets with light appearance could be occasionally observed in some micrographs. These droplets probably are oil droplets stabilised with the hydrophilic emulsifiers containing few or no inner water droplets inside. These small droplets could affect the mean droplet diameter of w/o/w emulsions quoted as the size of the populations in the size distributions (Figure 5.2). When using Tween 20 or OSA starch, there was no visible difference in the emulsion microstructure independent of aroma inclusion, type of aroma inclusion and sample age.

A


No aroma
+ diacetyl
+ 3-pentanone
Day of making
Day 2
Day 6

B


No aroma
+ diacetyl
+ 3-pentanone
Day of making
Day 2
Day 6

C

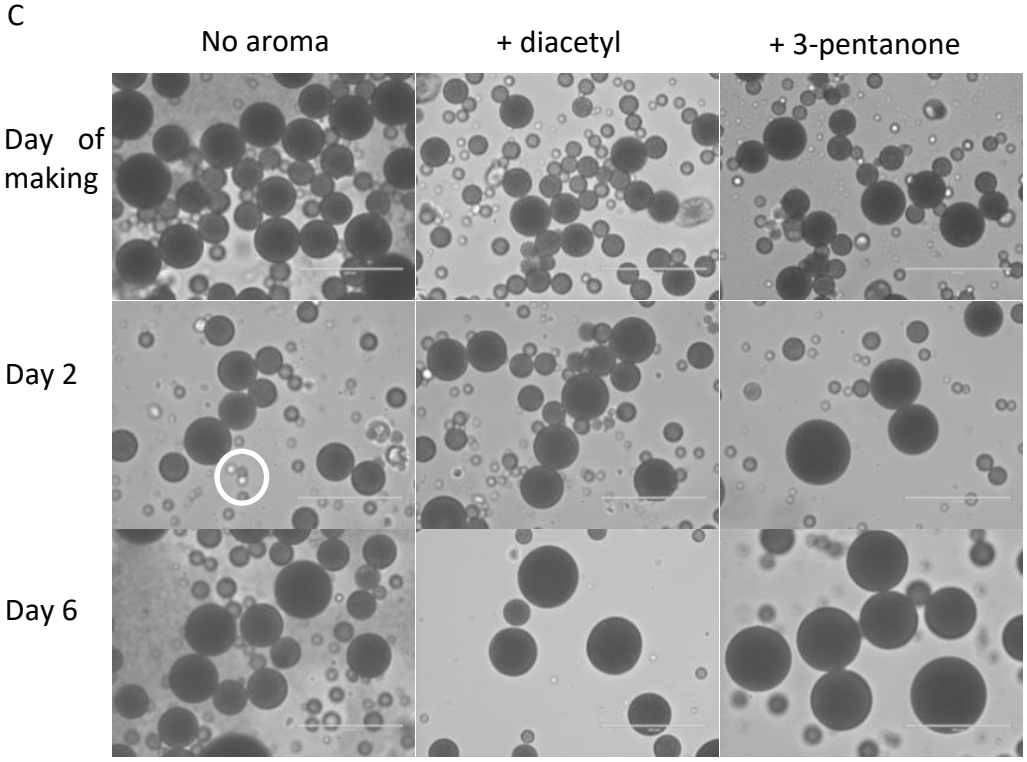
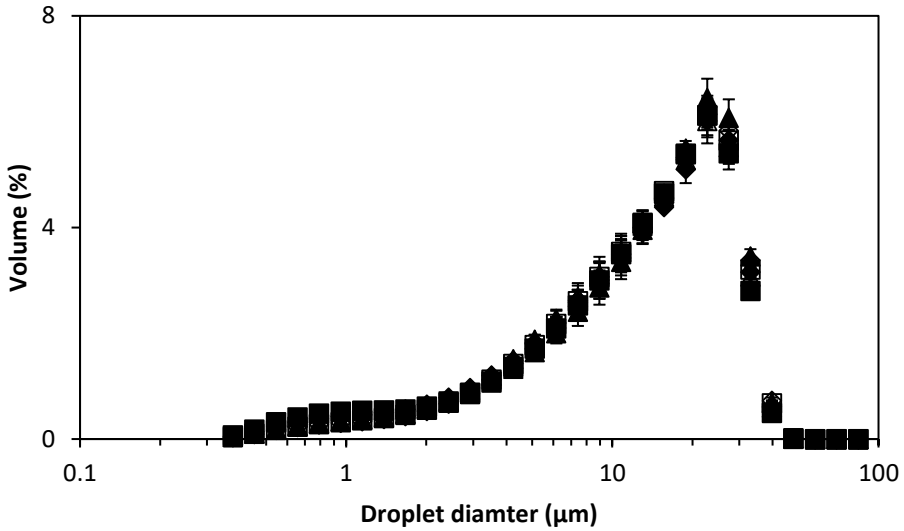


Figure 5.1 Micrographs of w/o/w emulsions imaged in the absence of aroma, or in the presence of diacetyl or 3-pentanone stored on day of making, day 2 and day 6: A) Tween 20 stabilised w/o/w emulsions; B) OSA starch stabilised w/o/w emulsions; C) PPI stabilised w/o/w emulsions. The circles indicate small oil droplets containing few w_1 droplets. Scale bar = 100 µm in all micrographs.

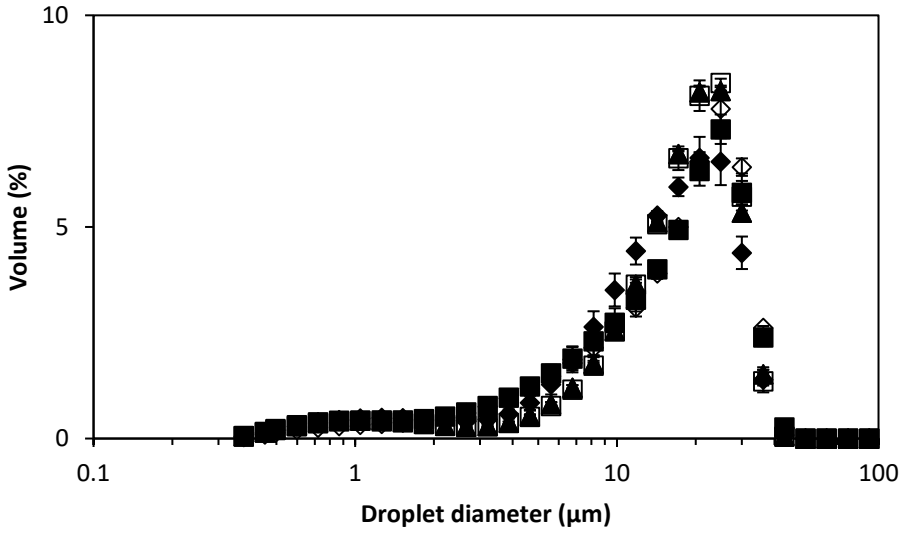
However, the oil droplets stabilised with PPI appeared larger on the micrographs than those stabilised with the other two emulsifiers. Also, coalescence was seen in the PPI stabilised oil droplets following the addition of 3-pentanone. The possible reasons behind this are discussed on page 102.

Figure 5.2 shows the volume based droplet size distributions of the w/o/w emulsions stabilised with Tween 20 (Figure 5.2A), with OSA starch (Figure 5.2B) or with PPI (Figure 5.2C) as the hydrophilic emulsifier.

A


8
4
0
Volume (%)
0.1
1
10
100
Droplet diamter (µm)

B


10
5
0
Volume (%)
0.1
1
10
100
Droplet diameter (µm)

C

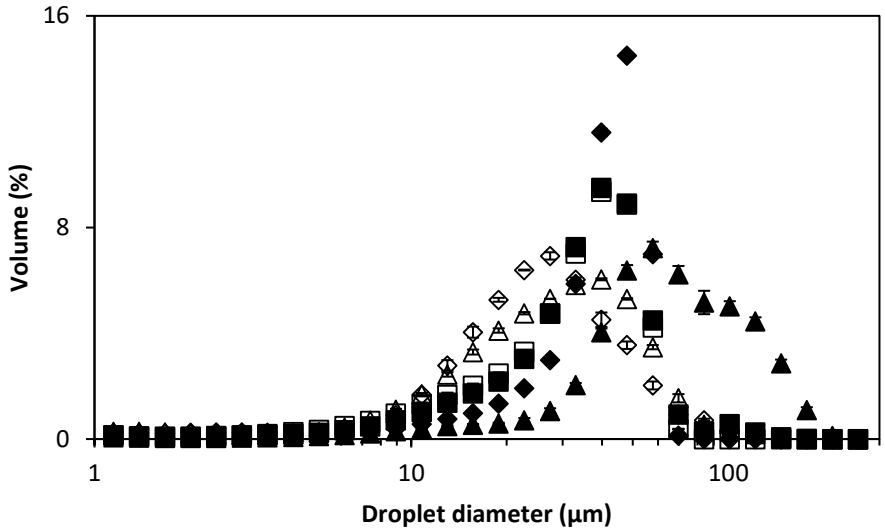


Figure 5.2 Averaged volume based droplet size distributions of A) Tween 20 stabilised w/o/w emulsions; B) OSA starch stabilised w/o/w emulsions; C) PPI stabilised w/o/w emulsions: □ Day of making; ■ Day 6; ◇ in the presence of diacetyl on Day of making; ◆ in the presence of diacetyl on Day 6; △ in the presence of 3-pentanone on Day of making; ▲ in the presence of 3-pentanone on Day 6.

The droplet size distributions of Tween 20 and OSA starch stabilised w/o/w emulsions remained unchanged for one week, which were independent of aroma inclusion and type of aroma inclusion. They had two populations with one peak at around 1 µm and another peak at around 20 µm. This quantifies the qualitative image given by microscopy for Tween 20 (Figure 5.1A) and OSA starch (Figure 5.1B). The peak around 1 µm in the droplet size distribution was

probably obtained from those small oil droplets and the peak around 20 μm was from the oil droplets with inner water droplets in the w/o/w emulsions.

The PPI stabilised w/o/w emulsions showed no change in droplet size distribution in the absence of aroma compound. There were also two peaks in the droplet size distribution, with one at around 10 μm and the other at around 40 μm. The peak around 10 μm would correspond with small oil droplets, which could be observed in the micrographs (Figure 5.1C). In the presence of diacetyl, the droplet size distribution became narrower within one week of storage with span decreased from 1.59 to 0.88, but the bigger peak shifted from approximately 25 μm on the day of making to roughly 45 μm on day 6. It suggests that Ostwald ripening/ coalescence took place in the PPI stabilised w/o/w emulsions in the presence of diacetyl. However, in the presence of 3-pentanone, the droplet size distribution on the day of making had two peaks with one around 1 μm and the other around 33 μm, while on day 6 the peaks shifted to around 50 μm and 100 μm. This accompanies with span changing from 1.62 to 1.58. It also suggested that coalescence took place in the PPI stabilised w/o/w emulsions with 3-pentanone.

As a numerical value of the characteristic droplet size parameter that is relevant to this work on aroma release, Sauter diameter ($d_{3,2}$) is reported in Tables 5.2. It is worth noting that the $d_{3,2}$ values in Table 5.2 do not reflect the real size of droplets with actual peaks in their size distributions.

Table 5.2 Average Sauter diameter ($d_{3,2}$) of w/o/w emulsions: stabilised with A) Tween 20, B) OSA starch or C) PPI; in the absence of aroma, or in the presence of diacetyl or 3-pentanone; on day of making, day 2 and day 6. Values are the mean of 3 replicates ± the standard deviation.

A

Emulsion	Day of making (µm)	Day 2 (µm)	Day 6 (µm)
wowT	7.22±0.30^{abc*}	7.56±0.22^{bc}	5.97±0.23^{a}
wowT + diacetyl	7.31±0.26^{abc}	8.07±0.78^{c}	6.38±0.05^{ab}
wowT + 3-pentanone	6.95±0.16^{abc}	7.18±0.15^{abc}	7.21±0.24^{abc}

* Different letters indicate statistically significant values (P < 0.05).

B

Emulsion	Day of making (µm)	Day 2 (µm)	Day 6 (µm)
wowS	7.71±0.06^{ab*}	8.42±0.25^{ab}	7.02±0.11^{a}
wowS + diacetyl	8.04±0.18^{ab}	8.58±0.17^{b}	7.08±0.12^{ab}
wowS + 3-pentanone	7.72±0.18^{ab}	7.83±0.25^{ab}	7.89±0.09^{ab}

* Different letters indicate statistically significant values (P < 0.05).

C

Emulsion	Day of making (µm)	Day 2 (µm)	Day 6 (µm)
wowP	13.19±0.05^{bc*}	13.98±0.06^{c}	14.25±0.09^{c}
wowP + diacteyl	10.85±0.12^{a}	14.41±0.11^{c}	17.69±0.04^{d}
wowP + 3-pentanone	12.07±0.12^{ab}	18.37±0.15^{d}	30.03±2.19^{e}

* Different letters indicate statistically significant values (P < 0.05).

The $d_{3,2}$ of Tween 20 and OSA starch stabilised w/o/w emulsions were similar. Specifically, the $d_{3,2}$ slightly decreased for both w/o/w emulsions in the absence of aroma or in the presence of diacetyl on day 6 compared to those on the day of making. However, there was no significant change in $d_{3,2}$ in both w/o/w emulsions independent of aroma inclusion, type of aroma inclusion and sample age. The w/o/w emulsions stabilised with PPI had a higher $d_{3,2}$ than the other two emulsions. There was no significant difference in $d_{3,2}$ of PPI stabilised w/o/w emulsions in the absence of aroma. In the presence of diacetyl or 3-pentanone in PPI stabilised w/o/w emulsions, $d_{3,2}$ significantly increased on day 6 compared with those on the day of making. Meanwhile, the $d_{3,2}$ of PPI stabilised w/o/w emulsions in the presence of diacetyl or 3-pentanone on day 6 was significantly larger than those of PPI stabilised w/o/w emulsions in the absence of aromas on day 6.

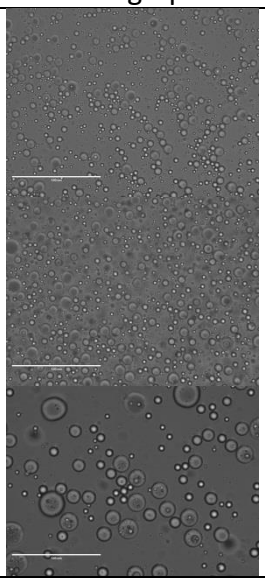
As suggested by the micrographs, droplet size distribution and $d_{3,2}$, coalescence would not be a factor impacting on aroma release for the Tween 20 and OSA starch stabilised w/o/w emulsions. The slight decrease of $d_{3,2}$ in Tween20 and OSA starch stabilised w/o/w emulsions in the absence or in the presence of diacetyl after 6-day storage might be due to w_1 in the oil droplets migrating to w_2 over time. The mechanisms of water and water soluble materials transport in w/o/w emulsions are discussed in section 2.1.3.6. Since the osmotic pressure was balanced, water transport between two aqueous phases might result from the thin lamellae of surfactant forming in the oil film, the PGPR micelles and/or Tween20 and OSA starch reverse micelles in the oil phase.

The larger droplet size of PPI stabilised w/o/w emulsions compared to Tween 20 and OSA starch stabilised w/o/w emulsions was possibly because PPI stabilised oil droplets coalesced during emulsification or immediately after emulsification. PPI was not the least surface active among the three emulsifiers as reported in Tables 6.1-2. Thus, it was speculated that protein tends to adsorb slower at the oil-water interface compared to the other two types of emulsifier leading to coalescence. It is well known that low molecular weight surfactants are more efficient to reduce the interfacial tension than the macromolecules such as polysaccharides and proteins (Beverung et al. 1999, Manglik et al. 2001). Tween 20 could decrease the oil-water interfacial tension in about 10 s (Schröder et al. 1998). It was also reported that pea protein reduced the interfacial tension by two stages: a rapid decrease during the first 15 min and a slow decrease until adsorption equilibrium reached after 5000 s (Gharsallaoui et al. 2009). OSA starch was found to reduce the interfacial tension approximately less than 1000 s (Tesch et al. 2002). This slower adsorption of protein might arise from several reasons: the protein possibly has a larger molecular weight than the starch and should have the large size than Tween 20; PPI mainly contains globular proteins, which usually rearrange themselves after they adsorb at the interface as described in section 2.2.2.3; the possible repulsive interactions between PPI molecules might have a negative influence on droplet formation. Besides, since PPI changes conformation gradually at the interface, it causes naked regions of oil to form and hence promoting coalescence. Ostwald ripening/ coalescence in presence of the hydrophilic aroma diacetyl in PPI stabilised w/o/w emulsions might be due to the hydrogen

bonding between diacetyl and the protein loop in water as previously discussed in section 2.4.2.4. Coalescence in PPI stabilised w/o/w emulsions in the presence of the hydrophobic aroma 3-pentanone could result from a hydrophobic interaction between 3-pentanone and the protein as also discussed in section 2.4.2.4. It is speculated that the interactions potentially removed protein from the droplet surface. The larger droplets size in the PPI stabilised w/o/w emulsions would negatively impact on stability as creaming velocity increases with increasing droplet size according to Stokes' law (section 2.1.3.1). Accelerated creaming would lead to a higher probability of droplet collisions which could result in coalescence. So, it appears that the protein stabilised emulsion was affected by aroma addition due to aroma-protein interactions whereas emulsifier-aroma interactions appeared to be largely absent for the Tween 20 and OSA starch stabilised emulsions.

The emulsion characteristics of control o/w emulsions using these three hydrophilic emulsifiers in the absence of aroma compound on the day of making are shown in Table 5.3. It can be seen that for each hydrophilic emulsifier, $d_{3,2}$ of the o/w emulsion was smaller than that of the respective w/o/w emulsion. This is because of the fact that there is the internal water phase in the oil phase of w/o/w emulsions as well as the hydrophobic emulsifier at the w_1-o interface and the viscosity is different. Similar to the w/o/w emulsions, the o/w emulsions stabilised with PPI had a larger mean droplet size and a smaller specific surface area than those using Tween 20 or OSA starch. This might result from coalescence of PPI stabilised o/w emulsions during or after emulsification.

Table 5.3 Emulsion characteristics of control o/w emulsions using Tween 20, OSA starch or PPI in the absence of aroma on day of making. Scale bar in micrographs is 100 µm.

Emulsion type	$d_{3,2}$(µm)	Micrographs
owT	3.15±0.02[a*]	
owS	3.11±0.07[a]	
owP	6.96±0.01[b]	

* Different letters indicate statistically significant values ($P < 0.05$).

5.4 AROMA RELEASE UNDER STATIC CONDITION

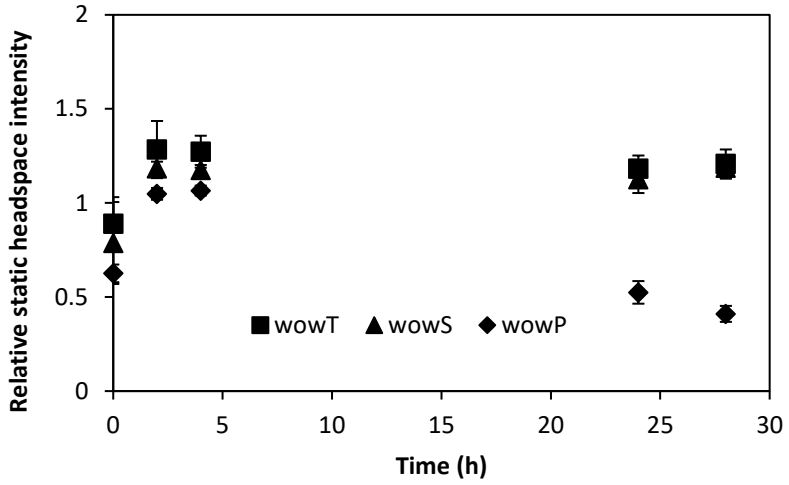
Aroma release behaviour under the static headspace analysis was measured to explore the time when the headspace intensity reached equilibrium. Relative headspace intensity was measured at five time slots. An equilibrium was supposed to be reached when there was no difference in the relative headspace intensity measured between two continuous time slots.

5.4.1 Hydrophilic aroma

Figure 5.3 shows the relative static headspace intensity of the hydrophilic aroma diacetyl above the w/o/w emulsions and the control o/w emulsions. The relative headspace intensity of diacetyl over w/o/w emulsions stabilised with Tween 20 or OSA starch remained unchanged over 4 h, which indicates an equilibrium at 4 h. However, it took roughly 24 h for the PPI stabilised w/o/w emulsion to reach equilibrium. Although the headspace intensity of PPI stabilised w/o/w emulsions was unchanged over 4 h, the intensity was lower after 24 h. It took less than 4 h for diacetyl to reach equilibrium in the headspace over all o/w emulsions (Figure 5.3B). For w/o/w emulsions or o/w emulsions, PPI stabilised emulsions always showed the lowest relative headspace intensity, compared with OSA starch stabilised emulsions and Tween 20 stabilised emulsions. This means that diacetyl tended to remain more in PPI stabilised emulsions than in Tween 20 or OSA starch stabilised emulsions.

At equilibrium, the experimental relative headspace intensities of diacetyl above w/o/w emulsions at 28 h and above o/w emulsions at 4 h were compared to the theoretical relative headspace intensity at equilibrium in Table 5.4. It can be seen that only the experimental relative headspace intensity over the PPI stabilised w/o/w emulsions at equilibrium was significantly lower than the theoretical value (Table 5.4A). The same was found for the PPI stabilised o/w emulsions (Table 5.4B).

A



B

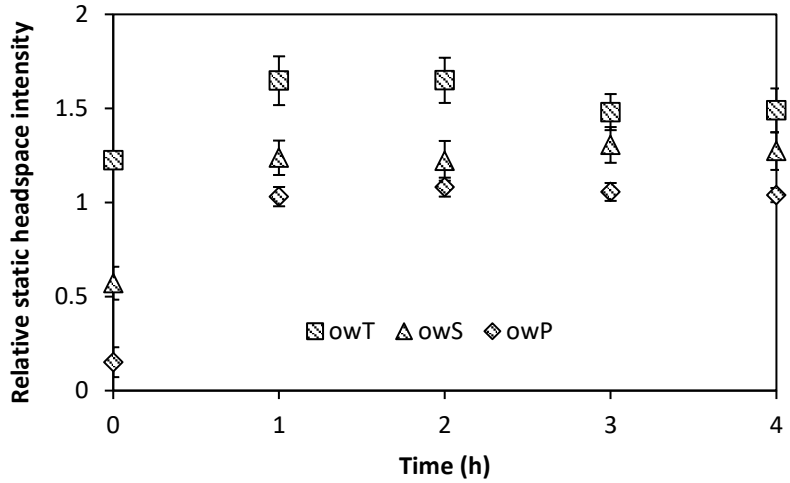


Figure 5.3 Relative static headspace intensity of diacetyl above A) w/o/w emulsions using Tween 20, OSA starch or PPI or B) control o/w emulsions over time. The analysis time lasted 28 h for w/o/w emulsions whereas it lasted 4 h for o/w emulsions. Each value is based on 3 replicates. The error bars show the standard deviation.

Table 5.4 Theoretical relative headspace intensity compared with experimental relative headspace intensity of diacetyl above A) w/o/w emulsion or B) o/w emulsion.

A

Emulsifier type	Relative headspace intensity
Theoretical	1.21^{b*}
Tween 20	1.21 ± 0.08^{b}
OSA starch	1.19 ± 0.06^{b}
PPI	0.41 ± 0.04^{a}

* Different letters indicate statistically significant values ($P < 0.05$).

B

Emulsifier type	Relative headspace intensity
Theoretical	1.4^{bc}
Tween 20	1.49 ± 0.12^{c}
OSA starch	1.27 ± 0.10^{b}
PPI	1.04 ± 0.04^{a}

* Different letters indicate statistically significant values ($P < 0.05$).

Since the prediction of the theoretical relative headspace intensity only takes account of the lipid effect (section 5.2.2), there should be other reasons responsible for these results. The big decline in relative headspace intensity for PPI stabilised emulsions could be because there were more oil droplets creaming. The larger the emulsion droplets, the more the droplets cream and the thicker the cream layer. The cream oil layer could be a barrier for the aroma diffusion from other droplets underneath the creamed oil droplets and for the diffusion from w_2 as well. Secondly, Tables 5.2 showed an increase in $d_{3,2}$ of PPI stabilised w/o/w emulsions respectively after 2 day storage. Although there was no data collected on day 1, it can be speculated that the droplet size in the

presence of diacetyl grew in the first 24 h of storage. One may not expect that the droplet size has a significant impact on aroma distribution in the headspace at equilibrium, since the Equations 5.1-9 (section 5.2.2) used to predict these theoretical equilibrium distributions in each phase of the emulsions and the headspace do not take account of the emulsion microstructure. Droplet size though can indirectly affect the aroma distribution in emulsions and in the headspace because of changes in the total emulsifier concentration, or in the relative distribution of emulsifiers between adsorbed and non-adsorbed states.

It has been reported that the aroma headspace concentrations at equilibrium above o/w emulsions were dependent on droplet size, presumably because there were aroma-emulsifier interactions and the interactions were different in the adsorbed and non-adsorbed states of emulsifier (Miettinen et al. 2002, van Ruth et al. 2002b, van Ruth et al. 2002c). A significant decrease in the headspace intensity of α-pinene, myrcene, limonene and β-caryophyllene and a decrease in total aroma headspace intensity was found with increasing droplet size (Paraskevopoulou et al. 2009). This was caused by the substantial increase in the thickness of the adsorbed casein layer when moving from a fine sized emulsion produced by high pressure homogenizer to the one with a much larger size made by high speed homogenizer. Besides, it was resulted from differences in the ratio of adsorbed to non-adsorbed casein emulsifier. As the droplet size of PPI stabilised w/o/w emulsions in the presence of diacetyl increased, the droplet surface area decreased, so the protein adsorbed at the interface decreased and non-adsorbed protein increased. It suggested diacetyl was likely to bind to the non-adsorbed protein. The hydrophilic aroma

compound diacetyl may interact with PPI due to a large amount of polar regions in the protein such as protein loops in water (section 2.4.2.4). Indeed, binding of diacetyl to sodium caseinate (Landy et al. 1995, Lubbers et al. 1998), raw egg albumin (Leland 1997) and gelatin (Bakker 1998) has previously been reported. It was also found that carbonyl flavour compounds can bind to soy proteins and β-lactoglobulin (Okeefe et al. 1991, Andriot et al. 2000). The nature of the binding could be determined by the measurement of binding constants or binding sites through chromatography, equilibrium dialysis, static headspace, fluorimetry and nuclear magnetic resonance spectroscopy (Guichard et al. 2000, Jouenne et al. 2000, Chalier et al. 2007, Tavel et al. 2008). On the other hand, this result may also result from the instability of the PPI stabilised w/o/w emulsions over time.

As a result, 24 h and 4 h were chosen for diacetyl release over w/o/w emulsions and o/w emulsions respectively.

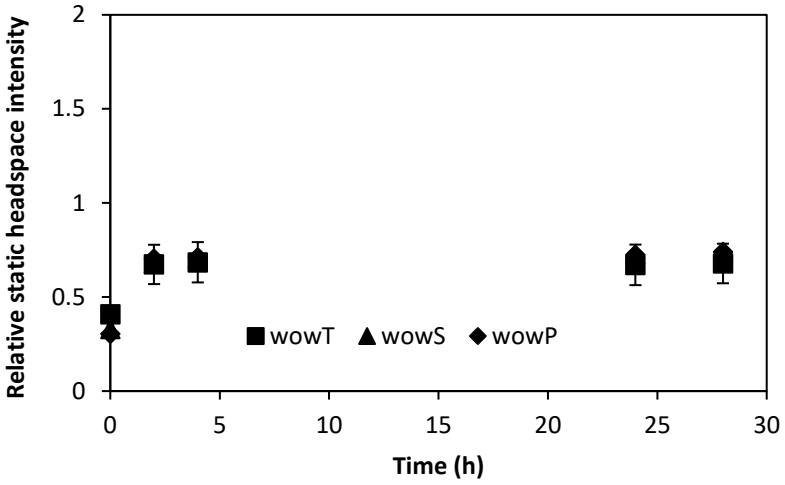
5.4.2 Hydrophobic aroma

Figure 5.4 shows the relative static headspace intensity of the hydrophobic aroma 3-pentanone above the w/o/w emulsions and the control o/w emulsions. It can be seen that the relative headspace intensity of 3-pentanone reached an equilibrium in 4 h for w/o/w emulsions (Figure 5.4A). After 24 h, the headspace intensities above the w/o/w emulsions were still unchanged independent of the type of emulsifier. There was also no difference in the headspace intensities above the w/o/w emulsions after 2 h. For o/w emulsions

(Figure 5.4B), the headspace intensities of 3-pentanone showed an equilibrium at less than 4 h. The headspace intensity above Tween 20 stabilised emulsions was always higher than that above the other two emulsions. There was not much difference in the headspace intensity between the OSA starch and the PPI stabilised o/w emulsions.

In Table 5.5, the experimental relative headspace intensity at equilibrium is compared with the theoretical relative headspace intensity above w/o/w emulsions at 28 h and above o/w emulsions at 4 h at equilibrium. The experimental intensities above w/o/w emulsions were all higher than the theoretical value, but only OSA starch and PPI stabilised w/o/w emulsions were significantly higher (Table 5.5A). o/w emulsions had a significantly higher headspace intensity in experiment than theory predicted independent of emulsifier type (Table 5.5B).

A



B

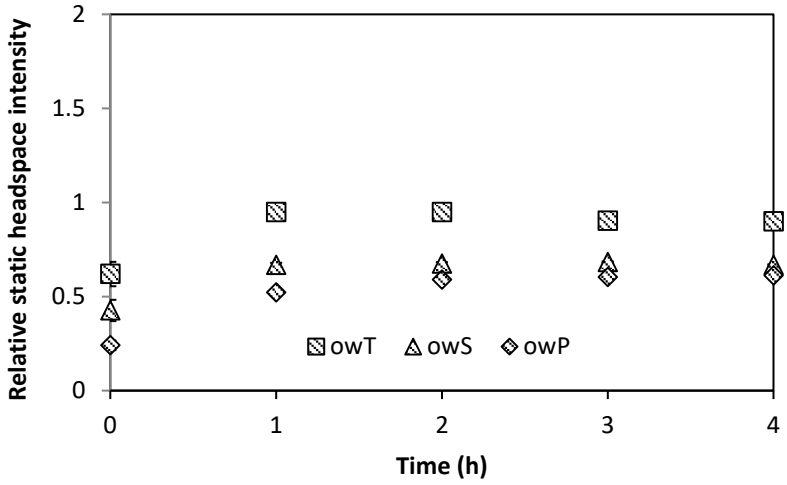


Figure 5.4 Relative static headspace intensity of 3-pentanone above A) w/o/w emulsions stabilise with Tween 20, OSA starch or PPI and B) control o/w emulsions over time. The analysis time lasted 28 h for w/o/w emulsions whereas it lasted 4 h for o/w emulsions. Each value is based on 3 replicates. The error bars show the standard deviation.

Table 5.5 Theoretical relative headspace intensity compared with experimental relative headspace intensity of 3-pentanone above A) w/o/w emulsion or B) o/w emulsion.

A

Emulsifier type	Relative headspace intensity
Theoretical	0.55^{a}
Tween 20	0.68 ± 0.11^{ab}
OSA starch	0.74 ± 0.01^{b}
PPI	0.74 ± 0.00^{b}

* Different letters indicate statistically significant values ($P < 0.05$).

B

Emulsifier type	Relative headspace intensity
Theoretical	0.42^{a}
Tween 20	0.90 ± 0.01^{d}
OSA starch	0.67 ± 0.00^{c}
PPI	0.61 ± 0.01^{b}

* Different letters indicate statistically significant values ($P < 0.05$).

Since the hydrophobic aroma favours oil, the oil phase has the main effect on the release of 3-pentanone above emulsions. Thus, as expected from Table 5.1, there was a big decline in the headspace intensity of 3-pentanone above emulsions. However, the experimental relative headspace intensities were all higher than the theoretical value and significant differences were found in OSA starch and PPI stabilised w/o/w emulsions. This result could be due to the creaming of all emulsions. It has been reported that creaming led to the oil droplets of egg yolk-stabilised o/w emulsions transferring very rapidly near the emulsion surface and therefore, the static headspace concentration of a hydrophobic aroma limonene above these emulsions was enhanced (Karaiskou

et al. 2008). OSA starch and PPI stabilised w/o/w emulsions had a lower headspace intensity than Tween 20 stabilised emulsions. This was also found for the o/w emulsions. It might be because there was a hydrophobic interaction through inclusion complex formed by the helical amylose of OSA starch and the hydrophobic aroma 3-pentanone (section 2.4.2.3) and between the non-polar part of PPI and 3-pentanone (section 2.4.2.4).

As a result, 24 h and 4 h were chosen for 3-pentanone release over w/o/w emulsions and o/w emulsions respectively.

5.5 AROMA RELEASE UNDER DYNAMIC CONDITION

Dynamic headspace analysis was carried out to evaluate the release behaviour over water, o/w emulsions and w/o/w emulsions. It reveals how fast the air-liquid interface replenish the headspace during headspace dilution. The rate to replenish a diluting headspace is attributed to one of two aspects, either the equilibrium headspace intensity is low, therefore the mass transfer required to achieve equilibrium is low (Linforth et al. 2010), or there was no ingredient-aroma interactions that limit aroma release to the headspace.

The first point in the dynamic headspace analysis was regarded as the equilibrium headspace intensity, which was set to 100%. Afterwards the equilibrium was disturbed during headspace dilution so the dynamic headspace intensity was decreasing. The headspace intensities measured after the first point were divided by the first point of average headspace intensity,

which indicate the remaining headspace intensity compared to the first point, 100%. As expected in Table 5.1, when only considering the lipid effect, the theoretical headspace concentration of the hydrophilic aroma diacetyl at equilibrium for all systems was relatively close, but highest over o/w emulsions, followed by w/o/w emulsions and water. Thus, the mass transfer required to replenish 100% of headspace should be most for o/w emulsions, then for w/o/w emulsions and last for water. For the hydrophobic aroma 3-pentanone, the theoretical headspace concentration at equilibrium was highest over water, followed by w/o/w emulsions and o/w emulsions. Hence, the mass transfer required to replenish 100% of headspace is most for water, then for w/o/w emulsions and last for o/w emulsions. If the experimental results do not follow the trend, there should be other factors that influenced the dynamic aroma release, such as the interactions between the aroma compounds and the hydrophilic emulsifier.

5.5.1 Hydrophilic aroma

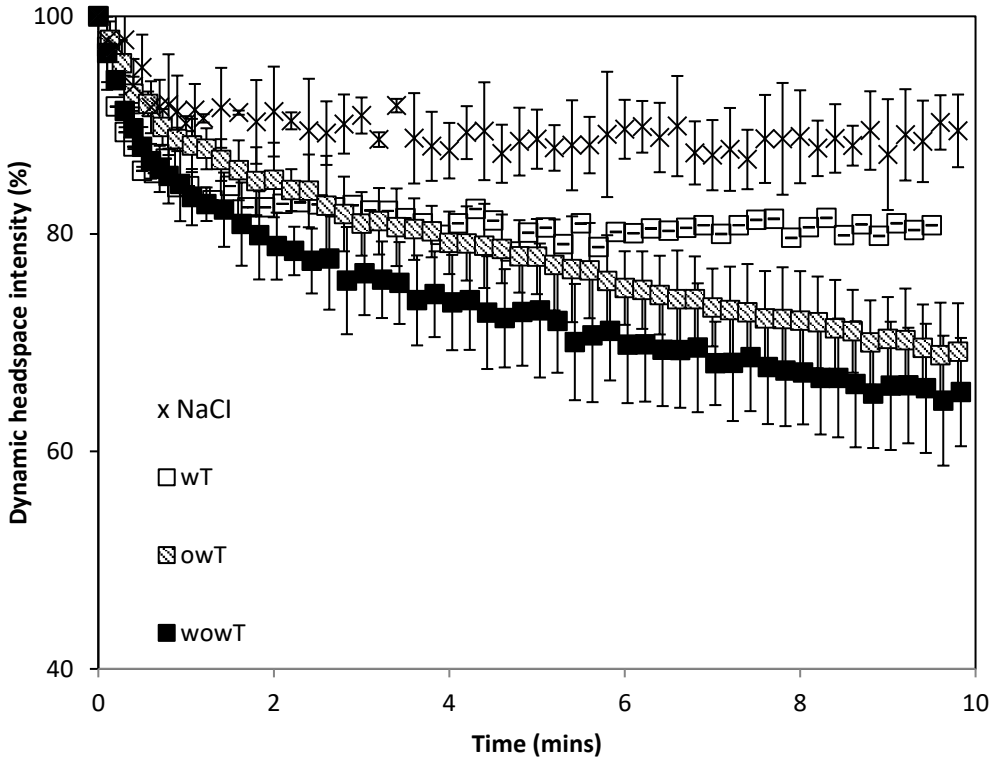
Figure 5.5 demonstrates the dynamic headspace intensity of the hydrophilic aroma diacetyl changing with time. For Tween 20 (Figure 5.5A), the water control ‘wT’ (preparation is described in section 5.2.1) had a lower headspace intensity than ‘NaCl‘. It suggests there were interactions between diacetyl and Tween 20 over 10 min. Diacetyl headspace intensity from ‘wT’ was similar as that from ‘owT’ at around 5 min, but afterwards it was higher than that from ‘owT’. Tween 20 stabilised w/o/w emulsions had a slightly lower headspace

intensity than Tween 20 stabilised o/w emulsions and Tween 20 in water.

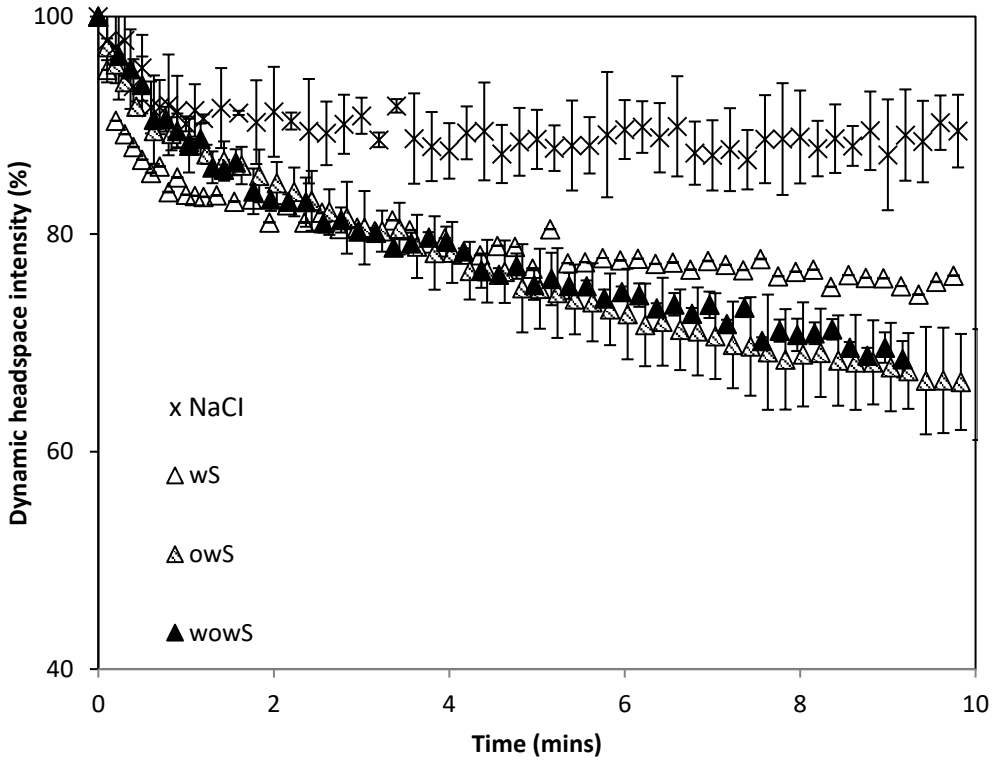
For OSA starch (Figure 5.5B), ‘wS’ also had a lower headspace intensity than ‘NaCl’, which indicates the OSA starch-diacetyl interaction in 10 min. Diacetyl replenished the headspace from OSA starch in water a bit faster than that over OSA starch stabilised o/w emulsions w/o/w emulsions, while the latter two were almost the same. Although there were significant differences in droplet size between the o/w emulsions and the w/o/w emulsions using Tween 20 or OSA starch (Table 5.4), the release behaviour of diacetyl from these systems did not show a big difference. This could be due to diacetyl favouring water. Although there is w_1 in the oil droplets of the w/o/w emulsions, the internal water phase volume in w/o/w emulsions (12%) is small. So the dispersed oil droplets in w/o/w emulsions had less influence on diacetyl release.

For PPI (Figure 5.5C), there was no difference in the headspace intensity between ‘wP’ and ‘NaCl’. PPI stabilised o/w emulsions had the fastest decline in headspace intensity for all samples. For PPI samples, the fastest headspace replenishment was found over ’owP’, then ‘wP’ and last ‘wowP’.

A


100
80
60
40
Dynamic headspace intensity (%)
0
2
4
6
8
10
Time (mins)
x NaCl
wT
owT
wowT

B


100
80
60
40
Dynamic headspace intensity (%)
0
2
4
6
8
10
Time (mins)
x NaCl
wS
owS
wowS

C

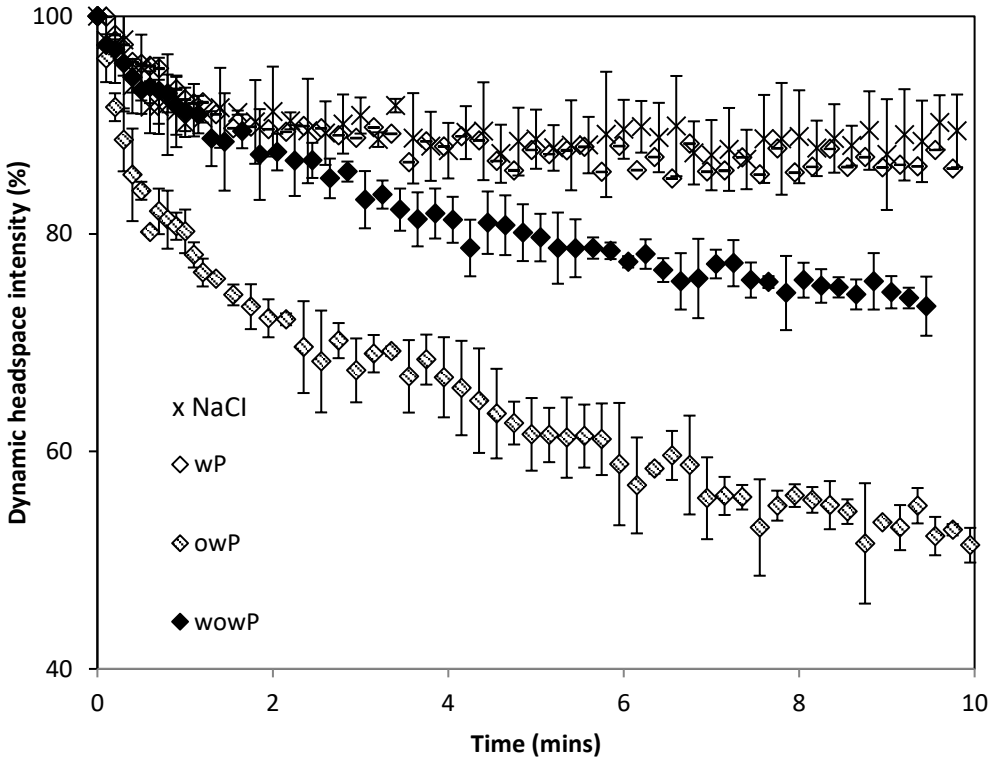


Figure 5.5 Dynamic headspace intensity of diacetyl over control water, control o/w emulsions and w/o/w emulsions over time in the presence of A) Tween 20 B) OSA starch C) PPI. Y axis starts from 40%.

In order to investigate the aroma retention in the headspace at the end of the 10-minute dynamic analysis period, the aroma headspace intensity (%) at the last point compared to the initial 100% is presented in Table 5.6. Lower aroma retention in the headspace suggests a stronger resistance of the air-liquid interface against aroma release. It can be seen that there was no significant difference in headspace intensity at the end of the dynamic headspace analysis among water controls independent of hydrophilic emulsifier type. Also, there was no significant difference among all emulsions, only except for PPI stabilised

o/w emulsions, which was significantly different from the other samples. In terms of the emulsifier type, only when using PPI, o/w emulsions showed significantly lower aroma retention in the headspace, then w/o/w emulsions and last water controls. But for Tween 20 and OSA starch, only water controls were significantly different from o/w emulsions and w/o/w emulsions. As a result, o/w emulsions and w/o/w emulsions had a stronger resistance to the movement of diacetyl than water controls, no matter which hydrophilic emulsifier was used.

In summary, the different replenishment trends of diacetyl in dynamic headspace over different samples could be due to the hydrophilic emulsifier type, the system type or/ and the difference in emulsion droplet size.

Table 5.6 Aroma retention of diacetyl at the end of the dynamic headspace analysis from different systems

System type	Aroma retention (%)
wT	$80.79\pm3.31^{de*}$
owT	69.16 ± 4.46^{bc}
wowT	65.45 ± 4.98^{b}
wS	76.18 ± 1.39^{cde}
owS	66.16 ± 5.10^{b}
wowS	68.49 ± 1.68^{bc}
wP	85.08 ± 1.75^{e}
owP	51.27 ± 0.90^{a}
wowP	74.32 ± 1.41^{bcd}

* Different letters indicate statistically significant values ($P < 0.05$).

5.5.2 Hydrophobic aroma

The changes in the dynamic headspace intensity of the hydrophobic aroma 3-pentanone with time are shown in Figure 5.6. As expected, there was a trend that water had the fastest decrease in the headspace intensity of 3-pentanone, then w/o/w emulsions and last is o/w emulsions. This is due to 3-pentanone favouring oil so the oil phase plays a major role of 3-pentanone release. However, 'wS' had a slower replenishment in the headspace than others among all water controls. A possible explanation is the hydrophobic interaction between the amylose molecules in water and 3-pentanone through the inclusion complex that inhibited the aroma moving across the air-liquid interface and to the headspace (Plug et al. 1993, Decourcelle et al. 2004, Keršienė et al. 2008). 3-pentanone from o/w emulsions replenishing the headspace faster than that from w/o/w emulsions might be because the aroma amount required to replenish 100% of headspace was less for o/w emulsions than for w/o/w emulsions (Table 5.1). The replenishment of 3-pentanone from Tween 20 stabilised emulsions was faster than that from OSA starch and PPI stabilised emulsions. This could be because a low molecular weight surfactant such as Tween 20 laden interface is thinner than an interface laden with a polymeric emulsifier such as protein or OSA starch (Hasenhuettl et al. 2008). Interfacial thickness has an impact on diffusion of the aroma molecules across the interface, with thicker interfaces decreasing release rate.

Table 5.7 shows the aroma retention in the headspace at the end of the 10-minute dynamic analysis period. There was no difference in each system type,

i.e. water, o/w emulsions and w/o/w emulsions, for all emulsifier types Tween 20, OSA starch or PPI. There was no difference between water controls and w/o/w emulsions no matter which hydrophilic emulsifier was used. However, water controls were significantly different from o/w emulsions for each hydrophilic emulsifier. Thus, it can be concluded that water controls had higher 3-pentanone retention than o/w emulsions independent of hydrophilic emulsifier type.

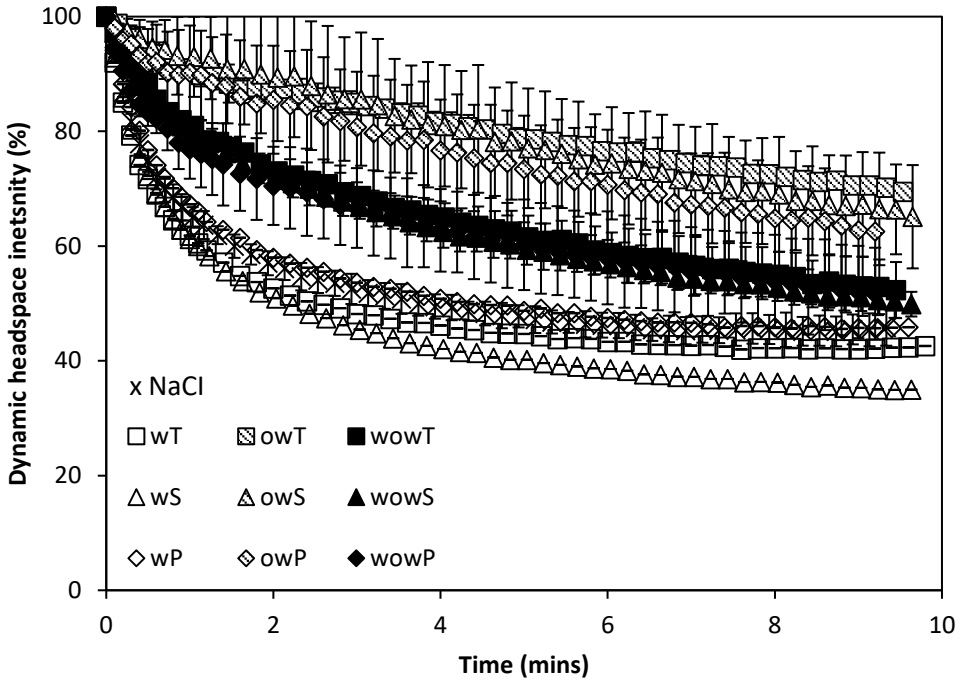


Figure 5.6 Dynamic headspace intensity of 3-pentanone over control water, control o/w emulsions and w/o/w emulsions over time. A lower headspace intensity corresponds to the system releasing less aroma.

Table 5.7 Aroma retention of 3-pentanone at the end of the dynamic headspace analysis from different systems

System type	Aroma retention (%)
wT	42.59 ± 4.23^{ab}
owT	69.49 ± 1.15^{e}
wowT	52.19 ± 3.46^{bcd}
wS	34.97 ± 0.51^{a}
owS	65.12 ± 6.37^{de}
wowS	49.88 ± 2.15^{abc}
wP	45.85 ± 5.11^{ab}
owP	62.53 ± 9.20^{cde}
wowP	51.70 ± 8.01^{bcd}

* Different letters indicate statistically significant values ($P < 0.05$).

In summary, the differences in the dynamic headspace intensity of 3-pentanone over the different samples were driven by the system type, where water showed the slowest headspace replenishment, followed by the o/w emulsions and lastly the w/o/w emulsions. OSA starch in water appeared to interact with the 3-pentanone.

5.6 CONCLUSIONS

The studies showed that Tween 20 and OSA starch stabilised w/o/w emulsions were stable independent of aroma inclusion, type of aroma inclusion and sample age. PPI stabilised w/o/w emulsions in the absence of aroma were stable for one week. But the PPI stabilised w/o/w emulsions in the presence of 3-pentanone or diacetyl were unstable. Under static headspace analysis, 4 h and 24 h were sufficient for the aroma equilibrium distribution over o/w

emulsions and w/o/w emulsions respectively. The system type including water, o/w emulsions and w/o/w emulsions and the hydrophilic emulsifier type including Tween 20, OSA starch and PPI as well as droplet size, emulsion stability and creaming had different impacts on aroma release. Thus, to investigate the hydrophilic emulsifier influence on aroma release alone, better control over emulsion microstructure should be addressed. The next main thesis Chapter 6 introduces the manufacturing route for w/o/w emulsions using stirred cell membrane emulsification to control the emulsion microstructure. The final main thesis Chapter 7 introduces how these emulsions were analysed for aroma release to validate the release behaviour.

6 DROPLET SIZE CONTROL OF W/O/W EMULSIONS THROUGH STIRRED CELL MEMBRANE EMULSIFICATION

In this chapter, the research to obtain better microstructure control of w/o/w emulsions destined to the study of aroma release is reported. The w/o/w emulsions were stabilised as throughout this PhD research with Tween 20, OSA starch or PPI as the representative of a low molecular weight surfactant, starch and protein respectively. These w/o/w emulsions were produced through stirred cell membrane emulsification in order to obtain similarly sized droplets. By visual observation, all emulsions creamed over time due to the oil-water density difference. A published model was used to predict the droplet size of all three types of w/o/w emulsions. Micrographs, droplet size and droplet uniformity of w/o/w emulsions are reported. Varying process parameters of the membrane emulsification including the rotational speed and the injection speed, and varying hydrophilic emulsifier concentration were applied. Emulsion stability over 13 day storage was also investigated.

6.1 INTRODUCTION

Emulsion stability is dependent on the droplet size distribution. An emulsion is more stable with narrower droplet size distribution to suppress Ostwald ripening as described in section 2.1.3.5. Broad droplet size distribution of an emulsion is usually obtained via conventional emulsification methods,

including high speed mixing, high pressure valve homogenisation, colloid mill processing, microfluidisation and ultrasonic methods (McClements 2005). These conventional emulsification methods rely on high shear or high pressure to disrupt and form droplets, which can also cause damage to temperature-sensitive or shear-sensitive ingredients in emulsions. Thus, novel emulsification methods including membrane emulsification and microchannel homogenising has been studied to obtain a narrow droplet size distribution (Schröder et al. 1998, Walstra et al. 1998, Joscelyne et al. 2000, Schubert et al. 2003, Spyropoulos et al. 2014). Meanwhile, these mild emulsification processes are protective for many temperature and shear sensitive ingredients used in emulsion systems, such as starches and proteins (van der Graaf et al. 2005).

Membrane emulsification (ME) is a drop-by-drop process instead of breaking down droplets. It is a process that forces the dispersed phase through a microporous membrane into the continuous phase with the solubilised emulsifier to form an emulsion (Safwat et al. 1994). The dispersed droplets with the emulsifier adsorbed at the surface will form and detach at the end of membrane pores with a desired droplet size. The droplet formation and detachment from the membrane surface are determined by four main forces including shear, pressure, interfacial tension and buoyancy forces, as well as the shape, material and porosity of the membrane and the shape of the flow channel (Spyropoulos et al. 2014). As a result, membrane emulsification could produce a range of emulsion droplet sizes and fairly monodisperse droplets under varying process conditions.

Cross-flow membrane emulsification is one of the most commonly used membrane emulsification types, which uses a tubular membrane with the continuous phase flowing along the inside or the outside of the tube (Spyropoulos et al. 2011, Hancocks et al. 2013). However, it has been reported to be unsuitable for producing droplets larger than 15 μm, as the dispersion needs to recycle over the membrane surface leading to damage of the previously formed droplets by the pump and system fittings (Gijsbertsen-Abrahamse et al. 2004). Larger emulsion droplets are appropriate for applications of controlled release or encapsulation in food (Schuch et al. 2014), due to less interfacial area of emulsion droplets available for the transfer of solutes which can contribute to a sustained and sufficient release (Dragosavac et al. 2012).

Rotating membrane emulsification is another commonly used membrane emulsification method. It is a process of rotating the membrane in the continuous phase and generating a centrifugal force for the dispersed phase permeating through the membrane (Lloyd et al. 2014). It was found that w/o/w emulsions manufactured by rotating membrane emulsification had a slower release rate of sodium chloride than those manufactured by cross-flow membrane emulsification and high shear emulsification, as a consequence of the magnitude and duration of shear forces acting on formed w/o droplets during emulsification (Pawlik et al. 2012). It also has been reported that when using whey protein isolate, the droplet size of o/w emulsions did not significantly change with increasing rotational velocity of the membrane, due to electrostatic repulsion of the negatively charged proteins slowing down the

adsorption process (Pawlik et al. 2013).

Stirred cell membrane emulsification is another established set up of membrane emulsification and this is the one used in this PhD research. It is available at laboratory scale and it is also a scalable technique for commercial production via scaling from the stirred cell approach to an oscillating membrane system (Holdich et al. 2010). The schematic set up of stirred cell membrane emulsification used here is shown in Figure 6.1 (Dragosavac et al. 2012).

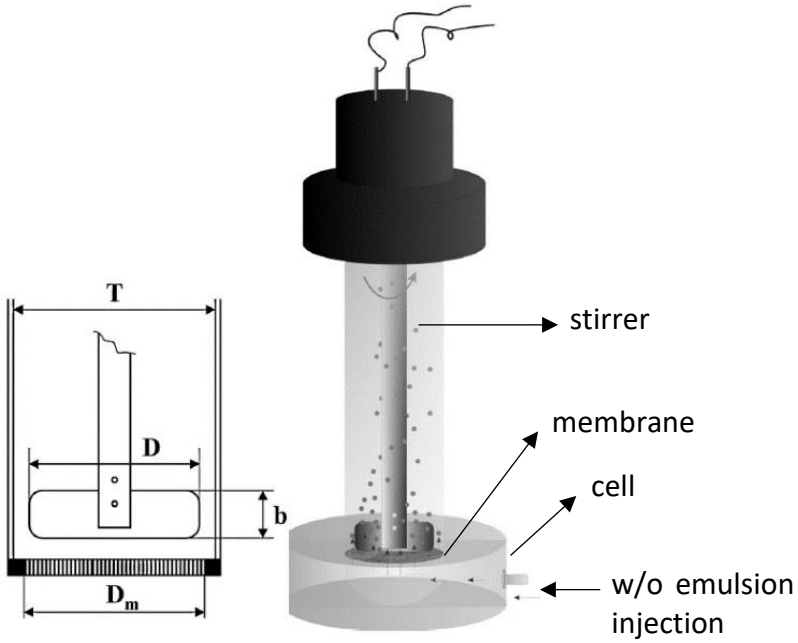


Figure 6.1 Schematic set up of Dispersion Cell with simple paddle stirrer above a flat-disc membrane (Dragosavac et al. 2012)

In this membrane emulsification, a flat disc microporous membrane is placed in a stirred cell. The dispersion phase, in this case a w/o emulsion, was injected

into the cell base through the membrane. A simple paddle stirrer above the membrane induced shear at the membrane surface. The setup resulted in droplet formation and detachment during membrane emulsification. A stirred cell is an unusual device for membrane emulsification. This is because one may prefer inducing a uniform shear field at the surface of the membrane for the generation of uniformly sized droplets. However, in previous studies it was found that a stirrer cell with a consequently varying radial shear field at the membrane surface could produce uniformly sized droplets of o/w emulsions (Kosvintsev et al. 2005, Stillwell et al. 2007) and w/o/w emulsions (Dragosavac et al. 2012). When using stirred cell membrane emulsification to produce w/o/w emulsions, a two-step emulsification method is also used. This first step involves processing w_1 with o to produce the primary w/o emulsion by high speed homogenising. The second step is processing the w/o emulsion into w_2 to form the w/o/w emulsion by stirred cell membrane emulsification. The w/o emulsion is injected through a hydrophilic membrane fitted in the cell base. The external water phase containing the hydrophilic emulsifier is circulated above the membrane by a stirrer. Using stirred cell membrane emulsification, w/o/w emulsions have previously been produced with PGPR as the hydrophobic emulsifier in the oil phase (o), and Tween 20 or polyoxyethylene-polyoxypropylen copolymer (Pluronic F-68) as the hydrophilic emulsifier in w_2. These emulsions had a wide range of uniform droplet sizes, between 100 and 430 µm with a span of around 0.5, and showed high encapsulation efficiency of copper in the internal water phase of more than 94% (Dragosavac et al. 2012). Uniform w/o/w emulsions stabilised with gelatin and poly-vinyl alcohol (PVA)

were also obtained through stirred cell membrane emulsification (Imbrogno et al. 2015). This membrane emulsification could also form uniform o/w emulsions with Tween 20 or Pluronic F-68 (Dragosavac et al. 2008) and w/o emulsions with modified polyether-polysiloxane (ABIL EM 90) (Morelli et al. 2016) with a range of droplet sizes.

In Chapter 5, emulsions were prepared by conventional emulsification and it was concluded that better control of emulsion microstructure should be addressed for aroma release analysis. Thus, the aim related to this chapter was to produce similar and well defined droplet sizes in w/o/w emulsions with the three hydrophilic emulsifiers Tween 20, OSA starch and PPI through stirred cell membrane emulsification. Aroma release analysis over these similarly sized w/o/w emulsions is introduced in Chapter 7.

In order to predict the droplet size, a published model (Dragosavac et al. 2008) for stirred cell membrane emulsification derived from a force balance of the capillary force (function of interfacial tension and pore size) and the drag force (function of a shear stress and the droplet size) acting on a strongly deformed droplet at a single membrane pore was used. The droplet diameter (x) was predicted with Equation 6.1, where τ_{max} is the maximum shear stress at membrane surface, r_p is the pore radius (10 µm) and γ is the interfacial tension.

$$x=\frac{\sqrt{18\tau_{max}^2 r_p^2+2\sqrt{81\tau_{max}^4 r_p^4+4\tau_{max}^2 r_p^2 \gamma^2}}}{3\tau_{max}}$$

Equation 6.1

The maximum shear stress over the whole membrane area was calculated with Equation 6.2, where η is the viscosity of continuous phase, ω is angular velocity, r_{trans} is the transitional radius (where the shear stress reaches the maximal value) and δ is the boundary layer thickness.

$$\tau_{max} = 0.825\eta\omega r_{trans}\frac{1}{\delta} \qquad \text{Equation 6.2}$$

The boundary layer thickness and the transitional radius are given in Equation 6.3 and Equation 6.4 respectively, where ρ is the density of the continuous phase, D is the stirrer diameter (3.2 cm), T is the tank diameter (4 cm), b is the blade height (1.2 cm), n_b is the number of impeller blades (2) and Re is the Reynolds number.

$$\delta = \sqrt{\frac{\eta}{\rho\omega}} \qquad \text{Equation 6.3}$$

$$r_{trans} = 1.23\frac{D}{2}(0.57+0.35\frac{D}{T})(\frac{b}{T})^{0.036}n_b{}^{0.116}\frac{Re}{1000+1.43Re}$$

Equation 6.4

The Reynolds number (Re) is given in Equation 6.5.

$$Re = \omega\rho D^2/(2\pi\eta) \qquad \text{Equation 6.5}$$

The interfacial tension between the disperse phase (w/o emulsion) and the continuous phase (w_2), the viscosity of w_2 and the density of w_2 were measured utilising the methods described in the following.

6.2 METHODS SPECIFIC TO THE RESULTS REPORTED IN THIS CHAPTER

6.2.1 Interfacial tension measurement

The surface tension of water or oil and the interfacial tension between water and oil at equilibrium was measured by a tensiometer (model DB2KS, White Electric Instrument Co. Ltd., UK) using the Du Nouy ring method at room temperature (21 ± 5 °C). The ring was cleaned before and after use by dipping in acetone, deionized water, Aqua Regia and deionized water in sequence, followed by heating in a flame to remove any residue. The glass beaker used for containing the sample was cleaned in detergent solution, deionized water, acetone and then Aqua Regia, before drying with the compressed air. Water or oil was placed at the bottom of the beaker. The ring was manually lowered to just under the surface of the water or oil and the tensiometer signal was set to zero. When measuring the water-oil interface, oil was slowly added onto the water surface and the tensiometer signal was ensured to be set to zero. The ring was then manually and slowly pulled out across the air-water, air-oil or water-oil interface until it was completely detached from the surface/ interface. The surface/ interfacial tension value was automatically shown on the tensiometer screen. Different water phases were prepared as follows: water, 0.1 M NaCl in water, 2% Tween 20 in water, 2% Tween 20 with 0.1 M NaCl in water, 4% OSA starch in water, 4% OSA starch with 0.1 M NaCl in water, 1.5% PPI in water and 1.5% PPI with 0.1 M NaCl in water. Different oil phases were prepared by mixing different ingredients in sunflower oil: oil, 4% PGPR in oil and w/o emulsion (made by the method described in section 6.2.4.1). All samples

were prepared in triplicate and each sample was analysed once.

6.2.2 Viscosity measurement

The viscosity of w_2 of the w/o/w emulsions was measured using a rheometer (MCR 301, Anton Paar, Germany) fitted with a concentric cylinder double gap geometry (DG26.7/T200). The test was run with a controlled shear rate in the range of 0.1-1000 s^{-1}. A total number of 21 points were acquired at a rate of 5 points/decade with each point measured every 5 s. Measurement temperature was 20 °C. Different water phases were prepared as follows: water, 2% Tween 20 with 0.1 M NaCl in water, 4% OSA starch with 0.1 M NaCl in water and 1.5% PPI with 0.1 M NaCl in water. All samples were prepared in triplicate and each sample was analysed once.

6.2.3 Density measurement

The density of w_2 of the w/o/w emulsions was measured using a density meter (DMA 5000, Anton Paar, Germany). Measurement temperature was 20 °C. Different water phases were prepared as follows: water, 2% Tween 20 with 0.1 M NaCl in water, 4% OSA starch with 0.1 M NaCl in water and 1.5% PPI with 0.1 M NaCl in water. All samples were prepared in triplicate and each sample was analysed once.

6.2.4 Preparation of w/o/w emulsions through stirred cell membrane emulsification

6.2.4.1 Stirred cell membrane emulsification

w/o/w emulsions were manufactured by two steps. First, w/o emulsions were produced by slowly adding w_1 into the oil phase under high shear mixing (Ultra Turrax, model T25, IKA Works, USA) at 24000 rpm for 5 min in an ice bath to avoid overheating. This process condition was used to ensure the mean diameter of the internal water droplets in w/o emulsions was around 0.5 μm (Vladisavljevic et al. 2003). The condition of processing the w/o emulsion was different from Chapter 4 and 5 in order to produce w/o emulsions into smaller droplet size for further processing of the w/o/w emulsions. The w/o/w emulsions were then manufactured using stirred cell membrane emulsification. The membrane emulsification was set up by placing a flat disc membrane (Micropore Technologies Ltd., Loughborough, UK) in the base of the Dispersion Cell (Micropore Technologies Ltd., Loughborough, UK) illustrated in Figure 6.1 (Dragosavac et al. 2012). A hydrophilic nickel membrane containing uniform cylindrical pores with a pore diameter of 20 μm and a pore spacing of 200 μm was used, see Figure 6.2. In order to increase the hydrophilicity of the membrane surface to avoid the dispersed phase (w/o emulsions) spreading over the membrane surface, the membrane was pre-soaked for at least 30 min in a 2% wetting agent solution. The 2% wetting agent solution was prepared by mixing a proprietary wetting agent in acetone and stored in a fridge.

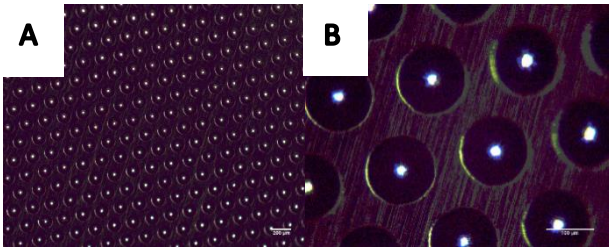


Figure 6.2 Micrographs of the membrane with a pore diameter of 20 µm and a pore spacing of 200 µm. The scale bar in A and B represents 200 µm and 100 µm respectively.

A cylinder glass bottle was fitted to the base with a paddle blade stirrer driven by a 24V DC motor and power supply (INSTEK Model PR 3060). Paddle rotational speed was controlled by applied voltage of 3, 5, 7, 9 and 11 V (approximately 197, 444, 706, 966, 1214, 1488 rpm respectively). The initial volume of w_2 in the cell was around 10 cm^3. The membrane was then placed into the cell, before adding the remaining volume of w_2 above the membrane in the glass bottle. Except when using PPI in w_2, deionized water instead of w_2 was filled into the cell first. Then the solution with PPI was poured above the membrane in the cylinder glass bottle to obtain a final PPI concentration of 1.5% in w_2. This is in order to prevent membrane blockage caused by the protein during emulsification if PPI was initially placed in the cell. The dispersed phase w/o emulsions contained in a glass syringe with a diameter of 29 mm were injected through the microporous membrane surface by a peristalic pump (Watson-Marlow-Bredel Pump 101U/R, Cornwall, UK) at constant injection speed between 1 and 15 ml/min. The experiments were run until the dispersed

phase volume fraction reached 10 vol.%, estimated from the syringe scale. Batches of 100 g were prepared. Once the desired amount of w/o emulsion had passed through the membrane, the pump and stirrer were switched off. The w/o/w emulsions were transferred into a glass beaker. Prepared sodium azide solution was then added to the w/o/w emulsion to obtain a final sodium azide concentration at 0.02% to prevent microbial spoilage. The addition of sodium azide after emulsion manufacture was to avoid causing damage to the membrane. The beaker was then covered by Cling film to avoid evaporation until further analysis and stored at room temperature (21 ± 5 °C). By visual observation, all emulsions creamed over time due to the oil-water density difference. The membrane was cleaned with detergent solution in an ultrasonic bath for 1 min, followed by ultrasonically rinsing for 1 min with deionized water three times and then with acetone, before drying using compressed air.

6.2.4.2 Emulsion phases

The formulation of the w/o/w emulsion corresponded to the formulation presented in section 5.2.1, except for the ratio of w_1/o: w_2. In Chapter 4 and 5, the ratio of w_1/o: w_2 was 3:7 (w/w). In this chapter, the ratio of w_1/o: w_2 of 1:9 (v/w) was used for the sake of simplicity. Because using a lower w/o emulsion volume fraction reduced the time required to prepare the number of samples required in this Chapter.

The hydrophilic emulsifier concentrations are described below. To investigate the concentration of hydrophilic emulsifier influencing on droplet size under

different process conditions, the final emulsifier concentrations in w_2 of 0.5%, 1%, 2% or 4% for Tween 20, 2% or 4% for OSA starch and 0.5%, 1.5%, 3% or 6% for PPI were used. Here, 4% was used as the maximum starch concentration since preliminary experiments showed that at higher concentrations the emulsions were not uniform in droplet size using the membrane emulsification set up. This could have been a result of the viscosity increase of w_2.

6.2.4.3 Process parameters

Process parameters of stirred cell membrane emulsification, including the injection speed applied to the w/o emulsion and the rotational speed applied to w_2, are described below.

To investigate the process parameter effect on droplet size and uniformity five injection speeds including 1, 3, 5, 10 and 15 ml/min and six rotational speeds including 197, 444, 706, 966, 1214 and 1488 rpm, w_2 containing a final concentration of 2% Tween 20, 4% OSA starch or 1.5% PPI were applied. Initially, Tween 20 stabilised w/o/w emulsions were started with the membrane emulsification setup. Their emulsion microstructure was only characterised by microscopy and image analysis as described in the subsequent section 6.2.5. For OSA starch and PPI stabilised w/o/w emulsions, microscopy and droplet size distribution analysis described in sections 6.2.5-6 were used for their microstructure characteristics. Only w/o/w emulsions manufactured at the injection speed of 1 ml/min and the rotational speed of 197, 706, 1214

and 1488 rpm were prepared in triplicate. All other w/o/w emulsions were prepared only once.

To investigate the effect of emulsifier concentration and rotational speed on droplet size, injection speed was set constant to 1 ml/min. The rotational speed was set to 197 rpm, 706 rpm or 1488 rpm, representing low, mid and high level respectively. w/o/w emulsions were prepared just once.

To investigate emulsion stability in terms of droplet size and droplet size distribution, w_2 contained a final concentration of 2% Tween 20, 4% OSA starch or 1.5% PPI. For each type of w/o/w emulsion, one sample was prepared through membrane emulsification at the injection speed of 1 ml/min and the rotational speed of 197, 706 and 1488 rpm.

6.2.5 Microscopy and image analysis

The microstructure of the w/o/w emulsions was visualised using an epifluorescence microscope (L3201LED, GT Vision Ltd., Sufflok, UK) immediately after emulsion preparation and regularly during 13 day storage. Day of making refers to the day when emulsions were prepared. Day 1, 2, 6 and 13 were 1, 2, 6 and 13 days after emulsion preparation respectively. Slides were prepared using a few drops of emulsion and micrographs were taken immediately. The magnification range was between x4 and x20 utilising a bright field objective. At least three randomly selected areas of each slide were imaged at each magnification and three slides were prepared for each

emulsion. Only when investigating the effect of process parameters on emulsion microstructure of Tween 20 stabilised w/o/w emulsions, the images were analysed. For processing the image, the droplets in the selected image were scanned and outlined by the software ImageJ (National Institutes of Health, USA). Then the number of the droplets and their size were analysed by the software. The average droplet size (d_{av}) and standard deviation (SD) were calculated based on at least 100 imaged droplets per sample. As an indication of droplet uniformity of the Tween 20 stabilised w/o/w emulsions, the coefficient of variation (CV) was determined as defined by Equation 6.6:

$$CV\ (\%) = SD / d_{av} \times 100 \qquad \text{Equation 6.6}$$

6.2.6 Droplet size measurement

The droplet size distribution of the secondary emulsion droplets (the emulsified w_1/o emulsion) of the w/o/w emulsion was analysed immediately after preparation and during storage over 13 days. A laser diffraction particle size analyser (Malvern Mastersizer 2000, Worcestershire, UK) was used with deionized water as the dispersing medium. The piece of the equipment used in this chapter is different to the one used in Chapters 4 and 5, so the method is described here. Measurement set up and analysis was controlled by the instrument's software package. The refractive indices of the dispersion medium (water) and the dispersed phase (oil) were 1.33 and 1.47 respectively. The absorption value of the dispersed phase was set to 0. Once the emulsion was dispersed in the water, three measurements were taken and the raw data

was fitted with a general model or single peak model. For each emulsion one sample was prepared, but for emulsions made at the injection speed of 1 ml/min and the rotational speed of 197 rpm, 706 rpm, 1214 rpm or 1488 rpm no matter which of the hydrophilic emulsifier was used were prepared in triplicate. The results are reported as the droplet size on a volume basis ($d_{4,3}$), and the Sauter diameter ($d_{3,2}$). Droplet size distributions are presented as cumulative volume distribution.

6.3 PREDICTION OF DROPLET DIAMETER

In order to predict the droplet diameter, different properties are required to be able to apply the published model (Equations 6.1-5). These properties including surface/ interfacial tension, viscosity and density are reported as follows.

6.3.1 Surface/ interfacial tension of all liquid phases

Table 6.1 shows the surface tension of deionized water at 20 °C was as expected at about 73 mN/m for the chosen measurement temperature (Vargaftik et al. 1983). There was no significant difference in surface tension of deionized water and water with 0.1 M NaCI. This is in agreement with a previous study in which it was reported that the addition of 0.1 M NaCI in water did not increase the surface tension by more than 0.5 mN/m at 20 °C (Lima et al. 2013). For each hydrophilic emulsifier, 0.1 M NaCI also had no influence on the surface tension.

Table 6.1 Surface tension of water or oil (liquid phase) at 20 °C based on Du Nouy ring analysis.

Aqueous phase	Surface tension (mN/m)
Deionized water	72.8±0.5[d]*
0.1 M NaCl	73.3±0.7[d]
2% Tween 20	38.6±0.6[a]
2% Tween 20, 0.1 M NaCl	38.9±0.5[a]
4% OSA starch	55±1.0[c]
4% OSA starch, 0.1 M NaCl	53.5±0.4[c]
1.5% PPI	50.0±1.0[b]
1.5% PPI, 0.1 M NaCl	49.5±0.6[b]
Oil phase	
oil	35.9±0.2[a]
4% PGPR in oil	35.9±0.1[a]
w/o emulsion**	36.2±0.2[a]

* Different letters indicate statistically significant values ($P < 0.05$). Statistics of the surface tension of aqueous phase and oil phase was analysed separately.

** w/o emulsion: 0.1 M NaCl in w, 4% PGPR in o and w:o = 2:3 (w/w).

As expected, the addition of the hydrophilic emulsifier lowered the surface tension and there were significant differences among the three emulsifiers. The lowest surface tension was found for Tween 20, followed by PPI and OSA starch. The surface tension values of the three emulsifiers are in agreement with those reported in literature (Niño et al. 1998, Prochaska et al. 2007, Krstonošić et al. 2011, Yusoff et al. 2011, Xu et al. 2012). As a non-ionic low molecular weight surfactant Tween 20 efficiently forms a compact interfacial layer where the hydrophilic head group is attached to the water phase and the hydrophobic tail region is attached to air or the oil phase (Hasenhuettl et al. 2008). While as macromolecules OSA starch and PPI form a thick viscoelastic layer as a

consequence of the configurational order of proteins and starch at the interface (Garti 1997b), only a fraction of the interface is actually covered by the protein and starch segments and the other regions of the interface remain at high free energy levels (Damodaran et al. 1997, McClements 2005). Therefore, the protein and starch are less surface active than the surfactant.

A lower surface tension of oil was found compared with the surface tension of water. But none of the surface tension data acquired on oil were significantly different from each other. The addition of the hydrophobic emulsifier PGPR, whether it was used in oil or to produce the w/o emulsion, did not significantly lower the surface tension of oil.

Table 6.2 shows the oil-water interfacial tension of all liquid phases used in the stirred cell membrane emulsification experiment. The addition of NaCI did not affect the oil-water interfacial tension. The addition of PGPR decreased the water-oil interfacial tension by a large extent as previously reported (Márquez et al. 2010). When using PGPR to produce the w/o emulsion, the w/o emulsion-water interfacial tension was significantly higher than 4% PGPR in oil-water interfacial tension. It was because some PGPR molecules adsorbed at the surface of the internal water droplets (40%) in the w/o emulsion. Non-adsorbed PGPR molecules distributed at the water-oil interface were responsible for the reduction of the interfacial tension. When adding 0.1 M NaCI in water, the interfacial tension between water with 0.1 M NaCI and 4% PGPR in oil was significantly lower than that between water and 4% PGPR in oil. It was expected that the availability of salt would enhance the adsorption of PGPR molecules at

the interfaces thus more lowering the oil-water interfacial tension (Hino et al. 2000, Fechner et al. 2007, Pawlik et al. 2010, Wolf et al. 2013).

Table 6.2 Interfacial tension between the different water and oil phases at 20 °C based on Du Nouy ring analysis.

water phase	Oil phase	Interfacial tension (mN/m)
water	oil	18.2±0.2^{i}*
	4% PGPR oil	3.7±0.2^{d}
	w/o emulsion**	15.8±0.4^{h}
0.1 M NaCl	oil	18.4±0.2^{i}
	4% PGPR oil	2.6±0.1^{bc}
	w/o emulsion	15.7±0.1^{h}
2% Tween 20, 0.1 M NaCl	oil	5.2±0.2^{e}
	4% PGPR oil	0.8±0.1^{a}
	w/o emulsion	5.9±0.4^{e}
4% OSA starch, 0.1 M NaCl	oil	14.5±0.2^{g}
	4% PGPR oil	3.0±0.2^{bcd}
	w/o emulsion	13.7±0.2^{g}
1.5% PPI, 0.1 M NaCl	oil	9.8±0.1^{f}
	4% PGPR oil	2.5±0.1^{b}
	w/o emulsion	10.5±0.4^{f}

* Different letters indicate statistically significant values ($P < 0.05$).

** w/o emulsion: 0.1 M NaCl in w, 4% PGPR in o and w:o = 2:3 (w/w).

As expected, Tween 20 lowered the interfacial tension most, followed by PPI and OSA starch. Their interfacial tension values are in agreement with literature (Tesch et al. 2002, Gharsallaoui et al. 2009, Biswal et al. 2016). Besides, the interfacial tension between w_2 and oil or between w_2 and w/o emulsion was significantly higher than that between w_2 and 4% PGPR in oil. This was in agreement with the surface tension findings. The interfacial tension values between w_2 containing Tween 20, PPI or OSA starch and the w/o emulsion were

used for the published model calculation to predict the droplet diameter of w/o/w emulsion by Equation 6.1.

6.3.2 Viscosity

Figure 6.3 reports the average viscosity of water and w_2 as a function of shear rate. The viscosity of aqueous phases fluctuated at the lower shear rate in the range of 0.1-10 s^{-1}. Hence the viscosity at the shear rate from 10-1000 s^{-1} was shown. w_2 contained 2% Tween 20, 4% OSA starch or 1.5% PPI with 0.1 M NaCl.

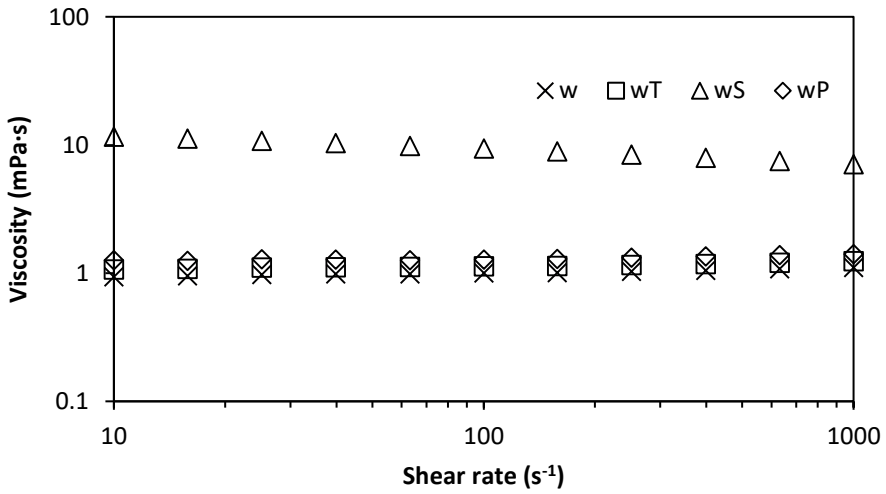


Figure 6.3 Average viscosity of water and w_2 with different emulsifiers measured at 20 °C. Standard deviation is within symbol size.

The viscosity behaviour of all phases was Newtonian in the investigated shear rate range. The OSA starch containing phase showed a slight indication of onset

of shear thinning at the higher shear rates, which has been reported in literature (Park et al. 2004, Dokic 2008). This system was also significantly higher viscous. The viscosity measured as the lowest shear rate as possible is more corresponding to the state of the aqueous phases at rest. Thus, the viscosity of w_2 at 10 s^{-1} was used for the published model calculation in Equations 6.2, 6.3 and 6.5, which was 1.01 mPa·s for added Tween 20, 11.57 mPa·s for added OSA starch and 1.26 mPa·s for added PPI.

6.3.3 Density

Table 6.3 shows the density of water and w_2, which was significantly different from each other. The density of w_2 with added Tween 20, OSA starch and PPI was used for the published model calculation in Equations 6.3 and 6.5.

Table 6.3 Densities of different water phase measured at 20 °C

Water phase	Density (g/cm^3)
Water	0.9982 ± 0.0000^{a}*
2% Tween 20, 0.1 M NaCl	1.0050 ± 0.0000^{b}
4% OSA starch, 0.1 M NaCl	1.0173 ± 0.0000^{d}
1.5% PPI, 0.1 M NaCl	1.0065 ± 0.0002^{c}

* Different letters indicate statistically significant values ($P < 0.05$).

6.3.4 Predicted droplet diameters

The droplet diameters predicted with the model based on Equations 6.1-5 as a function of rotational speed were shown in Figure 6.4. It is worth noting that

the model does not take account of the injection speed of the disperse phase.

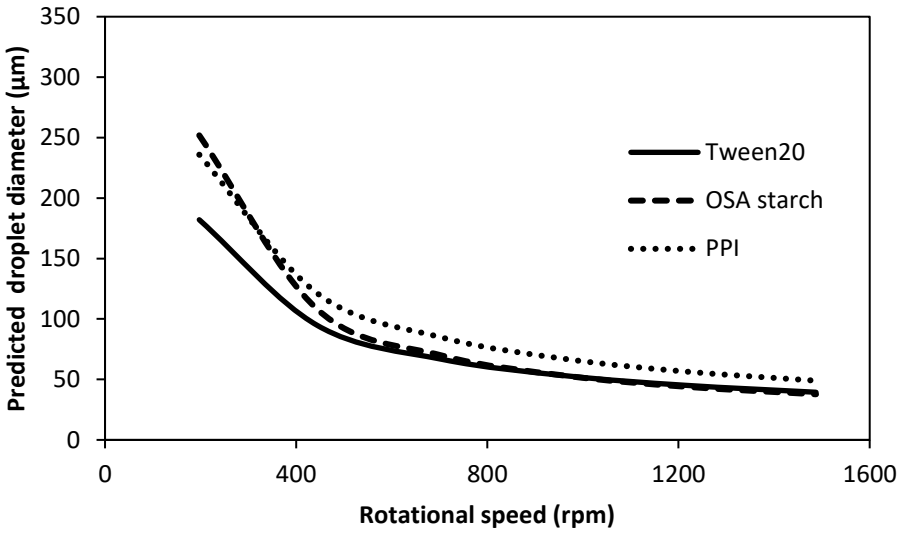


Figure 6.4 Predict droplet diameter of w/o/w emulsions stabilised with Tween 20, OSA starch or PPI based on a published model (Dragosavac et al. 2008)

The predicted droplet diameter decreased with increasing rotational speed. As expected based on the interfacial tension values (Table 6.2) the predicted droplet diameter for the Tween 20 stabilised system was the lowest at all rotational speeds. However, while the predicted droplet diameter of the OSA starch stabilised w/o/w emulsion was higher at low rotational speeds, it asymptotically approached the value of the Tween 20 stabilised system at higher rotational speeds. This might be explained by the fact that at low rotational speed, the droplet formation and detachment is mainly affect by the capillary force, which is as a function of interfacial tension. With increasing rotational speed, it is affected by both the capillary force and the drag force

(function of shear tress that is affected by the viscosity of the continuous phase). The shape of the predicted droplet diameter curve for the PPI stabilised system was very similar to that of the Tween 20 stabilised system and only shifted to slightly larger droplet diameters. This was because the viscosity of these two systems was comparable and interfacial tension as well as density slightly increased for the protein-stabilised system. The published model prediction was used to decide on the processing parameters for preparing w/o/w emulsions of comparable droplet size using these three different emulsifiers.

6.4 EFFECT OF PROCESS PARAMETERS ON DROPLET SIZE

The effect of five injection speeds (1-15 ml/min) and six rotational speeds (197-1488 rpm) on mean droplet size and uniformity of w/o/w emulsions is presented. w_2 of 2% Tween 20, 4% OSA starch or 1.5% PPI was used.

Figure 6.5 shows the micrographs of w/o/w emulsions stabilised with Tween 20, OSA starch or PPI manufactured at the injection speed of 1 ml/min and different rotational speeds. The micrographs of w/o/w emulsions produced at 3-15 ml/min were not shown, as they were similar to these micrographs in Figure 6.5. The micrographs show the characteristics of w/o/w emulsions as already seen in section 4.3. A better control of the emulsion droplets with the improvement in uniformity is clearly visible, compared to the micrographs of w/o/w emulsions manufactured by high shear mixing presented in Figure 5.1. It also can be found that droplet size independent of emulsifier type decreased with increasing rotational speed.

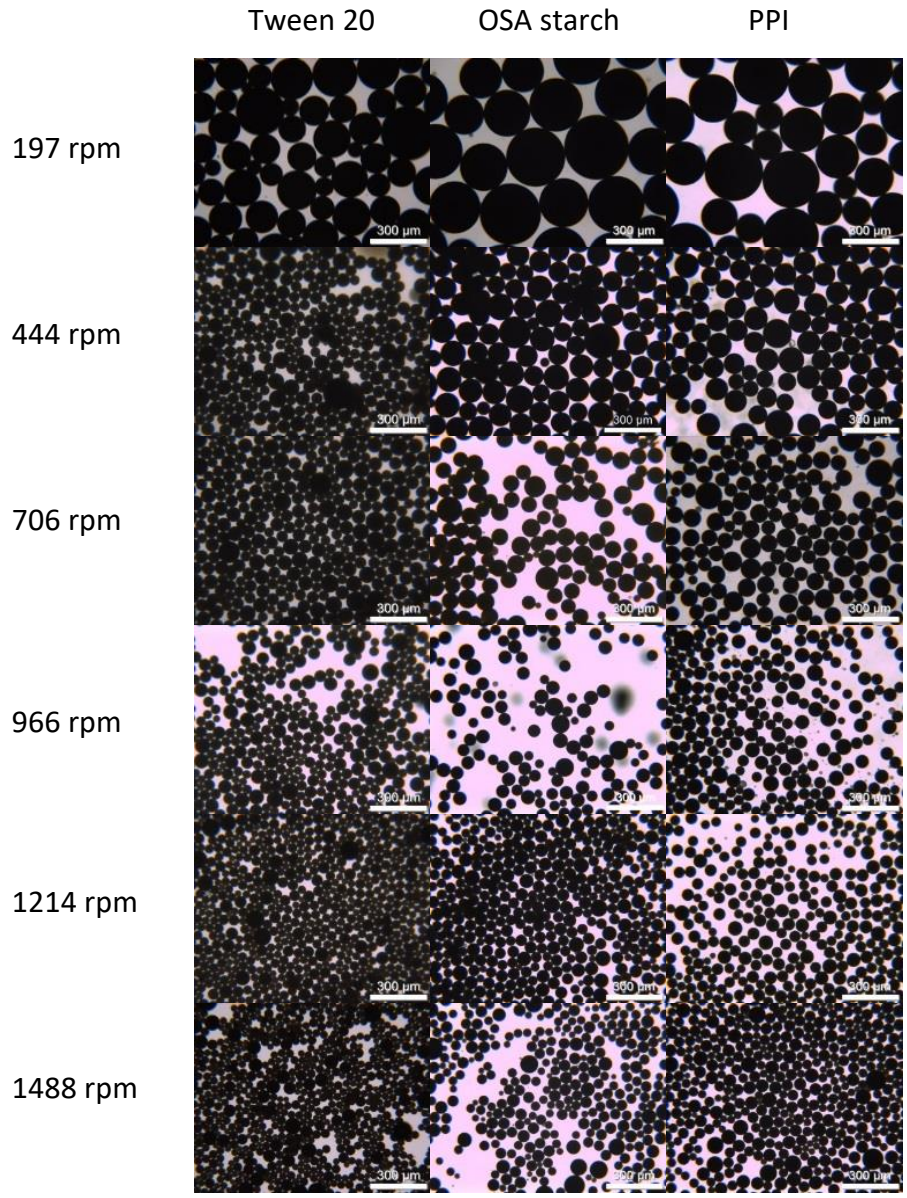


Figure 6.5 Micrographs of w/o/w emulsions stabilised with A) Tween 20 B) OSA starch or C) PPI through stirrer cell membrane emulsification under different injection speeds (1-15 ml/min) and rotational speeds (197-1488 rpm). The scale bar in each micrograph is 300 µm.

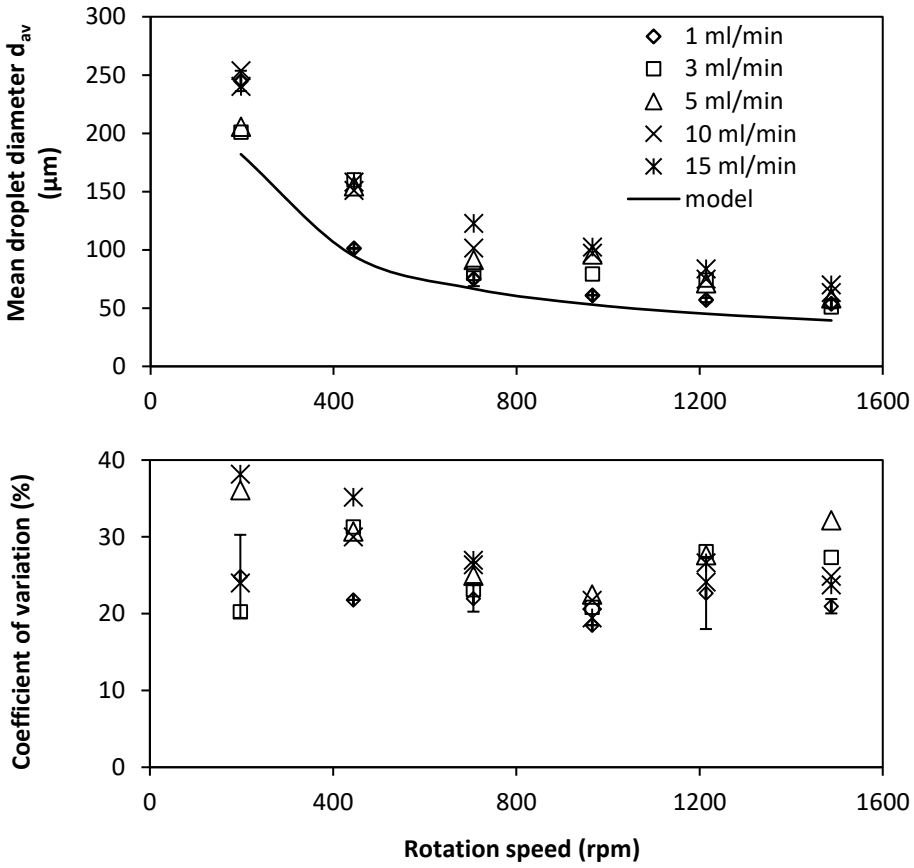
w/o/w emulsions stabilised with Tween 20 were initially produced to check the setup of stirred cell membrane emulsification making w/o/w emulsions under

different process parameters. Images analysis were only used to calculate the mean droplet size d_{av} and coefficient of variation CV (as emulsion uniformity) for their emulsion characteristics. The analysis results of Tween 20 stabilised w/o/w emulsions are presented in Figure 6.6A. When using the rotational speed of 197 rpm d_{av} was larger than 200 μm with the exception of the injection speed of 1 ml/min and this is larger than the pore spacing between the pores. As this means that the emulsion droplets needed to deform before detachment from the membrane surface, where the newly formed emulsion droplets built up at the membrane surface rather than immediately detachment (Pawlik et al. 2012). This was due to the small shear force leading a layer of droplets formed at the membrane surface, which then slowly dispersed into the bulk upon further shear stress. Besides, it could be that not all of the membrane pores were used to produce droplets during emulsification providing more space for droplets to grow on the membrane (Vladisavljevic et al. 2002). Otherwise coalescence would have occurred and the resulting CV would have been large rather than small. The lower the CV value, the more uniform the droplet size. When the lowest injection speed of 1 ml/min was applied, uniform emulsion droplets with the CV between 20% and 30% could be obtained. The lowest CV for the Tween 20 stabilised system was 18% at 1 ml/min injection speed and 966 rpm rotational speed. Droplets were less uniform with a CV of approximately 40% when the very high injection speed of 15 ml/min or/ and the extreme cases of lower and higher end of the rotational speed range was applied. This could be due to some droplets being broken up by the paddle stirrer under extreme high rotational speed (1500 rpm) and droplets being

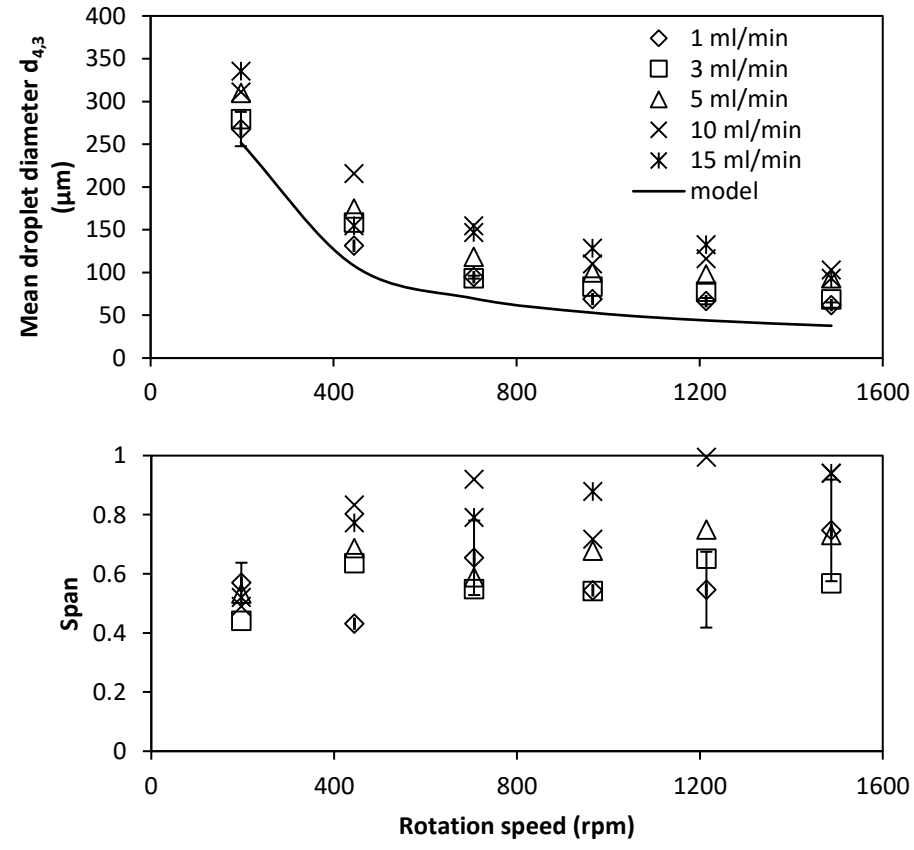
creaming under the extreme low rotational speed and/ or the highest injection speed (Dragosavac et al. 2012).

A similar trend was found for the OSA starch (Figure 6.6B) and the PPI stabilised w/o/w emulsions (Figure 6.6C) where mean droplet sizes decreased with increasing rotational speed and decreasing injection speed. This is in agreement with the micrograph findings. When the rotational speed was 197 rpm mean droplet sizes of both types of w/o/w emulsions were greater than 260 µm, which was also larger than the spacing between the pores of 200 µm. Span representing the emulsion uniformity is reported in Figure 6.6B and C. The lowest span for the OSA starch stabilised system was 0.4 when processed at 1ml/min injection speed and 444 rpm rotational speed. The lowest span for the PPI stabilised emulsions was 0.4 when processed at 10 ml/min injection speed and 197 rpm rotational speed. The same was found for the Tween 20 stabilised system, narrow droplet size distributions were generally produced when the lowest injection speed of 1 ml/min was applied. Here, spans of OSA starch and PPI stabilised w/o/w emulsions generated at the lowest injection speed of 1 ml/min were around 0.6. The droplet size (d_{av}) for Tween 20 is not comparable to the droplet size ($d_{4,3}$) for OSA starch and PPI. However, it is comparable in Figure 6.7, which is discussed in section 6.5.

A


Mean droplet diameter d_{av} (µm)
1 ml/min
3 ml/min
5 ml/min
10 ml/min
15 ml/min
model
Coefficient of variation (%)
Rotation speed (rpm)

B


Mean droplet diameter $d_{4,3}$ (µm)
1 ml/min
3 ml/min
5 ml/min
10 ml/min
15 ml/min
model
Span
Rotation speed (rpm)

C

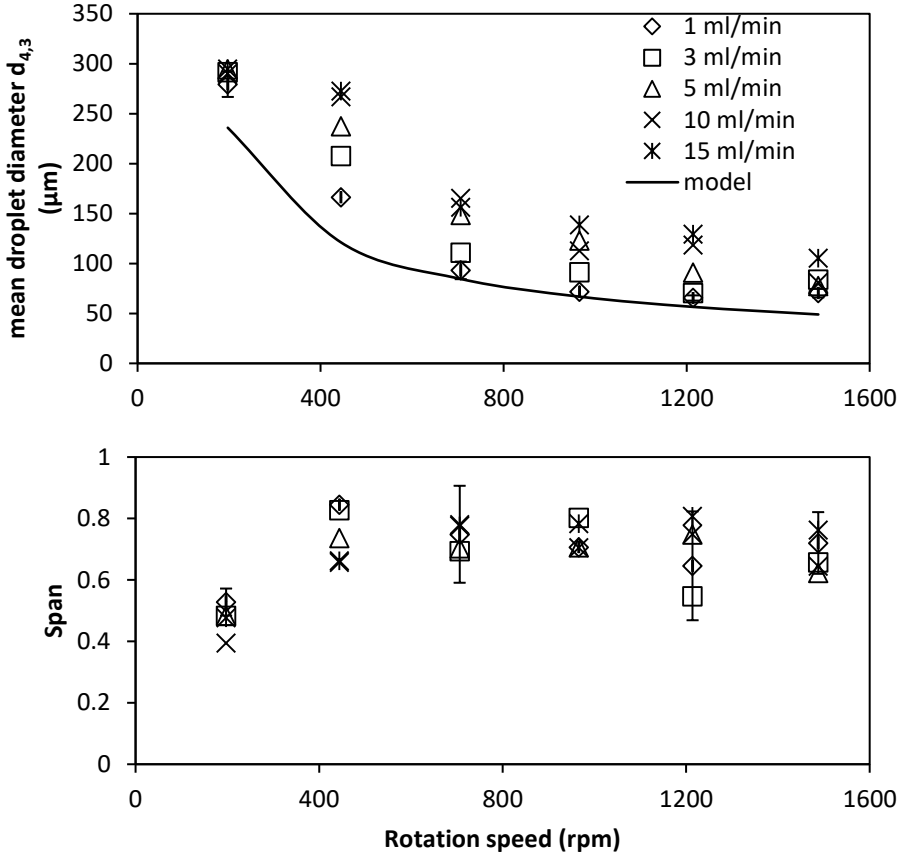


Figure 6.6 Effect of rotational speed (197-1488 rpm) and injection speed (1-15 ml/min) on mean droplet diameter (d_{av} or $d_{4,3}$) and coefficient of variation (CV) or span of w/o/w emulsions stabilised with A) Tween 20 (2%) B) OSA starch (4%) or C) PPI (1.5%) obtained experimentally and as predicted by the published model for comparison. $d_{av} = \sum_{i=1}^{n} \frac{d_i}{N}$, where d_i is the ith dimeter of the droplet and N is the total number of the droplets counted. $CV = \frac{\sum_{i=1}^{n}(d_i - d_{av})/N}{d_{av}} \times 100\ (\%)$. Volume mean diameter $d_{4,3} = \frac{\sum n_i d_i^4}{\sum n_i d_i^3}$, where 4 and 3 are the algebraic power of d_i. $span = \frac{d_{90} - d_{10}}{d_{50}}$, where d_{90}, d_{10} and d_{50} are the droplet sizes at which 90%, 50% and 10% of the distribution lies below in a cumulative undersize figure.

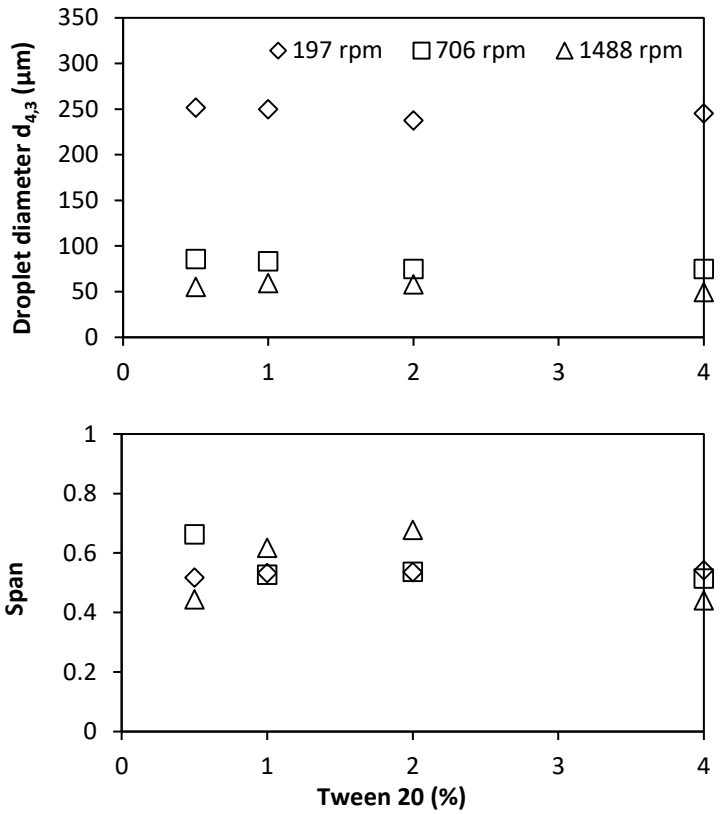
The experimental droplet size followed the same trend as the published model of predicted droplet diameter calculated by Equations 6.1-5, i.e., droplet size decreased with increasing rotational speed asymptotically reaching a droplet size specific to the system that does do significantly decreased further with increasing the rotational speed. At the same time, for each rotational speed droplet diameter decreased with decreasing injection speed. These findings are in agreement with literature (Vladisavljevic et al. 2003, Holdich et al. 2010, Dragosavac et al. 2012). The published model did not take account of the injection speed (Equations 6.1-6.5) and it is ideally valid for infinitesimal low injection speed. Because the lower the injection speed, the slower the droplet growth at the membrane pore, the more effectively the emulsifier reducing the interfacial tension, the smaller the droplet size formed before the detachment (Schröder et al. 1999). Thus, the experimental data obtained for the lowest injection speed at 1 ml/min are closest to the model prediction.

In conclusion, when using a relatively high rotational speed in the present set-up (966-1488 rpm) combined with a very low injection speed (i.e. 1 ml/min), w/o/w emulsions with comparable droplet size of around 60-70 µm could be produced with any of the three emulsifiers applied in this research. This was in line with the model prediction showcasing the validity of the model. So, this stirred cell membrane device enabled the generation of w/o/w emulsions of comparable microstructure for assessment to aroma release (reported in Chapter 7) with droplet size removed as an influencing factor.

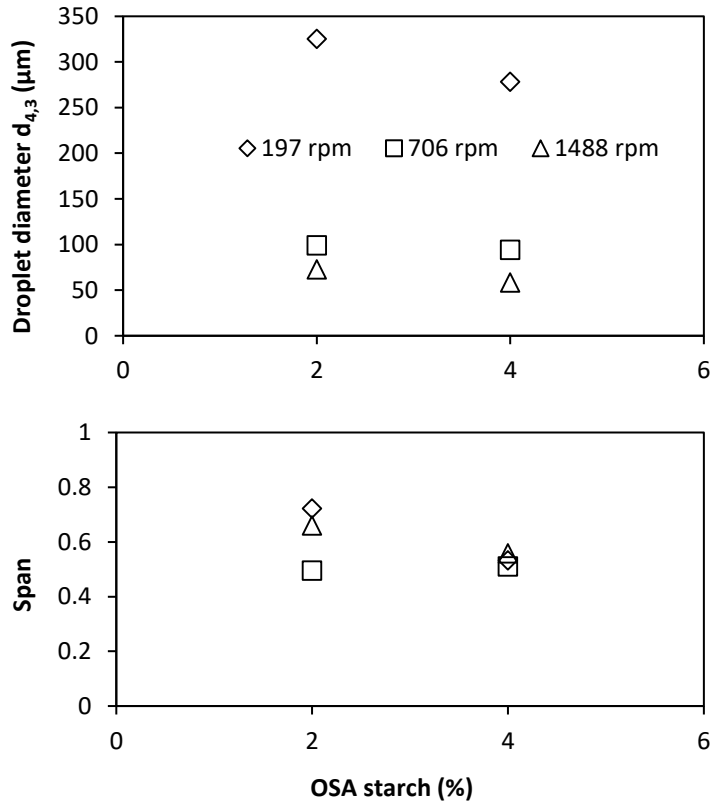
6.5 EFFECT OF EMULSIFIER CONCENTRATION AND ROTATIONAL SPEED ON EMULSION MICROSTRUCTURE

The same emulsifier concentration as used in the conventional emulsification (i.e. high shear mixing) in this study was applied for using in the membrane emulsification above. Additionally, the concentration effect for each emulsifier corresponding to the system generated via the membrane emulsification were tested. Droplet size was expected to decrease with increasing emulsifier concentration as interfacial tension decreases. But once upon a concentration (critical micelle concentration, CMC), droplet size did not decrease further because the emulsifier molecules were sufficient to decrease the oil-water interfacial tension and stabilise droplets against coalescence during emulsification. CMC indicates the minimum concentration of an emulsifier required to sufficiently cover the droplet surface against aggregation and coalescence. The effect of the concentration of Tween 20, OSA starch and PPI and the rotational speed of 197, 706 or 1488 rpm on the droplet size and span of the w/o/w emulsions is reported in Figure 6.7. Only 1 ml/min was used as injection speed, since the experimental droplet size obtained at this injection speed was closest to the model prediction (Figure 6.6).

A


197 rpm
706 rpm
1488 rpm
Droplet diameter $d_{4,3}$ (µm)
Span
Tween 20 (%)

B


197 rpm
706 rpm
1488 rpm
Droplet diameter $d_{4,3}$ (µm)
Span
OSA starch (%)

C

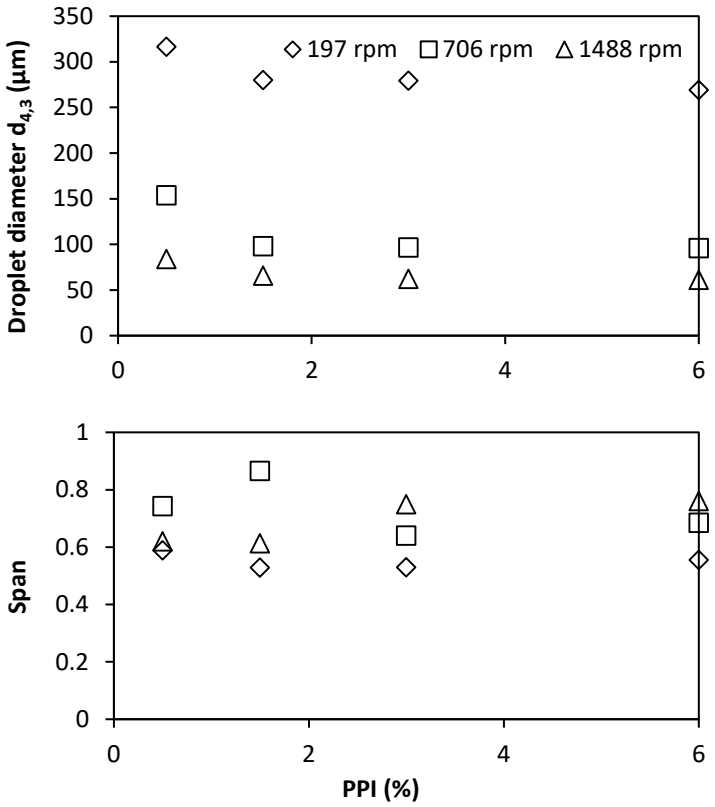


Figure 6.7 Effect of emulsifier concentration of A) Tween 20 B) OSA starch C) PPI to stabilise the w/o/w emulsion assessed at three rotational speeds (197rpm, 706 rpm and 1488 rpm) and at the injection speed of 1 ml/min on the droplet size ($d_{4,3}$) and span. Single experiments were carried out.

As expected, increase of emulsifier concentration was found to lead to a decrease of the droplet size for each emulsifier type. In the case of the Tween 20 stabilised w/o/w emulsions (Figure 6.7A), the span was between 0.45-0.68 and the increase of Tween 20 concentration from 0.5% to 4% had little impact on droplet size. It showed that Tween 20 was a strong emulsifier reducing interfacial tension to a large extent to form the oil droplets in w/o/w emulsions,

even at 0.5%. The CMC for Tween 20 corresponding to the w/o/w emulsion system is 0.5%. For OSA starch stabilised w/o/w emulsions (Figure 6.7B), the droplet size decreased with increasing OSA starch concentration from 2% to 4%. This was accompanied with a reduction in the span from 0.72 to 0.53 and from 0.66 to 0.56 for the rotational speed of 197 rpm and 1488 rpm respectively. The CMC for OSA starch in w/o/w emulsions is 4%. For PPI stabilised w/o/w emulsions (Figure 6.7C), a decrease in the droplet size was observed with increasing PPI concentration from 0.5% to 1.5%. Once the PPI concentration was above 1.5%, no further decrease of the droplet size was observed. Thus, the CMC for PPI is 1.5%. The span of the w/o/w emulsions stabilised with PPI was in a range of 0.53-0.76, except that the span of the PPI stabilised w/o/w emulsion manufactured at 706 rpm was about 0.87.

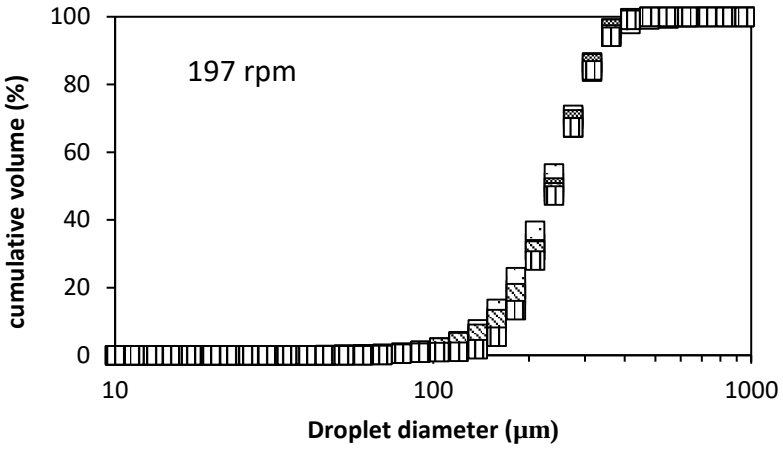
It also can be seen that for each rotational speed, w/o/w emulsions stabilised by 2% Tween 20 had a smaller droplet size ($d_{4,3}$) than those stabilised by 4% OSA starch or 1.5% PPI. This is probably because Tween 20 reduced the interfacial tension to a largest extent than other two emulsifiers (Table 6.2).

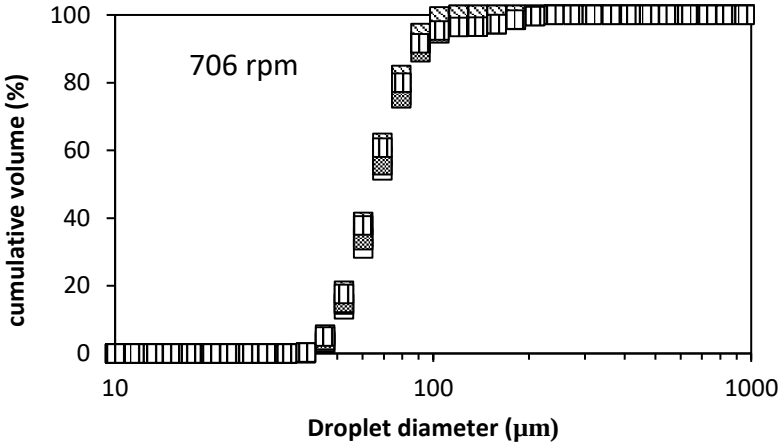
In summary, Tween 20 at 2%, OSA starch at 4% and PPI at 1.5% were sufficient to decrease the interfacial tension at the w/o and w_2 interface to produce stable droplets against coalescence. Thus, the same concentrations of each emulsifier used for the high shear processed emulsions reported in Chapter 5 can be used for the membrane emulsification processed emulsions.

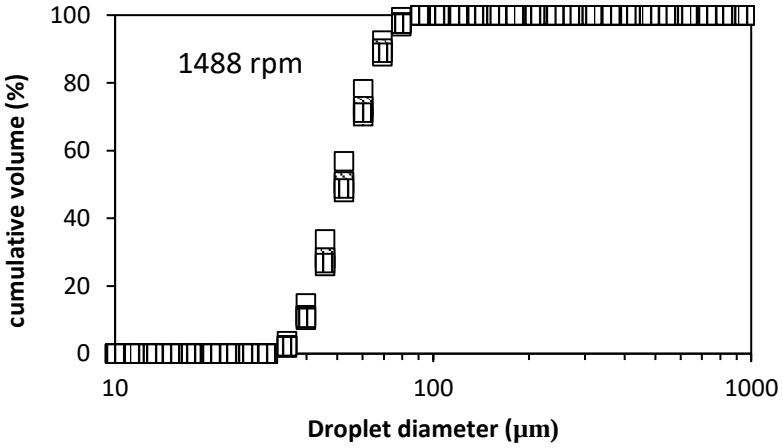
6.6 EMULSION STABILITY

The stability of w/o/w emulsions manufactured at the three rotational speeds of 197 rpm, 706 rpm and 1488 rpm was investigated over 13 day storage to check longer term stability instead of one week reported in Chapter 5. Figure 6.8 shows the droplet size distribution on cumulative volume basis of w/o/w emulsions stabilised with all three emulsifiers manufactured at three different rotational speeds (197, 706 and 1488 rpm) during 13 day storage. The emulsifier concentrations were 2% for Tween 20, 4% for OSA starch and 1.5% PPI, the same as used in high shear processed emulsions as described in Chapter 5. Only the injection speed of 1 ml/min was used since droplet size produced at this injection speed was closest to the published model as seen in Figure 6.6. As in agreement with Figure 6.6, the droplet size reduced with increasing rotational speed (197-1488 rpm) for each emulsifier. For each emulsion, the droplet size distributions independent of hydrophilic emulsifiers showed no difference over 13 days. Thus, these emulsions were suitable for aroma release measurement.

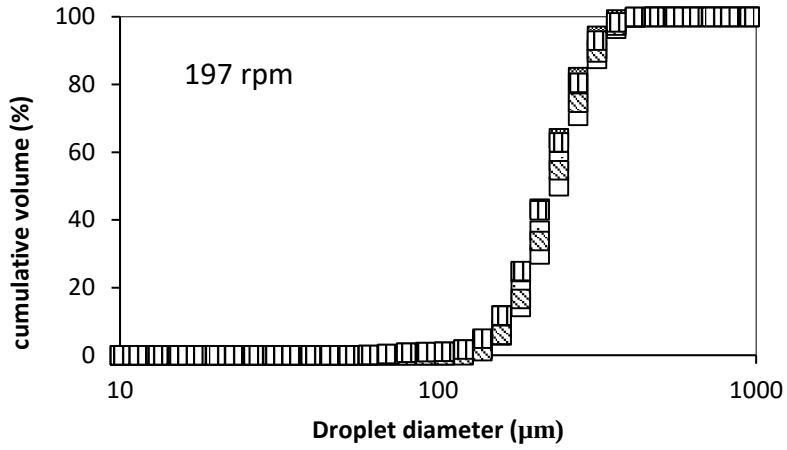
A

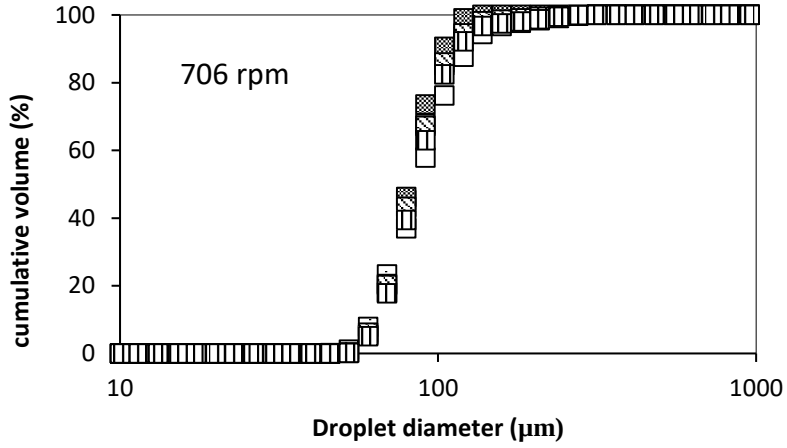

197 rpm
cumulative volume (%)
Droplet diameter (µm)
0
20
40
60
80
100
10
100
1000

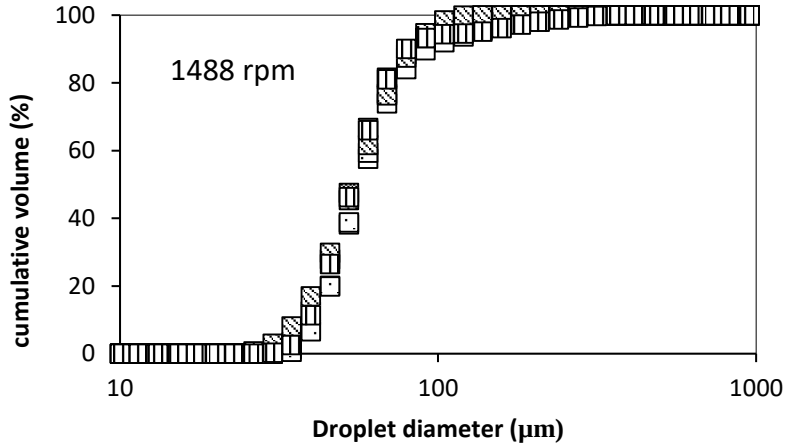

706 rpm
cumulative volume (%)
Droplet diameter (µm)
0
20
40
60
80
100
10
100
1000


1488 rpm
cumulative volume (%)
Droplet diameter (µm)
0
20
40
60
80
100
10
100
1000

B


197 rpm
cumulative volume (%)
100
80
60
40
20
0
10
100
1000
Droplet diameter (µm)


706 rpm
cumulative volume (%)
100
80
60
40
20
0
10
100
1000
Droplet diameter (µm)


1488 rpm
cumulative volume (%)
100
80
60
40
20
0
10
100
1000
Droplet diameter (µm)

C

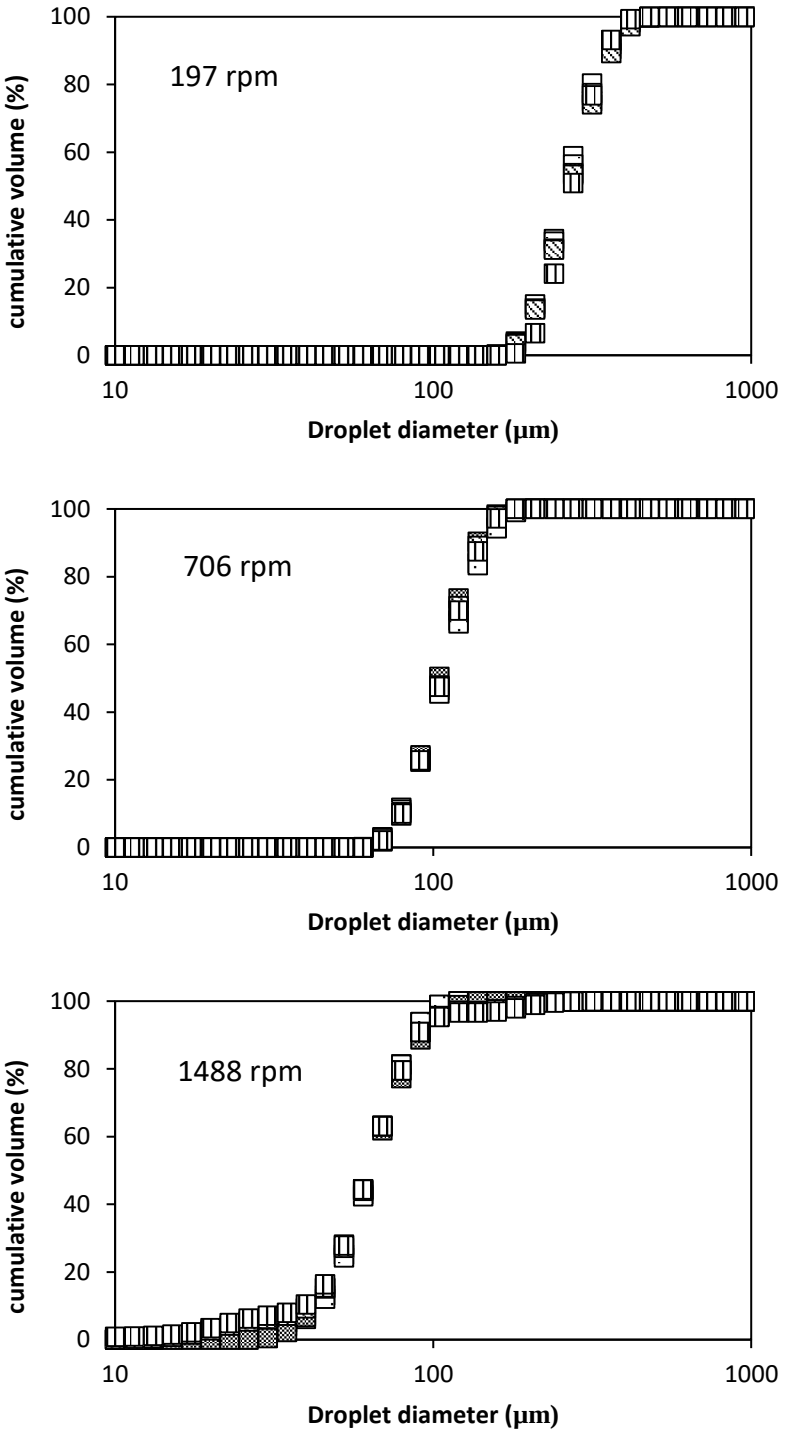


Figure 6.8 Droplet size distributions of w/o/w emulsions stabilised with A) 2% Tween 20 B) 4% OSA starch or C) 1.5% PPI. Days: □ day of making, ⁘ day 1, ▩ day 2, ▨ day 6, ▥ day 13. Cumulative volume is the total volume contained in droplets having diameter less than a given size.

6.7 CONCLUSIONS

Utilising stirred cell membrane emulsification narrow droplet size distributions of w/o/w emulsions stabilised with all three hydrophilic emulsifiers of interest in this PhD research (Tween 20, OSA starch and PPI) could be produced. Based on published model predictions experimental conditions to produce similarly sized w/o droplets in all three systems were successfully trialled. Agreement with model predictions was obtained for the lowest injection speed only since this is not a parameter considered in the model. This applied to all rotational speeds. At higher injection speed larger droplets than predicted were generated. All three emulsions systems were stable in terms of droplet size distribution and microstructure for at least 13 days. In terms of stirred cell membrane emulsification, this research has for the first time shown that complex food emulsifiers such as starch and protein can be applied to produce stable w/o/w emulsions with this technology. One should consider though that stabilisation with a low molecular surfactant such as Tween 20 would allow formation of slightly more uniform droplet size distributions (lower span) with a lower mean diameter. In conclusion, the research reported in this chapter enabled the production of uniformly sized w/o/w emulsions with similar average droplet diameters for the study of aroma release so that droplet size and droplet size distribution was no longer an influencing factor.

7 IMPACT OF HYDROPHILIC EMULSIFIER ON AROMA RELEASE OVER EMULSIONS GENERATED VIA STIRRED CELL MEMBRANE EMULSIFICATION AND THICKENED WITH XANTHAN GUM

In this chapter aroma release over similarly sized emulsions with xanthan gum as a thickener is reported. In order to eliminate the impact of droplet size on aroma release, emulsion droplets of similar diameter were generated via stirred cell membrane emulsification. w/o/w emulsions and control o/w emulsions stabilised with Tween 20, OSA starch or PPI as the hydrophilic emulsifier were produced. After emulsion manufacture, concentrated xanthan gum solution was added to slow down the creaming of the emulsion droplets to eliminate the impact of creaming on aroma release. Encapsulation efficiency of magnesium was measured by adding magnesium chloride to the internal water phase (w_1) and monitoring the amount of magnesium in the external water phase (w_2) over time. This was to explore the loss of w_1 into w_2 containing xanthan gum to understand the effect of the loss of w_1 on aroma release. The aroma compound, diacetyl or 3-pentanone, was added in the above produced w/o/w emulsions and o/w emulsions after emulsion manufacture. Microstructure characteristics of these xanthan gum added emulsions were also studied to evaluate the emulsion stability in the absence or in the presence of either aroma compound. The creaming velocity of the emulsions with or without xanthan gum was calculated to investigate the effect of xanthan gum on creaming. Emulsion viscosity was measured to investigate the effect of

viscosity on aroma release. Static headspace analysis and dynamic headspace analysis over samples were carried out to evaluate the impact of the three different hydrophilic emulsifiers on aroma release behaviour over w/o/w emulsions. To eliminate the impact of the oil phase (o), the hydrophobic emulsifier (PGPR) and w_2 on aroma release, release behaviour over w_2, o/w emulsions and w/o/w emulsions was quantified in the same way.

7.1 INTRODUCTION

The partitioning and release of aroma compounds over emulsions can be affected by various factors. For example, the droplet size or interfacial area can influence the equilibrium distribution of aroma molecules in an emulsion (Jacobsen et al. 1999). The droplet size in the w/o/w emulsion system with different hydrophilic emulsifiers could be well controlled by the membrane emulsification as discussed in Chapter 6. Besides, the droplet size for a o/w emulsion system could also be controlled (Dragosavac et al. 2008). Thus, the effect of droplet size or interfacial area in o/w or w/o/w emulsions stabilised with different emulsifier types on aroma release can be eliminated by producing the same droplet size.

The creaming of emulsion droplets could also affect aroma release by creating an oil barrier for aroma compounds diffusion underneath the oil layer, as reported in Chapter 5. To prevent the creaming, thickening or gelling agents can be used to modify texture by increasing the viscosity of the continuous phase of emulsions. Examples are natural gums like xanthan gum, gum Arabic,

guar gum and locust bean gum, starch, pectin and gelatin (Saha et al. 2010). Xanthan gum is one of the commonly used polysaccharides that are usually added to the aqueous phase of o/w emulsions (Long et al. 2013, Traynor et al. 2013). It is produced through microbial fermentation of glucose or sucrose by xanthomonas capestris (Morris 2006). The primary structure of xanthan gum consists of a β-(1-4)-D-glucose backbone with trisaccharide side chains at the C-3 positions of alternate glucose residues. The trisaccharide side chains consist of β-D-mannose, β-(1-4)-D-glucuronic acid and α-(1-2)-D-mannose. The molecular weight of xanthan gum ranges from $2x10^6$ to $5x10^7$ g/mol depending on the association between chains (Garcıa-Ochoa et al. 2000). Xanthan gum has the characteristics to increase the viscosity of the continuous aqueous phase at relatively low concentration and have high viscosity at low shear rate which corresponds to the state of emulsion at rest, e.g. creaming or sedimentation. It also has strong shear-thinning behaviour, compared to other thickeners (Sworn 2009). The flow behaviour of xanthan gum is a result of intermolecular association among the polymer chains which results in the formation a complex network of entangled rod-like molecules. At low shear rate, xanthan gum has a high viscosity preventing creaming of emulsion droplets (Akhtar et al. 2006). At high shear rate, such as oral processing during eating, viscosity decreases with the disentanglement of the network and the alignment of the individual macromolecules in the direction of shear, which would help to release flavour and induce good mouthfeel (Karaiskou et al. 2008).

In Chapter 6 a route of producing similarly sized w/o/w emulsions through stirred cell membrane emulsification was demonstrated. The aim of the research presented in this chapter was to study the aroma release behaviour over these similarly sized w/o/w and o/w emulsions produced through membrane emulsification. The effect of droplet size and creaming was eliminated. It is a comparison of the aroma release over emulsions produced through high shear mixing as reported in Chapter 5, where hydrophilic emulsifier-aroma interactions, droplet size, droplet thickness and creaming had the influence on aroma release. So, to study the effect of the hydrophilic emulsifier on aroma release behaviour alone, the same three hydrophilic emulsifiers, Tween 20, OSA starch and PPI, as well as the same two aroma compounds, diacetyl and 3-pentanone, were used.

7.2 METHODS SPECIFIC TO THE RESULTS REPORTED IN THIS CHAPTER

7.2.1 Sample formulations and process parameters

For w/o/w emulsions, the emulsion formulation and setup of stirred cell membrane emulsification was described in sections 5.2.1 and 6.2.4.1 respectively. According to Chapter 6, a range of droplet size of w/o/w emulsions stabilised with Tween 20, OSA starch or PPI could be obtained through stirred cell membrane emulsification by varying process parameters. When a high rotational speed (966-1488 rpm) and a very low injection speed (1 ml/min) was applied, similar droplet sizes independent of emulsifier type were obtained. Specifically, at the rotational speed of 1214 rpm uniform emulsion droplets

characterised by a low CV and span could be produced (Figure 6.6). Thus, a rotational speed at 1214 rpm and an injection speed of 1 ml/min were chosen as the process parameters to produce similar and uniform droplet size of around 60-70 µm (Figure 6.6) in the system type of w/o/w emulsions.

For control o/w emulsions, the formulation was same as that reported in section 5.2.1, except that 4% PGPR was added to the oil phase (o) and 0.1 M NaCI was added to the water phase (w). The addition of PGPR to the oil phase and NaCI to the water phase was to compare with the w/o/w emulsions and to be able to eliminate the effect of PGPR and NaCI on aroma release. Control o/w emulsions of equivalent droplet size between 60-70 µm were also produced using stirred cell membrane emulsification. To predict the droplet diameter of the o/w emulsions, the same model as presented in section 6.1 for the w/o/w emulsions was applied based on Equations 6.1-5. Predicted droplet diameters of the o/w emulsions are shown in Figure 7.1. In order to obtain a droplet size of around 60-70 µm, the process parameters as predicted were tested in preliminary experiments and following some trial and error experimentation the following parameters were fixed. Tween 20 stabilised o/w emulsions were to be manufactured at the rotational speed of 966 rpm and the injection speed of 1 ml/min. PPI and OSA starch stabilised o/w emulsions were to be manufactured at the rotational speed of 1214 rpm and the injection speed of 1 ml/min.

As with previous samples prepared in section 6.2.4.1, sodium azide solution was added to the w/o/w emulsions and the o/w emulsions after emulsion

manufacture to obtain a final sodium azide concentration at 0.02%.

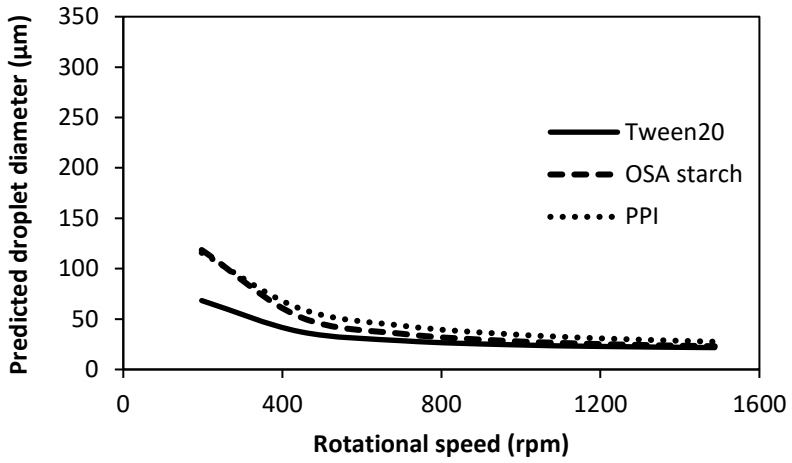


Figure 7.1 Predicted droplet diameter of o/w emulsions stabilised with Tween 20, OSA starch or PPI based on model calculated by Equations 6.1-5

The water control samples containing 0.1 M NaCl, 0.02% sodium azide and 2% Tween 20, 4% OSA starch or 1.5% PPI were prepared to explore the impact of the external water phase (w_2) on aroma release.

7.2.2 Xanthan gum addition and aroma inclusion

Xanthan gum stock solution contained 1% xanthan gum, 0.1 M NaCl and 0.02% sodium azide in deionized water. This solution was prepared by dispersing the xanthan gum powder into water pre-heated to 80°C, while mixing at 1500 rpm through an overhead mixer (RW20 fitted with a Propeller 4-bladed stirrer, IKA, Staufen, Germany) for 1 h. The temperature (80°C) was maintained by placing

the beaker containing the solution into a circulating water bath. The solution was continuously mixed during this time to minimise clumping. After preparation, the xanthan gum stock solution was allowed to cool down at room temperature and left overnight for complete hydration before use. 70 g of xanthan gum stock solution was added to 100 g emulsion sample after emulsion manufacture. The emulsion was then placed into a 600 ml glass beaker and mixed at 600 rpm on a magnetic stirrer for 30 min. It was confirmed that the droplet size of w/o/w and o/w emulsions did not change under this mixing condition. The final xanthan gum concentration in the external aqueous phase of the w/o/w and o/w emulsions was 0.5%. To prepare the xanthan gum containing aqueous control samples, 100 g of the xanthan gum stock solution was mixed with 100 g of water at 600 rpm to also obtain a final xanthan gum concentration of 0.5%. After mixing, 50 g of xanthan gum containing samples were transferred to a glass bottle with a total volume of 134 ml and a 25x6 mm magnetic stir bar was added at the bottom.

As before, the two aroma compounds diacetyl and 3-pentanone were chosen. 1020 µl/l aroma stock solution with the addition of 0.1 M NaCl was prepared. 1 ml of the stock solution was added into each glass bottle to obtain a final aroma concentration in liquid at 20 µl/l. After aroma addition, the bottle was immediately sealed and samples were stored at room temperature for further analysis.

7.2.3 Emulsion characteristics

For microscopy and droplet size measurement, single experiments were carried out, where each one of the w/o/w emulsions and o/w emulsions with the addition of xanthan gum and aroma compounds was prepared. Emulsion microstructure and droplet size characteristics were assessed immediately after sample preparation and during a 13 day storage period (day 1, 2, 6 and 13). Microscopy and droplet size measurement were carried out utilising the method in sections 6.2.5 and 6.2.6 respectively.

In order to calculate the creaming velocity with Equation 2.1, the density of o and w_2, as well as the viscosity of w_2, was measured.

For density measurement, three different oil phases were prepared: oil, oil with 4% PGPR and w/o emulsions. With regard to w_2, three different aqueous solutions containing 0.1 M NaCl and 0.5% xanthan gum as well as 2% Tween 20, 4% OSA starch or 1.5% PPI were prepared. The aqueous phases were labelled 'wT+XG', 'wP+XG' and 'wS+XG' respectively. Samples were prepared in triplicate and the density was measured following the method as described in section 6.2.3.

For viscosity measurement, four aqueous phases were prepared: water with 0.5% xanthan gum, 2% Tween 20 solution in 0.1 M NaCl and 0.5% xanthan gum, 4% OSA starch solution in 0.1 M NaCl and 0.5% xanthan gum and 1.5% PPI solution in 0.1 M NaCl and 0.5% xanthan gum. o/w and w/o/w emulsions with xanthan gum addition after emulsion manufacture were prepared as described in sections 7.2.1-2. They were labelled 'owT+XG', 'owP+XG', 'owS+XG',

'wowT+XG', 'wowP+XG' and'wowS+XG' respectively. Samples were prepared in triplicate. The viscosity of the continuous phases and the emulsions was measured with a concentric cylinder geometry (CC 27) following the method outlined in section 6.2.2.

7.2.4 Assessing encapsulation efficiency

Assessing encapsulation efficiency was carried out by adding magnesium chloride to the internal water phase (w_1) of the w/o/w emulsions. This was to measure the loss of the internal water phase (w_1) into the external water phase (w_2) and assessing release of magnesium has previously been reported as a suitable method (Bonnet et al. 2009). It helps to understand the loss of w_1 on aroma release. This was investigated for test emulsion and these w/o/w emulsions with magnesium chloride instead of NaCl added to w_1 were not used for aroma release measurement.

Initially, $MgCl_2 \cdot 6H_2O$ (magnesium chloride hexahydrate) was dried at 95°C in the vacuum oven overnight to remove free water. 1600 ppm $MgCl_2 \cdot 6H_2O$ was dissolved in water to be the internal aqueous phase of the w/o/w emulsions. This magnesium concentration was chosen to maintain the osmotic pressure balance between two aqueous phases of w/o/w emulsions. o contained 4% PGPR. w_2 contained 0.1 M NaCl and 2% Tween 20, 4% OSA starch or 1.5% PPI. Emulsions were produced in triplicate by the method described in section 7.2.1. Thickened emulsions containing xanthan gum were prepared using the method presented in section 7.2.2. The emulsions were inspected for microstructure

and droplet size distribution immediately after preparation, with results labelled ‘day of making’, and during storage applying the methods described in sections 6.2.5-6. Stored w/o/w emulsions were evaluated 1, 2, 6, 13 days after emulsion manufacture and results are labelled ‘day 1’, ‘day 2’, ‘day 6’ and ‘day 13’, respectively. This was to ensure the addition of $MgCl_2$ to the w/o/w emulsions had no influence on the microstructure and droplet size distribution, so the method is valid to make a statement about the encapsulation efficiency for the actual emulsions assessed for aroma release.

For the magnesium release measurement, magnesium concentration was measured with a flame atomic absorption spectroscope (Spectra AA-200 Varian, UK) at the wavelength of 285.2 nm. Standard solutions containing 100 times dilution of w_2 (with 0.5% xanthan gum) and $MgCl_2 \cdot 6H_2O$ at the concentrations of 0 ppm, 0.02 ppm, 0.05 ppm, 0.1 ppm, 0.5 ppm and 1 ppm were prepared to acquire a standard curve. Standard curves with the magnesium concentration as a function of the measurement signal (absorption) are shown in Figure 7.2. The absorption obtained from the spectroscopy increased with increasing magnesium concentration. The relationships were linear and repeatable.

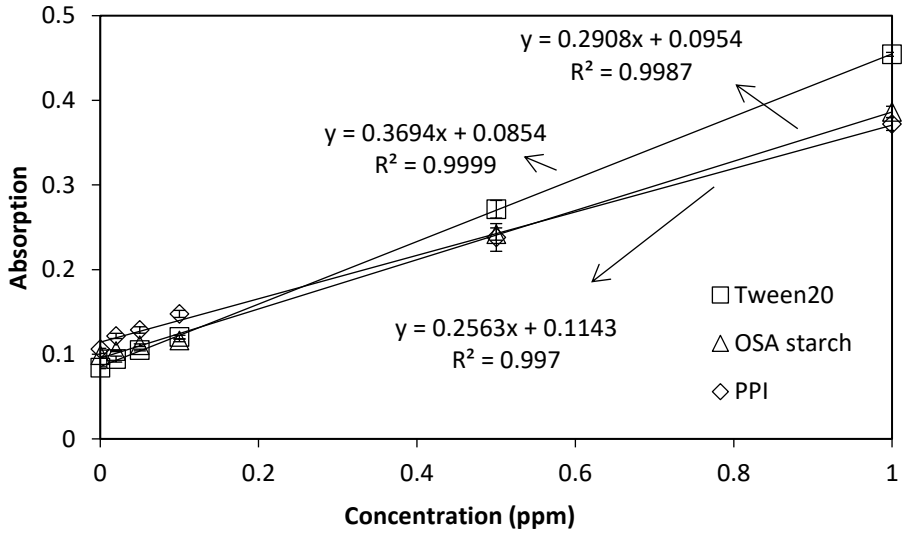


Figure 7.2 Standard curves of magnesium in standard solutions with Tween20, OSA starch or PPI

To assess the external aqueous emulsion phase (w_2) for leakage of internal aqueous phase and thus magnesium into w_2, the concentration of magnesium in w_2 was calculated based on the standard curve. The percentage of magnesium (Mg %) released from w_1 into w_2 of the w/o/w emulsions was calculated by Equation 7.1:

$$Mg\ (\%) = (C_{Mg} * 100 * V_{w_2} / (V_{w_1} * C_t)) * 100 \qquad \text{Equation 7.1}$$

where C_{Mg} is the magnesium concentration in w_2, which was calculated by the equations in the standard curves (Figure 7.2) with the experimental value (adsorption) measured by the spectroscope. V_{w_2} is the volume of w_2, V_{w_1} is the volume of w_1 and C_t is the total magnesium concentration initially added in the

internal water phase. This equation was used to convert the magnesium concentration into percent released.

w_2 was separated through centrifugation at 2383 g for 30 min (3500 rpm) using a Heraeus Labofuge 400R centrifuge (Thermo Scientific, Germany). The bottom layer was then carefully taken out by pipette and centrifuged again at the same conditions to ensure that the external emulsion phase was void of oil droplets. Via microscopic observation and droplet size analysis of the creamed emulsion droplets it was verified that the chosen centrifugation conditions had not changed the droplet size distribution of the emulsions. The methods described in sections 6.2.5-6 were applied for these analyses. Finally, 1 ml of separated external water phase was diluted with deionized water to a volume of 100 ml using a volumetric flask. All samples were prepared in triplicate. Measurements were taken over 13 days at the same days as emulsion droplet size was checked.

7.2.5 Aroma release measurement

For static headspace analysis, samples stored in glass bottles (a total volume of 134 ml) were stirred at 200 rpm for 1 min to ensure homogeneous distribution of the aroma compound. The first aroma release measurement taking place immediately after mixing was labelled ‘0 h’. Further measurements were undertaken 1 h, 2 h, 3 h and 4 h after aroma addition and results were labelled ‘1 h’, ‘2 h’, ‘3 h’ and ‘4 h’ respectively. For ‘0 h’, ‘2 h’ and ‘4 h’ time slots, emulsion samples and water controls were prepared in triplicate. For the other two time slots of ‘1 h’ and ‘3 h’ the samples and water controls were prepared once. A

water standard with the same amount of added aroma was always measured at the same time. Static headspace analysis was carried out at room temperature using the method described in section 3.2.5.1. The calculation of relative headspace intensity and the reason to calculate it was described in section 5.2.2. Theoretical aroma concentrations at equilibrium in the static headspace over water, o/w emulsion and w/o/w emulsion with xanthan gum addition were calculated with Equations 5.1-12, based on the mass fraction of each phase and the physiochemical properties of the aroma compounds (Table 3.1). As a result, for diacetyl, the ratio between the theoretical equilibrium static headspace concentration over water, o/w emulsion and w/o/w emulsion was 1: 1.2: 1.1. For 3-pentanone, the ratio between the theoretical equilibrium static headspace concentration over water, o/w emulsion and w/o/w emulsion was 1: 0.6: 0.7.

For dynamic headspace analysis, samples were allowed to equilibrate for 4 h. At the end of the static headspace analysis, two of the 50 ml samples were combined into one 100 ml sample in a glass bottle (a total volume of 134 ml). 4 h was chosen for the aroma equilibration because it was the aroma equilibration time suggested by the results of the static headspace analysis presented in Figures 7.10-11. Samples were prepared in triplicate. They were stirred at 200 rpm for 10 secs and maintained at zero speed for 1-2 min before the dynamic headspace analysis. Dynamic headspace analysis was carried out using the method described in section 3.2.5.2.

7.3 PROPERTIES OF EMULSIONS PREPARED THROUGH STIRRCED CELL MEMBRANE EMULSIFICATION

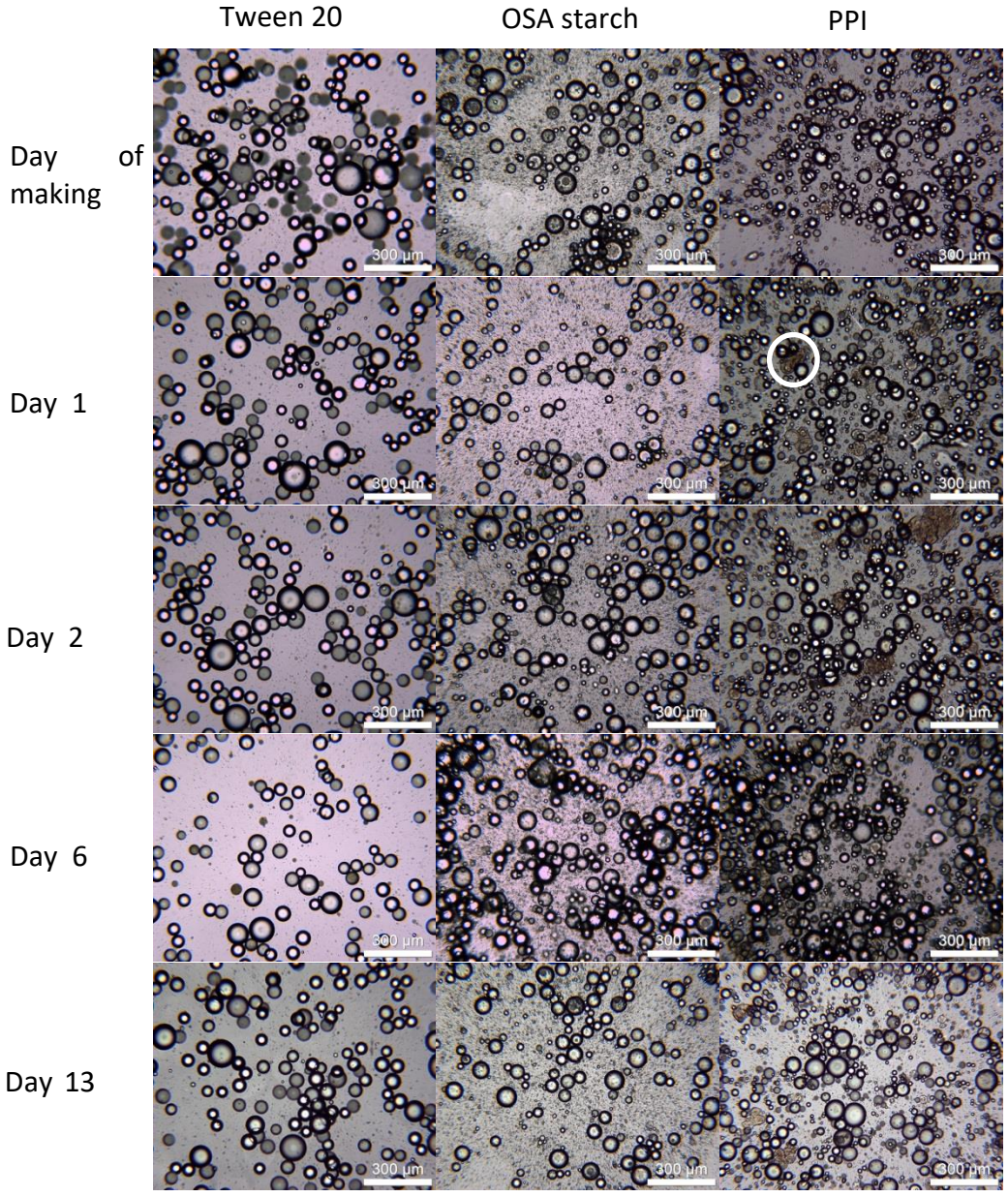
7.3.1 Emulsion microstructure during storage

The stability of the o/w and w/o/w emulsions produced through stirred cell membrane emulsification whereby xanthan gum and aroma were added afterwards was determined through the changes in microstructure. Emulsion microstructure was observed by micrographs (Figure 7.1) and droplet size distribution profiles (Tables 7.1-3) over 13 day storage. This is to ensure that the emulsions are stable during storage so suitable for further aroma release measurement.

The microstructure of w/o/w emulsions prepared with aroma addition (diacetyl or 3-pentanone) had the same microstructure, so only micrographs of the w/o/w emulsion in absence of aroma are shown in Figure 7.1. It is worth emphasising that droplet size independent of emulsion type and emulsifier type appeared visually similar. Pea protein isolate could be occasionally seen no matter in PPI stabilised o/w emulsions (Figure 7.1A) and w/o/w emulsions (Figure 7.1B). For each emulsion, there was no apparent change in microstructure independent of aroma inclusion and sample age, which indicates no coalescence. For o/w emulsions (Figure 7.1A), it can be seen that the dispersed oil droplets of the o/w emulsions were discernible with light appearance. For w/o/w emulsions (Figure 7.1B), the micrographs confirmed the successful formation of w/o/w emulsions through the dark appearance of the droplets, as discussed in section 4.3. The micrographs of w/o/w emulsions

also do not show evidence of loss of internal aqueous phase into the external aqueous phase, which would be recognisable by translucent droplets. The addition of xanthan gum after emulsion manufacture did not affect the emulsion microstructure for all emulsions.

A



B

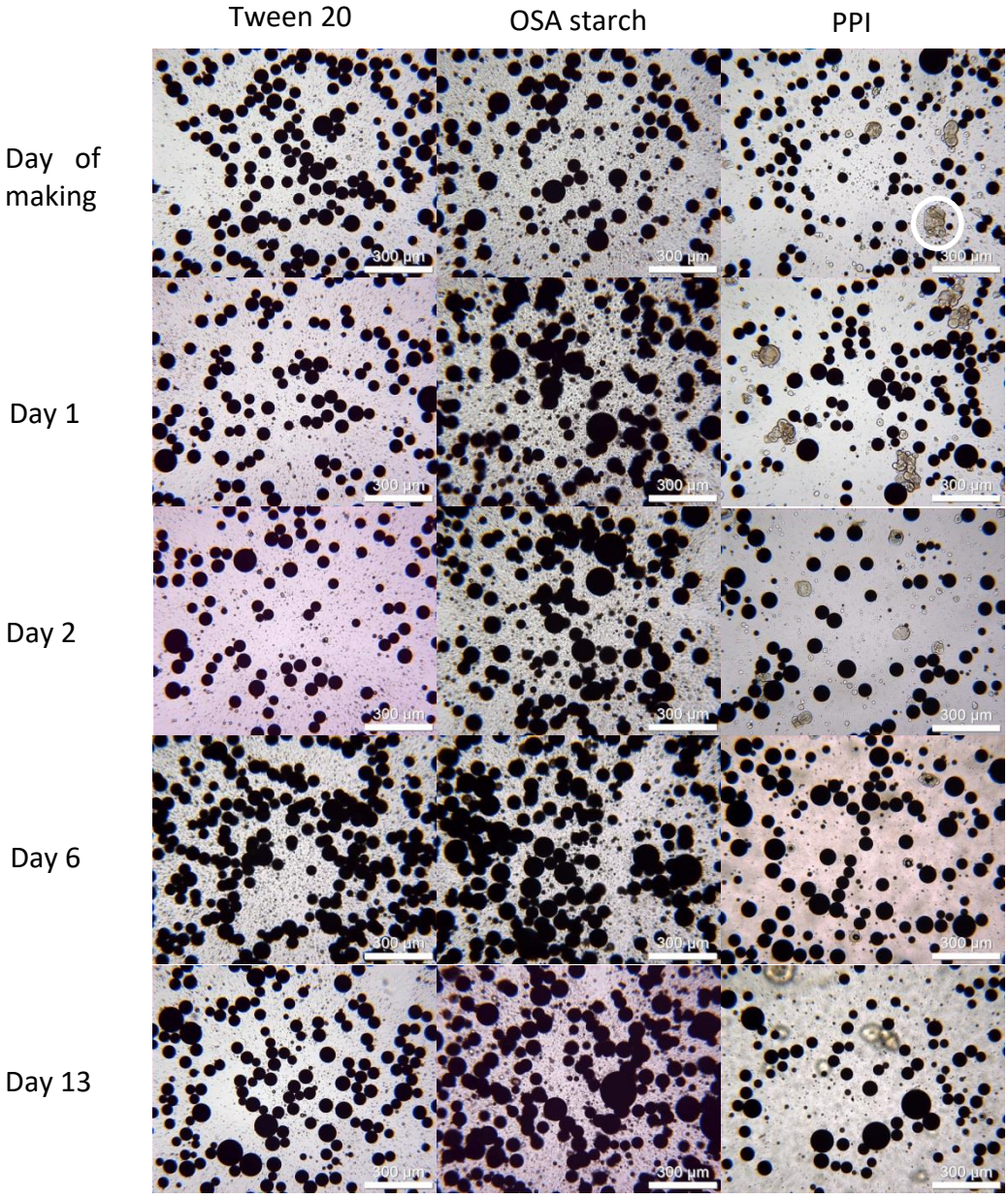


Figure 7.3 Micrographs of A) o/w and B) w/o/w emulsions stabilised with Tween 20, OSA starch or PPI in the absence aromas stored over 13 days. Scale bar = 300 µm. The circles indicate pea protein isolate.

The numerical results of droplet size distributions of emulsions stabilised with Tween 20, OSA starch and PPI are reported in Tables 7.1-3 respectively. The droplet size distribution profiles include the droplet size on volume basis ($d_{4,3}$), the Sauter diameter ($d_{3,2}$), the span and the specific surface area (SSA) for each emulsion. As predicted, the droplet size of all emulsions is similar, approximately 60-70 µm. $d_{4,3}$, $d_{3,2}$ and SSA of all of the emulsions remained constant independent of aroma inclusion, type of aromas and sample age. All Tween 20 stabilised emulsions had spans of less than 0.6, which showed a good uniformity of emulsion droplets. The span of the OSA starch stabilised emulsions was approximately 0.7, similar as reported in Figure 6.6B. The span of PPI stabilised emulsions was more than 0.8. The large span of the emulsions stabilised with PPI could be due to the fact that protein particles also scattered light and thus be a measurement artefact.

The 6 day stability of the w/o/w emulsions with the same emulsion formulation processed by high shear mixing was previously observed, except for PPI stabilised w/o/w emulsions (see section 5.3). The stability of w/o/w emulsions stabilised with PPI was improved by producing more uniform droplets through membrane emulsification.

Since all emulsions generated via stirred cell membrane emulsification were produced with predicted droplet size, approximately around 60-70 µm and all emulsions were stable over 13 days, these manufactured emulsions were suitable for further aroma release measurement.

Table 7.1 Droplet sizes on volume basis ($d_{4,3}$), the Sauter diameter ($d_{3,2}$), span and specific surface area (SSA) of Tween 20 stabilised o/w and w/o/w emulsions over 13 day storage. Tween 20 stabilised o/w and w/o/w emulsions are labelled 'owT' and 'wowT' respectively.

owT		$d_{4,3}$ (μm)	$d_{3,2}$ (μm)	span	SSA (m^2/g)
no aroma	day of making	66.75	63.96	0.568	0.104
	day 1	66.51	63.75	0.563	0.105
	day 2	66.87	64.04	0.566	0.104
	day 6	67.47	64.62	0.567	0.103
	day 13	67.73	64.91	0.564	0.103
+ diacetyl	day of making	66.54	63.74	0.569	0.105
	day 1	66.34	63.6	0.562	0.102
	day 2	66.94	64.14	0.566	0.104
	day 6	67.38	64.53	0.566	0.103
	day 13	66.87	63.89	0.588	0.104
+ 3-pentanone	day of making	66.47	63.68	0.568	0.105
	day 1	66.37	63.63	0.562	0.105
	day 2	66.94	64.13	0.568	0.104
	day 6	67.35	64.5	0.568	0.103
	day 13	67.15	64.16	0.586	0.104
wowT		$d_{4,3}$ (μm)	$d_{3,2}$ (μm)	span	SSA (m^2/g)
no aroma	day of making	59.7	56.94	0.583	0.117
	day 1	59.76	57.03	0.580	0.117
	day 2	59.49	56.8	0.578	0.117
	day 6	59.42	56.66	0.585	0.118
	day 13	60.5	57.71	0.581	0.116
+ diacetyl	day of making	60.75	58.09	0.559	0.115
	day 1	60.84	58.09	0.574	0.115
	day 2	60.88	58.16	0.566	0.115
	day 6	61.87	59.19	0.558	0.113
	day 13	61.9	59.26	0.546	0.113
+ 3-pentanone	day of making	61.23	58.47	0.565	0.114
	day 1	62.03	59.35	0.558	0.112
	day 2	62.48	59.75	0.553	0.112
	day 6	62.06	59.31	0.558	0.112
	day 13	63.77	61.12	0.534	0.109

Table 7.2 Droplet sizes on volume basis ($d_{4,3}$), the Sauter diameter ($d_{3,2}$), span and specific surface area (SSA) of OSA starch stabilised o/w and w/o/w emulsions over 13 day storage. OSA starch stabilised o/w and w/o/w emulsions are labelled 'owS' and 'wowS' respectively.

owS		$d_{4,3}$ (μm)	$d_{3,2}$ (μm)	span	SSA (m^2/g)
no aroma	day of making	70.45	61.3	0.697	0.109
	day 1	72.03	62.83	0.701	0.106
	day 2	72.32	63	0.688	0.106
	day 6	72.51	65.67	0.68	0.102
	day 13	72.04	65.05	0.705	0.102
+ diacetyl	day of making	70.82	62.13	0.695	0.107
	day 1	71.72	62.47	0.701	0.107
	day 2	72.18	62.8	0.691	0.106
	day 6	71.9	62.7	0.695	0.106
	day 13	71.9	64.91	0.707	0.103
+ 3-pentanone	day of making	70.28	61.03	0.701	0.109
	day 1	71.5	62.25	0.703	0.107
	day 2	72.03	62.65	0.692	0.106
	day 6	71.78	62.53	0.695	0.107
	day 13	71.77	64.8	0.709	0.103
wowS		$d_{4,3}$ (μm)	$d_{3,2}$ (μm)	span	SSA (m^2/g)
no aroma	day of making	68.43	64.4	0.685	0.104
	day 1	69.6	65.56	0.685	0.102
	day 2	70.08	66.11	0.676	0.101
	day 6	70.73	66.65	0.691	0.1
	day 13	70.45	66.45	0.68	0.1
+ diacetyl	day of making	68.71	64.68	0.684	0.103
	day 1	69.43	65.46	0.676	0.102
	day 2	70.01	66.07	0.67	0.101
	day 6	70.31	66.35	0.671	0.1
	day 13	70.31	66.31	0.678	0.101
+ 3-pentanone	day of making	68.98	64.9	0.689	0.103
	day 1	69.63	65.63	0.678	0.102
	day 2	70.36	66.41	0.67	0.1
	day 6	70.47	66.51	0.672	0.1
	day 13	70.37	66.39	0.674	0.1

Table 7.3 Droplet sizes on volume basis ($d_{4,3}$), the Sauter diameter ($d_{3,2}$), span and specific surface area (SSA) of PPI stabilised o/w and w/o/w emulsions over 13 day storage. PPI stabilised o/w and w/o/w emulsions are labelled 'owP' and 'wowP' respectively.

owP		$d_{4,3}$ (μm)	$d_{3,2}$ (μm)	span	SSA (m^2/g)
no aroma	day of making	63.96	58.51	0.852	0.114
	day 1	64.86	59.04	0.884	0.113
	day 2	65.46	60.15	0.809	0.111
	day 6	66.87	61.39	0.807	0.109
	day 13	67.21	61.56	0.817	0.108
+ diacetyl	day of making	63.64	58.21	0.856	0.115
	day 1	64.62	58.91	0.874	0.113
	day 2	65.4	60.14	0.805	0.111
	day 6	66.55	61.09	0.811	0.109
	day 13	66.81	61.19	0.821	0.109
+ 3-pentanone	day of making	63.81	58.41	0.847	0.114
	day 1	64.54	58.86	0.871	0.113
	day 2	65.22	59.98	0.803	0.111
	day 6	66.43	60.97	0.812	0.109
	day 13	66.86	61.28	0.815	0.109
wowP		$d_{4,3}$ (μm)	$d_{3,2}$ (μm)	span	SSA (m^2/g)
no aroma	day of making	67.27	61.84	0.840	0.108
	day 1	66.52	61.39	0.816	0.109
	day 2	67.22	61.81	0.839	0.108
	day 6	67.93	62.1	0.876	0.107
	day 13	68.21	62.59	0.852	0.107
+ diacetyl	day of making	66.71	61.39	0.838	0.109
	day 1	67.73	61.99	0.866	0.108
	day 2	67.35	61.86	0.847	0.108
	day 6	68.05	62.27	0.869	0.107
	day 13	68.07	62.51	0.846	0.107
+ 3-pentanone	day of making	66.64	61.44	0.823	0.109
	day 1	68.08	62.4	0.855	0.107
	day 2	67.05	61.68	0.836	0.108
	day 6	68.16	62.49	0.854	0.107
	day 13	68.16	62.62	0.842	0.106

7.3.2 Creaming velocity

Creaming velocity was estimated based on Equation 2.1 as it affects aroma release behaviour over emulsions, see section 5.4. The only two important parameters that would lead to different creaming velocity would be density and viscosity of the continuous emulsion phase since droplet size was similar. Table 7.4 shows the densities of different phases of the o/w and w/o/w emulsions.

Table 7.4 Densities of different dispersed phases and continuous phases at 20 °C

		Density (g/cm^3)
Dispersed phase	o	$0.9156 \pm 0.0031^{a*}$
	4% PGPR	0.9183 ± 0.0091^{a}
	w/o emulsion	0.9357 ± 0.0045^{b}
Continuous phase	wT+XG	1.0054 ± 0.0004^{c}
	wS+XG	1.0126 ± 0.0005^{c}
	wP+XG	1.0026 ± 0.0029^{c}

* Different letters indicate statistically significant values ($P < 0.05$).

The average viscosity of the different external emulsion phase after addition of xanthan gum is depicted in Figure 7.4. All of the external emulsion phases were shear thinning. The viscosity of 'wS+XG' was different from others, which was lower than others at the shear rate approximately in the range of 0.1-100 s^{-1}. It was found that the viscosity of a suspension containing 6% (w/v) OSA starch and 0.5% (w/v) xanthan gum dramatically decreased at low shear rate (< 0.2 s^{-1}) (Ntawukulilyayo et al. 1996). This was explained by an interaction between the non-ionic amylopectin molecules of OSA starch and rod-like xanthan gum. Same finding was reported (Krstonošić et al. 2011) and it was also suggested

that OSA starch and xanthan gum form mixed micelles at CMC of OSA starch and continually form complexes with increasing OSA starch concentration. The viscosity measured as lowest as possible is more corresponding to the state of all phases at rest. Hence, the viscosities at the shear rate of 0.1 s^{-1} were used to calculate the creaming rate in Equation 2.1. They were $1.73 \cdot 10^4$ mPa·s for Tween 20, $5.37 \cdot 10^3$ mPa·s for OSA starch and $1.74 \cdot 10^4$ mPa·s for PPI respectively.

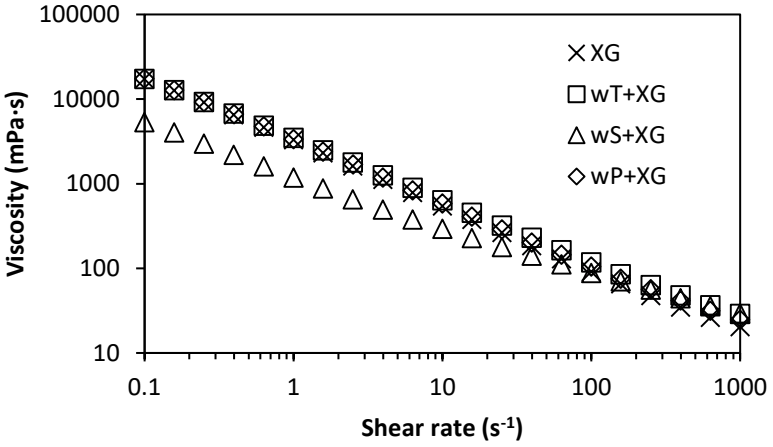


Figure 7.4 Average viscosity of the different external emulsion phases measured at 20 °C. Error bar is within symbol size.

Using the data including the droplet size ($d_{4,3}$) of emulsions produced on day of making without aroma addition reported in Tables 7.1-3, the density presented in Table 7.4 and the viscosity at 0.1 s^{-1} reported in Figure 7.4, creaming velocity was calculated for emulsions with xanthan gum addition. For the original emulsions i.e., before adding xanthan gum, the creaming velocity was calculated using the data including the droplet size of w/o/w emulsions

produced at the rotational speed of 1214 rpm and the injection speed of 1 ml/min reported in Figure 6.6, density reported in Table 6.3 and the viscosity at 10 s^{-1} reported in Figure 6.3. The droplet size of o/w emulsions used in this calculation for original emulsions were considered all at 65 μm. After calculation, creaming velocity is shown in Table 7.5. The estimation of the creaming velocity suggests that xanthan gum could effectively minimise the creaming of emulsion droplets. Thus, there would be no creaming impact on the aroma release behaviour over these xanthan gum added emulsions.

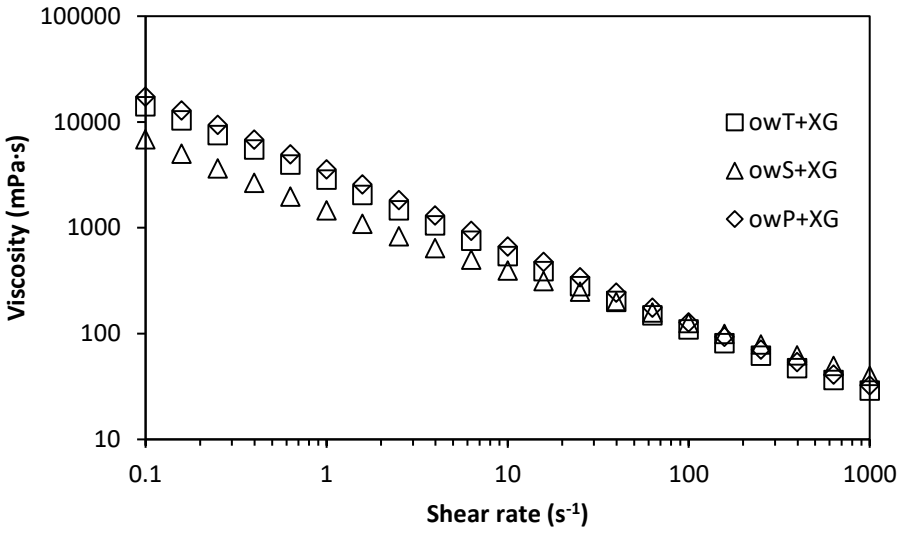
Table 7.5 Predicted creaming velocity of different emulsions at 20 °C

	Emulsion	Predicted creaming velocity (m/s)
No xanthan gum	owT	$1.87x10^{-4}$
	owS	$1.97x10^{-5}$
	owP	$1.61x10^{-4}$
	wowT	$1.15x10^{-4}$
	wowS	$1.7x10^{-5}$
	wowP	$1.31x10^{-4}$
+ xanthan gum	owT	$1.22x10^{-8}$
	owS	$4.75x10^{-8}$
	owP	$1.08x10^{-8}$
	wowT	$7.83x10^{-9}$
	wowS	$3.65x10^{-8}$
	wowP	$9.45x10^{-9}$

7.3.3 Emulsion viscosity with xanthan gum

In order to investigate the impact of the emulsion viscosity on aroma release, average viscosity of the o/w and w/o/w emulsions with xanthan gum addition after emulsion manufacture was measured. The results are shown in Figure 7.5.

A



B

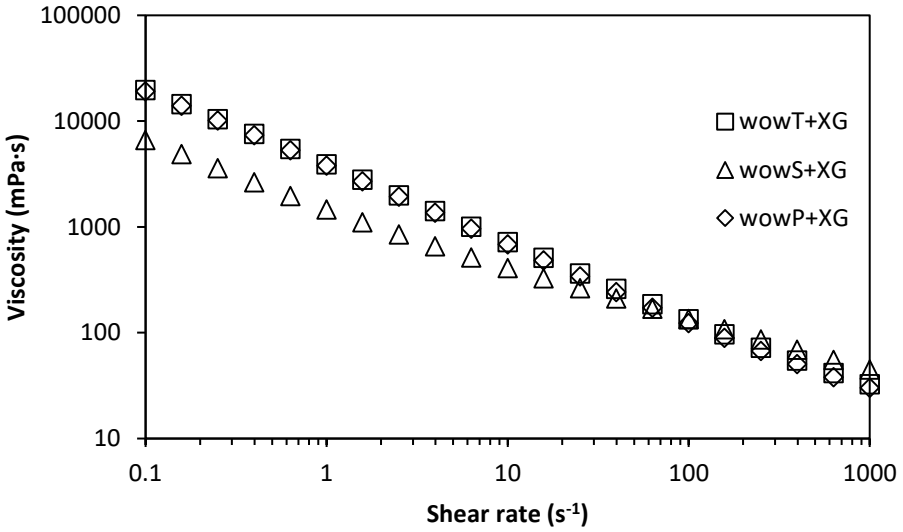


Figure 7.5 Average viscosity of A) o/w and B) w/o/w emulsions with xanthan gum measured at 20 °C. Error bar is within symbol size.

There was no apparent difference in the viscosity between o/w emulsions (Figure 7.7A) and w/o/w emulsions (Figure 7.7B) for each emulsifier type. It is worth noting that y axis for both systems was the same. This suggests that the viscosity was not affected by the presence of w_1. As expected all of the emulsions exhibited shear thinning flow behaviour. There was a difference in the viscosity between the Tween 20 and PPI stabilised emulsions and OSA starch stabilised emulsions when the shear rate was low. This difference would be taken into account when discussing the aroma release behaviour over these emulsions.

7.3.4 Encapsulation efficiency

Encapsulation efficiency of magnesium was measured in order to explore the diffusion of the internal water phase (w_1) into the external water phase (w_2) of the w/o/w emulsions. The diffusion of w_1 to w_2 would have an influence on the aroma distribution. Encapsulation efficiency was measured by adding magnesium chloride to w_1 and the concentration of magnesium in w_2 measured over 13 days. Initially however it was ascertained through microscopic inspection and acquisition of droplet size distribution data that the addition of magnesium chloride instead of NaCI into w_1 had no impact on the microstructure of Tween 20 stabilised w/o/w emulsions, see Figure 7.6 and Table 7.6.

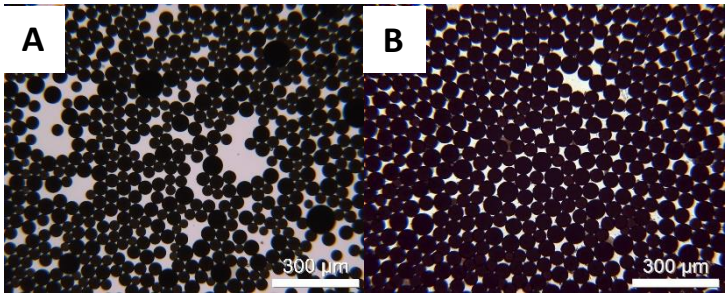


Figure 7.6 Micrographs of Tween 20 stabilised w/o/w emulsions with A) NaCl or B) $MgCl_2 \cdot 6H_2O$ added into w_1. The scale bar is 300 µm. Droplets shown in micrograph B were more crowded because the small drop of emulsion placed onto the slide was less diluted with water.

Table 7.6 Droplet size distribution characteristics of Tween 20 stabilised w/o/w emulsion with NaCl or $MgCl_2 \cdot 6H_2O$ added in w_1

w_1	$d_{4,3}$ (µm)	$d_{3,2}$ (µm)	span	SSA (m^2/g)
NaCl	57.7	55.17	0.561	0.121
$MgCl_2 \cdot 6H_2O$	59.61	57.1	0.533	0.117

Then the w/o/w emulsions stabilised with three types of emulsifiers included in this research using magnesium chloride into w_1 for up to 13 days of sample age were imaged, see Figure 7.7. There was no apparent change in the microstructure of the w/o/w emulsions using magnesium chloride instead of NaCl in w_1 compared to Figures 7.3. The w/o/w emulsions with magnesium chloride addition in w_1 were also stable for at least 13 days.

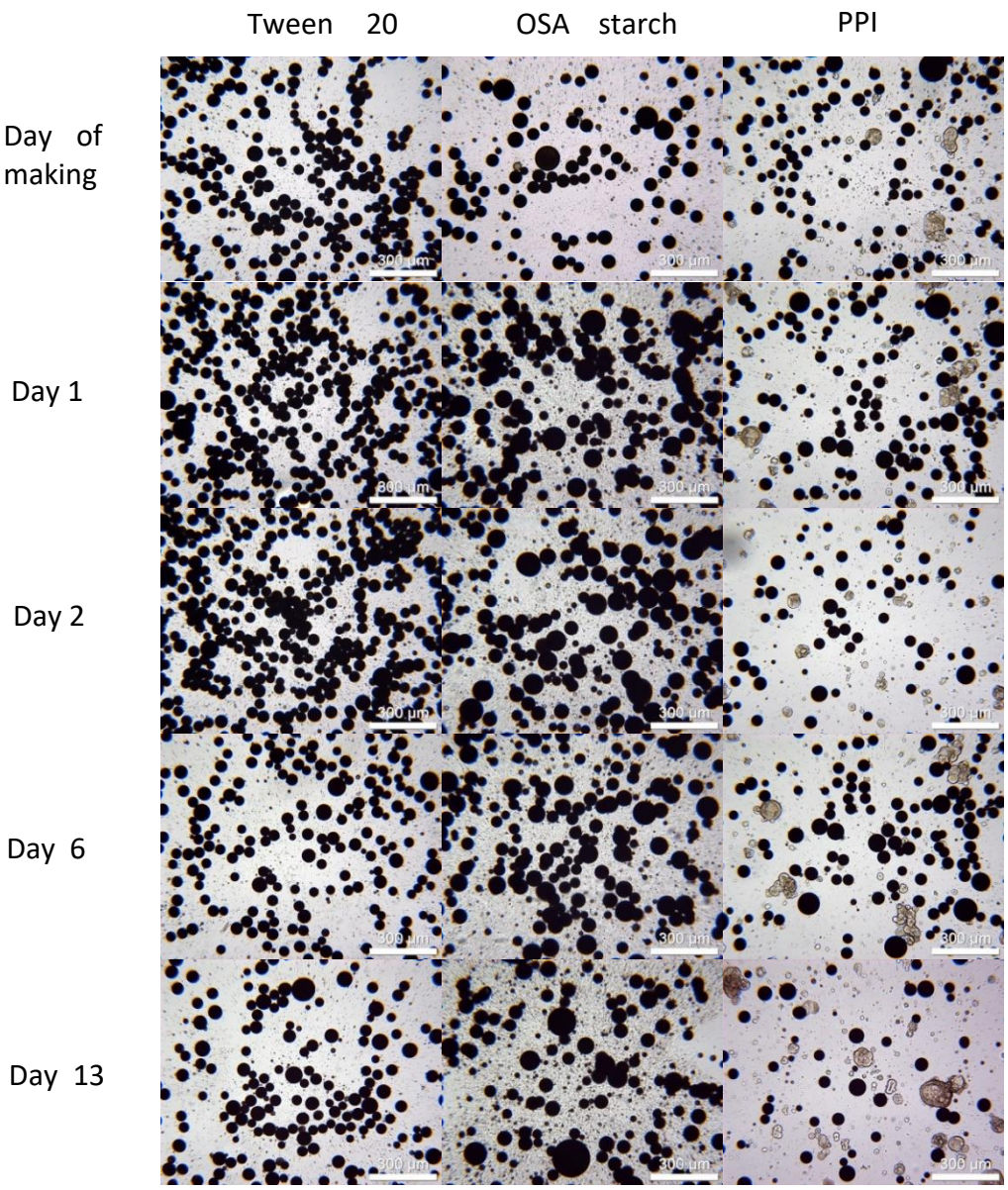


Figure 7.7 Micrographs of w/o/w emulsions stabilised with Tween 20, OSA starch or PPI with $MgCl_2 \cdot 6H_2O$ in w_1 over 13 days.

Figure 7.8 shows the release of magnesium from w_1 into w_2 of the xanthan gum thickened w/o/w emulsions over 13 days. The OSA starch and PPI stabilised w/o/w emulsions showed a release only between 3 days and 6 days after emulsion preparation. Approximately 1% of magnesium were detected in w_2

on day 6. Release continued at a slow rate and reached roughly 3% on day 13. So, these two types of emulsions appeared relatively stable against magnesium release from the encapsulated water phase and thus it is assumed that there was limited diffusion of w_1 into w_2 setting on only between 3 and 6 days after emulsion generation. It was found that the presence of hydroxylated octenyl succinate groups in OSA starch chains could bind to metal ions such as magnesium (Królikowska et al. 2017). Although there was no study reporting the interaction between magnesium and PPI, it has been reported that sodium caseinate bound to magnesium ions leading to a reduction in the ion release rate (Bonnet et al. 2009). Thus, the limited release of magnesium from OSA starch or PPI stabilised w/o/w emulsions in Fig. 7.10 could be resulted from the binding between these two hydrophilic emulsifiers and the metal ions.

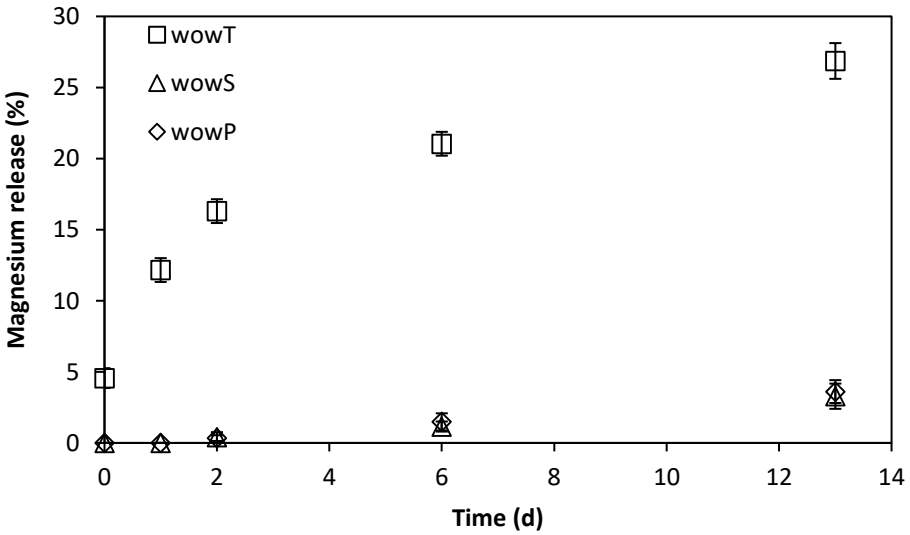


Figure 7.8 Magnesium release from w_1 to w_2 of w/o/w emulsions

The Tween 20 stabilised w/o/w emulsion was the least stable against magnesium release. 5% magnesium release was noted on the day of emulsion generation. This could be indicative of a rapidly setting on of diffusion of w_1 into w_2 or loss of w_1 into w_2 during the emulsification process. Magnesium was continuously leaked into the external water phase albeit at decreasing rate over time. 13 days after emulsion generation 27% of encapsulated magnesium had been released into the external water phase. Similar observations for Tween 20 stabilised w/o/w emulsions but manufactured at a higher injection speed (about 5 ml/min) so having a larger droplet size ($d_{3,2}$ = 107 µm) and encapsulating copper in w_1 have previously been reported (Dragosavac et al. 2012). In that case around 50% of the encapsulated copper had been release within 13 days of emulsion generation. The mechanism was explained by not one of unstable w/o/w drops and not simple diffusion from within the w/o/w droplet, because clear drops were seen after 15 days of release but the droplet size and spans did not vary substantially during 15 days. In this current study, there was no apparent change in the droplet appearance of Tween 20 stabilised w/o/w emulsions after 13 day storage. But it might be because 27% loss of w_1 into w_2 of Tween 20 stabilised w/o/w emulsions on day 13 was not high enough to show the apparent droplet appearance change. There still might be the diffusion of w_1 into w_2. The transfer mechanisms of water soluble materials were discussed in section 2.1.3.6. Thus, the higher release of magnesium and water of Tween 20 stabilised w/o/w emulsions could be resulted from the thin lamellae of Tween 20 and/ or PGPR forming in the oil film, the PGPR micelles and/or Tween20 and OSA starch reverse micelles in the oil phase. For aroma

release measurement, the increasing release of w_1 of Tween 20 stabilised w/o/w emulsions over time suggested that aroma release measurement over these emulsions was better performed within short time.

7.4 AROMA RELEASE UNDER STATIC CONDITION

Aroma release behaviour under static headspace analysis over water controls, o/w emulsions and w/o/w emulsions was plotted with the measurement signal (relative headspace intensity) as a function of time. This was to explore when the aroma intensity in the headspace over the liquids could reach an equilibrium. Five time slots were chosen to measure the relative headspace intensity. An equilibrium was supposed to be reached when the relative headspace intensities measured at two continuously measured time slots were not different. Under the static condition, aroma release is affected by the liquid system as a whole.

7.4.1 Hydrophilic aroma

Figure 7.11 shows the relative static headspace intensity of the hydrophilic aroma diacetyl above the controls of water, the o/w emulsions and the w/o/w emulsions. The relative headspace intensity of diacetyl over all liquid samples independent of the emulsifier type remained unchanged over 4h, which indicates an equilibrium within 4 h. The relative static headspace intensities of diacetyl at '4 h' were statistically analysed using the two factor ANOVA statistics

analysis (section 3.2.6). The two analysed factors were the emulsifier type (Tween 20, OSA starch and PPI) and the system type (water, o/w emulsion and w/o/w emulsion). As a result, no significant difference was found between the two factors and in each one of the factors ($P > 0.05$). It indicates the headspace intensity of hydrophilic aromas was independent of the emulsifier type and the system type at the equilibrium point. Also, as expected from the theoretical equilibrium headspace concentration ratio (section 7.2.5), the headspace intensity of diacetyl for different systems was similar, i.e. w: o/w: w/o/w = 1: 1.2: 1.1.

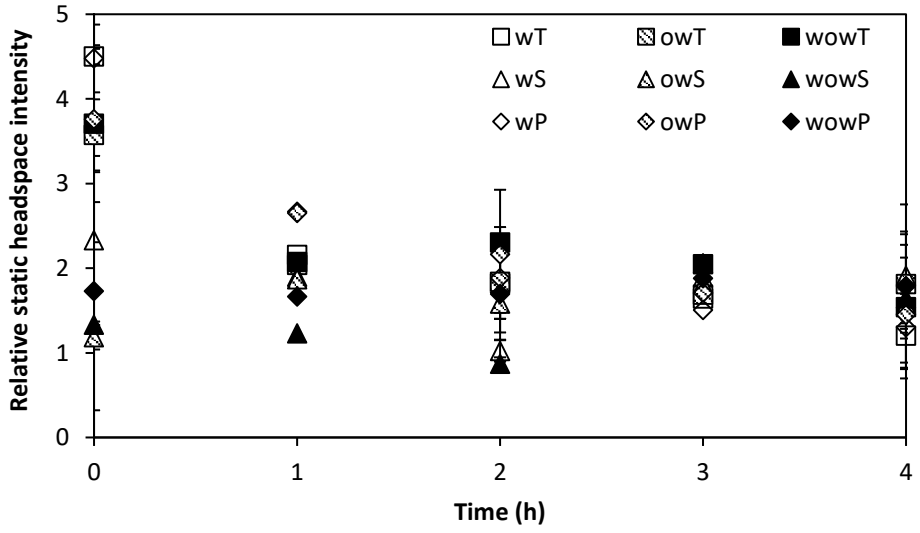


Figure 7.9 Relative static headspace intensity of diacetyl above water, o/w emulsions and w/o/w emulsions stabilised with Tween 20, OSA starch or PPI with xanthan gum. Values at 0, 2 and 4 h are based on 3 replicates and the error bars show the standard deviation.

It is generally reported that aroma release decreases with increasing viscosity in liquid systems (Malone et al. 2003). There was a lower viscosity of OSA starch stabilised o/w and w/o/w emulsions with xanthan gum at 0.1 s^{-1} compared to Tween 20 and PPI stabilised emulsions (Figure 7.5), but the aroma release behaviour was not affected by the viscosity differences. Maybe the difference in viscosity was not big enough to affect aroma release.

Although there could be a loss of the internal water phase of Tween 20 stabilised w/o/w emulsions with time (Figure 7.8), this did not show an effect of the loss of w_1 on the release of diacetyl, which could result in a higher headspace intensity over Tween 20 stabilised w/o/w emulsions than the other two w/o/w emulsions.

7.4.2 Hydrophobic aroma

Figure 7.10 presents the relative static headspace intensity of the hydrophobic aroma 3-pentanone above water, o/w emulsions and w/o/w emulsions.

The relative headspace intensity of 3-pentanone over all samples reached equilibrium within 4 h. At '4 h', the relative static headspace intensity over water controls was higher than that over the o/w and w/o/w emulsions. Since 3-pentanone is hydrophobic this result suggests that it diffused into the oil phase of both types of emulsions whereas in the water system the only hydrophobic phase available for partitioning was the gas phase. The relative static headspace intensities of 3-pentanone at '4 h' were statistically analysed.

There was no interaction between the emulsifier type and the system type ($P > 0.05$). There was no significant difference in the emulsifier type, while there was significant difference in the system type. The headspace intensity over water was significantly higher than that over the o/w emulsions and w/o/w emulsions. This is in agreement with the theory, where the equilibrium headspace concentration over water is higher than those over o/w emulsions and w/o/w emulsions (section 7.2.5), i.e. w: o/w: w/o/w = 1: 0.6: 0.7.

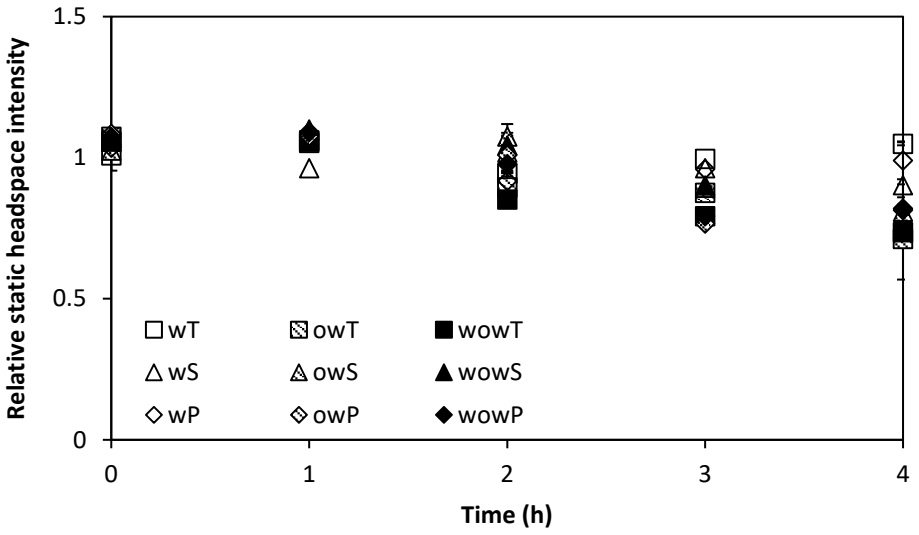


Figure 7.10 Relative static headspace intensity of 3-pentanone above water, o/w emulsions and w/o/w emulsions stabilised with Tween 20, OSA starch or PPI with xanthan gum. Values at 0, 2 and 4 h are based on 3 replicates and the error bars show the standard deviation.

7.5 AROMA RELEASE UNDER DYNAMIC CONDITION

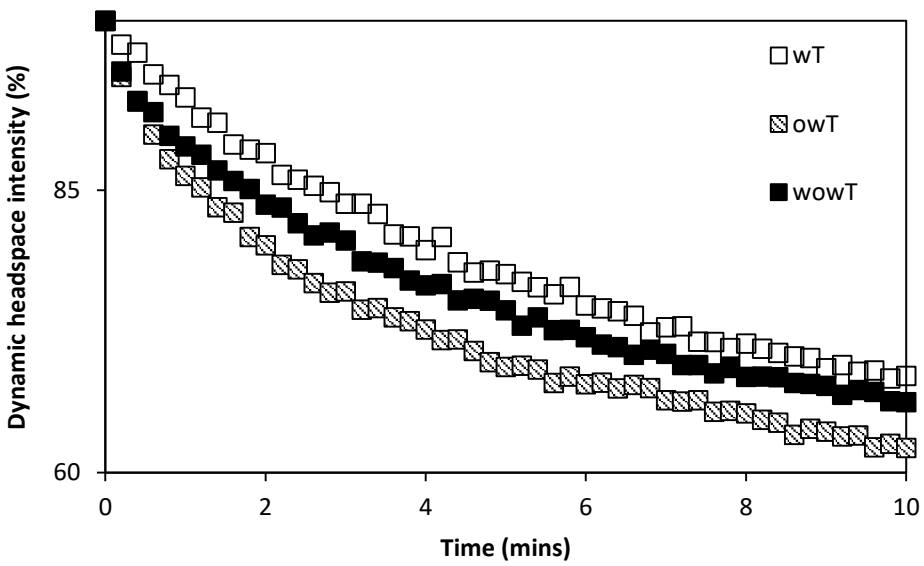
Aroma release under dynamic headspace analysis was carried out to investigate how fast the air-liquid interface replenish the headspace during headspace dilution. Dynamic release behaviour was reported with the headspace intensity as a function of time during 10 min and the first point in the headspace intensity was regarded as 100%. As described in section 5.5, during headspace dilution, the mass transfer required to replenish 100% of headspace was expected to be different depending on the aroma hydrophobicity and the system type, i.e. for the hydrophilic aroma diacetyl, o/w > w/o/w > w; for the hydrophobic aroma 3-pentanone, w > w/o/w > o/w.

7.5.1 Hydrophilic aroma

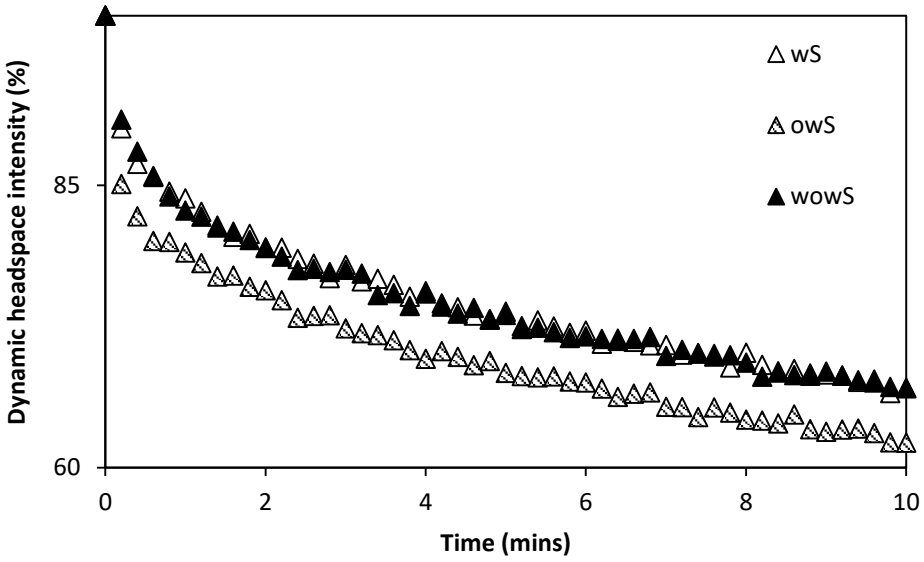
Figure 7.11 shows the dynamic headspace intensity of diacetyl over water, o/w emulsions and w/o/w emulsions. Since the data was all overlap, the y-axis scale starts from 60% instead of to zero to show the differences in intensity.

Statistical analysis of the headspace intensity by the two factor ANOVA method at the time points of 2, 5 and 10 min was carried out to facilitate the discussion of the results. 2, 5 and 10 min were chosen as early stage, mid stage and late stage of dynamic headspace analysis. Two factors including the emulsifier type and the system type were analysed. Statistics showed there was no interaction between the two factors ($P > 0.05$). The results shown in Table 7.7 show the significant differences in the dynamic headspace intensity for each factor.

A


wT
owT
wowT
Dynamic headspace intensity (%)
85
60
0
2
4
6
8
10
Time (mins)

B


wS
owS
wowS
Dynamic headspace intensity (%)
85
60
0
2
4
6
8
10
Time (mins)

C

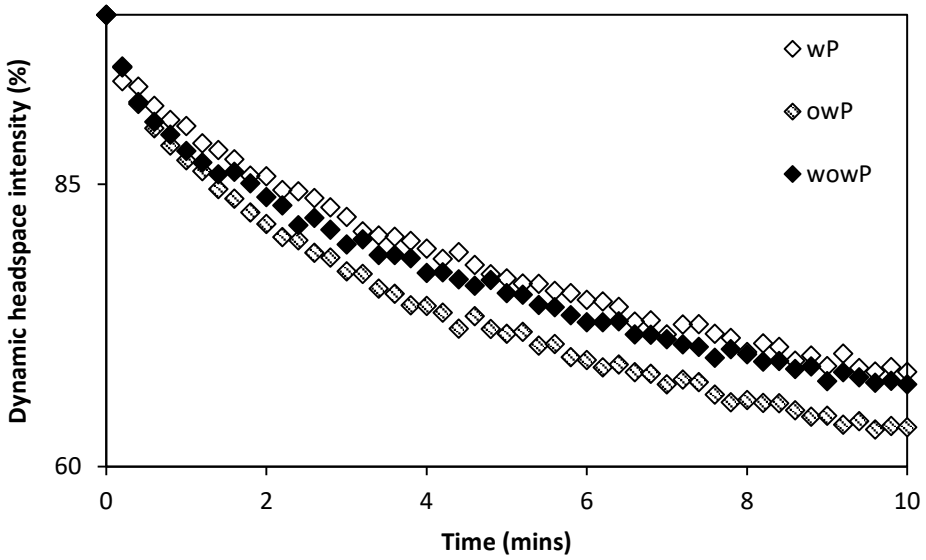


Figure 7.11 Dynamic headspace intensity of diacetyl above water, o/w emulsions and w/o/w emulsions stabilised with A) Tween 20, B) OSA starch or C) PPI with xanthan gum. Values are based on 3 replicates. Y axis starts from 60%.

Table 7.7 Statistics significant differences in the dynamic headspace intensities of diacetyl at 2, 5 and 10 min

	Emulsifier type (T, S, P)	System type (w, ow, wow)
2 min	S was significantly lower than P and T.	ow was significantly lower than wow.
5 min	No significant difference	ow was significantly lower than wow.
10 min	No significant difference	No significant difference

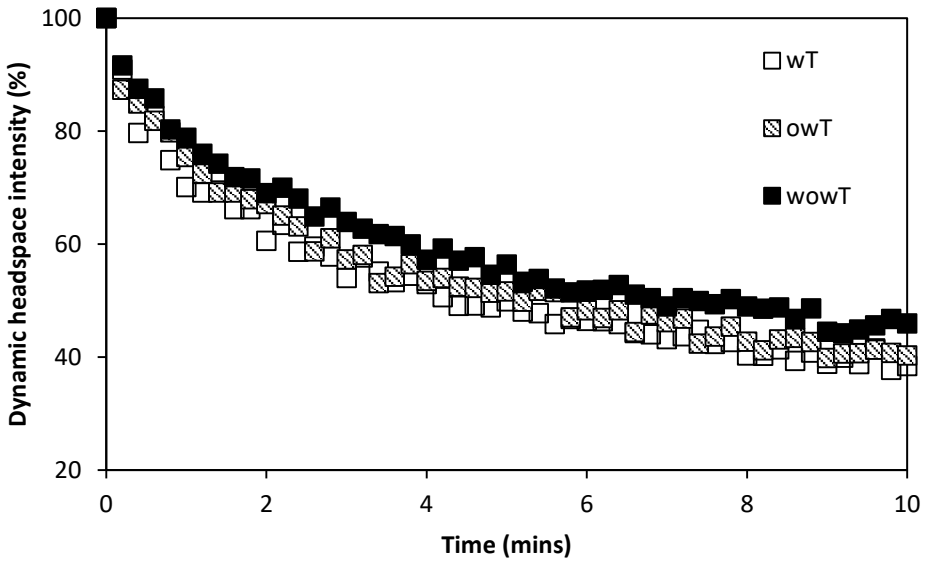
In terms of the emulsifier type, the dynamic headspace intensity over OSA starch water control was significantly lower than over the Tween 20 and PPI water controls at 2 min ($P < 0.05$). However, the significant difference disappeared at 5 and 10 min. This was also found for the OSA starch stabilised

o/w and w/o/w emulsions. Afterwards the headspace intensities over the same system were similar. It indicates that there was an interaction between diacetyl and OSA starch, but it was a weak and reversible physical interaction rather than irreversible chemical interaction. This diacetyl-OSA starch interaction was also observed in the emulsions generated conventionally, see section 5.5.1. Hydrogen bonding was discussed as a possible mechanism behind this, see section 2.4.2.4. In terms of system type, the headspace intensities over o/w emulsions were slightly lower than those over water and w/o/w emulsions at 2 and 5 min. Nonetheless, there was no difference for all system types at 10 min. This could be due to the hydrophilic aroma compound diacetyl favouring water. Since there was more water in water controls and w/o/w emulsions than in o/w emulsions, diacetyl tended to remain more in water controls and w/o/w emulsions than in o/w emulsions so less was released into the headspace of o/w emulsions.

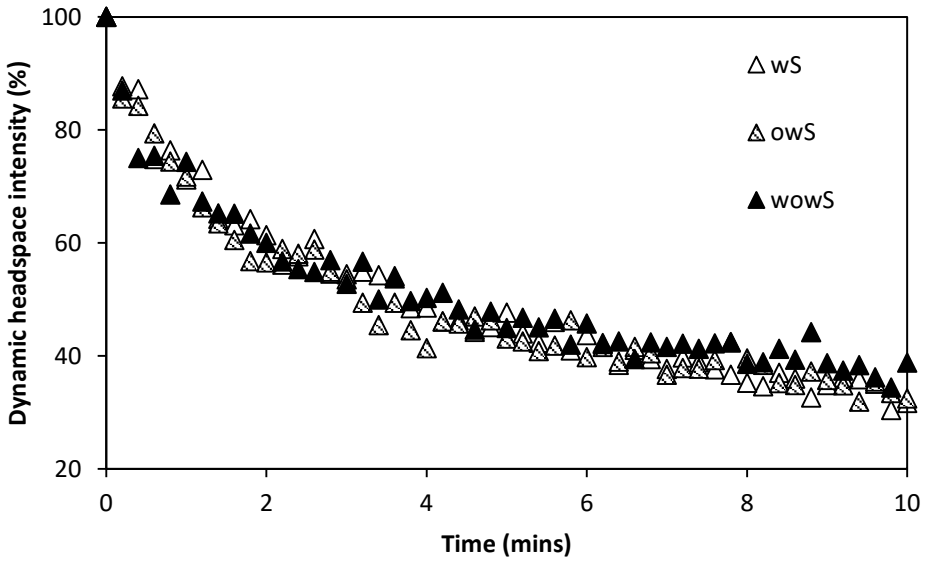
7.5.2 Hydrophobic aroma

Figure 7.12 shows the headspace intensity of the hydrophobic aroma 3-pentanone over water, o/w emulsions and w/o/w emulsions. The data overlapped. Thus, in accordance with the hydrophilic aroma data, the dynamic headspace intensities at the time points of 2, 5 and 10 min were also statistical analysed and results are reported in Table 7.8. There was also no interaction between the two factors, the emulsifier type and the system type ($P > 0.05$).

A


100
80
60
40
20
0
2
4
6
8
10
Dynamic headspace intensity (%)
Time (mins)
wT
owT
wowT

B


100
80
60
40
20
0
2
4
6
8
10
Dynamic headspace intensity (%)
Time (mins)
wS
owS
wowS

C

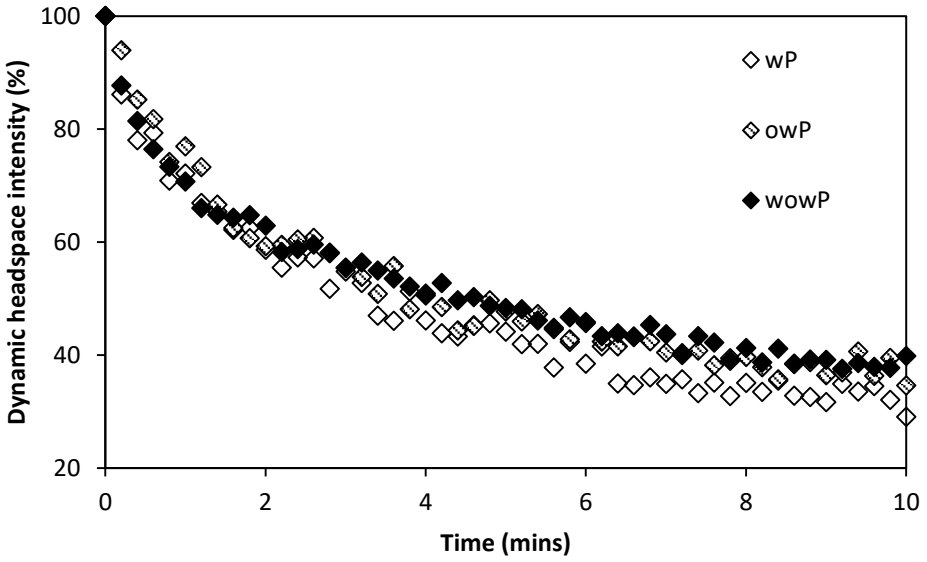


Figure 7.12 Dynamic headspace intensity of 3-pentanone above water, o/w emulsions and w/o/w emulsions stabilised with A) Tween 20, B) OSA starch or C) PPI with xanthan gum. Values are based on 3 replicates. Y axis starts from 20%.

Table 7.8 Statistics significant differences in the dynamic headspace intensities at 2, 5 and 10 min

	Emulsifier type (T, S, P)	System type (w, ow, wow)
2 min	No significant difference	No significant difference
5 min	S was significantly lower than T.	No significant difference
10 min	S and P were significantly lower than T.	w was significantly lower than wow.

Based on Table 7.8, there was no significant difference in the dynamic headspace over all samples at 2 min. However, Tween 20 samples had higher

headspace intensities than PPI and OSA starch samples at 5 and 10 min. The increase of the headspace intensity for Tween 20 samples was also observed for the high shear processed emulsions and the possible mechanism was explained by the thinner interface laden by Tween 20 as discussed in section 5.5.2. It was also suggested that there might be interactions between 3-pentanone and PPI or OSA starch through the hydrophobic bonding described in sections 2.4.2.3-4, which hindered the dynamic release of 3-pentanone starting from 5 min. The headspace intensities of 3-pentanone over Tween 20 stabilised w/o/w emulsions were also higher than those over OSA starch and PPI stabilised w/o/w emulsions. At 10 min, the dynamic headspace intensity of 3-pentanone over water was lower than that over w/o/w emulsions. Since 3-pentanone is hydrophobic, it favoured oil so more remained in w/o/w emulsions than water and less was released in the headspace.

7.6 CONCLUSIONS

Compared to the Chapter 5 results, the impact of droplet size and creaming as well as emulsion stability on aroma release were eliminated in this Chapter to investigate the aroma-emulsifier interactions alone. This was achieved by producing similarly sized and 13 day stable o/w and w/o/w emulsions stabilised with different hydrophilic emulsifiers using stirred cell membrane emulsification. Besides, the addition of xanthan gum after emulsion manufacture prevented the droplets to cream. Aroma release analysis above these emulsions showed that there was an interaction between the hydrophilic

aroma diacetyl and OSA starch possibly by reversible physical hydrogen bonding. There were interactions between the hydrophobic aroma 3-pentanone and OSA starch or PPI possibly through hydrophobic bonding. Interface thickness might also influence on the 3-pentanone release over w/o/w emulsions, where a thicker interface laden by OSA starch or PPI than an interface laden by Tween 20 might decrease the release rate.

8 OVERALL CONCLUSIONS AND FUTURE WORK

A brief summary of the research undertaken is presented first, before the overall conclusions in section 8.1 followed by suggestions for future work in section 8.2.

The overall aim of this PhD research was to explore the impact of interaction between aroma compounds and hydrophilic emulsifiers and the impact of emulsion microstructure including droplet size, droplet size distribution and emulsion stability on aroma release behaviour over w/o/w emulsions using *in vitro* methods. As w/o/w emulsions are suitable vehicles for aroma delivery as well as fat-reduced systems, it is necessary to understand the factors affecting aroma release behaviour. This research started with the questions below: Can w/o/w emulsions be used to entrap aroma compounds and If so, how can aroma compounds be entrapped? Do the emulsion ingredients in particularly the hydrophilic emulsifier as well as emulsion microstructure stabilised with the hydrophilic emulsifier have an impact on aroma release over w/o/w emulsions? If so, can the effect of the emulsion microstructure in particularly droplet size as well as creaming be eliminated to investigate the effect of hydrophilic emulsifier on aroma release alone? What kind of interactions exist between the hydrophilic emulsifier and aroma compounds?

To answer these questions, polyglycerol polyricinoleate (PGPR) was used as the only hydrophobic emulsifier to stabilise the primary w/o emulsion in w/o/w emulsions throughout this research. The aroma entrapment in a w/o/w emulsion manufactured via high shear mixing affected by the hydrophobicity

of aroma compounds was initially investigated. Then three hydrophilic emulsifiers, polyoxyethylene 20 sorbitan monolaurate (Tween 20), octenyl succinic anhydride (OSA) starch and pea protein isolate (PPI), were used to produce w/o/w emulsions and control o/w emulsions through high shear mixing. Emulsion microstructure was characterised in terms of droplet appearance, droplet size, droplet size distribution as well as emulsion stability over time. The aroma release behaviour under static and dynamic headspace analyses over these emulsions was evaluated. Apart from the nature of aromas, the differences in the headspace intensity of aromas were explained by aroma-emulsifier interactions and the impact of emulsion microstructure. To further understand the impact of aroma-emulsifier interaction alone, w/o/w emulsions with similarly sized droplets were produced through stirred cell membrane emulsification and emulsion microstructure was characterised over time. Aroma release behaviour over these controlled w/o/w and o/w emulsions with xanthan gum addition to prevent droplet creaming during assessment was measured. The loss of the internal water phase (w_1) into the external water phase (w_2) was evaluated by encapsulating magnesium in w_1 and measuring magnesium in w_2 over time. Emulsion microstructure characteristics plus emulsion viscosity after xanthan gum addition were also investigated.

8.1 CONCLUSIONS

The conclusions are presented by research question as follows:

- Can w/o/w emulsions be used to entrap aroma compounds and If so, how can aroma compounds be entrapped?

w/o/w emulsions were shown to be a suitable vehicle for short time aroma entrapment. This entrapment depended on the hydrophobicity of aroma compounds, which was most successful for a hydrophilic aroma (acetoin). The entrapment of the hydrophilic aroma in w/o/w emulsions resulted from the barrier of the oil phase in w/o droplets to delay its diffusion or the micelles of the hydrophobic emulsifier to entrap it inside.

- Do the emulsion ingredients in particularly the hydrophilic emulsifier as well as emulsion microstructure stabilised with the hydrophilic emulsifier have an impact on aroma release over w/o/w emulsions?

The hydrophilic emulsifier (Tween 20, OSA starch and PPI) as well as the emulsion microstructure including droplet size, emulsion stability, interface thickness, creaming and diffusion of w_1 into w_2 of w/o/w emulsions had an effect on the release of both investigated aromas (i.e. a hydrophilic aroma diacetyl and a hydrophobic aroma 3-pentanone) over w/o/w emulsions. Aroma release over w/o/w emulsions was slowed down for the reasons of the hydrophilic emulsifier-aroma interactions, instability of PPI stabilised emulsions, creaming of all emulsions, thicker interface laden by OSA starch or PPI and/ or the water diffusion from w_1 to w_2.

- If so, can the effect of the emulsion microstructure in particularly droplet size and creaming be eliminated to investigate the effect of hydrophilic emulsifier on aroma release alone?

The impact of droplet size on aroma release was eliminated by producing similarly sized emulsion droplets independent of hydrophilic emulsifier type through the membrane emulsification. It was the first time showed that complex food emulsifiers can be successfully used in stirred cell membrane emulsification to stabilise w/o/w emulsions. This followed the trend of the theoretical droplet diameter predicted by the published model. The effect of creaming on aroma release was eliminated by the addition of xanthan gum xanthan gum to the continuous phase of emulsions after emulsion manufacture to prevent droplets creaming. These emulsions were also stable independent of aroma inclusion, type of aroma inclusion, sample age and xanthan gum addition. Thus, the effect of aroma-emulsifier interactions could be investigated alone.

- What kind of interactions exist between the hydrophilic emulsifier and aroma compounds?

The thinner interface laden by Tween 20 possibly led to a quicker diffusion of 3-pentanone from the w/o droplets in w_2, as the thicker interface laden by OSA starch or PPI could decreasing the release rate. OSA starch interacted with the hydrophilic aroma diacetyl possibly through hydrogen bonding, while it interacted with 3-pentanone possibly through inclusion complex. PPI interacted with 3-pentanone possibly through hydrophobic bonding. These

were independent of whether these emulsions were of broad droplet size distribution as generally created through high shear mixing or had much more uniform droplet sizes when processed via stirred cell membrane emulsification.

Thus, this research presents a better understanding of aroma release behaviour influenced by the hydrophilic emulsifier and emulsion microstructure and a novel study to produce similarly sized of o/w and w/o/w emulsions stabilised with complex food emulsifiers in order to eliminate the effect of droplet size on aroma release.

8.2 FUTURE WORK

Based on this research, a few recommendations for future work are discussed as follows.

- In the current research, mainly two aroma compounds, diacetyl and 3-pentanone, were investigated for release behaviour over w/o/w emulsions. Although they were chosen as a hydrophilic aroma and a hydrophobic aroma respectively, a wider range of hydrophobicity of aroma compounds especially for hydrophilic (log P < 0) or more hydrophobic (log P > 1) aromas can be used to explore whether the interactions with the hydrophilic emulsifiers are still valid. This is to cover more aromas with the hydrophilic character since the w/o/w emulsions have the capability to entrap hydrophilic aromas inside, but also to cover more aromas with the hydrophobic character since the

majority of aroma compounds in food are hydrophobic (Taylor et al. 2010). It is expected that theses interactions between the emulsifiers and a hydrophilic aroma compound possibly through hydrogen bonding would be enhanced if a more hydrophilic aroma is used and same is for a more hydrophobic aroma.

- In the present research the three hydrophilic emulsifiers Tween 20, OSA starch and PPI were included for the stabilisation of the w/o/w emulsions as representatives of a low molecular weight surfactant, a hydrophobically modified starch and a protein respectively. There was much less loss of w_1 into w_2 for the starch and the protein stabilised w/o/w emulsions than the surfactant stabilised w/o/w emulsions. But the PPI stabilised w/o/w emulsions manufactured through high shear mixing had poor stability. Thus, it might be useful to use other proteins possibly with a higher surface activity, such as sodium caseinate and whey protein isolate, to stabilise w/o/w emulsions (Midmore et al. 1999, Bonnet et al. 2009, Lutz et al. 2009) through conventional and membrane emulsification. Then the effect of loss of w_1 and whether these proteins have the interaction with aroma compounds can be investigated.

- The nature of the proposed OSA starch-diacetyl, OSA starch-3-pentanone and PPI-3-pentanone interactions could be tested. It is suggested to measure such bonding through methods of determining binding constants or binding sites by chromatography, equilibrium

dialysis, static headspace, fluorimetry and nuclear magnetic resonance spectroscopy (Harrison et al. 1997, Guichard et al. 2000, Jouenne et al. 2000, Chalier et al. 2007, Tavel et al. 2008, Shimizu et al. 2017). This is to confirm the bonding between the hydrophilic emulsifiers (i.e. OSA starch and PPI) and aroma compounds (i.e. diacetyl and 3-pentanone), which was speculated to occur as one of the aroma release mechanisms.

- It was reported that more hydrophobic aroma compounds have a greater significant decrease in both interfacial elasticity and interfacial viscosity than hydrophilic aromas (Neville 2014). The decrease in the elastic behaviour of the interface suggests that interfaces are more susceptible to deformation and have an increased flow. Thus, interfacial rheological measurement at the w/o-w_2 interface stabilised with PGPR as the hydrophobic emulsifier and OSA starch or PPI as the hydrophilic emulsifier in the presence of the aroma compound 3-pentanone can also be carried out. This is to explore whether 3-pentanone significantly decreases the interfacial elasticity and interfacial viscosity as an indication of interface susceptibility to deformation, which may impact on emulsion stability and aroma release behaviour.

REFERENCES

Abd El-Hady, E. A. and Habiba, R. A. (2003). "Efffect of soaking and extrusion conditions on antinutrients and protein digestibility of legume seeds." Lebensmittel-Wissenschaft Und-Technologie-Food Science and Technology **36**(3): 285-293.

Adams, R. L., Mottram, D. S., Parker, J. K. and Brown, H. M. (2001). "Flavor-protein binding: disulfide interchange reactions between ovalbumin and volatile disulfides." J Agric Food Chem **49**(9): 4333-4336.

Adebiyi, A. P. and Aluko, R. E. (2011). "Functional properties of protein fractions obtained from commercial yellow field pea (Pisum sativum L.) seed protein isolate." Food Chemistry **128**(4): 902-908.

Aditya, N. P., Aditya, S., Yang, H.-J., Kim, H. W., Park, S. O., Lee, J. and Ko, S. (2015). "Curcumin and catechin co-loaded water-in-oil-in-water emulsion and its beverage application." Journal of Functional Foods **15**: 35-43.

Akhtar, M., Murray, B. S. and Dickinson, E. (2006). "Perception of creaminess of model oil-in-water dairy emulsions: Influence of the shear-thinning nature of a viscosity-controlling hydrocolloid." Food Hydrocolloids **20**(6): 839-847.

Almonds, B. B., Beetroot, G. E., Belitz, H. D., Grosch, W. and Schieberle, P. (2009). Aroma compounds. In: Food Chemistry,4th edition. Belitz, H. D., Grosch, W. and Schieberle, P. Berlin, Springer. 5**:** 340-341.

Andriot, I., Harrison, M., Fournier, N. and Guichard, E. (2000). "Interactions between methyl ketones and beta-lactoglobulin: Sensory analysis, headspace analysis, and mathematical modeling." Journal of Agricultural and Food Chemistry **48**(9): 4246-4251.

Arancibia, C., Jublot, L., Costell, E. and Bayarri, S. (2011). "Flavor release and sensory characteristics of o/w emulsions. Influence of composition, microstructure and rheological behavior." Food Research International **44**(6): 1632-1641.

Arvisenet, G., Voilley, A. and Cayot, N. (2002). "Retention of aroma compounds in starch matrices: competitions between aroma compounds towards amylose and amylopectin." J. Agric. Food Chem. **50**(25): 7345-7349.

Atkins, P. W. and J. de, P. (2014). Physical chemistry,10th edition. Oxford, Oxford University Press.

Augustin, M. A. and Sanguansri, L. (2008). Encapsulation of bioactives. In: Food Materials Science: Principles and Practice. Aguilera, J. M. and Lillford, P. J. New York, NY, Springer New York**:** 577-601.

Aveyard, R., Binks, B. P. and Clint, J. H. (2003). "Emulsions stabilised solely by colloidal particles." Adv Colloid Interface Sci **100**: 503-546.

Azhar, Y. K., Sushama, T., Zeenat, I., Farhan, J. A. and Roop, K. K. (2006). "Multiple emulsions : an overview." Current Drug Delivery **3**(4): 429-443.

Bahtz, J., Gunes, D. Z., Syrbe, A., Mosca, N., Fischer, P. and Windhab, E. J. (2016). "Quantification of spontaneous w/o emulsification and its impact on the swelling kinetics of multiple w/o/w emulsions." Langmuir **32**(23): 5787-5795.

Bai, Y., Shi, Y.-C., Herrera, A. and Prakash, O. (2011). "Study of octenyl succinic anhydride-modified waxy maize starch by nuclear magnetic resonance spectroscopy." Carbohydrate Polymers **83**(2): 407-413.

Bakker, J. (1995). Flavour interactions with the food matrix and their effects on perception. In: Ingredient interactions: effects on food quality. Gaonkar, A. G. New York, M. Dekker**:** 411-439.

Bakker, J., Boudaud, N., Harrison, M. (1998). "Dynamic release of diacetyl from liquid gelatin in the headspace." Journal of Agricultural and Food Chemistry **46**(7): 2714-2720.

Bandyopadhyay, P., Ghosh, A. K. and Ghosh, C. (2012). "Recent developments on polyphenol-protein interactions: effects on tea and coffee taste, antioxidant properties and the digestive system." Food & Function **3**(6): 592-605.

Barac, M., Cabrilo, S., Pesic, M., Stanojevic, S., Zilic, S., Macej, O. and Ristic, N. (2010). "Profile and Functional Properties of Seed Proteins from Six Pea (Pisum sativum) Genotypes." International Journal of Molecular Sciences **11**(12): 4974-4991.

Bastida-Rodriguez, J. (2013). "The food additive polyglycerol polyricinoleate (e-476): Structure, applications, and production methods." ISRN Chemical Engineering **2013**: 21.

Benichou, A., Aserin, A. and Garti, N. (2004). "Double emulsions stabilized with hybrids of natural polymers for entrapment and slow release of active matters." Adv Colloid Interface Sci **108-109**: 29-41.

Benjamin, O., Silcock, P., Beauchamp, J., Buettner, A. and Everett, D. W. (2014). "Emulsifying properties of legume proteins compared to β-lactoglobulin and tween 20 and the volatile release from oil-in-water emulsions." Journal of Food Science **79**(10): E2014-E2022.

Beverung, C. J., Radke, C. J. and Blanch, H. W. (1999). "Protein adsorption at the oil/water interface: characterization of adsorption kinetics by dynamic interfacial tension measurements." Biophysical Chemistry **81**(1): 59-80.

Bhosale, R. and Singhal, R. (2006). "Process optimization for the synthesis of octenyl succinyl derivative of waxy corn and amaranth starches." Carbohydrate Polymers **66**(4): 521-527.

Bishop, J. R. and White, C. H. (1986). "Assessment of dairy product quality and potential shelf-life - a review." Journal of Food Protection **49**(9): 739-753.

Biswal, N. R. and Singh, J. K. (2016). "Interfacial behavior of nonionic Tween 20 surfactant at oil-water interfaces in the presence of different types of nanoparticles." RSC Advances **6**(114): 113307-113314.

Bonnet, M., Cansell, M., Berkaoui, A., Ropers, M. H., Anton, M. and Leal-Calderon, F. (2009). "Release rate profiles of magnesium from multiple W/O/W emulsions." Food Hydrocolloids **23**(1): 92-101.

Borwankar, R. P., Lobo, L. A. and Wasan, D. T. (1992). "Emulsion stability — kinetics of flocculation and coalescence." Colloids and Surfaces **69**(2): 135-146.

Boutboul, A., Giampaoli, P., Feigenbaum, A. and Ducruet, V. (2002a). "Influence of the nature and treatment of starch on aroma retention." Carbohydrate Polymers **47**(1): 73-82.

Boutboul, A., Giampaoli, G., Feigenbaum, A. and Duvruet, V. (2002b). "Use of inverse gas chromatography with humidity control of the carrier gas to characterize aroma-starch interactions." Food Chemistry **71**: 387-392.

Brooks, B. W., Richmond, H. N. and Zerfa, M. (1998). Phase inversion and drop formation in agitated liquid–liquid dispersions in the presence of nonionic surfactants. In: Modern Aspects of Emulsion Science**:** 175-204.

Brückner, M., Bade, M. and Kunz, B. (2007). "Investigations into the stabilization of a volatile aroma compound using a combined emulsification and spray drying process." European Food Research and Technology **226**(1-2): 137-146.

Burova, T. V., Grinberg, N. V., Grinberg, V. Y. and Tolstoguzov, V. B. (2003). "Binding of odorants to individual proteins and their mixtures. Effects of protein denaturation and association. A plasticized globule state." Colloids and Surfaces A: Physicochemical and Engineering Aspects **213**(2–3): 235-244.

Buttery, R. G., Guadagni, D. G. and Ling, L. C. (1973). "Flavour compounds: volatiles in vegetable oil and oil-water mixtures." Journal of Agricultural and Food Chemistry **21**: 198.

Capek, I. (2004). "Degradation of kinetically-stable o/w emulsions." Adv Colloid Interface Sci **107**(2-3): 125-155.

Chalier, P., Angot, B., Delteil, D., Doco, T. and Gunata, Z. (2007). "Interactions between aroma compounds and whole mannoprotein isolated from Saccharomyces cerevisiae strains." Food Chemistry **100**(1): 22-30.

Chanamai, R. and McClements, D. J. (2002). "Comparison of gum arabic, modified starch, and whey protein isolate as emulsifiers: Influence of ph, cacl2 and temperature." Journal of Food Science **67**(1): 120-125.

Chang, D., Abbas, S., Hayat, K., Xia, S., Zhang, X., Xie, M. and Kim, J. M. (2010). "Original article: Encapsulation of ascorbic acid in amorphous maltodextrin employing extrusion as affected by matrix/core ratio and water content." International Journal of Food Science & Technology **45**(9): 1895-1901.

Charles, M., Rosselin, V., Beck, L., Sauvageot, F. and Guichard, E. (2000). "Flavor Release from Salad Dressings: Sensory and Physicochemical Approaches in Relation with the Structure." Journal of Agricultural and Food Chemistry **48**(5): 1810-1816.

Chattopadhyay, A. K., Ghaicha, L., Oh, S. G. and Shah, D. O. (1992). "Salt effects on monolayers and their contribution to surface viscosity." Journal of Physical Chemistry **96**(15): 6509-6513.

Chattopadhyay, A. K., Ghaicha, L., Oh, S. G., Knight, J., Moaddel, T. and Friberg, S. E. (1993). "Some anomalies between the surfactants comprising linear and branched hydrocarbon chains." Journal of the Indian Chemical Society **70**(4-5): 353-364.

Cheng, J., Chen, J.-F., Zhao, M., Luo, Q., Wen, L.-X. and Papadopoulos, K. D. (2007). "Transport of ions through the oil phase of W-1/O/W-2 double emulsions." J Colloid Interface Sci **305**(1): 175-182.

Chiu, N., Hewson, L., Fisk, I. and Wolf, B. (2015). "Programmed emulsions for sodium reduction in emulsion based foods." Food & Function **6**(5): 1428-1434.

Chiu, N., Tarrega, A., Parmenter, C., Hewson, L., Wolf, B. and Fisk, I. D. (2017). "Optimisation of octinyl succinic anhydride starch stablised w1/o/w2 emulsions for oral destablisation of encapsulated salt and enhanced saltiness." Food Hydrocolloids **69**: 450-458.

Chobpattana, W., Jeon, I. J., Smith, J. S. and Loughin, T. M. (2002). "Mechanisms of interaction between vanillin and milk proteins in model systems." Journal of Food Science **67**(3): 973-977.

Choi, J.-K., Girek, T., Shin, D.-H. and Lim, S.-T. (2002). "Structural and physical characterization of octenylsuccinyl β-cyclodextrin." Carbohydrate Polymers **49**(3): 289-296.

Cosgrove, T. (2010). Colloid science: principles, methods and applications,2nd. West Sussex, United Kingdom, John Wiley & Son Ltd**:** 47-49.

Cottrell, T. and van Peij, J. (2015). Sorbitan esters and polysorbates. In: Emulsifiers in food technology. Norn, V. West Sussex, UK, Wiley Blackwell. 12**:** 276-282.

Dagorn-Scaviner, C., Gueguen, J. and Lefebvre, J. (1987). "Emulsifying Properties of Pea Globulins as Related to Their Adsorption Behaviors." Journal of Food Science **52**(2): 335-341.

Damodaran, S. and Kinsella, J. E. (1980a). "Flavor protein interactions. Binding of carbonyls to bovine serum albumin: thermodynamic and conformational effects." Journal of Agricultural and Food Chemistry **28**(3): 567-571.

Damodaran, S. and Kinsella, J. E. (1980b). "Stabilization of proteins by solvents. Effect of pH and anions on the positive cooperativity of 2-nonanone binding to bovine serum albumin." Journal of Biological Chemistry **255**(18): 8503-8508.

Damodaran, S. and Kinsella, J. E. (1981). "Interaction of carbonyls with soy protein: thermodynamic effects." Journal of Agricultural and Food Chemistry **29**(6): 1249-1253.

Damodaran, S. and Paraf, A. (1997). Food proteins and their applications. New York, Marcel Dekker, Inc.

Davis, H. T. (1994). "Factors determining emulsion type: Hydrophile—lipophile balance and beyond." Colloids and Surfaces A: Physicochemical and Engineering Aspects **91**: 9-24.

Davis, R. H. (1996). Velocities of sedimenting particles in suspensions. In: Sedimentation of small particles in a viscous liquid. Tory, E. M., Ed. Southampton, UK, Computational Mechanics Publications. Chapter 6.

Decourcelle, N., Lubbers, S., Vallet, N., Rondeau, P. and Guichard, E. (2004). "Effect of thickeners and sweeteners on the release of blended aroma compounds in fat-free stirred yoghurt during shear conditions." International Dairy Journal **14**(9): 783-789.

Delarue, J. and Giampaoli, P. (2000). "Study of interaction phenomena between aroma compounds and carbohydrate matrixes by inverse gas chromatography." Journal of Agricultural and Food Chemistry **48**(6): 2372-2375.

Dickinson, E., Evison, J. and Owusu, R. K. (1991). "Preparation of fine protein-stabilized water-in-oil-in-water emulsions." Food Hydrocolloids **5**(5): 481-485.

Dickinson, E. (1992). Introduction to food colloids, Oxford University Press.

Dickinson, E., Evison, J., Gramshaw, J. W. and Schwope, D. (1994). "Flavour release from a protein-stabilized water-in-oil-in-water emulsion." Food Hydrocolloids **8**(1): 63-67.

Dickinson, E. (1997). "Properties of emulsions stabilized with milk proteins: Overview of some recent developments." Journal of Dairy Science **80**(10): 2607-2619.

Dickinson, E. (2003). "Hydrocolloids at interfaces and the influence on the properties of dispersed systems." Food Hydrocolloids **17**(1): 25-39.

Dickinson, E. (2009). "Hydrocolloids as emulsifiers and emulsion stabilizers." Food Hydrocolloids **23**(6): 1473-1482.

Dickinson, E. (2010). "Flocculation of protein-stabilized oil-in-water emulsions." Colloids Surf B Biointerfaces **81**(1): 130-140.

Dokić, L., Krstonošić, V. and Nikolić, I. (2012). "Physicochemical characteristics and stability of oil-in-water emulsions stabilized by OSA starch." Food Hydrocolloids **29**(1): 185-192.

Dokic, P. (2008). Colloid characteristics and emulsifying properties of osa starches.

Doyen, K., Carey, M., Linforth, R. S. T., Marin, M. and Taylor, A. J. (2001). "Volatile release from an emulsion: Headspace and in-mouth studies." Journal of Agricultural and Food Chemistry **49**(2): 804-810.

Dragosavac, M. M., Sovilj, M. N., Kosvintsev, S. R., Holdich, R. G. and Vladisavljević, G. T. (2008). "Controlled production of oil-in-water emulsions containing unrefined pumpkin seed oil using stirred cell membrane emulsification." Journal of Membrane Science **322**(1): 178-188.

Dragosavac, M. M., Holdich, R. G., Vladisavljević, G. T. and Sovilj, M. N. (2012). "Stirred cell membrane emulsification for multiple emulsions containing unrefined pumpkin seed oil with uniform droplet size." Journal of Membrane Science **392–393**: 122-129.

Druaux, C. and Voilley, A. (1997). "Effect of food composition and microstructure on volatile flavour release." Trends in Food Science & Technology **8**(11): 364-368.

Ducel, V., Richard, J., P. and Y., B., F. (2004). "Adsorption kinetics and rheological interfacial properties of plant proteins at the oil−water interface." Biomacromolecules **5**(6): 2088-2093.

Dumont, J. P. and Land, D. G. (1986). "Binding of diacetyl by pea proteins." Journal of Agricultural and Food Chemistry **34**(6): 1041-1045.

Escher, F. E., Nuessli, J. and Conde-Petit, B. (2000). Interactions of flavor compounds with starch in food processing. In: Flavor Release, American Chemical Society. 19**:** 230-245.

Fechner, A., Knoth, A., Scherze, I. and Muschiolik, G. (2007). "Stability and release properties of double-emulsions stabilised by caseinate-dextran conjugates." Food Hydrocolloids **21**(5-6): 943-952.

Ficheux, M.-F., Bonakdar, L., Leal-Calderon, F. and Bibette, J. (1998). "Some stability criteria for double emulsions." Langmuir **14**(10): 2702-2706.

Fisk, I. D. (2014). Aroma release. In: Flavour development, analysis and perception in food and beverages. Parker, J. K., Elmore, S. and Methven, L. Oxford, UK, Elsevier. 105-123**:** 105-123.

Frasch-Melnik, S., Spyropoulos, F. and Norton, I. T. (2010). "W1/O/W2 double emulsions stabilised by fat crystals--formulation, stability and salt release." J Colloid Interface Sci **350**(1): 178-185.

Garcıa-Ochoa, F., Santos, V., Casas, J. and Gomez, E. (2000). "Xanthan gum: production, recovery, and properties." Biotechnology advances **18**(7): 549-579.

Garti, N. and Aserin, A. (1996). "Double emulsions stabilized by macromolecular surfactants." Adv Colloid Interface Sci **65**: 37-69.

Garti, N. (1997a). "Double emulsions — scope, limitations and new achievements." Colloids and Surfaces A: Physicochemical and Engineering Aspects **123-124**(Supplement C): 233-246.

Garti, N. (1997b). "Progress in stabilization and transport phenomana of double emulsions in food applications." Lebensm.-Wiss.u.-Technol **30**: 222-235.

Garti, N., Aserin, A., Tiunova, I. and Binyamin, H. (1999). "Double emulsions of water-in-oil-in-water stabilized by alpha-form fat microcrystals. Part 1: Selection of

emulsifiers and fat microcrystalline particles." Journal of the American Oil Chemists Society **76**(3): 383-389.

Gerald, M. and Eric, D. (2017). "Double Emulsions Relevant to Food Systems: Preparation, Stability, and Applications." Comprehensive Reviews in Food Science and Food Safety **16**(3): 532-555.

Gharsallaoui, A., Cases, E., Chambin, O. and Saurel, R. (2009). "Interfacial and emulsifying characteristics of acid-treated pea protein." Food Biophysics **4**(4): 273-280.

Gharsallaoui, A., Saurel, R., Chambin, O. and Voilley, A. (2012). "Pea (pisum sativum, l.) protein isolate stabilized emulsions: A novel system for microencapsulation of lipophilic ingredients by spray drying." Food and Bioprocess Technology **5**(6): 2211-2221.

Gijsbertsen-Abrahamse, A. J., van der Padt, A. and Boom, R. M. (2004). "Status of cross-flow membrane emulsification and outlook for industrial application." Journal of Membrane Science **230**(1–2): 149-159.

Giroux, H. J., Constantineau, S., Fustier, P., Champagne, C. P., St-Gelais, D., Lacroix, M. and Britten, M. (2013). "Cheese fortification using water-in-oil-in-water double emulsions as carrier for water soluble nutrients." International Dairy Journal **29**(2): 107-114.

Griffin, W. C. (1949). "Classification of surface active agnets by HLB." J. Soc. Cosmet. Chem. **1**: 311-326.

Gueguen, J., Chevalier, M., Barbot, J. and Schaeffer, F. (1988). "Dissociation and aggregation of pea legumin induced by pH and ionic strength." Journal of the Science of Food and Agriculture **44**(2): 167-182.

Guichard, E. and Langourieux, S. (2000). "Interactions between β-lactoglobulin and flavour compounds." Food Chemistry **71**(3): 301-308.

Guichard, E. (2002). "Interactions between flavor compounds and food ingredients and their influence on flavor perception." Food Reviews International **18**(1): 49-70.

Guyot, C., Bonnafont, C., Lesschaeve, I., Issanchou, S., Voilley, A. and Spinnler, H. E. (1996). "Effect of fat content oil odor intensity of three aroma compounds in model emulsions: delta-decalactone, diacetyl, and butyric acid." Journal of Agricultural and Food Chemistry **44**(8): 2341-2348.

Hadnađev, T. D., Hadnađev, M., Pojić, M., Rakita, S. and Krstonošić, V. (2015). "Functionality of OSA starch stabilized emulsions as fat replacers in cookies." Journal of Food Engineering **167**: 133-138.

Hamada, D., Kuroda, Y., Tanaka, T. and Goto, Y. (1995). "High helical propensity of the peptide fragments derived from β-lactoglobulin, a predominantly β-sheet protein." Journal of Molecular Biology **254**(4): 737-746.

Hancocks, R. D., Spyropoulos, F. and Norton, I. T. (2013). "Comparisons between membranes for use in cross flow membrane emulsification." Journal of Food Engineering **116**(2): 382-389.

Harrison, M. and Hills, B. P. (1997). "Mathematical model of flavor release from liquids containing aroma-binding macromolecules." Journal of Agricultural and Food Chemistry **45**(5): 1883-1890.

Harrison, M. (2000). Mathematical models of release and transport of flavors from foods in the mouth to the olfactory epithelium. In: Flavor Release, American Chemical Society. 15**:** 179-191.

Harvey, B. A., Druaux, C. and Voilley, A. (1995). Effect of protein on the retention and transfer of aroma compounds at the lipid-water interface. In: Food macromolecule and colloids. Dickison, E., Lorient, D., eds. Cambridge, The Royal Scociety of Chemistry**:** 154-163.

Hasenhuettl, G. L. and Hartel, R. (2008). Food emulsifier and their applications,second edition. New York, Springer**:** 389-392.

Hasenhuettl, G. L. and Hartel, R. (2008). Food emulsifiers and their applications,Second Edition. New York, Springer**:** 1-8.

Heinze, F. H. (2000). Encapsulation technology with modified starches. Proceedings of the International Symposium on the Controlled Release of Bioactive Materials. **27:** 1326-1327.

Hemar, Y. and Horne, D. S. (1998). "Electrostatic interactions in adsorbed protein layers probed by a sedimentation technique." J Colloid Interface Sci **206**(1): 138-145.

Heng, L., van Koningsveld, G. A., Gruppen, H., van Boekel, M. A. J. S., Vincken, J. P., Roozen, J. P. and Voragen, A. G. J. (2004). "Protein–flavour interactions in relation to development of novel protein foods." Trends in Food Science & Technology **15**(3): 217-224.

Hermansson, A. M. and Svegmark, K. (1996). "Developments in the understanding of starch functionality." Trends in Food Science & Technology **7**(11): 345-353.

Hino, T., Kawashima, Y. and Shimabayashi, S. (2000). "Basic study for stabilization of w/o/w emulsion and its application to transcatheter arterial embolization therapy." Advanced Drug Delivery Reviews **45**(1): 27-45.

Holdich, R. G., Dragosavac, M. M., Vladisavljević, G. T. and Kosvintsev, S. R. (2010). "Membrane emulsification with oscillating and stationary membranes." Industrial & Engineering Chemistry Research **49**(8): 3810-3817.

Imbrogno, A., Dragosavac, M. M., Piacentini, E., Vladisavljević, G. T., Holdich, R. G. and Giorno, L. (2015). "Polycaprolactone multicore-matrix particle for the simultaneous encapsulation of hydrophilic and hydrophobic compounds produced by membrane emulsification and solvent diffusion processes." Colloids and Surfaces B: Biointerfaces **135**: 116-125.

Israelachvili, J. N. (2011). Thermodynamic principles of self-assembly. In: Intermolecular and Surface Forces,3rd Edition. Israelachvili, J. N. San Diego, USA, Academic Press**:** 503-534.

Jacobsen, C., Schwarz, K., Stöckmann, H., Meyer, A. S. and Adler-Nissen, J. (1999). "Partitioning of Selected Antioxidants in Mayonnaise." Journal of Agricultural and Food Chemistry **47**(9): 3601-3610.

Jager-Lezer, N., Terrisse, I., Bruneau, F., Tokgoz, S., Ferreira, L., Clausse, D., Seiller, M. and Grossiord, J. L. (1997). "Influence of lipophilic surfactant on the release kinetics of water-soluble molecules entrapped in a W/O/W multiple emulsion." Journal of Controlled Release **45**(1): 1-13.

Jiao, J. and Burgess, D. J. (2008). Multiple emulsion stability: pressure balance and interfacial film strength. In: Multiple emulsions: technology and applications. Aserin, A. Hoboken, New Jersey, John Wiley & Sons, Inc.**:** 1-18.

Jiménez-Colmenero, F. (2013). "Potential applications of multiple emulsions in the development of healthy and functional foods." Food Research International **52**(1): 64-74.

Joscelyne, S. M. and Tragardh, G. (2000). "Membrane emulsification - a literature review." Journal of Membrane Science **169**(1): 107-117.

Jouenne, E. and Crouzet, J. (2000). "Determination of apparent binding constants for aroma compounds with β-lactoglobulin by dynamic coupled column liquid chromatography." Journal of Agricultural and Food Chemistry **48**(11): 5396-5400.

Jouenne, E. and Crouzet, J. (2000). "Effect of pH on Retention of Aroma Compounds by β-Lactoglobulin." Journal of Agricultural and Food Chemistry **48**(4): 1273-1277.

Kaimainen, M., Marze, S., Järvenpää, E., Anton, M. and Huopalahti, R. (2015). "Encapsulation of betalain into w/o/w double emulsion and release during in vitro intestinal lipid digestion." LWT - Food Science and Technology **60**(2, Part 1): 899-904.

Karaiskou, S., Blekas, G. and Paraskevopoulou, A. (2008). "Aroma release from gum arabic or egg yolk/xanthan-stabilized oil-in-water emulsions." Food Research International **41**(6): 637-645.

Kaur, M., Sandhu, K. S. and Singh, N. (2007). "Comparative study of the functional, thermal and pasting properties of flours from different field pea (Pisum sativum L.) and pigeon pea (Cajanus cajan L.) cultivars." Food Chemistry **104**(1): 259-267.

Kawakatsu, T., Trägårdh, G. and Trägårdh, C. (2001). "Production of W/O/W emulsions and S/O/W pectin microcapsules by microchannel emulsification." Colloids and Surfaces A: Physicochemical and Engineering Aspects **189**(1): 257-264.

Kawashima, Y., Hino, T., Takeuchi, H. and Niwa, T. (1992). "Stabilization of water oil-water multiple emulsion with hypertonic inner aqueous phase." Chemical & Pharmaceutical Bulletin **40**(5): 1240-1246.

Keršienė, M., Adams, A., Dubra, A., Kimpe, N. D. and Leskauskaitė, D. (2008). "Interactions between flavour release and rheological properties in model custard desserts: Effect of starch concentration and milk fat." Food Chemistry **108**(4): 1183-1191.

Kim, H. and Min, D. B. (1988). Interaction of flavour compounds with protein. In: Flavour chemistry of lipid foods. D. B. Min and T. H. Smouse, e. Washington, D. C., American Chemical Society**:** 404-420.

Kim, H. J., Decker, E. A. and McClements, D. J. (2002a). "Role of Postadsorption Conformation Changes of β-Lactoglobulin on Its Ability To Stabilize Oil Droplets against Flocculation during Heating at Neutral pH." Langmuir **18**(20): 7577-7583.

Kim, H. J., Decker, E. A. and McClements, D. J. (2002b). "Impact of Protein Surface Denaturation on Droplet Flocculation in Hexadecane Oil-in-Water Emulsions Stabilized by β-Lactoglobulin." Journal of Agricultural and Food Chemistry **50**(24): 7131-7137.

Kinsella, J. E. (1988). Flavour perception and binding to food components. In: Flavour Chemistry of Lipid Foods. Min, D. B. a. S., T. H. Washington, DC, American Chemical Society**:** 376-403.

Kolb, B., Welter, C. and Bichler, C. (1992). "Determination of partition coefficients by automatic equilibrium headspace gas chromatography by vapor phase calibration." Chromatographia **34**(5): 235-240.

Koroleva, M. Y. and Yurtov, E. V. (2003). "Water Transport by Nanodispersion Droplets in a Water-in-Oil Emulsion." Colloid Journal **65**(1): 35-39.

Kosvintsev, S. R., Gasparini, G., Holdich, R. G., Cumming, I. W. and Stillwell, M. T. (2005). "Liquid−liquid membrane dispersion in a stirred cell with and without controlled shear." Industrial & Engineering Chemistry Research **44**(24): 9323-9330.

Królikowska, K., Fortuna, T., Pietrzyk, S. and Gryszkin, A. (2017). "Effect of modification of octenyl succinate starch with mineral elements on the stability and rheological properties of oil-in-water emulsions." Food Hydrocolloids **66**: 118-127.

Krstonošić, V., Dokić, L. and Milanović, J. (2011). "Micellar properties of OSA starch and interaction with xanthan gum in aqueous solution." Food Hydrocolloids **25**(3): 361-367.

Krstonošić, V., Dokić, L., Nikolić, I. and Milanović, M. (2015). "Influence of xanthan gum on oil-in-water emulsion characteristics stabilized by OSA starch." Food Hydrocolloids **45**: 9-17.

Kuhn, J., Considine, T. and Singh, H. (2008). "Binding of flavour compounds and whey protein isolate as affected by heat and high pressure treatments." J. Agric. Food Chem. **56**: 10218-10224.

Lad, M., Hewson, L. and Wolf, B. (2012). "Enhancing saltiness in emulsion based foods." Flavour **1**(1): 13.

Landy, P., Druaux, C. and Voilley, A. (1995). "Retention of aroma compounds by proteins in aqueous-solution." Food Chemistry **54**(4): 387-392.

Landy, P., Courthaudon, J. L., Dubois, C. and Voilley, A. (1996). "Effect of interface in model food emulsions on the volatility of aroma compounds." Journal of Agricultural and Food Chemistry **44**(2): 526-530.

Leal-Calderon, F., Bibette, J. and V., S. (2007). Emulsion Science: Basic Principles,2nd edition. New York, Springer**:** 173.

Leal-Calderon, F., Homer, S., Goh, A. and Lundin, L. (2012). "W/O/W emulsions with high internal droplet volume fraction." Food Hydrocolloids **27**(1): 30-41.

Leland, J. V. (1997). "Flavor interactions: The greater whole." Food Technology **51**(1): 75-&.

Lesmes, U. and McClements, D. J. (2009). "Structure–function relationships to guide rational design and fabrication of particulate food delivery systems." Trends in Food Science & Technology **20**(10): 448-457.

Light, J. M. (1990). "Modified food starch: why, what, where, and why." Cereal foods world **35**(11): 1081-1092.

Lima, E., De Melo, B., Baptista, L. and Paredes, M. (2013). "Specific ion effects on the interfacial tension of water/hydrocarbon systems." Brazilian Journal of Chemical Engineering **30**(1): 55-62.

Linforth, R. and Taylor, A. (2010). "Expression of multidisciplinary favour science. Flavour delivery from the oral cavity to the nose." Expression of multidisciplinary favour science: 101e104.

Lloyd, D. M., Norton, I. T. and Spyropoulos, F. (2014). "Processing effects during rotating membrane emulsification." Journal of Membrane Science **466**: 8-17.

Lobato-Calleros, C., Rodriguez, E., Sandoval-Castilla, O., Vernon-Carter, E. J. and Alvarez-Ramirez, J. (2006). "Reduced-fat white fresh cheese-like products obtained from W1/O/W2 multiple emulsions: Viscoelastic and high-resolution image analyses." Food Research International **39**(6): 678-685.

Lobato-Calleros, C., Recillas-Mota, M. T., Espinosa-Solares, T., Alvarez-Ramirez, J. and Vernon-Carter, E. J. (2009). "Microstructural and rheological properties of low-fat stirred yoghurts made with skim milk and multiple emulsions." Journal of Texture Studies **40**(6): 657-675.

Long, Z., Zhao, Q., Liu, T., Kuang, W., Xu, J. and Zhao, M. (2013). "Influence of xanthan gum on physical characteristics of sodium caseinate solutions and emulsions." Food Hydrocolloids **32**(1): 123-129.

Lubbers, S., Landy, P. and Voilley, A. (1998). "Retention and release of aroma compounds in foods containing proteins." Food Technology **52**(5): 68-+.

Lutz, R., Aserin, A., Wicker, L. and Garti, N. (2009). "Release of electrolytes from W/O/W double emulsions stabilized by a soluble complex of modified pectin and whey protein isolate." Colloids and Surfaces B: Biointerfaces **74**(1): 178-185.

Madene, A., Jacquot, M., Scher, J. and Desobry, S. (2006). "Flavour encapsulation and controlled release - a review." International Journal of Food Science and Technology **41**(1): 1-21.

Malone, M. E., Appelqvist, I. A. M., Goff, T. C., Homan, J. E. and Wilkins, J. P. G. (2000). A novel approach to the selective control of lipophilic flavor release in low fat food. In: Flavor Release, American Chemical Society. 18**:** 212-227.

Malone, M. E., Appelqvist, I. A. M. and Norton, I. T. (2003). "Oral behaviour of food hydrocolloids and emulsions. Part 2. Taste and aroma release." Food Hydrocolloids **17**(6): 775-784.

Manglik, R. M., Wasekar, V. M. and Zhang, J. (2001). "Dynamic and equilibrium surface tension of aqueous surfactant and polymeric solutions." Experimental Thermal and Fluid Science **25**(1): 55-64.

Mao, L., Roos, Y. H. and Miao, S. (2014). "Flavour Release from Monoglyceride Structured Oil-in-Water Emulsions through Static Headspace Analysis." Food Biophysics **9**(4): 359-367.

Marefati, A., Sjöö, M., Timgren, A., Dejmek, P. and Rayner, M. (2015). "Fabrication of encapsulated oil powders from starch granule stabilized W/O/W Pickering emulsions by freeze-drying." Food Hydrocolloids **51**: 261-271.

Márquez, A. L., Medrano, A., Panizzolo, L. A. and Wagner, J. R. (2010). "Effect of calcium salts and surfactant concentration on the stability of water-in-oil (w/o) emulsions prepared with polyglycerol polyricinoleate." J Colloid Interface Sci **341**(1): 101-108.

Matos, M., Timgren, A., Sjöö, M., Dejmek, P. and Rayner, M. (2013). "Preparation and encapsulation properties of double Pickering emulsions stabilized by quinoa starch granules." Colloids and Surfaces A: Physicochemical and Engineering Aspects **423**: 147-153.

Matos, M., Gutiérrez, G., Coca, J. and Pazos, C. (2014). "Preparation of water-in-oil-in-water (W1/O/W2) double emulsions containing trans-resveratrol." Colloids and Surfaces A: Physicochemical and Engineering Aspects **442**: 69-79.

Matsumoto, S. and Kohda, M. (1979). Rheological properties of water-in-oil-in water type multiple-phase systems. In: Food texture and rheology. Sherman, P. London, Academic Press**:** 437-452.

Matsumoto, S., Inoue, T., Kohda, M. and Ikura, K. (1980). "Water permeability of oil layers in W/O/W emulsions under osmotic pressure gradients." J Colloid Interface Sci **77**(2): 555-563.

McClements, D. J. (2002). "Modulation of Globular Protein Functionality by Weakly Interacting Cosolvents." Critical Reviews in Food Science and Nutrition **42**(5): 417-471.

McClements, D. J. (2005). Food emulsions: principles, practice and techniques,2nd edition. Bora Raton, CRC Press**:** 122-146.

McClements, D. J. (2005). Food emulsions: principles, pratices and techniques,2nd Edition. Bora Raton, CRC Press**:** 269-338.

McClements, D. J. (2005). Food emulsions: principles, practice and techniques,2nd Edition. Bora Raton, CRC Press**:** 249-259.

McClements, D. J. (2005). Food emulsions: principles, practice and techniques. Bora Raton, CRC press**:** 422-428.

Meynier, A., Garillon, A., Lethuaut, L. and Genot, C. (2003). "Partition of fove aroma compounds between air and skim milk, anhydrous milk fat or full-fat cream." Lait **83**: 223-235.

Meynier, A., Rampon, V., Dalgalarrondo, M. and Genot, C. (2004). "Hexanal and t-2-hexenal form covalent bonds with whey proteins and sodium caseinate in aqueous solution." International Dairy Journal **14**(8): 681-690.

Meynier, A., Lecoq, C. and Genot, C. (2005). "Emulsification enhances the retention of esters and aldehydes to a greater extent than changes in the droplet size distribution of the emulsion." Food Chemistry **93**(1): 153-159.

Mezzenga, R., Folmer, B. M. and Hughes, E. (2004). "Design of Double Emulsions by Osmotic Pressure Tailoring." Langmuir **20**(9): 3574-3582.

Mezzenga, R. (2007). "Equilibrium and non-equilibrium structures in complex food systems." Food Hydrocolloids **21**(5-6): 674-682.

Midmore, B. R. and Herrington, T. M. (1999). Silica-stabilised multiple emulsions. In: Trends in Colloid and Interface Science XIII. Težak, D. and Martinis, M. Berlin, Heidelberg, Springer Berlin Heidelberg**:** 115-120.

Miettinen, S.-M., Tuorila, H., Piironen, V., Vehkalahti, K. and Hyvönen, L. (2002). "Effect of Emulsion Characteristics on the Release of Aroma As Detected by Sensory Evaluation, Static Headspace Gas Chromatography, and Electronic Nose." Journal of Agricultural and Food Chemistry **50**(15): 4232-4239.

Mirhosseini, H., Tan, C. P., Aghlara, A., Hamid, N. S. A., Yusof, S. and Chern, B. H. (2008). "Influence of pectin and CMC on physical stability, turbidity loss rate, cloudiness and flavor release of orange beverage emulsion during storage." Carbohydrate Polymers **73**(1): 83-91.

Morelli, S., Holdich, R. G. and Dragosavac, M. M. (2016). "Chitosan and Poly (Vinyl Alcohol) microparticles produced by membrane emulsification for encapsulation and pH controlled release." Chemical Engineering Journal **288**: 451-460.

Morris, V. J. (2006). Bacterial polysaccharides. In: Food polysaccharides and their applications,2nd Edition. S., A. M., Glyn, O. P. and Peter, A. W. Boca Raton, CRC Press. 12**:** 413-454.

Mun, S., Choi, Y., Rho, S.-J., Kang, C.-G., Park, C.-H. and Kim, Y.-R. (2010). "Preparation and characterization of water/oil/water emulsions stabilized by polyglycerol polyricinoleate and whey protein isolate." Journal of Food Science **75**(2): E116-E125.

Naknean, P. and Meenune, M. (2010). "Factors affecting retention and release of flavour compounds in food carbogydrates." International Food Research Journal **17**: 23-34.

Napper, D. H. (1977). Steric stabilization. In: Plenary and Invited Lectures, Elsevier**:** 413-430.

Nawar, W. W. (1971). "Some variables affecting composition of headspace aroma." Journal of Agricultural and Food Chemistry **19**(6): 1057-&.

Neville, M. E. (2014). Impact of aroma compounds on oil-water interfacial properties. Food Science. Nottingham, UK, Univeristy of Nottingham. **BSc.**

Nilsson, L. and Bergenståhl, B. (2007). "Emulsification and Adsorption Properties of Hydrophobically Modified Potato and Barley Starch." Journal of Agricultural and Food Chemistry **55**(4): 1469-1474.

Niño, M. R. R. and Patino, J. R. (1998). "Surface tension of bovine serum albumin and tween 20 at the air-aqueous interface." Journal of the American Oil Chemists' Society **75**(10): 1241.

Normand, V., Dradelle, G., Bouguerand, P. E., Nicolas, L. and Johnston, D. J. (2005). "Flavor Encapsulation in Yeasts: Limonene Used as a Model System for Characterization of the Release Mechanism." Journal of Agricultural and Food Chemistry **53**(19): 7532-7543.

Norn, V. (2015). Introduction to food emulsifiers and colloidal system. In: Emulsifiers in food technology,2nd edition. Norn, V. West Sussex, UK, Wiley Blackwell. 1**:** 1-18.

Ntawukulilyayo, J. D., De Smedt, S. C., Demeester, J. and Remon, J. P. (1996). "Stabilisation of suspensions using sucrose esters and low substituted n-octenylsuccinate starch-xanthan gum associations." International Journal of Pharmaceutics **128**(1): 73-79.

O'Kane, F. E., Vereijken, J. M., Gruppen, H. and Van Boekel, M. A. J. S. (2005). "Gelation Behavior of Protein Isolates Extracted from 5 Cultivars of Pisum sativum L." Journal of Food Science **70**(2): C132-C137.

O'Neill, T. and Kinsella, J. E. (1988). "Effect of heat treatment and modification on conformation and flavor binding by β-lactoglobulin." Journal of Food Science **53**(3): 906-909.

O'Neill, T. E. and Kinsella, J. E. (1987). "Flavor protein interactions: Characteristics of 2 - nonanone binding to isolated soy protein fractions." Journal of Food Science **52**(1): 98-101.

Obradović, S. and Poša, M. (2017). "The influence of the structure of selected Brij and Tween homologues on the thermodynamic stability of their binary mixed micelles." The Journal of Chemical Thermodynamics **110**: 41-50.

Okeefe, S. F., Resurreccion, A. P., Wilson, L. A. and Murphy, P. A. (1991). "Temperature effect on binding of volatile flavor compounds to soy protein in aqueous model systems." Journal of Food Science **56**(3): 802-806.

Owusu-Ansah, Y. J. and McCurdy, S. M. (1991). "Pea proteins: A review of chemistry, technology of production, and utilization." Food Reviews International **7**(1): 103-134.

Paraskevopoulou, A., Tsoukala, A. and Kiosseoglou, V. (2009). "Monitoring air/liquid partition of mastic gum oil volatiles in model alcoholic beverage emulsions: Effect of emulsion composition and oil droplet size." Food Hydrocolloids **23**(4): 1139-1148.

Park, S., Chung, M.-G. and Yoo, B. (2004). "Effect of Octenylsuccinylation on Rheological Properties of Corn Starch Pastes." Starch - Stärke **56**(9): 399-406.

Pawlik, A., Cox, P. W. and Norton, I. T. (2010). "Food grade duplex emulsions designed and stabilised with different osmotic pressures." J Colloid Interface Sci **352**(1): 59-67.

Pawlik, A. K. and Norton, I. T. (2012). "Encapsulation stability of duplex emulsions prepared with SPG cross-flow membrane, SPG rotating membrane and rotor-stator techniques-A comparison." Journal of Membrane Science **415**: 459-468.

Pawlik, A. K. and Norton, I. T. (2013). "SPG rotating membrane technique for production of food grade emulsions." Journal of Food Engineering **114**(4): 530-537.

Pays, K., Giermanska-Kahn, J., Pouligny, B., Bibette, J. and Leal-Calderon, F. (2002). "Double emulsions: how does release occur?" Journal of Controlled Release **79**(1-3): 193-205.

Plug, H. and Haring, P. (1993). "The influence of flavour-ingredient interactions on flavour perception." Food Qual. Prefer **5**: 95-102.

Plug, H. and Haring, P. (1993). "The role of ingredient-flavour interactions in the development of fat-free foods." Trends in Food Science & Technology **4**(5): 150-152.

Poole, S. K. and Poole, C. F. (2003). "Separation methods for estimating octanol–water partition coefficients." Journal of Chromatography B **797**(1–2): 3-19.

Prochaska, K., Kędziora, P., Le Thanh, J. and Lewandowicz, G. (2007). "Surface activity of commercial food grade modified starches." Colloids and Surfaces B: Biointerfaces **60**(2): 187-194.

Raynal, S., Grossiord, J. L., Seiller, M. and Clausse, D. (1993). "A topical W/O/W multiple emulsion containing several active substances: formulation, characterization and study of release." Journal of Controlled Release **26**: 129-140.

Reineccius, G. A. (1991). "Carbohydrates for flavor encapsulation." Food Technology **45**(3): 144-&.

Rojas, E. C., Staton, J. A., John, V. T. and Papadopoulos, K. D. (2008). "Temperature-induced protein release from water-in-oil-in-water double emulsions." Langmuir **24**.

Rosen, M. J. and Kunjappu, J. T. (2012). Surfactants and interfacial phenomena. Hoboken, NJ, John Wiley and Sons.

Safwat, S. M., Kassem, M. A., Attia, M. A. and EI-Mahdy, M. (1994). "The formation-performancerelationship of mutiple emulsions and ocular activity." Journal of Controlled Release **32**(3): 259-268.

Saha, D. and Bhattacharya, S. (2010). "Hydrocolloids as thickening and gelling agents in food: a critical review." Journal of food science and technology **47**(6): 587-597.

Sapei, L., Naqvi, M. A. and Rousseau, D. (2012). "Stability and release properties of double emulsions for food applications." Food Hydrocolloids **27**(2): 316-323.

Saveyn, P., Cocquyt, E., Zhu, W., Sinnaeve, D., Haustraete, K., Martins, J. C. and Van der Meeren, P. (2009). "Solubilization of flurbiprofen within non-ionic Tween 20 surfactant micelles: a 19F and 1H NMR study." Physical Chemistry Chemical Physics **11**(26): 5462-5468.

Schröder, V., Behrend, O. and Schubert, H. (1998). "Effect of Dynamic Interfacial Tension on the Emulsification Process Using Microporous, Ceramic Membranes." J Colloid Interface Sci **202**(2): 334-340.

Schröder, V. and Schubert, H. (1999). "Production of emulsions using microporous, ceramic membranes." Colloids and Surfaces A: Physicochemical and Engineering Aspects **152**(1–2): 103-109.

Schubert, H. and Ax, K. (2003). Engineering food emulsions. In: Texture in food, volume 1: semid-solid foods,1st Edition. McKenna, B. M. Boca Raton, FL, USA, CRC Press. 8**:** 185-198.

Schuch, A., Wrenger, J. and Schuchmann, H. P. (2014). "Production of W/O/W double emulsions. Part II: Influence of emulsification device on release of water by coalescence." Colloids and Surfaces A: Physicochemical and Engineering Aspects **461**: 344-351.

Seifriz, W. (1925). "Studies in Emulsions. III-V." The Journal of Physical Chemistry **29**(6): 738-749.

Sela, Y., Magdassi, S. and Garti, N. (1995). "Release of markers from the inner water phase of W/O/W emulsions stabilized by silicone based polymeric surfactants." Journal of Controlled Release **33**(1): 1-12.

Semenova, M. G., Antipova, A., S.,, Belyakova L. E., Polikarpov, Y. N., Wasserman, L., A.,, Misharina, T. A., Terenina, M., B., and Golovnya, R. V. (2002c). "Binding of aroma compounds with legumin. III. Thermodynamics of competitive binding of aroma compounds with 11S globulin depending on the structure of aroma compounds." Food Hydrocolloid **16**(6): 573-584.

Shamil, S., Wyeth, L. J. and Kilcast, D. (1991). "Flavour release and perception in reduced-fat foods." Food Quality and Preference **3**(1): 51-60.

Shima, M., Morita, Y., Yamashita, M. and Adachi, S. (2006). "Protection of Lactobacillus acidophilus from the low pH of a model gastric juice by incorporation in a W/O/W emulsion." Food Hydrocolloids **20**(8): 1164-1169.

Shimizu, S., Abbott, S. and Matubayasi, N. (2017). "Quantifying non-specific interactions between flavour and food biomolecules." Food & Function **8**(9): 2999-3009.

Shogren, R. L., Viswanathan, A., Felker, F. and Gross, R. A. (2000). "Distribution of octenyl succinate groups in octenyl succinic anhydride modified waxy maize starch." Starch - Stärke **52**(6-7): 196-204.

Singh, J., Kaur, L. and McCarthy, O. J. (2007). "Factors influencing the physico-chemical, morphological, thermal and rheological properties of some chemically modified starches for food applications—A review." Food Hydrocolloids **21**(1): 1-22.

Sostmann, K. and Guichard, E. (1998). "Immobilized β-lactoglobulin on a HPLC-column: a rapid way to determine protein—flavour interactions." Food Chemistry **62**(4): 509-513.

Souilem, S., Kobayashi, I., Neves, M. A., Sayadi, S., Ichikawa, S. and Nakajima, M. (2014). "Preparation of Monodisperse Food-Grade Oleuropein-Loaded W/O/W Emulsions Using Microchannel Emulsification and Evaluation of Their Storage Stability." Food and Bioprocess Technology **7**(7): 2014-2027.

Spyropoulos, F., Hancocks, R. D. and Norton, I. T. (2011). "Food-grade emulsions prepared by membrane emulsification techniques." Procedia Food Science **1**: 920-926.

Spyropoulos, F., Lloyd, D. M., Hancocks, R. D. and Pawlik, A. K. (2014). "Advances in membrane emulsification. Part A: recent developments in processing aspects and microstructural design approaches." Journal of the Science of Food and Agriculture **94**(4): 613-627.

St Angelo, A. J. (1989). A brief introduction to food emulsions and emulsifiers. In: Food emulsifiers: chemistry, technology, functional properties and applications. Charalambous, G. and Doxastakis, G. Amsterdam, Elsevier Science Publishers B. V.**:** 1-8.

Stauffer, C. E. (1999). Emulsifiers. St. Paul, Minnesota, Eagan Press**:** 25-45.

Stillwell, M. T., Holdich, R. G., Kosvintsev, S. R., Gasparini, G. and Cumming, I. W. (2007). "Stirred cell membrane emulsification and factors influencing dispersion drop size and uniformity." Industrial & Engineering Chemistry Research **46**(3): 965-972.

Suppavorasatit, I. and Cadwallader, K. R. (2012). "Effect of enzymatic deamidation of soy protein by protein–glutaminase on the flavor-binding properties of the protein under aqueous conditions." Journal of Agricultural and Food Chemistry **60**(32): 7817-7823.

Surh, J., Vladisavljevic, G. T., Mun, S. and McClements, D. J. (2007). "Preparation and characterization of water/oil and water/oil/water emulsions containing biopolymer-gelled water droplets." Journal of Agricultural and Food Chemistry **55**(1): 175-184.

Suryaprakash, P., Kumar, R. P. and Prakash, V. (2000). "Thermodynamics of interaction of caffeic acid and quinic acid with multisubunit proteins." International Journal of Biological Macromolecules **27**(3): 219-228.

Sweedman, M. C., Tizzotti, M. J., Schäfer, C. and Gilbert, R. G. (2013). "Structure and physicochemical properties of octenyl succinic anhydride modified starches: A review." Carbohydrate Polymers **92**(1): 905-920.

Sworn, G. (2009). Xanthan gum. In: Handbook of hydrocolloids,2nd Edition. Phillips, G. O. and Williams, P. A. Boca Raton, CRC Press. 8**:** 186-202.

Tadros, T. (2015). "Viscoelastic properties of sterically stabilised emulsions and their stability." Adv Colloid Interface Sci **222**: 692-708.

Tadros, T. F. (1991). "Steric stabilisation and flocculation by polymers." Polymer journal **23**(5): 683.

Tadros, T. F. (2013). Emulsion formation and stability,1st Edition. Weinheim, Germany, Wiley-VCH Verlag Gmbh & Co. KGaA**:** 3-5.

Taggart, P. and Mitchell, J. R. (2009). Starch. In: Handbook of hydrocolloids,2nd edition. Phillips, G. O., Williams, P. A. Cambridge, CRC Press. 5**:** 108-120.

Tari, T. A. and Singhal, R. S. (2002). "Starch based spherical aggregates: reconfirmation of the role of amylose on the stability of a model flavouring compound, vanillin." Carbohydrate Polymers **50**(3): 279-282.

Tavel, L., Andriot, I., Moreau, C. and Guichard, E. (2008). "Interactions between β-lactoglobulin and aroma compounds: Different binding behaviors as a function of ligand structure." Journal of Agricultural and Food Chemistry **56**(21): 10208-10217.

Tavel, L., Moreau, C., Bouhallab, S., Li-Chan, E. C. Y. and Guichard, E. (2010). "Interactions between aroma compounds and β-lactoglobulin in the heat-induced molten globule state." Food Chemistry **119**(4): 1550-1556.

Taylor, A. J. and Roozen, J. P. (1996a). "Volatile flavor release from foods during eating." Critical Reviews in Food Science and Nutrition **36**(8): 765-784.

Taylor, A. J. and Linforth, R. S. T. (1996b). "Flavour release in the mouth." Trends in Food Science & Technology **7**(12): 444-448.

Taylor, A. J. (1998). "Physical chemistry of flavour." International Journal of Food Science & Technology **33**(1): 53-62.

Taylor, A. J. and Linforth, R. S. T. (2010). Food flavour technology,2nd. West Sussex, John Wiley and Sons Ltd.**:** 178.

Taylor, A. J. and Linforth, R. S. T. (2010). Food flavour technology,2nd edition. West Sussex, John Wiley and Sons Ltd.**:** 190-200.

Taylor, M. S. (2011). Stabilisation of water-in-oil emulsions to improve the emollient properties of Lipstick. School of Chemical Engineering, The University of Birmingham. **MRes thesis**.

Tesch, S., Gerhards, C. and Schubert, H. (2002). "Stabilization of emulsions by OSA starches." Journal of Food Engineering **54**(2): 167-174.

Thompson, K. L., Mable, C. J., Lane, J. A., Derry, M. J., Fielding, L. A. and Armes, S. P. (2015). "Preparation of pickering double emulsions using block copolymer worms." Langmuir **31**(14): 4137-4144.

Thomson, D. M. H. (1986). The meaning of flavour. In: Developments in food flavour. Birch, G. G., Lindley, M. G. and Eds. London, Elsevier Applied Science**:** 1-19.

Traynor, M., Burke, R., Frias, J. M., Gaston, E. and Barry-Ryan, C. (2013). "Formation and stability of an oil in water emulsion containing lecithin, xanthan gum and sunflower oil." International Food Research Journal **20**(5): 2173-2181.

Ushikubo, F. Y. and Cunha, R. L. (2014). "Stability mechanisms of liquid water-in-oil emulsions." Food Hydrocolloids **34**(Supplement C): 145-153.

van der Graaf, S., Schroën, C. G. P. H. and Boom, R. M. (2005). "Preparation of double emulsions by membrane emulsification—a review." Journal of Membrane Science **251**(1–2): 7-15.

van Ruth, S. M., O'Connor, C. H. and Delahunty, C. M. (2000). "Relationships between temporal release of aroma compounds in a model mouth system and their physico-chemical characteristics." Food Chemistry **71**(3): 393-399.

van Ruth, S. M., King, C. and Giannouli, P. (2002a). "Influence of lipid fraction, emulsifier fraction, and mean particle diameter of oil-in-water emulsions on the release of 20 aroma compounds." Journal of Agricultural and Food Chemistry **50**(8): 2365-2371.

van Ruth, S. M., de Vries, G., Geary, M. and Giannouli, P. (2002b). "Influence of composition and structure of oil-in-water emulsions on retention of aroma compounds." Journal of the Science of Food and Agriculture **82**(9): 1028-1035.

van Ruth, S. M., King, C., Delarue, M. and Giannouli, P. (2002c). "Release of volatile compounds from emulsions: Influence of β-lactoglobulin and pH." Italian journal of food science **14**(2).

Vargaftik, N., Volkov, B. and Voljak, L. (1983). "International tables of the surface tension of water." Journal of Physical and Chemical Reference Data **12**(3): 817-820.

Versic, R. J. (1988). Flavour encapsulation: an overview. In: Flavour encapsulation. Reineccius, S. J. R. a. G. A. Washington, D. C., American Chemical Society**:** 1-11.

Vladisavljevic, G. T. and Schubert, H. (2002). "Preparation and analysis of oil-in-water emulsions with a narrow droplet size distribution using Shirasu-porous-glass (SPG) membranes." Desalination **144**(1): 167-172.

Vladisavljevic, G. T. and Schubert, H. (2003). "Influence of process parameters on droplet size distribution in SPG membrane emulsification and stability of prepared emulsion droplets." Journal of Membrane Science **225**(1-2): 15-23.

Voilley, A., Simatos, D. and Loncin, M. (1977). "Gas phase concentration of volatiles in equilibrium with a liquid aqueous phase." Lebensm.-Wiss.u.-Technol **10**: 45-49.

Voilley, A. and Etievant, P. (1996). Flavour in food,2nd edition. Cambridge, Woodhead Publishing Ltd.

Walstra, P. and Smulders, P. E. A. (1998). Emulsion formation. In: Modern aspects of emulsion science,1st Edition. Binks, B. P. Cambridge, UK, The Royal Society of Chemistry. 2**:** 56-97.

Wang, K. and Arntfield, S. D. (2014). "Binding of carbonyl flavours to canola, pea and wheat proteins using GC/MS approach." Food Chemistry **157**(Supplement C): 364-372.

Wang, K. and Arntfield, S. D. (2015). "Binding of selected volatile flavour mixture to salt-extracted canola and pea proteins and effect of heat treatment on flavour binding." Food Hydrocolloids **43**(Supplement C): 410-417.

Wilson, R., Van Schie, B. J. and Howes, D. (1998). "Overview of the preparation, use and biological studies on poltglycerol polyricinoleate (PGPR)." Food and Chemical Toxicology **36**: 711-718.

Wolf, F., Koehler, K. and Schuchmann, H. P. (2013). "Stabilization of water droplets in oil with pgpr for use in oral and dermal applications." Journal of Food Process Engineering **36**(3): 276-283.

Wulff, G., Steinert, A. and Höller, O. (1998). "Modification of amylose and investigation of its inclusion behavior." Carbohydrate Research **307**(1–2): 19-31.

Wulff, G., Avgenaki, G. and Guzmann, M. S. P. (2005). "Molecular encapsulation of flavours as helical inclusion complexes of amylose." Journal of Cereal Science **41**(3): 239-249.

Xu, Y. Y., Howes, T., Adhikari, B. and Bhandari, B. (2012). "Investigation of relationship between surface tension of feed solution containing various proteins and surface composition and morphology of powder particles." Drying Technology **30**(14): 1548-1562.

Yusoff, A. and Murray, B. S. (2011). "Modified starch granules as particle-stabilizers of oil-in-water emulsions." Food Hydrocolloids **25**(1): 42-55.

Zhu, Q., Qiu, S., Zhang, H., Cheng, Y. and Yin, L. (2018). "Physical stability, microstructure and micro-rheological properties of water-in-oil-in-water (W/O/W) emulsions stabilized by porcine gelatin." Food Chemistry **253**: 63-70.